
Electronic Thesis and Dissertation Repository

11-14-2018 3:00 PM

Continuous Monitoring of Neutral Grounding Resistors and Reactors

Rahim Jafari
The University of Western Ontario

Supervisor
Sidhu, Tarlochan Sing.
The University of Western Ontario

Graduate Program in Electrical and Computer Engineering
A thesis submitted in partial fulfillment of the requirements for the degree in Doctor of Philosophy
© Rahim Jafari 2018

Follow this and additional works at: <https://ir.lib.uwo.ca/etd>



Part of the [Power and Energy Commons](#)

Recommended Citation

Jafari, Rahim, "Continuous Monitoring of Neutral Grounding Resistors and Reactors" (2018). *Electronic Thesis and Dissertation Repository*. 5877.
<https://ir.lib.uwo.ca/etd/5877>

This Dissertation/Thesis is brought to you for free and open access by Scholarship@Western. It has been accepted for inclusion in Electronic Thesis and Dissertation Repository by an authorized administrator of Scholarship@Western. For more information, please contact wlsadmin@uwo.ca.

Abstract

Electrical power system components are designed three-phase balanced and symmetric with the internal connection of wye or delta. The common point of the wye-connected equipments, which is called neutral, is impedance grounded for many reasons such as fault ride through by controlling transient overvoltages, and limiting the ground overcurrents. Depending on the application, different neutral impedance grounding methods exist that employ resistors or reactors with/without neutral grounding transformers. These apparatuses are known as Neutral Grounding Devices (NGD). The most well-known sort of NGDs are the Neutral Grounding Resistor (NGR) and Neutral Grounding Reactor (NGL) which are the main focus of this research work.

As said, NGDs provide many benefits; however, they fail due to many reasons such as corrosion, lightning, and extended service life. Upon this failure, the advantages of impedance grounding are replaced by disadvantages of the ungrounded or solidly grounded traditional systems. Consequences of such a failure are false sense of security, ungrounded system, transient overvoltages, overcurrents, line-to-ground voltage test non-safety, and so on. In order to prevent these issues, the intactness and integrity of the neutral-to-ground circuit shall be ensured. However, this cannot be done easily since the neutral-to-ground circuit is dead or de-energized during the steady-state condition. However, there has to be a continuous and online monitor, which without it there is no guarantee or indication that these apparatuses have failed. That is why the Canadian Electric Code (CEC) mandates monitoring of the neutral-to-ground circuit in industrial and commercial networks.

Accordingly, this research work first reviews the existing monitoring methods to understand the fundamentals, and performance of these techniques. The performed literature survey results in a conceptual classification of the existing methods into three categories called passive, active, and passive-active. This part of the carried-out research highlights the advantages and disadvantages of the methods on one hand, and the evolution trend of the methods on the other. It also reveals that all of the existing methods suffer from one shared issue which is the hard-to-achieve continuous monitoring. In fact, they cannot provide continuous or uninterrupted operation in all system conditions, i.e., normal, faulted, and de-energized. It is this major shortcoming of the literature which motivates towards making a difference. Therefore, the mission is to resolve this issue relying on the existing measurement instruments and protection installations. As the results, three new or enhanced methods are achieved.

The first technique is a cost-effective combination of two existing techniques resulted in a better performance. The performance of this proposed method is comprehensively studied using software analysis, and a fabricated prototype of the invented mechanism for full-range neutral voltage measurement. The resulted method provides reliable monitoring during both faulted and unfaulted conditions of the power system which is the most prominent advantage of the proposed technique since none of the existing methods, with the same measurements, provide the such a performance.

The second proposed technique is an economical solution that employs the third harmonic of neutral and residual voltages for monitoring the NGR installed at the neutral of the unit-connected generators. The proposed technique is comprehensively studied including further hardware validations using an available industrial generator protective relay. The required measurement instruments and protection infrastructures are readily available which means that the proposed method could be implemented with no additional cost. In fact, the proposed method could be easily incorporated into the core of the existing digital protective relays.

Lastly, the third technique employs an existing sub-harmonic injection based generator stator ground protection for monitoring the neutral-to-ground circuit of the same generator, which is equipped with either the neutral grounding resistor or neutral grounding reactor. This alternative is also a money-saving solution since it only demands a current sensor to measure the injected current. It is also easily retrofitted to installed digital protective relays. The other advantage of this proposed method is its functionality in de-energized condition of the power system beside its reliable performance in both faulted and unfaulted operation conditions. It is this one last accomplishment that brings the mission to completion.

Keywords: Neutral grounding devices, neutral grounding resistor, neutral grounding reactor, continuous monitoring, resistance grounding, sensing resistor, third harmonic, sub-harmonic injection, passive, active.

Dedicated to my dear mother for her love and boundless support from the Heaven.

Acknowledgments

I would like to express my deep gratitude to Professor Tarlochan Singh Sidhu for his patient guidance, enthusiastic encouragement, and useful critiques of this research work. Furthermore, Dr. Mital Kanabar from GE Grid Solutions provided me with his very valuable guidance throughout my graduate studies. It has been a great privilege to pursue my higher education under their supervision.

I must express my very profound gratitude to my parents and spouse for providing me with unfailing support and continuous encouragement throughout my years of study and through the process of researching and writing this thesis. This accomplishment would not have been possible without them.

I am grateful to my friends in London, ON for helping me through the difficult times, for their support, and care.

My special thanks are extended to NSERC and GE Grid Solutions, Markham, ON, Canada for their financial support, to pursue this research work.

Contents

List of Figures	x
List of Tables	xviii
Nomenclature	xix
1 Introduction	1
1.1 Neutral Grounding Devices	1
1.2 Problem Definition	2
1.3 Literature Survey	3
1.4 Challenges	8
1.5 Objectives and Motivations	8
1.6 Thesis Outlines	9
2 Literature Review: Existing Monitoring Methods	11
2.1 Neutral Impedance Grounding	11
2.1.1 Neutral Grounding Methods	12
2.1.2 Neutral Grounding Devices	15
2.1.3 Failure of Neutral Grounding Devices	16
2.2 Importance of Monitoring The Neutral-to-Ground Path	18
2.3 Existing Monitoring Methods – Passive Category	19
2.3.1 Method P1 – Preventive maintenance	20
2.3.2 Method P2 – Neutral Current Supervision	21
2.3.3 Method P3 – Impedance Supervision Using V_N and I_N	22
2.3.4 Method P4 – Impedance Supervision Using V_0 and I_N	24
2.3.5 Method P5 – Impedance Supervision Using V_{RPD} and I_N	25
2.3.6 Method P6 – Impedance Supervision Using V_{TVS} and I_N	27
2.4 Existing Monitoring Methods – Active Category	30
2.4.1 Method A1 – Injected Neutral Current Supervision	30

2.4.2	Method A2 – Impedance Supervision Using Injected DC Signal	32
2.4.3	Method A3 – Neutral Grounding System Time Constant Supervision based on Pulse Injection	34
2.5	Existing Monitoring Methods – Passive-Active Category	34
2.6	Comparison of Existing Monitoring Methods	36
2.7	Summary	37
3	Modeling and Behavior Analysis of Two Existing Monitoring Methods	39
3.1	Method P6 - NGR Monitoring Using Sensing Resistor and Neutral CT	40
3.1.1	Monitoring Algorithm	40
	Decision Making Flowchart	41
	Dead Zones of The Algorithm	43
3.1.2	Performance Analysis	44
	Configuration 1 — High Resistance Grounded Generator	45
	Configuration 2 - High Resistance Grounded DYg Transformer	54
	Configuration 3 - High Resistance Grounded YD Transformer	55
3.2	Method P5 - NGR Monitoring Using Resistive Potential Divider (RPD) and Neutral CT	62
3.2.1	Monitoring Algorithm	63
	Decision-Making Flowchart	63
	Dead Zones of The Algorithm	66
3.2.2	Performance Analysis	68
	Configuration 1 — High Resistance Grounded Generator	68
	Configuration 2 — High Resistance Grounded DYg Transformer	79
	Configuration 3 — High-resistance-grounded YD transformer	80
3.3	Summary	81
4	An Improved NGR and NGL Monitoring Method With Hardware Validation	83
4.1	Proposed Monitoring Method	84
4.1.1	Monitoring Scheme	84
4.1.2	Neutral Voltage Measurement	85
4.2	Modeling and Behavior Analysis of The Proposed Voltage Metering Method	89
4.2.1	Software Verification	89
4.2.2	Hardware Validation	92

4.3	Performance of The Monitoring Scheme	93
4.4	Summary	105
5	A Passive NGR Monitoring Method for Unit-Connected Generators	106
5.1	Fundamentals and Concepts	106
5.2	Proposed Monitoring Technique and Challenges	108
5.2.1	NGR Monitoring Logics	108
5.2.2	Monitoring Challenges	111
	Load Variation	111
	Step-up Transformer Bank Saturation	112
	Ground Faults	113
5.2.3	Monitoring Algorithm	113
5.3	Validation	116
5.3.1	Study System Specifications and Modeling	116
5.3.2	NGR Failure Detection In Unfaulted Condition	117
5.3.3	Distinguishing Ground Faults from NGR Failure	127
5.3.4	Load Variation and Step-up Transformer Saturation	130
5.4	Discussion	131
5.5	Summary	132
6	NGR and NGL Monitoring based on Sub-Harmonic Signal Injection	134
6.1	Configuration 1 — High Resistance Grounding	135
6.1.1	Proposed Monitoring Method	136
6.1.2	Simulation Verification	137
6.2	Configuration 2 — Resonant Grounding	143
6.2.1	Proposed Monitoring Method	144
6.2.2	Simulation Verification	145
6.3	Summary	149
7	Summary, Conclusions, and Future Works	150
7.1	Summary	150
7.2	Contributions and Conclusions	152
7.3	Future Works	153
	Bibliography	155

Appendix A Simulation Settings	161
Appendix B Sensing Resistor Modeling and Verification	162
B.1 Implementation of Zener Diode In PSCAD	163
B.2 Implementation of A Single Cell TVS DIODE (Thyrector diode)	172
B.3 Implementation of TVS in PSCAD	180
Appendix C Additional Results for Chapter 4	182
Appendix D Additional Results for Chapter 5	193
Appendix E Additional Results For Chapter 6	204
Curriculum Vitae	213

List of Figures

2.1	High resistance grounded generator	14
2.2	A typical NGR	16
2.3	Thermal failure of NGR	17
2.4	Overvoltage due to undesired effect of NGR inductance	17
2.5	Melted neutral point junction	17
2.6	Connection diagram of the monitoirng method P1	21
2.7	Connection diagram of the monitoirng method P3	23
2.8	Monitoring algorithm of method P3	24
2.9	Connection diagram of the monitoirng method P4	25
2.10	Connection diagram of the monitoirng method P5	26
2.11	Monitoring algorithm of method P5	27
2.12	Connection diagram of the monitoirng method P6	28
2.13	I-V characteristic of a sample TVS diode	28
2.14	Monitoring algorithm of method P6	29
2.15	Injected current supervision based NGR monitoring	31
2.16	Connection diagram of the monitoring method A2	33
2.17	Connection diagram of the monitoring method P6A2	35
2.18	Evolution of the existing NGR monitoring methods	36
3.1	Decision making flowchart of the monitoring method P6.	41
3.2	The dead zones of the monitoring algorithm	43
3.3	High-resistance-grounded generator	46
3.4	Sequential network of the configuration 1 for LG fault	52
3.5	Behavior analysis using the dead zones of the algorithm.	53
3.6	High resistance grounded DYg distribution transformer	54
3.7	High resistance grounded wye-delta distribution transformer	56
3.8	The zig-zag connection modeled in PSCAD	57
3.9	Sequential network of the configuration 3 for LG fault	58

3.10	Decision making flowchart of the monitoring method P5.	64
3.11	The dead zones characteristic of the method P5	67
3.12	High-resistance-grounded generator	68
3.13	Monitoring algorithm operation representation based on dead zones characteristic for scenarios 11-14	76
3.14	Monitoring algorithm operation representation based on dead zones characteristic for scenarios 15-20	77
3.15	Monitoring algorithm operation representation based on dead zones characteristic for scenarios 21-24.	78
3.16	High-resistance-grounded DYg distribution transformer.	79
3.17	High resistance grounded YD distribution transformer.	81
4.1	Neutral voltage metering techniques. a) Resistive Potential Divider (RPD), b) Sensing Resistor (SR), and c) Advanced Sensing Resistor (ASR). . . .	85
4.2	I-V characteristics of voltage metering mechanisms.	87
4.3	Characteristic and operation of the proposed technique.	88
4.4	Breaking voltage extraction and neutral voltage recovery.	89
4.5	Neutral voltage measurement: a) Devised measurement circuit, and b) Temperature impact on breaking voltage and its extraction.	90
4.6	A sample neutral voltage recovery.	91
4.7	Measurement error of the proposed voltage metering technique compared to the other methods, considering 12-bit resolution.	91
4.8	Hardware test setup.	92
4.9	Experimental results (150 V across the prototype).	93
4.10	Study power system equipped with high or low resistance grounding apparatuses, and the proposed voltage metering mechanism.	94
4.11	Failed-short LNGR during unfaulted condition	96
4.12	Failed-open LNGR during unfaulted condition. a) Neutral voltage, b) Neutral current, c) NGR resistance, d) Measurement error of NGR resistance, e) NGR failure detection by SR-based monitoring method, f) NGR failure detection by RPD-based monitoring method, and g) NGR failure detection by proposed monitoring method.	97

4.13	Failed-short LNGR during single-line-to-ground fault at terminals of the transformer. a) Neutral voltage, b) Neutral current, c) NGR resistance, d) Measurement error of NGR resistance, e) NGR failure detection by SR-based monitoring method, f) NGR failure detection by RPD-based monitoring method, and g) NGR failure detection by proposed monitoring method.	98
4.14	Failed-open LNGR during single-line-to-ground fault at terminals of the transformer. a) Neutral voltage, b) Neutral current, c) NGR resistance, d) Measurement error of NGR resistance, e) NGR failure detection by SR-based monitoring method, f) NGR failure detection by RPD-based monitoring method, and g) NGR failure detection by proposed monitoring method.	99
4.15	Failed-short HNGL during unfaulted condition. a) Neutral voltage, b) Neutral current, c) NGL reactance, d) Measurement error of NGL reactance, e) NGL failure detection by SR-based monitoring method, f) NGL failure detection by RPD-based monitoring method, and g) NGL failure detection by proposed monitoring method.	100
4.16	Failed-open HNGL during unfaulted condition. a) Neutral voltage, b) Neutral current, c) NGL reactance, d) Measurement error of NGL reactance, e) NGL failure detection by SR-based monitoring method, f) NGL failure detection by RPD-based monitoring method, and g) NGL failure detection by proposed monitoring method.	101
4.17	Failed-short HNGL during single-line-to-ground fault at terminals of the transformer. a) Neutral voltage, b) Neutral current, c) NGL reactance, d) Measurement error of NGL reactance, e) NGL failure detection by SR-based monitoring method, f) NGL failure detection by RPD-based monitoring method, and g) NGL failure detection by proposed monitoring method.	102
4.18	Failed-open HNGL during single-line-to-ground fault at terminals of the transformer. a) Neutral voltage, b) Neutral current, c) NGL reactance, d) Measurement error of NGL reactance, e) NGL failure detection by SR-based monitoring method, f) NGL failure detection by RPD-based monitoring method, and g) NGL failure detection by proposed monitoring method.	103

5.1	High-resistance-grounded unit-connected generator.	107
5.2	Simplified third harmonic model of the system.	107
5.3	Comprehensive algorithm for monitoring the NGR at neutral of the unit-connected generator restrained against ground faults, load and temperature variation, and step-up transformer saturation.	114
5.4	Rate of change of magnitude of the third harmonic of neutral and residual normalized voltage phasors in respect to NGR resistance (absolute values).	117
5.5	Failed-short NGR case (scenario number B5, $r = 1 \rightarrow 0.05$ pu, $Load = 0.94 + j0.2$ pu, and $e3 = 0.5\%$)	119
5.6	Failed-short NGR case ($r = 1 \rightarrow 0.6$ pu, $Load = 0.94 + j0.2$ pu, and $e3 = 0.5\%$): (a) Residual voltage, (b) Neutral voltage, (c) Normalized neutral and residual third harmonic voltages, (d) Rate of change of the normalized third harmonic voltages, (e) NGR resistance, (f) Ground fault detection, (g) NGR failure detection, and (h) NGRS State.	120
5.7	Failed-open NGR case (scenario G5, $r = 1 \rightarrow 2$ pu, $Load = 0.94 + j0.2$ pu, and $e3 = 0.5\%$): (a) Residual voltage, (b) Neutral voltage, (c) Normalized neutral and residual third harmonic voltages, (d) Rate of change of the normalized third harmonic voltages, (e) NGR resistance, (f) Ground fault detection, (g) NGR failure detection, and (h) NGRS State.	121
5.8	Failed-open NGR case (scenario H5, $r = 1 \rightarrow 5$ pu, $Load = 0.94 + j0.2$ pu, and $e3 = 0.5\%$): (a) Residual voltage, (b) Neutral voltage, (c) Normalized neutral and residual third harmonic voltages, (d) Rate of change of the normalized third harmonic voltages, (e) NGR resistance, (f) Ground fault detection, (g) NGR failure detection, and (h) NGRS State.	122
5.9	Hardware test setup.	123
5.10	Schematics of the hardware test setup.	124
5.11	Relay detections for LG fault at 5% of the generator stator winding.	125
5.12	Relay detections for failed-short NGR in unfaulted condition.	126
5.13	Ground fault case followed by NGR failure ($r=1 \rightarrow 0.5$ pu, $Load = 1.0 + j0.0$ pu, and $e3 = 0.5\%$)	128

5.14	Single-phase-to-ground fault at terminal of the generator for intact NGR condition, $E3 = 1\%$, and $e3 = 0.5\%$: (a) Neutral and residual voltages, (b) Neutral current (c) Normalized neutral and residual third harmonic voltages, (d) Rate of change of the normalized third harmonic voltages, (e) NGR resistance, (f) Ground fault detection, and (g) NGR failure detection.	129
5.15	Load variation $(1.0 + j0.0) \rightarrow (0.6 + j0.35)$ pu, and step-up transformer saturation ($e3 = 0 \rightarrow 0.5\%$) case for intact NGR: (a) Neutral and residual voltages, (b) Neutral current (c) Normalized neutral and residual third harmonic voltages, (d) Rate of change of the normalized third harmonic voltages, (e) NGR resistance, (f) Ground fault detection, and (g) NGR failure detection.	131
6.1	Connection diagram of the high resistance grounded unit-connected generator equipped with sub-harmonic signal injection based generator stator ground protection.	135
6.2	NGR monitoring logic and ground fault detection scheme.	137
6.3	Case–1: Failed-short NGR in unfaulted condition	139
6.4	Case–2: Failed-open NGR in unfaulted condition: a) Neutral voltage, b) Neutral current, c) Injected 20 Hz current, d) Generator stator winding insulation resistance, e) NGR resistance, f) Ground Fault (GF), g) Resistor Failure (RF), and h) Resistor Status (RS).	140
6.5	Case–3: Failed-short NGR during an internal single-line-to-ground fault: a) Neutral voltage, b) Neutral current, c) Injected 20 Hz current, d) Generator stator winding insulation resistance, e) NGR resistance, f) Ground Fault (GF), g) Resistor Failure (RF), and h) Resistor Status (RS).	141
6.6	Case–4: Failed-open NGR during an internal single-line-to-ground fault: a) Neutral voltage, b) Neutral current, c) Injected 20 Hz current, d) Generator stator winding insulation resistance, e) NGR resistance, f) Ground Fault (GF), g) Resistor Failure (RF), and h) Resistor Status (RS).	142
6.7	Connection diagram of the resonant grounded unit-connected generator equipped with 20 Hz signal injection based generator stator winding ground protection.	143
6.8	NGL monitoring logic and ground fault detection scheme.	144
6.9	Case–5: Failed-short HNGL in unfaulted condition	145

6.10	Case–6: Failed-open HNGL in unfaulted condition: a) Neutral voltage, b) Neutral current, c) Injected 20 Hz current, d) Generator stator winding insulation resistance, e) HNGL reactance, f) Ground fault, g) Reactor Failure (RF), and h) Reactor Status (RS).	146
6.11	Case–7: Failed-short HNGL during an internal single-line-to-ground fault: a) Neutral voltage, b) Neutral current, c) Injected 20 Hz current, d) Generator stator winding insulation resistance, e) HNGL reactance, f) Ground fault, g) Reactor Failure (RF), and h) Reactor Status (RS).	147
6.12	Case–8: Failed-open HNGL during an internal single-line-to-ground fault: a) Neutral voltage, b) Neutral current, c) Injected 20 Hz current, d) Generator stator winding insulation resistance, e) HNGL reactance, f) Ground fault, g) Reactor Failure (RF), and h) Reactor Status (RS).	148
B.1	PSCAD statement-based model of diode.	164
B.2	Zener diode SPICE macro-model	164
B.3	Zener diode I-V characteristic	165
B.4	Zener diode simplified macro-model	165
B.5	I-V characteristic of an avalanche Zener diode	166
B.6	Macro-model of the Zener diode simulated in PSCAD.	167
B.7	PSCAD simulation result for $8 \times 20 \mu\text{s}$ current waveform scenario.	167
B.8	SPICE simulation result of $8 \times 20 \mu\text{s}$ waveform scenario	168
B.9	Bench test measurement result of $8 \text{ A} \times 20 \mu\text{s}$ scenario	168
B.10	PSCAD simulation result for $8 \times 20 \mu\text{s}$ scenario.	169
B.11	$1 \times 1000 \mu\text{s}$ current waveform scenario	169
B.12	PSCAD results for $1 \text{ A} \times 1000 \mu\text{s}$ current waveform scenario when $R_z = 1.28 \Omega$.	170
B.13	PSCAD results for $1 \text{ A} \times 1000 \mu\text{s}$ current waveform scenario when $R_z = 8 \Omega$.	170
B.14	PSCAD results for $1 \times 1000 \mu\text{s}$ current waveform bench test when $R_z = 8 \Omega$.	171
B.15	I-V characteristic of the PSCAD based Zener diode.	171
B.16	Symbolical representation of Thyrector diode.	172
B.17	Voltage clamping by TVS	172
B.18	Thyrector diode macro-model	173
B.19	Test circuit for performance investigation of the Thyrector diode	173
B.20	AC dynamic resistance of the TVS diode versus HPM pulse power at different operating frequencies	174
B.21	I-V characteristic of the Thyrector diode at different operating frequencies	174

B.22	PSCAD test circuit for analysis of the Thyrector diode.	175
B.23	HPM current profile for DC pulse test.	176
B.24	PSCAD model of the Thyrector diode.	177
B.25	I-V characteristic of the Thyrector diode in PSCAD.	178
B.26	R_{DYN} versus the power of the HPM DC pulse characteristic of the Thyrector diode in PSCAD.	179
B.27	The TVS simulated test circuit in PSCAD.	180
B.28	TVS operation during normal and faulted conditions.	181
B.29	TVS operation clamping sensed voltage during transition from normal to faulted conditions.	181
C.1	Failed-short HNGR ($288\ \Omega \rightarrow 144\ \Omega$) during unfaulted condition	183
C.2	Failed-open HNGR ($288\ \Omega \rightarrow 576\ \Omega$) during unfaulted condition	184
C.3	Failed-open HNGR ($288\ \Omega \rightarrow 1440\ \Omega$) during unfaulted condition	185
C.4	Failed-short HNGR ($288\ \Omega \rightarrow 144\ \Omega$) during LG fault	186
C.5	Failed-open HNGR ($288\ \Omega \rightarrow 576\ \Omega$) during LG fault	187
C.6	Failed-open HNGR ($288\ \Omega \rightarrow 1440\ \Omega$) during LG fault	188
C.7	Failed-open LNGR ($50\ \Omega \rightarrow 250\ \Omega$) in unfault condition	189
C.8	Failed-open LNGR ($50\ \Omega \rightarrow 250\ \Omega$) during LG fault condition	190
C.9	Failed-open HNGL ($784\ \Omega \rightarrow 4\ \text{k}\Omega$) in unfault condition	191
C.10	Failed-open HNGL ($784\ \Omega \rightarrow 4\ \text{k}\Omega$) during LG fault condition	192
D.1	Failed-short NGR case (scenario number B6, $r = 1 \rightarrow 0.5 \rightarrow 0.05$ pu, Load= $0.94+j0.2$ pu, and $e3 = 1\%$)	194
D.2	Failed-short NGR case (scenario number B8, $r = 1 \rightarrow 0.5 \rightarrow 0.05$ pu, Load= $0.85+j0.4$ pu, and $e3 = 0.5\%$)	195
D.3	Failed-short NGR case (scenario number B5 with catastrophic dynamic, $r = 1 \rightarrow 0.5 \rightarrow 0.05$ pu, Load = $0.94 + j0.2$ pu, and $e3 = 0.5\%$)	196
D.4	Failed-open NGR case (scenario number G6, $r = 1 \rightarrow 2$ pu, Load= $0.94+j0.2$ pu, and $e3 = 1\%$)	197
D.5	Failed-open NGR case (scenario number G8, $r = 1 \rightarrow 2$ pu, Load= $0.85+j0.4$ pu, and $e3 = 0.5\%$)	198
D.6	Failed-open NGR case (scenario number G5 with catastrophic dynamic, $r = 1 \rightarrow 5$ pu, Load = $0.94 + j0.2$ pu, and $e3 = 0.5\%$)	199
D.7	External double-line-to-ground fault at generator terminals	200

D.8	External line-to-line and three-phase fault at generator terminals	201
D.9	External three-phase-to-ground fault at generator terminals	202
D.10	External line-to-ground fault in 345 kV system	203
E.1	Failed-short NGR in de-energized condition	205
E.2	Failed-open NGR in de-energized condition	206
E.3	Failed-open NGR during LG fault at 12.47 kV busbar	207
E.4	Failed-open NGR during LG fault in 345 kV system	208
E.5	Failed-short NGL in de-energized condition	209
E.6	Failed-open NGL in de-energized condition	210
E.7	Failed-open NGL during LG fault at 12.47 kV busbar	211
E.8	Failed-open NGL during LG fault in 345 kV system	212

List of Tables

2.1	Comparison of the existing NGR monitoring methods	37
3.1	Case 1 –Monitoring a healthy NGR during various system faults.	46
3.2	Case 2 –Monitoring various NGR degradations in a healthy system. . . .	48
3.3	Case 3 –Monitoring various NGR degradations during a solid LG fault. .	49
3.4	Case 4 –Monitoring a failed-short NGR during various system faults. . .	50
3.5	Case 5 –Monitoring a failed-open NGR during various system faults. . . .	51
3.6	Case 1 – Monitoring a healthy NGR during various system faults.	59
3.7	Case 2 – Monitoring the failed NGR during unfaulted condition.	60
3.8	Case 3 – Monitoring the failed NGR during a LG fault at 12.47kV busbar.	61
3.9	Case 4 – Monitoring a failed-short NGR during various system faults. . .	61
3.10	Case 5 –Monitoring a failed-open NGR during various system faults. . . .	62
3.11	Case 1 - Monitoring a healthy NGR during various system faults.	69
3.12	Case 2 - Monitoring various NGR degradations in a healthy system. . . .	71
3.13	Case 3 - Monitoring various NGR degradations during a LG fault.	73
3.14	Case 4 - Monitoring a shorted NGR during the ground faults.	74
3.15	Case 5 - Monitoring a failed-open NGR during various system faults. . .	75
4.1	NGD status detection: Normal (NM), Failed-short (SH), or Failed-open (OP)	104
5.1	Power system specifications.	116
5.2	NGR failure detection in unfaulted condition. (NGR Status: NM=Normal, SH=Failed-Short, and OP=Failed-Open).	118
B.1	Electrical specifications of the Zener diode	166
B.2	Default specifications of the SPICE diode	166

Nomenclature

NGD	Neutral Grounding Device
NGR	Neutral Grounding Resistor
LNGR	Low resistance Neutral Grounding Resistor
HNGR	High resistance Neutral Grounding Resistor
NGRF	Neutral Grounding Resistor Failure
NGRS	Neutral Grounding Resistor Status
NGL	Neutral Grounding Inductor
LNGL	Low reactance Neutral Grounding Inductor
HNGL	High reactance Neutral Grounding Inductor
NGLF	Neutral Grounding Inductor Failure
NGLS	Neutral Grounding Inductor Status
SR	Sensing Resistor
RPD	Resistive Potential Divider
PM	Proposed Method
TVS	Transient Voltage Suppressor
GF	Ground Fault

Chapter 1

Introduction

1.1 Neutral Grounding Devices

Power system components are designed to be three-phase balanced and symmetric with the internal connection of wye/star or delta. The common node of the wye-connected equipment such as generators and transformers is known as neutral point. In conventional and traditional power networks, this node is left floating known as ungrounded neutral, or directly connected/wired to earthing point known as solidly grounded neutral [1].

Modern power networks maintain a safe electrical connection between the neutral and earthing nodes to solve many of issues and challenges associated with ungrounded and solidly grounded networks. A few of the most prominent advantages of this practice are to ride through the first ground fault and avoid operation interruption, control the transient overvoltages, limit the ground fault current, overcome electromechanical and electrostatic stresses, avoid the risk of arc flash hazards to personnel associated with high ground-fault current, etc. The requirements of neutral grounding, also known as neutral earthing, are fulfilled by means of Neutral Grounding Devices (NGD) [2, 3].

Due to variety of neutral grounding methods, different types of the NGDs exist. First, resistance grounding connects the neutral and earthing nodes to each other via a resistor that is known as Neutral Grounding Resistor (NGR). This resistor comes with various resistances for different strategies such as low, medium and high resistance grounding. Second, effective grounding employs a very small inductor to limit the single-line-to-ground fault current to the same level as the three-phase-to-ground fault current. Third,

resonant grounding uses a very small inductor behind a single phase Neutral Grounding Transformer (NGT) to limit the neutral current to a few amperes during the ground faults [4, 5, 6, 7, 8].

1.2 Problem Definition

Properly designed neutral grounding systems eliminate many of the issues and challenges associated with solidly grounded and ungrounded traditional systems while maintaining their advantages [9]. Failure of NGDs is a well-reported issue in industrial and commercial power networks that can happen due to natural incidents such as welding breakage [10], lightning, storm, earthquakes, extended service life, corrosive atmosphere, extreme temperature variations, and hail. The other causes are third harmonic currents, manufacturing defects, and vibration [11].

Another possible mechanism of NGR failure has been discussed in [12]. The authors show that how an NGR fails due to local high frequency transients involving the inherent inductance of the resistor and the transformer terminal-to-ground-point coupling capacitance.

Coal mining industry has widely reported the NGRs failure. This industry experiences change in resistance of the NGRs which is a serious problem in safety and protection aspect of view. Many events have been reported by this industry that a failed NGR has been identified as the main reason. A few reported events are: 1) a victim at an underground coal mine in Virginia on November 11, 1991, 2) soft starter failure due to open NGR, and 3) nine loose connections in Eastern Canada on a 200 A, 4160 V NGR [9].

Any kind of degradation of NGDs causes the risk of the ungrounded or solidly grounded neutral and the consequent issues [9]. Depending on the failure mode, i.e., failed-open or failed-short, this can disable ground protection system, cause significant damage to the power system equipment during ground faults, risk the safety of site personnel, etc. As such, most of the utilities perform periodical investigations to detect such a failure. However, planned-maintenances or periodical inspections/tests guarantee the intactness of these apparatuses only during the investigation as the failed-short and

failed-open NGRs have been detected right after preventive maintenances reported by [11].

Indeed, without continuous monitoring of NGDs, there is no indication that they have failed. Therefore, relaying industry needs a reliable solution for detecting the failed NGDs installed at neutral system of generators and distribution transformers. In fact, the NGDs must be continuously monitored to avoid false sense of security, as recommended in article 250 of National Electrical Code (NEC) 2005 [13], and Sections 1-6 and 10-1102.3 of Canadian Electrical Code (CEC) 2011 [14].

Accordingly, as the initial goal of this research work, the existing methods and techniques for monitoring NGDs will be reviewed to understand their behavior and performance. These methods are known to have shortcomings and issues that motivate this research work to search for better alternatives. Thereby, main goal is to devise new or enhanced methods for monitoring the NGDs that can be easily adopted/retrofitted to multi-functional digital protective relays or available protection platforms. Although this criteria limits the work to rely on available infrastructures and installations; however, it makes the outcomes of the research to be economical, cost-effective and money-saving solutions. In other words, it motivates the work to employ the existing installations of monitoring, control, and protection systems which are already in use in power networks to not only reduce the cost of the proposed monitoring mechanisms but also to boost the value of the previous investments.

1.3 Literature Survey

The continuity of service and intactness of the NGRs has been an unavoidable concern to many industries for decades worldwide, especially in Canada. It can be said that Canada is the frontier in the field of continuous NGR monitoring due to industries that are well-known in the area of NGR monitoring.

On the basis of the performed literature survey for existing NGD monitoring techniques, ten methods have been explored that are explained briefly in this section. It should be mentioned that almost all of the existing explorable monitoring techniques

focus on only the resistive type of the NGDs, i.e., the NGR. These methods are classified into three different categories based on their principles and concepts. The first category is called passive methods. The main reason behind such naming is that these methods do not change the operation characteristic of the power network and rely on existing electrical parameters of the neutral system, i.e., neutral voltage and current. These methods claim that although the neutral system is theoretically supposed to not experience any electrical energy flow, however, it always conducts a very negligible current (in the order of milliamperes) due to inherent asymmetry or imbalance of the three-phase components of the power system such as the transformers, generators, transmission lines, loads, and system charging capacitances. Six methods are classified under the passive category. On the other hand, the second category is called active methods since they inject signals to neutral system. People who have proposed these methods believe that the neutral voltage and current are not sufficient to be accurately and safely measured; hence, some means of signal injection should be used to solve this issue. Three methods are classified under this category. The third category is called passive-active since it uses both passive and active concepts. In fact, the passive concept is used when the neutral voltage and current are high enough to be accurately measured to provide a reliable monitoring. Furthermore, the active concept is used when the neutral voltage and current are very low or absent.

The first passive method has a very long history that goes back to even the first days of appearance of the power systems which is nothing but the periodical or planned inspections, tests, maintenances or investigations. The [11] mentions this method with minimum degree of satisfaction since it guarantees the integrity of the assets only during the investigation and not after that. It means that the inspected equipment could fail even right after the test [15]. Therefore, this method is not a continuous monitor and not of interest.

The second passive technique measures and employs the negligible current in neutral wire, which flows through the NGR itself, to detect the NGR failure by supervising the level of this current. In fact, two level thresholds are used to detect whether the current is absent or abnormally very high. This method, referred to as neutral current supervision

logic, is mostly known as ground overcurrent protection since it only functions during the ground faults, and besides, it cannot detect partial failure of the NGR [9, 11].

The third passive method employs the neutral current and voltage to monitor the NGR using neutral current supervision and NGR impedance supervision. The neutral current supervision is employed during the normal operation condition of the power system where both neutral current and voltage are less than 0.1 pu. As mentioned earlier, this logic cannot detect the partially failed NGR condition. However, the impedance supervision logic that is employed during the faulted condition of the power system detects all kinds of NGR degradation. It should be noted that although this technique guarantees an acceptable monitoring during the ground faults, however, it is not that much interested since NGR failure detection is required and necessary before the incidence of the ground faults to guarantee a safe operation during the ground faults [9, 11].

The fourth passive method benefits from the same monitoring principles and concepts as the previous method. The only difference is the neutral voltage measurement instrument. This technique uses the residual voltage instead of neutral voltage since the applicable configurations do not have the neutral PT. It uses the neutral current supervision logic only when both neutral voltage and current become less than 0.01 pu. Otherwise, the impedance supervision logic functions which is highly reliable [16, 17]. As such, this method provides a better monitoring than the previous method.

The fifth passive method uses the same principles as the previous methods with better performance. The neutral voltage is measured by Resistive Potential Divider (RPD) which can cover wider range of neutral voltage. However, the very weak voltages appearing across neutral system cannot be measured by this technique unless if very high sampling resolutions are employed. The impedance measurement functions when both neutral voltage and current are higher than 0.1%, which is the minimum accuracy limit of the RPD. Otherwise, the neutral current supervision logic operates to detect the failed-open or disconnected NGR condition. This method has been applied to distribution systems up to 1000 V [18]. In fact, in order to employ this technique in MV systems, the monitoring relays requires high sampling resolution to measure the very low voltage of the neutral point.

The sixth and last passive method employs both the neutral current supervision and NGR impedance supervision as well, but in a different way. It uses a sensitive CT to measure the neutral current, and a sensing resistor for metering neutral voltage. The sensing resistor provides error-less measurement of the neutral voltage in unfaulted condition where the neutral voltage is low, and invalid voltage measurement in faulted condition. As a result, this new mechanism does not provide neutral voltage metering during the ground faults. As such, this monitoring method employs the impedance supervision during the unfaulted condition, and the neutral current supervision during the faulted condition. As explained earlier, since the impedance supervision logic detects partial failure of the NGR, this monitoring method functions very strong in unfaulted condition. However, since the neutral current supervision logic cannot detect partial failures of the NGR, the performance of this monitoring technique is very limited during the ground faults [19, 20, 21, 22]. Additionally, since reliable monitoring in unfaulted condition is more of interest, this method is very practical.

As mentioned, the passive methods rely on existing electrical parameters of the neutral system. As such, if these parameters disappear for any reason such as de-energization or power outage, the passive methods will become non-functional.

The seventh method is classified under active methods. It is basically the enhanced version of the second passive method. In this technique, the neutral current is assumed not sufficient to be accurately measured. Therefore, a current signal is injected between the neutral and ground nodes. This current must move back and forth only through the grounding path. Therefore, the application of this monitoring method is limited to specific configurations. Moreover, the presence or absence of the injected current is the only criteria to detect the failed NGR resulting in an imperfect monitor [23, 24]. As a result, this method is suitable for monitoring the continuity and connectivity of the grounding path but not for NGR monitoring.

The eighth monitoring method is classified under active category too. In this technique, a DC voltage or current signal is injected to neutral node to guarantee the existence of the neutral voltage and current. The DC voltage and current of the NGR are then measured, and the calculated impedance of the NGR is used to monitor its status. Neutral

current supervision is also used to detect the failed-short or failed-open NGR [10, 25, 26].

In the third and last active monitoring method, an AC pulse is injected to grounding system, and the time constant (RC) of the grounding path is supervised. The injected pulse to grounding network is damped due to resistance of the grounding path. Hence, the damping inertia known as time-constant is a very beneficial criteria for detecting variations of the grounding path resistance. If the time constant becomes greater than a predefined value, the disconnected grounding path is reported. Although this technique has been designed to monitor the connectivity of the grounding path; however, it can be set to continuously monitor the NGR as well [27]. This technique is applicable to very low voltage distribution systems since the injection device is not well-protected against the transients that happen in medium voltage power networks.

The active methods need means of signal injection and coupling filters to protect the injection installations against the faulted condition. As a result, this technique causes more costs compared to passive methods specially when its decoupling during the ground faults is considered. In fact, this technique cannot function during the ground faults since the protection or decoupling filters isolate the monitoring system from the neutral. Furthermore, the injected current shall circulate through the NGR, and shall not penetrate to the network. Therefore, its application is limited to wye connected transformers that supply the ungrounded networks or delta connected loads that can be found in coal mining distribution systems. The other application is the unit-connected generators. Therefore, the active methods cause more expense with limited performance. The other issue facing this technique is the DC stray influence, and continuity through probable ground faults [9]. Furthermore, the integrity and continuity of the injection circuit itself should be monitored which adds to the complexity of the active monitoring methods. However, the active methods are well-known due to their functionality in de-energized operation condition.

Understanding that 1) the active methods function reliably when the neutral voltage and current are very low or absent, and 2) the passive methods operate strongly when the neutral voltage and current are high enough to be accurately measured, the power system engineers came across the most reliable solution by combining the active and

passive methods resulted in active-passive methods [28, 29, 30]. These method mostly rely on NGR impedance supervision due to availability of neutral current and voltage over their full range. However, when these parameters fade completely, still the injection remains in the picture to check the disconnected grounding path.

1.4 Challenges

Three-phase power system networks are highly symmetric and balanced. As such, the neutral node is dead during the normal operation condition of the power system which means that the neutral system does not experience any energy under this situation. Theoretically, his fact results in zero or very weak voltage and current in neutral system. On the other hand, if any kind of system faults or failures occurs, the same dead neutral will experience thousands of amperes and volts depending on the application. As may be realized, unlike the line voltage and current that always remain very close to the rating level, the neutral system including the NGD experiences wide range of voltage and current from just a few volts or amperes during the unfaulted condition to thousands of volts or amperes during the faulted condition. Here, the accuracy limits of the conventional metering instruments come to the picture. Most of the existing measurement instruments cannot guarantee metering both extremely low and very high voltages and currents. They provide an acceptable performance for only the very high or very low levels of the electrical parameters. This fact is the major challenge of the existing NGR monitoring techniques. None of them have succeeded in proposing or providing a mechanism or technique that can overcome this challenge. As a result, the existing techniques cannot cover both the normal and faulted conditions.

1.5 Objectives and Motivations

The objectives and motivations of this research work are to propose new or enhanced NGR and NGL monitoring methods that fulfill the following principles required for a well-designed monitoring scheme:

- Proposed methods should detect the NGD failure during both normal and faulted operation conditions of the power system.
- Monitoring mechanism should rely on existing measurement instruments and protection/control installation in order to be cost-effective.
- Adoptable or retrofittable to existing protection or monitoring platforms which means avoiding very complex algorithms that pose high computation burden or risk of malfunctioning.
- Monitor the whole grounding path from neutral node to earthing point including grounding connections and wiring.
- Monitoring means should be properly decoupled from the high voltage neutral during the system faults.

1.6 Thesis Outlines

Second chapter reviews the fundamentals and concept of the neutral grounding methods, and existing NGD monitoring techniques. In this chapter, first the neutral grounding and various NGDs are introduced. A brief explanation of the structure of a sample NGD is included as well. Thereafter, the existing NGD monitoring techniques that are categorized into three different categories will be explained in detail.

In Chapter 3, the behavior of two existing monitoring methods will be thoroughly analyzed for various conditions of the NGDs and power system as well. The main goal of this chapter is to understand the behavior/performance, shortcomings, challenges, advantages and disadvantages of the existing techniques. This knowledge will later on help to devise and develop new or enhanced methods, and avoid intellectual property infringement.

In the fourth chapter, the first proposed method will be introduced. This technique is the cost-effective combination of two existing techniques which provides better performance than each of the originals. The combination methodology itself is novel. Hence,

first the combination technique will be explained and thoroughly analyzed. Thereafter, the performance of the monitoring technique itself will be studied under various conditions.

In Chapter 5, the second proposed technique will be introduced. This method monitors the high resistance NGR at neutral of unit-connected generators. It does not demand any new measurement instruments and uses the existing generator protection installations, i.e., third harmonic voltage comparator (59D).

Chapter 6 introduces the third technique which injects a sub-harmonic to the neutral and monitors the NGR or NGL based on its calculated impedance at the same injected frequency. The performance of the technique will be thoroughly studied as well.

The summary and conclusions will be presented in Chapter 7.

Lastly, five appendices are included that present the simulation settings, and additional simulation results.

Chapter 2

Literature Review: Existing Monitoring Methods

In this chapter, first various neutral grounding methods are reviewed followed by introducing different existing NGDs. Thereafter, the importance of monitoring the NGDs, and various existing industrial techniques upon this practice are explained in detail. Lastly, a thorough comparison of these methods will be presented considering the characteristics of the existing monitoring techniques such as measurements, applicable configurations, issues, challenges and shortcomings.

2.1 Neutral Impedance Grounding

In traditional power systems such as mining distribution networks, the neutral node was left floating or directly connected/wired to earthing point, known as ungrounded or solidly grounded neutral respectively. In fact, the neutral-to-ground impedance was either zero or infinite. Obviously, the zero impedance causes very high ground fault currents providing sensitive overcurrent protection and very low transient overvoltages. On the other hand, the infinite impedance between neutral and earthing points causes very high neutral voltage in case of ground faults guaranteeing a safe ground protection, but causing excessive transient overvoltages across neutral side of the equipment. Due to consequences of transient overvoltages and very high ground fault currents such as the risk

of arc flash hazard, and electromechanical stresses on equipment windings and structure, the impedance grounding emerged in late 70's. Impedance grounding means that a safe electrical connection between neutral and earthing nodes via electrical elements such as resistors, inductors, capacitors and/or any possible beneficial combination of these key assets. Moreover, various levels of neutral grounding impedances are used for different strategies. High impedance means less ground current but higher overvoltages since the higher impedance causes higher electrical distance from earth potential. On the other hand, low impedance means high ground currents and low transient overvoltage since the electrical distance to earthing point is low. Compromising between these two cases, the medium impedance neutral grounding, and hybrid grounding techniques emerge, which result in better performance controlling both the transient overvoltages and overcurrents. Therefore, various neutral grounding methods exist that are explained in the next section.

2.1.1 Neutral Grounding Methods

In this section, all existing techniques for neutral grounding are reviewed followed by their most prominent characteristics, advantages and disadvantages.

Ungrounded system means neutral node is intentionally left floating which means there is no direct connection between the neutral node and earthing point. However, the distributed system charging capacitors, and potential transformers cause other high impedance paths to the closest earthing point. This method is called capacitive grounding too [2]. As such, this method does not introduce any NGD whereas grounding impedance is very high and capacitive. During the normal operation condition of the power system, a very weak voltage is sensed across the neutral which appears due to inherent asymmetry of the power system components; however, very high transient overvoltages are experienced in the presence of ground faults. Indeed, the ungrounded systems are no longer interested since these transients can easily be controlled by means of neutral impedance grounding. However, the ungrounded systems do not sense the first single-phase-to-ground (LG) fault which helps the power network, especially the coal mining motor loads, to ride through the first ground fault, avoid operation interruption, and reduce the reconnection costs. Ungrounded neutral can be found in unit-connected generators, and common bus

generators without feeders as well [5]. The only available electrical parameter is the neutral voltage obtained by either neutral PT or line PTs.

Solid grounding means neutral node is directly wired/connected to earthing point without any intentionally inserted impedance introducing no NGD [2]. This method was traditionally used to avoid the risk of the very high transient overvoltages appearing during the restriking ground faults. However, solid grounding causes extremely high ground fault currents and mechanical damages [5], yet very beneficial in protection aspect [8]. This method is mostly used in transmission systems and the only available measurement is the neutral current [7].

Effective grounding means neutral node is connected to earth potential via a very small inductor directly inserted between neutral and earthing points which hereafter will be called Low reactance Neutral Grounding Inductor (LNGL). The main goal behind such a grounding scheme is to limit the LG fault current to the same level as the three-phase-to-ground fault current. In fact, the zero sequence impedance becomes less than the positive sequence impedance when using the solid grounding, which was traditionally solved by effective grounding [4]. This method is mostly used in generation and distribution levels of the power system [7, 8].

Low inductance grounding is achieved in the same manner as effective grounding, but using a reactor with higher reactance, hereafter called Medium reactance Neutral Grounding Inductor (MNGL). The ground fault current is still relatively high, and the risk of damage to iron-core caused by internal faults is noticeable. However, the transient overvoltages are well-controlled to 230% of the system voltage rating [5].

Low resistance grounding is when the neutral node is grounded using a Low resistance Neutral Grounding Resistor (LNGR) that is directly inserted between neutral and earthing nodes. This resistor controls the neutral current to 400-1200 A. Sensitive and selective ground overcurrent protection is well-achieved with this level of the ground current. This method guarantees the lowest transient overvoltages among all impedance grounding methods. That is why low resistance grounding is known as a satisfactory replacement of the effective grounding [7].

Medium resistance grounding means neutral is grounded using a medium resis-

tance Neutral Grounding Resistor (MNGR) that limits the neutral current to 200-400 A. This method is known as a variant of the low resistance grounding method that further limits the ground current to fulfill the requirements of selective ground protection [3].

High resistance grounding is accomplished using a high resistance Neutral Grounding Resistor (NGR). This NGR is obtained by a very small resistor, i.e., less than 1Ω , behind a single phase Neutral Grounding Transformer (NGT) with the turn ratio of 40-100. The resistor suppresses the LG fault current to 3.75-25 A to maintain the operation of the power network during the first ground fault. The primary terminals of the NGT are connected to neutral and earthing nodes. The other way to obtain this kind of grounding is to install the small resistor at secondary of grounded-wye-to-broken-delta line PTs, or terminal grounding transformers [31]. It should be noted that the high resistance grounding can be performed without the NGT as well, but it is not an economical alternative [3, 5]. Lastly, the available measurements with this method are the neutral current, and neutral or residual voltage. In general, the resulted NGD with this grounding method is either an NGR, NGR+NGT, or NGR+GT as shown in the following figures for a generator.

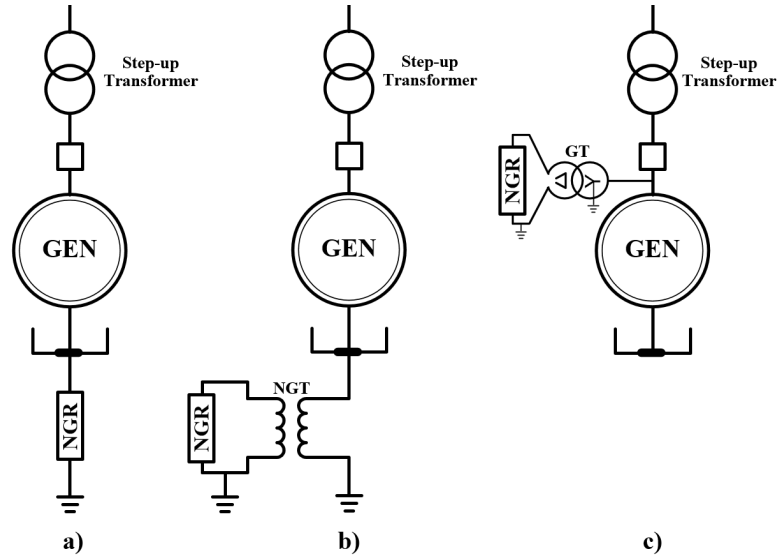


Figure 2.1: High resistance grounded generator. a) without NGT, b) with NGT, and c) with terminal grounded-wye-to-broken-delta grounding transformer [3, 5, 31].

Resonant grounding also known as tuned reactor or ground fault neutralizer means that the neutral is connected to earthing point via a very small inductor behind a NGT

in the same way as shown in Figure 2.1(b). The inductor is so designed that the seen reactance at primary of the NGT is equal to one-third of the system line-to-ground capacitance. This apparatus suppresses the LG fault current to 5 A to maintain the operation of the power network during the first ground fault. Hence, the resulted NGD is a reactor plus a NGT referred to as NGL+NGT or HNGL. The available measurements by this method are the neutral current and voltage. In fact, the NGT operates as a Potential Transformer.

Hybrid grounding is the combination of solid and high resistance grounding techniques. In this method, the solid grounding serves in the absence of the ground faults. Once the ground fault occurs, and ground current is sensed, the protection system switches from the solid grounding to high-resistance grounding. Through such a strategy, the solid grounding controls the transient overvoltages that appear right after the fault incidence. Moreover, it provides sufficient current for ground fault detection and instantaneous overcurrent protection. The high resistance grounding which comes to service after a few power frequency cycles suppresses the ground fault current to a few amperes to avoid the mechanical and thermal damages to the equipment. The resulted NGD is actually an NGR which shows zero resistance in unfaulted condition and high resistance in the presence of ground faults [3]. It should be noted that hybrid grounding can be achieved by combining any of the aforementioned grounding techniques, e.g., solid and resonant grounding methods.

2.1.2 Neutral Grounding Devices

On the basis of the introduced neutral grounding methods, following NGDs exist which are explained.

The **Neutral Grounding Resistor (NGR)** is used in low-resistance, medium-resistance, high-resistance, and hybrid neutral grounding methods. This apparatus is obtained by series and parallel combination of the small resistive elements that interconnectedly construct the desired rated resistor. These resistive elements are constructed with resistive wire or metal strips coiled and wrapped around porcelain insulators. A sample NGR is demonstrated below. The quality factor of this resistor (R/X) is usually

about 100 since it contains very negligible inductance as well [12].

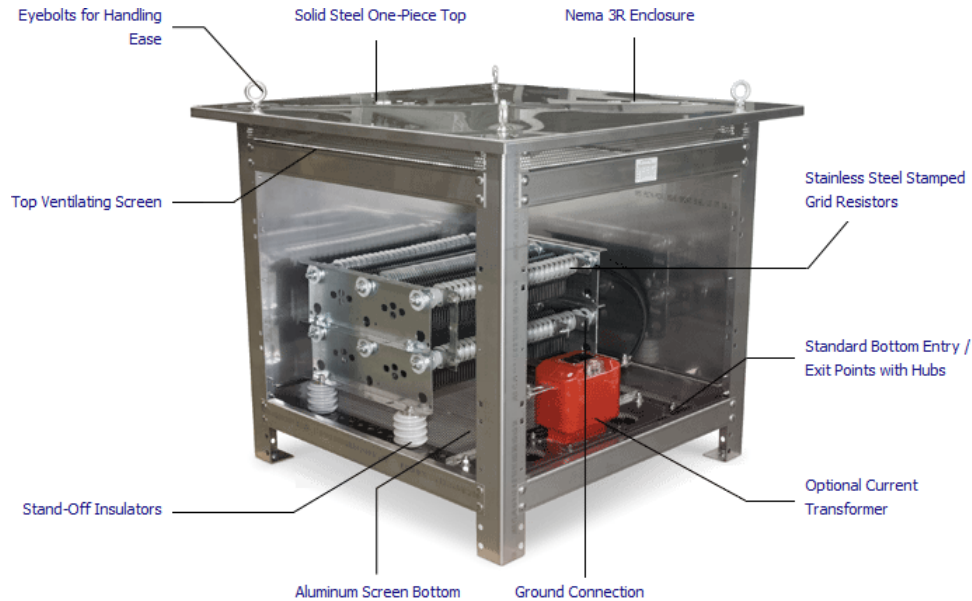


Figure 2.2: A typical NGR constructed with 6 series edge-wound resistive elements closed with a bar type current transformer [32].

The **Neutral Grounding Transformer (NGT)** is another apparatus that is used for neutral grounding. It can be found in high resistance and resonant grounding.

Lastly, the **Neutral Grounding Inductor (NGL)** is used in effective, low-reactance and resonant neutral grounding methods. Unlike the NGR, it is composed of one single coil reactors. The quality factor of this element (X/R) is about 20.

2.1.3 Failure of Neutral Grounding Devices

NGRs fail due to natural incidents such as lightning, storm, earthquakes, extended service life, corrosive atmosphere, extreme temperature variations, and hail. The other causes are third harmonic currents, manufacturing defects, and vibration [11, 17]. A sample failed NGR due to thermal issues is shown in Figure 2.3.

The [10] mentions that the history of NGR failure mostly contains the mechanical defection since it is highly interconnected with edge wound resistive inter-elements that are mechanically joint to two supporting steel frames. This resource relates the NGR failure to structure defections such as breakage of spot and fillet welding used for mechan-



Figure 2.3: Thermal failure of NGR [11].

ical assembly. The spot welding defect occurs due to wide range temperature variation and fault current thermal forces. The fillet welding breakage happens due to mechanical stress caused by fault currents, corrosion, and uneven thickness of the welding. Depending on the location of the defection, the NGR can be partially or completely failed-short or failed-open.

Furthermore, another work shows that NGR can be burnt because of overvoltage transients initiated by high-frequency (125 kHz) oscillations involving the inherent inductance of the NGR and system charging capacitances. This phenomenon is known as ferroresonance [12]. The waveform of the neutral voltage containing the 125 kHz oscillations, and resulted failed-open NGR are shown in Figures 2.4 and 2.5.

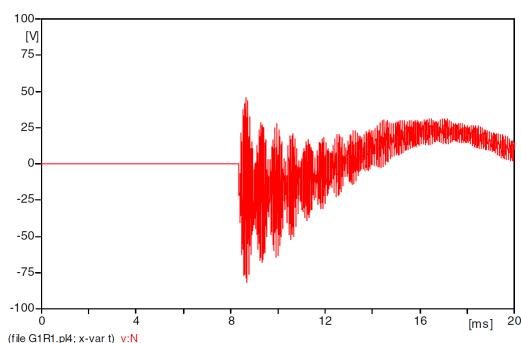


Figure 2.4: Overvoltage due to undesired effect of NGR inductance [12].

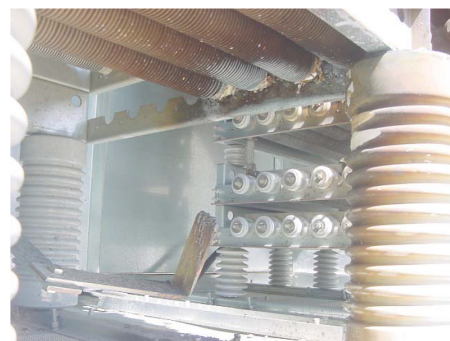


Figure 2.5: Melted neutral point junction [12].

Unlike the NGRs, the NGLs do not have lots of mechanical connections and are constructed using a single coil or winding. Hence, failure of these elements is not as popular as the NGRs.

2.2 Importance of Monitoring The Neutral-to-Ground Path

Properly designed neutral grounding systems eliminate many of the issues and challenges associated with solidly grounded and ungrounded traditional systems while maintaining the same advantages. Any kind of degradation of NGDs causes the risk of ungrounded or solidly grounded neutral and the consequent issues [9]. Depending on the failure mode, i.e. failed-open or failed-short, this can disable ground protection system, cause significant damage to the power system equipments during ground faults, risk the safety of site personnel, etc. As such, most of the utilities perform periodical investigations to detect such a failure. However, planned-maintenances or periodical inspections/tests guarantee the intactness of these apparatuses only during the investigation as the failed-short and failed-open NGRs have been detected right after preventive maintenances [11].

Coal mining industry has widely mentioned this issue regarding the NGRs. This industry experiences change in resistance of NGRs that is a major problem in protection aspect of view. Many events have been reported by this industry that a failed NGR has been identified as the main reason. A few reported events are: 1) a victim at an underground coal mine in Virginia on November 11, 1991, 2) soft starter failure due to an open NGR, and 3) nine loose connections in Eastern Canada on a 200 A, 4160 V NGR [9].

Indeed, without continuous monitoring of neutral grounding systems, there is no indication that NGDs have failed. Therefore, relaying industry needs a reliable solution for detecting the failed NGDs installed at neutral system of generators and distribution transformers. In fact, the NGDs must be continuously monitored to avoid false sense of security, as mandated for NGRs installed in mining systems per article 250 of National

Electrical Code (NEC) 2005 [13], and for all NGR applications per Sections 1-6 and 10-1102.3 of Canadian Electrical Code (CEC) 2018 [14]. As understood from these resources, industries of the North America shall continuously monitor the NGRs to guarantee a safe operation during the likely-to-happen ground faults [15].

2.3 Existing Monitoring Methods – Passive Category

Continuity of service, integrity and intactness of the NGRs have been unavoidable concerns of many industries for decades worldwide especially in Canada. It can be said that Canada is one of the frontiers in the field of continuous NGR monitoring due to industries that are well-known in competition [19, 20, 21, 28, 29]. The [16, 17] also show the record of this practice in Slovenia. In USA, the continuity of service and connectivity of the grounding path has been focused as can be found in [23, 24, 27]. India has contributed in this industrial field as well [25].

On the basis of the performed literature survey for existing NGD monitoring techniques, ten different concepts have been explored that are explained in this section. The explored methods are classified into three different categories based on their principles and concepts, i.e., passive, active, and passive-active. The first category is the passive methods since they rely on existing electrical parameters of the neutral system, i.e., neutral voltage and current, without polluting the electrical characteristics of the power network. These methods claim that although the neutral system is theoretically supposed to not experience any electrical energy flow; however, it always conducts a very negligible current, less than 100 mA, due to inherent asymmetry or imbalance of the three-phase components of the power system such as the transformers, generators, transmission lines, loads, and system charging capacitances. Obviously, presence of this current in neutral system is a must for these methods since monitoring will be disabled if this current disappears for any reason except the failed-open NGR condition. Six methods are classified under the passive category, called methods P1-P6. The main issue with the passive

methods is that none of them could provide monitoring in de-energized state of the power system. As mentioned earlier, these techniques do not inject signals and rely on existing electrical parameters of the neutral system. Hence, the monitoring will be disabled if these electrical parameters become absent due to any reason.

2.3.1 Method P1 – Preventive maintenance

The first method, hereafter referred to as preventive maintenance or method P1, has a very long history that goes back to even the first days of appearance of the power systems which is nothing but the periodical or planned inspections, tests, maintenances or investigations. This practice exists even these days where the power systems are highly advanced. The [11] mentions this method with minimum degree of satisfaction since it guarantees the integrity of the assets only during the investigation and not after that. This means the inspected device could fail even right after the test. Moreover, the [11] mentions that a few open NGRs have been detected after completion of a planned maintenance. Thus, this method cannot guarantee continuous monitoring of the NGDs. It is classified under passive methods since it does not inject any signals to the power network. Although this method is not a continuous monitoring alternative; however, it provides a minimum level of monitoring applicable to almost any possible kind of NGDs.

A few case studies are presented for preventive-maintenance-based NGR monitoring. As the first record, a conducted inspection of the NGRs in a 60-year-old chemical plant with 80 substations of various ages has resulted detection of two failed-open NGRs among ten high-resistance grounded substations yielding 20% chance for NGR failure [11].

Second, five NGRs have been detected faulty at a P&G's facilities during an investigation of eight NGRs shortly before they were about to be empowered. These NGRs were unintentionally left disconnected after transformer testing. The issue was solved by manually reconnecting the NGRs. This case means even the inspection itself could cause failed-open NGR situation. How long would these undetected failed-open NGRs have risk the network safety without continuous monitoring [15]?

Third, a physically damaged NGR has been noticed during visiting the processing plant at a mine in Northern Minnesota, USA in 2001. The NGR was mounted too close

to the overhang of the building, and an iceberg sized icicle had fallen over the screened enclosure. The enclosure and the resistor were both crushed by the impact. The same question rises here which holds the importance of continuous monitoring [15].

2.3.2 Method P2 – Neutral Current Supervision

Second technique, hereafter referred to as method P2 or method IN, is classified under passive methods. This technique measures the negligible current of the neutral wire that flows through the NGR as well. This current is induced in neutral system due to inherent asymmetry of the power system components. Figure 2.6 shows a sample resistance grounded wye-connected transformer or generator configuration. A very negligible imbalance of the phase-to-ground capacitors of this system causes the residual current. This current which will be referred to as leakage current circulates through the neutral system including the NGR as well.

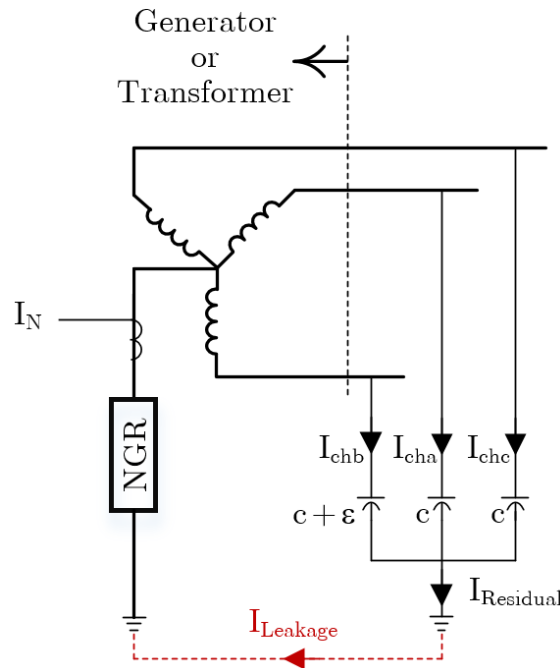


Figure 2.6: Connection diagram of the monitoring method P2.

This monitoring technique employs the measured neutral current to detect the NGR failure through supervising the level. In fact, two thresholds are used to detect whether the current is absent or abnormally very high. In other words, dissatisfaction of the

following constraint turns the NGR failure detection signal on.

$$0.01\% < I_N < 120\% \quad (2.1)$$

where the base value is neutral let-through current (I_{let}). The failed-open NGR is detected only if the NGR current declines to less than the lower threshold disregarding the operation mode of the power system. This means that the NGR is completely disconnected. Therefore, if the NGR fails partially open, this method will not be able to detect it. Moreover, the failed-short NGR is detected only if the neutral current rises beyond the maximum expected level which is 120% of the I_{let} that is experienced during the LG fault. Obviously, if the NGR fails partially shorted in the absence of ground faults, its failure will remain undetected until a ground fault occurs. As such, this method has many shortcomings even though it is very economical since the only needed measurement instrument is already installed for the protection system. The first issue with this method is that it cannot detect partial failure of the NGR. Second, neutral current is not a reliable or satisfying parameter for the aimed monitoring system. Third, it is mainly an overcurrent ground protection scheme rather than a continuous monitoring technique. Yet, it provides a very limited performance for monitoring the NGR. It should be noted that neutral current supervision can be used for monitoring the other types of NGDs, and even the continuity of service of the solid grounding [9, 11].

2.3.3 Method P3 – Impedance Supervision Using V_N and I_N

As known, the impedance is the best parameter to detect the intactness, integrity, and continuity of service of power system components. This concept appears in following monitoring techniques causing better performance .

The third method, hereafter referred to as method P3 or method VNIN, is classified under passive methods. The measurement points and connection diagram of the configuration are shown in Figure 2.7. This technique benefits from two logics that are neutral current supervision, and NGR impedance supervision. The neutral current supervision is employed during the normal operation condition of the power system where the neutral

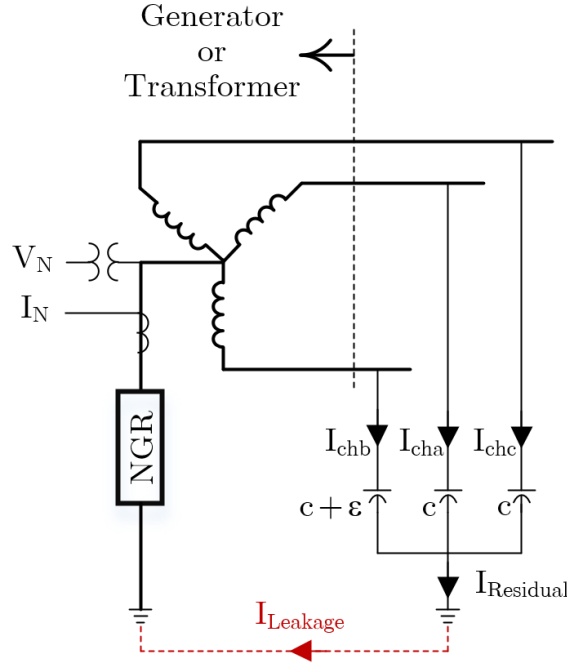


Figure 2.7: Connection diagram of the monitoring method P3.

voltage is so low that the utilized voltage metering instrument (PT) cannot provide an accurate measurement. As such, only the neutral current is used which is applied to neutral current supervision logic. As mentioned for previous method, this logic cannot detect partial failure. As a result, the method VNIN cannot detect partial failure during the normal operation condition. However, the impedance supervision logic, Equation 2.2, that is employed during the faulted condition of the power system detects all kinds of degradation of the NGR.

$$80\% < |Z_N| < 120\% \quad [9] \quad (2.2)$$

As known, the ground fault overcurrent or overvoltage protection pickup settings are tuned to 10-20% of the maximum voltage or current that is expected in neutral system during the ground faults. The complete monitoring algorithm is presented in Figure 2.8.

This technique is applicable to high impedance NGDs such as HNGR used in high resistance grounding with/without NGT, and HNGL used in resonant grounding [9, 10, 11]. It should be noted that although this technique guarantees an acceptable monitoring during the ground faults; however, it's performance is very limited since NGR failure

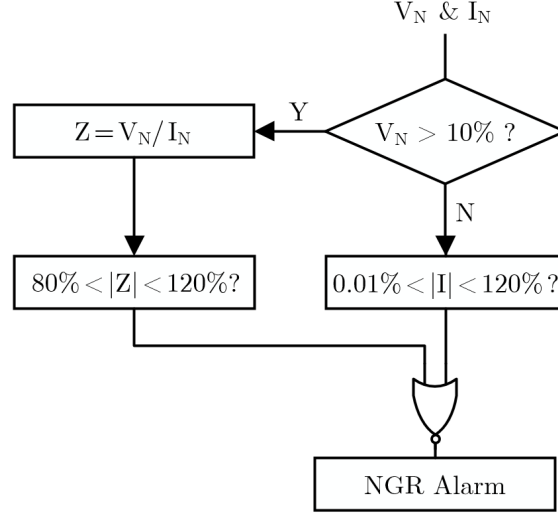


Figure 2.8: Monitoring algorithm of method P3.

detection is required and necessary before ground faults incidence to guarantee a safe operation during the likely to happen ground faults.

2.3.4 Method P4 – Impedance Supervision Using V_0 and I_N

The fourth method, hereafter referred to as method P4 or method V0IN, is classified under passive methods category. The measurement points and connection diagram of the configuration are shown in Figure 2.9. The monitoring principles and concepts of this technique are the same as the method VNIN. The only difference is the neutral voltage metering mechanism. This technique uses the residual voltage instead of neutral voltage since the applicable configurations do not have the neutral PT. However, the neutral voltage is obtained by grounded-wye-broken-delta PT configuration that provides the residual voltage at terminals of the generators and transformers, as shown in Figure 2.9 [16, 17].

This technique uses the neutral current supervision logic if residual voltage is less than 1%, and the impedance supervision logic when the residual voltage is higher than 1%. The performance of this technique is believed to be better than the previous method since the minimum accuracy limit of the residual voltage is around 1% which is lower than that of the neutral voltage, i.e., 10%. Hence, this technique relies on impedance measurement if the neutral current is more than 1% instead of 10%. As a result, this monitoring

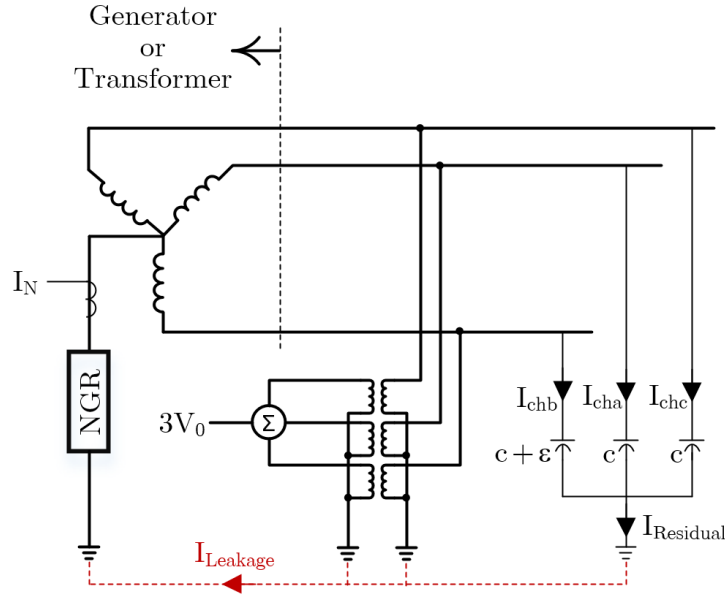


Figure 2.9: Connection diagram of the monitoring method P4 [16, 17].

method relies on impedance supervision on a wider range compared to previous method resulting a better performance. The monitoring algorithm is the same as shown in Figure 2.8 except that the voltage threshold is 1% instead of 10%.

Again, it should be noted that although this technique guarantees an acceptable monitoring during the ground faults, however, it is not an widely used practice since NGR failure detection is required and necessary before ground faults incidence to guarantee a safe operation during the ground faults.

2.3.5 Method P5 – Impedance Supervision Using V_{RPD} and I_N

The fifth method, hereafter referred to as method P5 or method VRPDIN, is classified under passive methods. Its concept is very close to methods P3 or P4, but with better performance. In other words, this practice is toward an enhanced version of the monitoring methods P3 and P4 by employing a more accurate voltage metering instrument. The measurement points and connection diagram of the configuration are shown in Figure 2.10. The neutral voltage is measured by Resistive Potential Divider (RPD) technique. The minimum accuracy limit of the RPD is less than the neutral and residual voltages obtained by neutral PT and terminal PTs, respectively. Hence, it can cover wider range

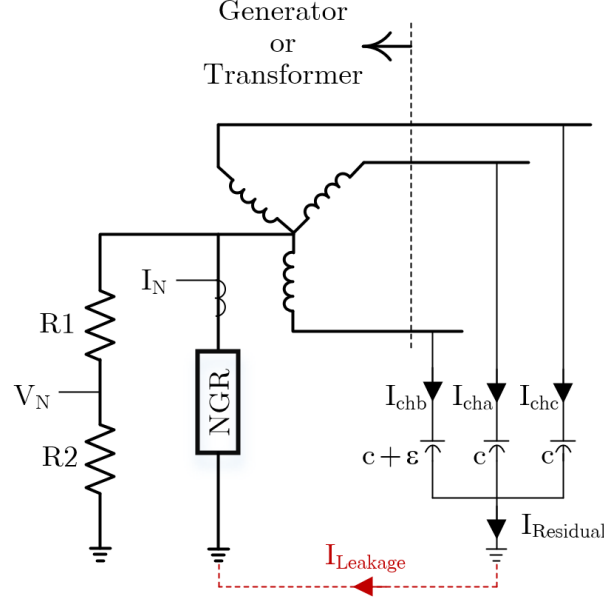


Figure 2.10: Connection diagram of the monitoring method P5 [18].

of NGR voltage measurement from 0.1%, to the phase voltage rating. However, the very weak voltages appearing across neutral system, i.e., less than 0.1% which happen during the normal condition, cannot be measured by this technique unless a high sampling resolutions is employed. This monitoring method uses the same algorithm as the previous method with some enhancements as shown in Figure 2.11. The enhancements are the switching level between the neutral current and impedance measurement logics. This level indicates the reliability of the method. In fact, the lower this threshold declines the more reliable it becomes since lower levels of this threshold makes the impedance supervision logic more dominant than the current supervision logic. The impedance supervision logic functions very strong, while the neutral current supervision logic functionality is very limited since the neutral current supervision logic only detects the completely disconnected or failed-open NGR while the impedance supervision logic detects even the partial failure of the apparatus. The ground fault constraint is now changed to following constraint which is the switching criteria between monitoring logics.

$$V_N > 0.1\% \quad (2.3)$$

In short, the impedance supervision logic is used during the faulted conditions or when the neutral voltage is sufficient during the unfaulted condition. Moreover, the neutral current

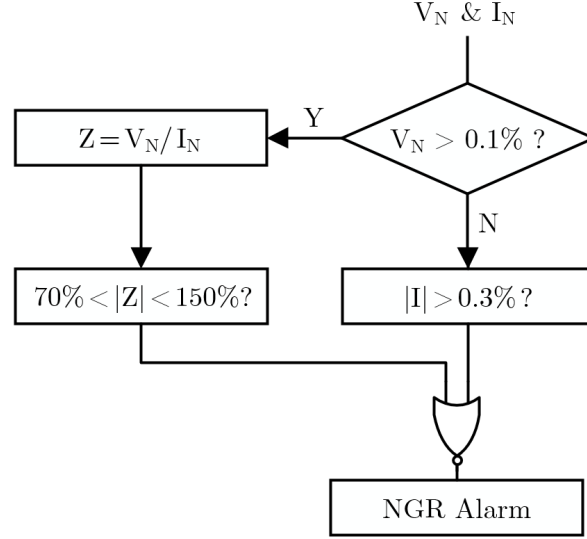


Figure 2.11: Monitoring algorithm of method P5.

supervision logic functions during the unfaulted conditions that the neutral voltage is very weak and less than the minimum accuracy limit of the used RPD [18].

2.3.6 Method P6 – Impedance Supervision Using V_{TVS} and I_N

The sixth monitoring technique, hereafter referred to as method P6 or method VTVSIN, is classified under passive category. The functionality of this method is inverse of the methods P4 and P5. It uses a sensitive CT, and a new mechanism for neutral voltage metering called sensing resistor, as shown in Figure 2.12. It is mainly composed of a Transient Voltage Suppressing (TVS) diode, and an isolation or protective resistor. It provides very accurate voltage metering in unfaulted systems where the neutral voltage is very weak and in the order of a few volts even in medium voltage distribution systems.

The isolation resistor (R_1) limits the TVS current to its maximum tolerating overcurrent level. Thereby, the monitoring relay is protected against ground faults in the high voltage system. For example, a $100\text{ k}\Omega$ isolation resistor is used in distribution networks up to 35 kV to limit the TVS current to 250 mA . On the other hand, the TVS diode is composed of two back-to-back zener diodes making the device bidirectional. This device comes in parallel to the NGR and neutral voltage measurement points. When the neutral voltage is less than the clamping level of the zener diode, chosen 1% of line-to-ground

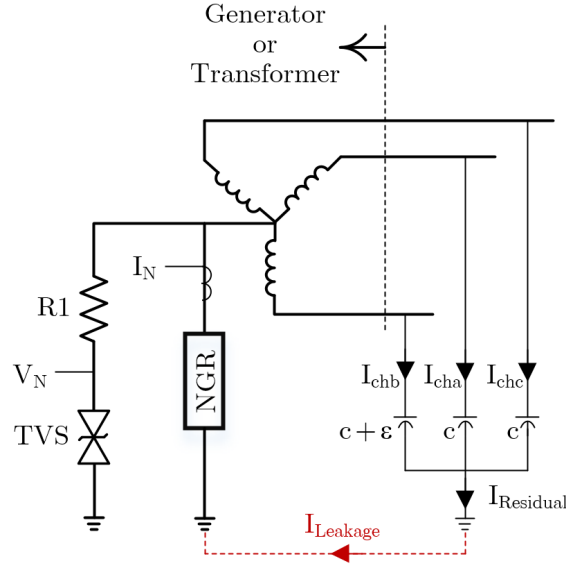


Figure 2.12: Connection diagram of the monitoring method P6.

voltage, the TVS acts open, and the neutral voltage is accurately measured. However, if neutral voltage becomes noticeable such as during ground faults, the TVS acts shorted bypassing the measurement points to protect the relay against the neutral transient over-voltages. Hence, it can be said that the neutral voltage measurement is not valid when it becomes greater than the clamping level of the TVS diode. As a result, this new mechanism does not provide neutral voltage metering during the ground faults. The I-V characteristic of a sample TVS diode with the breaking voltage equal to 9 V is shown in the following graph.

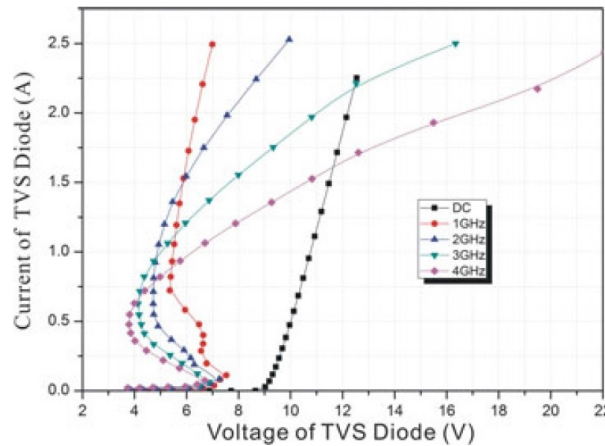


Figure 2.13: I-V characteristic of a sample TVS diode [33].

On the basis of the understood operation modes of the sensing resistor technique, this monitoring method employs the impedance supervision logic during the unfaulted condition, and the neutral current supervision logic during the faulted condition. It should be mentioned that the clamping level of the TVS diode is designed greater than the maximum known voltage at neutral in absence of ground faults. As explained earlier, since the impedance measurement logic can detect partial failure of the NGR, this monitoring method functions very strong in unfaulted condition. However, since the neutral current supervision logic cannot detect partial failures of the NGR, the performance of this monitoring technique is very limited during the ground faults. Yet, it can detect the failed-short and failed-open NGR conditions in the presence of ground faults. The monitoring algorithm is shown in Figure 2.14 [1, 9, 19, 20, 21, 22].

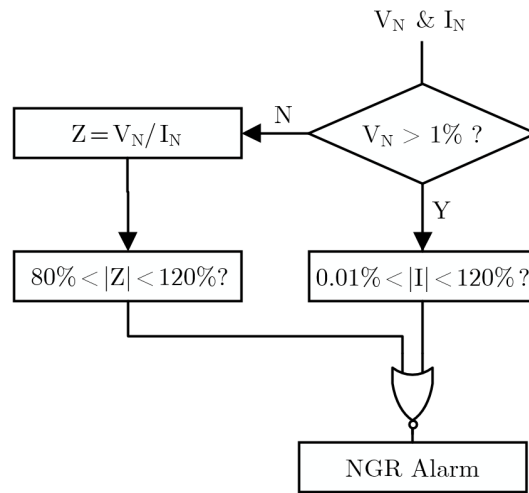


Figure 2.14: Monitoring algorithm of method P6.

Lastly, it should be noted that although this monitoring technique cannot guarantee a safe operation during the ground fault, however, it is the most popular passive technique since it operates strongly in unfaulted condition. In fact, detecting degraded NGR before incidence of ground faults is more of interest to guarantee protecting the power system equipment in case of an upcoming ground fault. Following, a few case studies that have been solved by this technique are reviewed briefly.

As the first case, after finding three left-open NGRs of a stationary surface substation of an Anglo Coal mine in Australia in 2004, this industry used this monitoring method and

reported it beneficial. Furthermore, this method has tripped on a 5 year old installation reported by Assistant Maintenance Manager at Cargill Fertilizer Inc. in Bradley Junction Florida. The NGR was hit and burnt out by a lightning strike [15].

2.4 Existing Monitoring Methods – Active Category

The second category of the existing NGR monitoring techniques is called active methods since they inject AC/DC signals to neutral system and do change the operation characteristics of the system. The main philosophy behind appearance of these methods is that the neutral voltage and current are not sufficient to be accurately measured, and some means of signal injection should be employed to solve this issue. The injection source should be decoupled from the power network in case of ground faults which is accomplished by means of coupling filters. These filters do not let the power frequency harmonics to penetrate to the injection equipment, however, when the ground faults occur, the signal processing of the injected signal becomes challenging since the level of the power frequency signal is remarkably higher than the injected signal. Furthermore, the injection circuit itself shall be monitored to ensure being failsafe. Three methods are classified under this category that are called methods A1-A3. The most prominent advantage of the active methods is the functionality in de-energized operation mode of the power network. However, the injection means and coupling filters add to the implementation costs compared to the passive methods.

2.4.1 Method A1 – Injected Neutral Current Supervision

The seventh monitoring method, hereafter referred to as method A1, is classified under active methods. It is basically the enhanced version of the method P2 used to monitor the bonding system which earths the entire structure of a distribution network. The method P2 supervised the presence of the neutral current that exists due to inherent asymmetry of the power system while the method A1 monitors the neutral system via supervising the injected AC or DC current signals.

The main reason behind emerging this technique is that the neutral current due to

power system asymmetry is not sufficient for a secure measurement as it sometimes fades completely. Therefore, a current signal is injected to neutral system to resolve this issue. This current must only back and fourth through the pilot and grounding conductors, as shown in Figure 2.15 [23]. This concept can be used for NGR monitoring as well. However, it will only detect the failed-open NGR condition. In fact, the current is injected to ensure the connectivity of the grounding circuit. These methods are mostly known as continuous monitoring of grounding/bonding circuit. Yet, they are counted as a continuous monitoring principle that can be used for monitoring the connectivity of the NGDs as well.

A sample technique, that relies on this concept, injects DC pulses to neutral and monitors the continuity of the bonding path through supervising the level of the injected current in two directions. The connection diagram of this technique is demonstrated in Figure 2.15 [23]. The power source can be a generator or transformer. The monitoring relay injects a current that circulates through the pilot and bonding wires that earth the chassis of the ungrounded load. The measured current should be zero in one direction and non-zero in the other. If the bonding wire is disconnected, this current will be zero

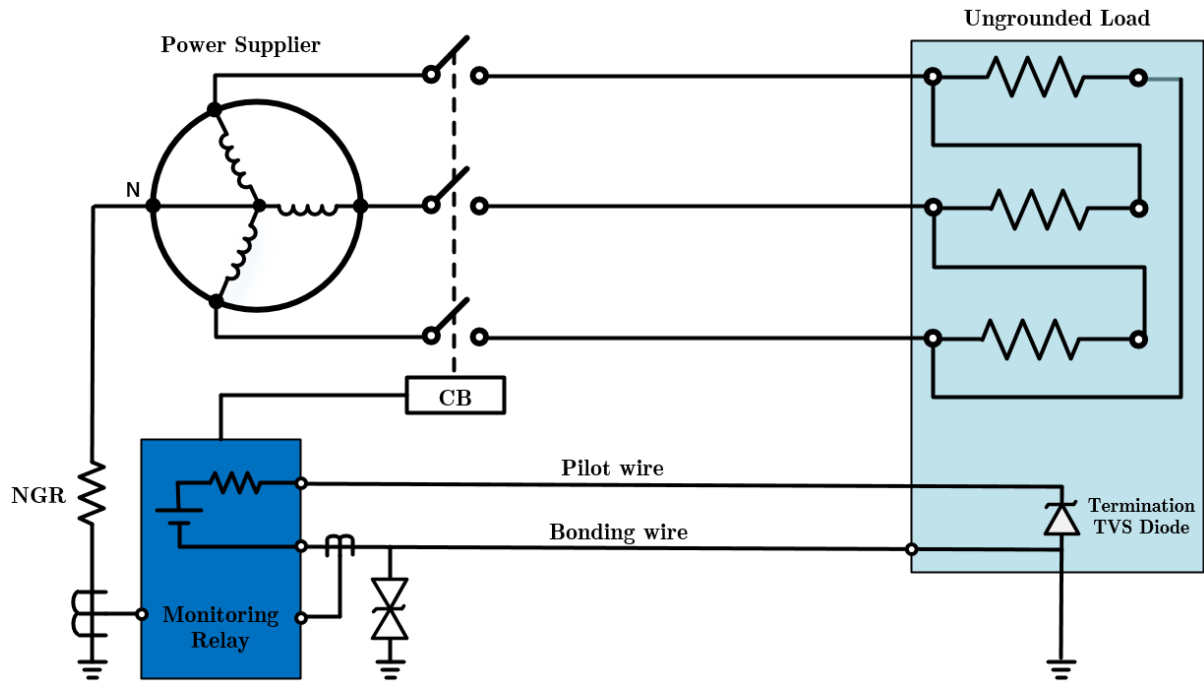


Figure 2.15: Injected current supervision based pilot monitor [23].

in both directions. Thereby, the disconnected bonding circuit is easily identified.

2.4.2 Method A2 – Impedance Supervision Using Injected DC Signal

The eighth monitoring method, hereafter referred to as method A2, is classified under active methods. In this technique, a DC voltage is injected between neutral and ground nodes to guarantee the existence of the neutral electrical parameters. The DC voltage and current of the NGR are then measured to calculate its impedance for monitoring purpose. The neutral current supervision logic is also used to detect the dis-connectivity of the NGR [10, 26, 25]. This technique needs means of signal injection and coupling filters to protect the injection installations against the high voltage system faults. As a result, this technique causes more costs compared to passive methods specially when its decoupling during the ground faults is considered. In fact, this technique cannot function during the ground faults since the protection or decoupling filters isolate the monitoring system from the neutral. Furthermore, the injected current has to mostly flow through the NGR and shall not penetrate to the network. Hence, its application is limited to wye-connected transformers that supply the ungrounded networks or delta-connected loads that can be found in coal mining distribution network. As a conclusion, this method, alongside with the other active methods, cause more expense with limited performance.

The other application of this technique is the unit-connected generators. The stator winding of these kinds of generators is protected against near the neutral ground faults by supervising the seen impedance from neutral using injected sub-harmonic [34], inter-harmonics [31], or multi-harmonics [35]. The injection and coupling filters are already installed. Thereby, the NGR continuous monitoring is easily achieved employing these installations resulting an efficient solution.

A sample approach of this monitoring method is shown in Figure 2.16 [26], which includes only the NGR and voltage injection means. The coupling resistor, R_C , is used for voltage isolation in case of ground faults in high voltage side of the system to protect the injection means. Its resistance shall be equal to the resistance of the

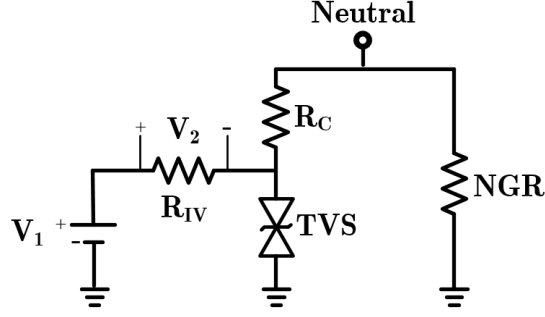


Figure 2.16: Connection diagram of the monitoring method A2 [26].

NGR. Practically, its resistance cannot be very high due to probable challenges caused by sampling resolution. This fact limits the performance of this technique to low voltage applications. The bidirectional TVS diode, together with the coupling resistor protect the DC source against the system ground faults. The logic resistor, R_{IV} , is a $1\ \Omega$ resistor used to convert the injected current to DC voltage shown as V_2 . In the absence of the ground faults, and when the existing voltage across the NGR is less than the clamping level of the TVS, the battery injects a DC current that flows through the logic resistor, coupling resistor and NGR. Thereby, the Equation (2.4) can be used to calculate the NGR resistance in unfaulted condition.

$$R_{NGR} = \frac{1}{2} \frac{V_1}{V_2} \quad (2.4)$$

The $1/2$ coefficient reflects the fact that the coupling resistor and NGR have the same resistance that both are noticeably higher than that of the logic resistor. Indeed, the V_2/V_1 is twice as the resistance of the NGR for intact NGR in unfaulted condition. The impedance supervision logic represented by Relation (2.2) detects the failed NGR in unfaulted condition.

This method suffers from few issues. First, if the neutral voltage grows due to possible asymmetry of the power system, filtration of the injected DC signals from the AC profile of the neutral voltage current and voltage will be struggling. Therefore, this method cannot obtain the NGR impedance when the neutral voltage increases due to asymmetry of the system. Another probable issue facing this technique is the DC/AC strays or influences that appear at neutral node due to environmental effects. Furthermore, continuity

through a ground fault may be recognized as NGR continuity [9].

2.4.3 Method A3 – Neutral Grounding System Time Constant Supervision based on Pulse Injection

The last active monitoring method, hereafter referred to as method A3, is introduced here. In this technique, an short duty impulse is injected into the grounding system, and the time constant of the neutral-to-ground system (RC) is supervised. The injected impulse causes the appearance of an exponentially damping sinusoidal signal. The damping inertia of this signal known as time-constant is a very beneficial criteria for detecting variations of the grounding path resistance. The analog circuit calculates the subtraction of the damped signal by the grounding system from an internally damped signal. If the difference becomes more than a predefined threshold, the disconnected grounding path is identified. Although this technique is designed to monitor the grounding path, however, it can be set to continuously monitor the NGR as well. This technique is very old and uses analog calculations for supervision. The connection diagram of this technique is obsolete and out of the scopes of this research work. However, it can be found with complete details in [27].

2.5 Existing Monitoring Methods – Passive-Active Category

The active monitoring methods function very well in the absence of the ground faults specially when the existing neutral voltage is very low. On the other hand, the passive methods operate satisfactorily in the presence of the ground faults or when the neutral voltage exists. As may be realized, the passive and active methods are perfect compliments to each other. In fact, if both of them are used simultaneously, a continuous monitoring method will be achieved that guarantees NGR monitoring in all de-energized, unfaulted, and faulted conditions of the power system. Such a combination yields to the third category of existing NGR motoring methods which is called passive-active [28, 29, 30]. A

sample approach is introduced here which combines the methods P6 and A2, hereafter referred to as method P6A2, with the connection diagram shown in 2.17.

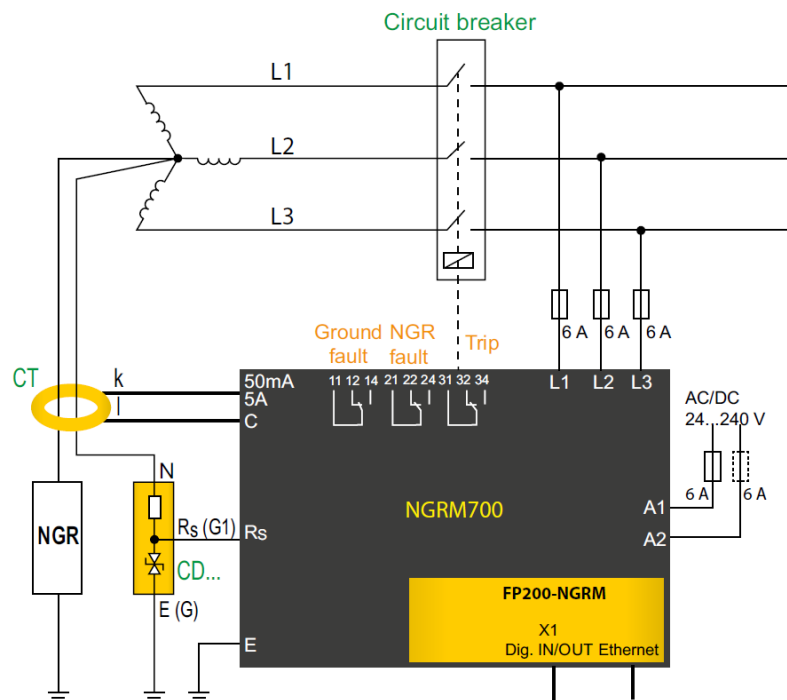


Figure 2.17: Connection diagram of the monitoring method P6A2 [30].

In this method, the sensitive CT at neutral provides wide range current measurement with less than 10% error. On the other hand, the neutral voltage is measured by the vector sum of the line voltages that are measured by the relay. The measurements achieved by these instruments are used for NGR resistance supervision if they exist. In other words, these parameters shall be more than a minimum level which is known as 10% [30]. If not, the signal injection comes to the operation. Under this condition, the very same methodology shown in Figure 2.16 is employed. In fact, the line PTs and neutral CT are switched off the service. Again, the resistance of the NGR is obtained using the injected voltage and current, and the NGR resistance supervision functions to detect the failed NGR. Obviously, the NGR resistance is available over its full range which provides a dependable indication of its status. As such, the neutral current supervision is removed from the monitoring scheme increasing the reliability of the monitor. Although this method costs more, but it guarantees a better performance than all other previously mentioned methods.

2.6 Comparison of Existing Monitoring Methods

In this section, the existing NGR monitoring methods will be compared in two ways. First, the evolution of the art of NGR monitoring will be shown using a trend graph, and second, a table will be provided which lists all of the existing methods mentioning the employed measurement instruments and the guaranteed operation conditions.

In Figure 2.18, three categories of the existing monitoring methods are demonstrated. Further, the evolution trend of these methods is depicted yielding the most recent techniques, i.e., passive-active methods. In fact, this graph not only shows different existing concepts of NGR monitoring, but also represents the way these methods have been enhanced. The most recent generation of these methods are the passive-active techniques that are nothing but efficient combination of the passive and active methods.

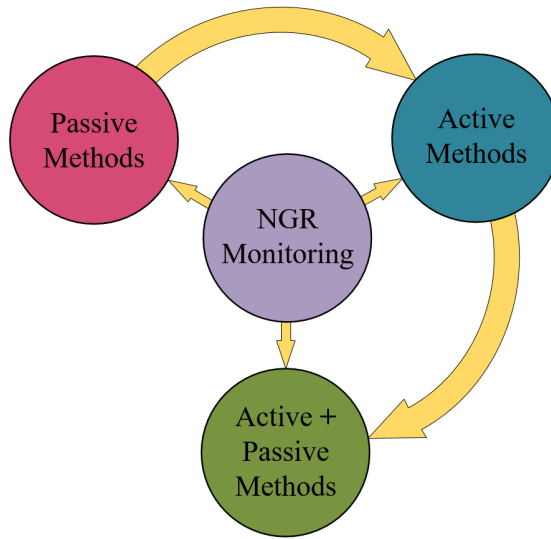


Figure 2.18: Evolution of the existing NGR monitoring methods.

Furthermore, the existing methods are compared based on the employed measurement instruments, and their performance under various operation conditions of the power system, as shown in Table 2.1. The most essential requirement of a well-designed NGR monitoring method is its continuity which means it could identify the precise status of the NGR in all de-energized, normal, and faulted operation conditions of the system. As such, the strength of different existing NGR monitoring methods are ranked relying on this parameter, as shown in the following table. Besides, the required measurement

instruments is the other factor that is considered in the comparison since it limits the methods to specific applications.

Table 2.1: Comparison of the existing NGR monitoring methods.

	Method	Measurement Instruments		Performance in various operation modes		
		I_N	V_N	De-energized	Unfaulted	Faulted
Passive	P1	N/A	N/A	Good	Poor	Poor
	P2	Neutral CT	N/A	Poor	Fair	Average
	P3	Neutral CT	Neutral PT	Poor	Fair	Good
	P4	Neutral CT	Line PTs	Poor	Average	Excellent
	P5	Neutral CT	Neutral RPD	Poor	Good	Excellent
	P6	Neutral EFCT	Neutral SR	Poor	Excellent	Fair
Active	A1	Logic Resistor	Neutral SR	Average	Average	Poor
	A2	Logic Resistor	Neutral SR	Excellent	Excellent	Poor
	A3	N/A	Neutral RPD	Good	Good	Poor
P-A	P6A2	Neutral CT and Logic Resistor	Neutral SR And Line PTs	Excellent	Excellent	Excellent

2.7 Summary

In this chapter, different existing neutral grounding methods were reviewed resulted in introducing various existing neutral grounding devices such as the NGR. Thereafter, the NGR failure and importance of monitoring the NGR were highlighted. Lastly, various existing NGR monitoring methods were reviewed. On the basis of the employed measurement instruments, these methods were classified into three categories named passive, active, and passive-active.

The passive methods rely on existing neutral voltage and/or current of the neutral system that appear due to inherent asymmetry of the power network components such as the generators and transformers. The most prominent issue with these methods is the non-functionality in de-energized operation condition of the power system which causes the appearance of the active category.

The active methods rely on the injected voltage and/or current to the neutral system which results in an excellent performance in de-energized and unfaulted operation conditions. Unlike the passive methods that rely on existing measurement instruments, the active methods come with further implementation cost due to additional measurement instruments to be installed. Besides, these methods cannot monitor the NGR in the presence of the ground faults due to coupling filters that protect the injection source.

Therefore, the third and most recent category of the NGR monitoring methods appeared in the line of the review which is the passive-active category. These methods combine the passive and active methods in such a way that NGR could be monitored in all de-energized, unfaulted and faulted operation conditions of the system. Although these methods are more expensive compared to the other methods, however, they provide the best performance specially in de-energized operation condition.

Chapter 3

Modeling and Behavior Analysis of Two Existing Monitoring Methods

In this chapter, the performance of two existing NGR monitoring methods is investigated. The primary purpose of this investigation is to comprehend the fundamentals and operation principles of these methods. Understanding their concepts and fundamentals helps developing new or enhanced methods that could solve the shortcomings of the existing monitoring methods. Furthermore, the value of the proposed techniques will be clear after understanding the issues and challenges facing the investigated methods. The efficiency of the methods is thoroughly investigated for different operating conditions of the simulated power system configurations, and the degree of their effectiveness is identified. On the basis of the performed studies, three new methods for monitoring the NGRs will be proposed and verified in the next chapters.

Although there are various monitoring methods, as reviewed in the previous chapter, only two methods are analyzed since 1) they are well-known and popular, and 2) understanding their principles and concepts is required in Chapter 4 where the first proposed monitoring method is presented. Following, the monitoring algorithm of each of the methods will be extracted based on their logics of operation provided by available resources. Thereafter, the shortcomings of the methods will be shown through comprehensive scenario-based analysis performed considering three well-known power system configurations.

3.1 Method P6 - NGR Monitoring Using Sensing Resistor and Neutral CT

In this section, the performance of the sixth passive monitoring method, i.e., method P6, is studied. This method has been implemented, verified and widely employed in distribution systems during recent years [19, 20]. Hence, it will be worthwhile to study and understand its performance. The main concepts and principles of this method have been reviewed in the second chapter. This section conducts the detailed studies on modeling and behavior analysis of this method. This technique employs a sensitive CT and a sensing resistor to measure the neutral current and voltage respectively. Both of the utilized measurement instruments are not conventional instruments that could be readily available in most of the applications which causes additional implementation costs.

Following, the detail principles and concepts of operation of the method are extracted and employed by its developed monitoring algorithm. The dead zones of the algorithm are also derived to show the blind regions of its operation. Moreover, the performance and functionality of the method for three different power system configurations are investigated through 150 scenarios. Finally, the learned lessons will be included summarizing the defects, issues, advantages, and disadvantages of this method.

3.1.1 Monitoring Algorithm

The monitoring algorithm of this method has been extracted from the available resources [19, 20]. This decision making flowchart might not reflect the exact operation of the original method. However, it employs the same logics of operation of this technique that have been mentioned in the available publications. The algorithm has different elements for both NGR monitoring and ground fault protection that will be explained one by one. After understanding the employed elements of monitoring, the dead zones of the algorithm will be derived and represented. In fact, the conditions that the proposed monitoring algorithm fails to function correctly will be shown and discussed using the dead zones of the algorithm.

Decision Making Flowchart

The main principles of the monitoring algorithm are divided into four major protection/monitoring elements. Two elements provide ground fault protection. The other two elements monitor the status of the NGR. The complete flowchart of the monitoring algorithm is shown in Figure 3.1. It should be noted that ground fault protection is not a focus of this research work; however, it is believed that the NGR monitoring is very much connected to ground fault protection. As such, the ground fault protection is

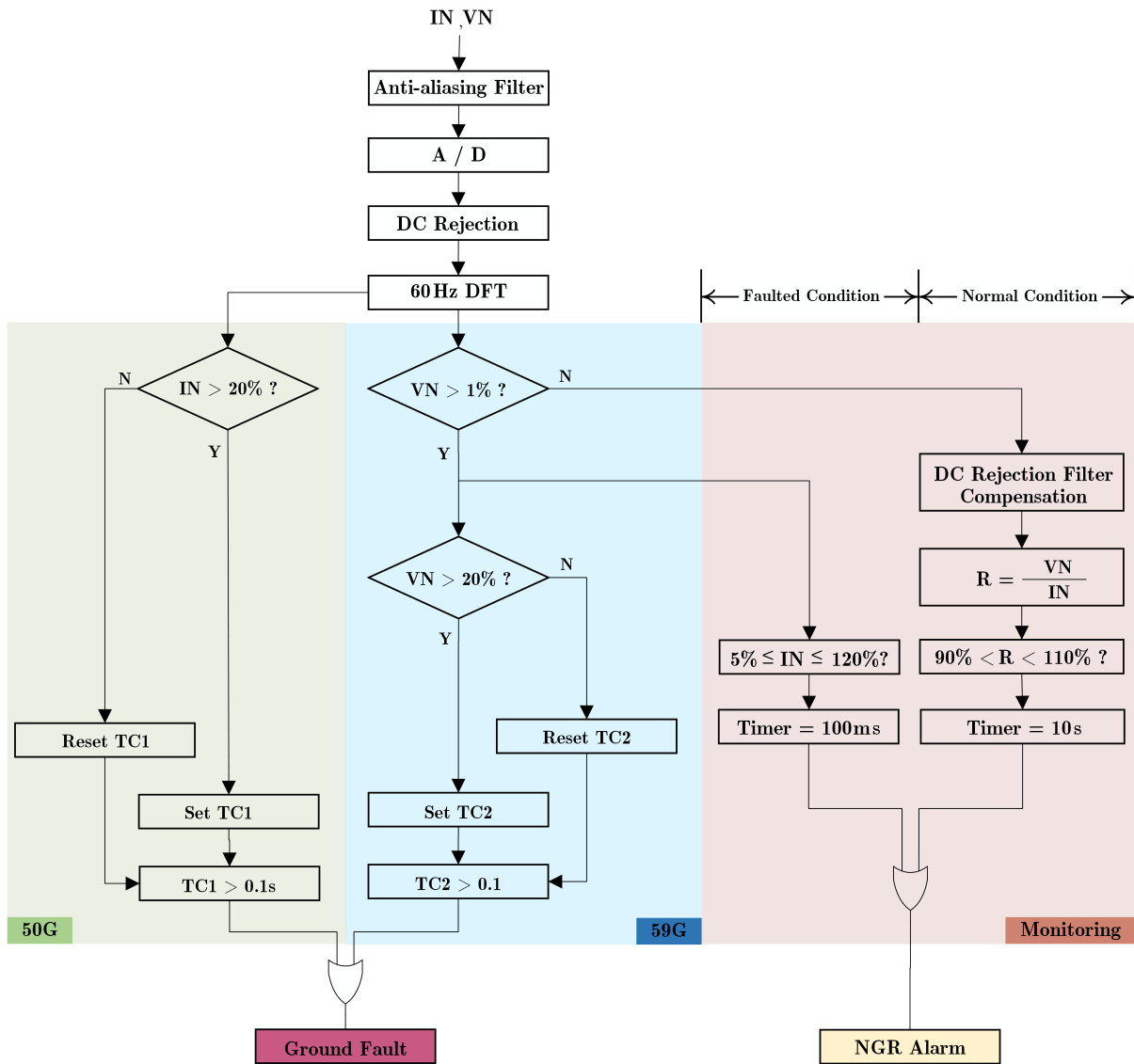


Figure 3.1: Decision making flowchart of the monitoring method P6.

investigated as well.

In order to clearly introduce each part of the scheme, a different color is assigned to each element. For example, the overcurrent ground fault protection element is differentiated by green color and coded as 50G. The other element is the overvoltage ground fault protection, represented in blue and coded as 59G. This element detects the very high impedance ground faults where the 50G fails to function. The last element, shown in red, is the monitoring scheme which is the main focus of this research work. It itself consists of two separate logics, as mentioned on top of the monitoring block. The left part functions during the faulted condition, while the right side element operates during the normal operation condition where the voltage across the NGR is very low.

Since the main focus of the work is the monitoring part of the algorithm, the protection elements are not discussed anymore. The only challenge facing the monitoring part is the neutral voltage metering mechanism which is the sensing resistor. In Appendix B, detail explanations and operation principles of the sensing resistor have been presented that are followed by its detail modeling in PSCAD software. The main issue is the accuracy limits of the sensing resistor that measures the neutral voltage. On the basis of [19], the neutral voltage can be measured with less than 1% error when it is less than 1% of the system line-to-ground voltage rating, e.g., 100 V. This means that the very weak voltage across the neutral system, less than 100 V, that appear during the normal operation condition can be measured accurately. As such, both of the voltage and current signals of the NGR become available with an acceptable accuracy. Thereby, the impedance of the NGR can be used as shown in the algorithm. A calibration margin is used to identify the intact NGR, which is 90-110% of the rated resistance of the NGR. The failed NGR is identified if its resistance goes out of this preset region considering 10 s time delay.

When the sensed voltage is higher than 1%, which is not measured accurately, the monitoring algorithm relies on I_N . It supervises the magnitude of this parameter, and if it does not fall within a preset safe region, i.e., 5-120% of neutral let through current (I_{let}), then the failed NGR is reported considering 0.1 s time delay. It should be noted that the used 0.1 s time delay is to detect NGR failure before that the ground fault trip is commanded. If the current measured by neutral current transformer becomes less than

5%, the failed-open NGR will be reported, and if it is more than 120%, the failed-short NGR.

Dead Zones of The Algorithm

The following figure shows the dead zones of the aforementioned algorithm. The dead zones point out to the conditions that the algorithm cannot function correctly. For this monitoring algorithm, it fails if the operating point falls inside the areas of the (V_N, R_{NGR}) plane that are gray, as shown in the following figure. It should be advised that this characteristic is not a protection zone. It is derived just for figuring out the dependability of the algorithm and finding ideas to improve the proposed algorithm. Further improvements can be obtained by reducing the gray area. The gray areas cover around 20% of the plane meaning that the dependability of the algorithm is around

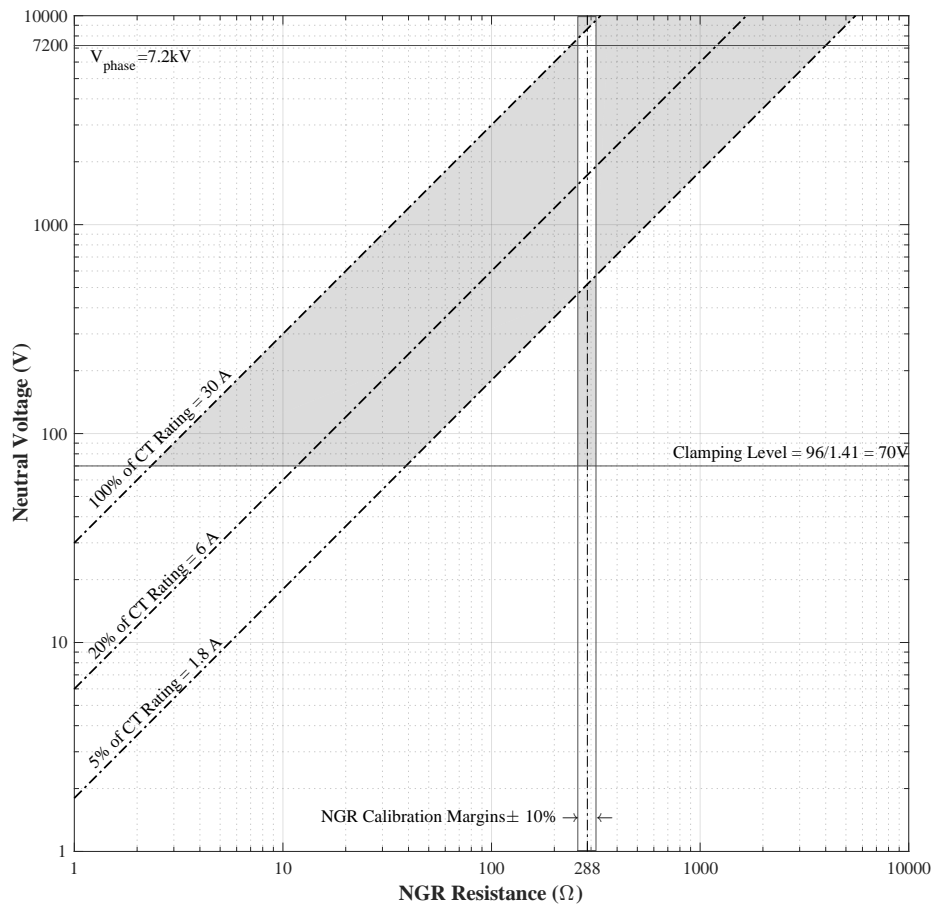


Figure 3.2: Dead zones of the monitoring algorithm.

20%; however, it is 100% reliable during the unfaulted condition. This characteristic will mostly be used to explain the conditions that this algorithm fails to function correctly.

As shown, the characteristic is effected by two current thresholds, one voltage level, and the NGR calibration margins. The neutral voltage is securely measured during the normal operation condition where it is less than 70 V RMS or 100 V peak. Under this condition, the resistance of the NGR is obtained accurately, and the calibration margins are used to detect the failed NGR. The algorithm operates strongly during this mode of operation. There is no dead zone for this condition which means that the algorithm does not maloperate at all. However, when a ground faults occurs, the neutral voltage rises beyond the minimum accuracy limit, i.e., 1%, where the neutral voltage is not measured accurately. Under this condition, the algorithm only uses the current signal and the safe region defined as 1.8-30 A.

3.1.2 Performance Analysis

Following, the performance of the monitoring method P6 is studied for high-resistance NGR during different system conditions. Three of the popular-in-the-art power system configurations will be simulated in PSCAD. The current and voltage waveforms captured from PSCAD will be played back to Matlab-based model of the monitoring algorithm to investigate its performance for various NGR failures and/or system faults. The studied configurations have been selected from [2, 3, 16, 17], which are listed below:

- Configuration 1 — High-resistance-grounded generator.
- Configuration 2 — High-resistance-grounded DYg distribution transformer.
- Configuration 3 — High-resistance-grounded YD distribution transformer.

The proposed algorithm is expected to monitor the status of the NGR during both unfaulted and faulted conditions. Furthermore, the resistance of the NGR will be changed so as to represent various kinds of NGR degradations during both the faulted and unfaulted conditions of the power system configurations. As such, there will be five different cases to analyze the performance of the monitoring method, as listed below:

- Case 1 — Monitoring a healthy NGR during various system faults.
- Case 2 — Monitoring various NGR degradations in a healthy system.
- Case 3 — Monitoring various NGR degradations during a LG fault.
- Case 4 — Monitoring a failed-short NGR during various system faults.
- Case 5 — Monitoring a failed-open NGR during various system faults.

These five cases are investigated through 50 scenarios, 10 scenarios per case. Since three configurations are studied, the total number of the scenarios is 150 resulting a comprehensive study of the performance of this monitoring method.

Configuration 1 — High Resistance Grounded Generator

On the basis of IEEE Standard C37.101 [3], the generators are mostly unit-connected rather than directly loaded. The main reason behind this principle is the zero sequence isolation of the generation side from the rest of the power system. The neutral of such generators is often resistance grounded. Therefore, analysis of the operation and functionality of the monitoring method for a high-resistance-grounded unit-connected generator is worthwhile as performed here. The high-resistance grounding is carried out using a small resistor at the secondary of a single-phase Neutral Grounding Transformer (NGT) which actually makes the grounding easier since the ratings of the grounding component decrease strikingly. In fact, the voltage at the secondary of the NGT is usually 50-100 times smaller than the system voltage level. Additionally, the impedance of NGR decreases by a factor of 2500-10000.

The connection diagram of the configuration is shown in Figure 3.3. It represents a LV distribution system supplied by a 14MVA generator. As shown, the generator neutral is grounded using a 9.6/0.240 kV NGT, and a $0.18\ \Omega$ resistor, resulting $288\ \Omega$ at primary. The system charging capacitors are also demonstrated. An imbalance of 1% has been considered in system charging capacitors to induce a milliampere current in the neutral wire. This phenomenon happens in real practice since the three-phase power system is inherently asymmetric and does have some negligible levels of imbalance.

The induced current is called residual or leakage current and is employed by passive monitoring methods. The measurements, V_N and I_N , are transmitted to the monitoring relay, and the status of the NGR is monitored using the obtained resistance of the NGR, and neutral current supervision logic.

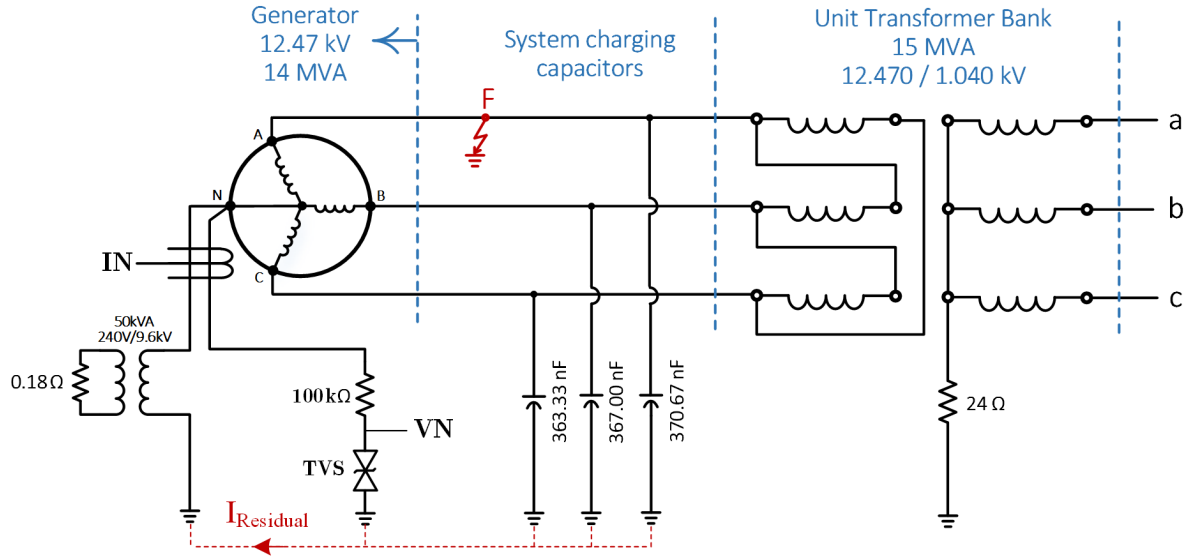


Figure 3.3: High resistance grounded unit-connected generator.

Case 1 – Monitoring the healthy NGR During Various System Faults: First, a healthy NGR is monitored during different faulted conditions, i.e., case 1. The monitoring and protection outcomes for investigated scenarios are presented in Table 3.1. The NGR status is reported by NF or F representing the healthy (non-failed) or failed NGR,

Table 3.1: Case 1 –Monitoring a healthy NGR during various system faults.

Scenario No.	GF Type	V_N / V_{LG}	NGR (p.u.)	NGR Status	GF Trip
1	—	0.0008	1.0	NF	0
2	AG	0.2	1.0	NF	1
3	AG	0.4	1.0	NF	1
4	AG	0.6	1.0	NF	1
5	AG	0.8	1.0	NF	1
6	AG	1.0	1.0	NF	1
7	BC	0.0006	1.0	NF	0
8	BCG	1.0	1.0	NF	1
9	ABC	0.0005	1.0	NF	0
10	ABCG	0.0004	1.0	NF	0

respectively. In addition, the Ground Fault (GF) detection is identified by 1 or 0.

In this case, NGR remains healthy even during the faults. The scenario 1 models monitoring a healthy NGR during the loading condition because the neutral voltage is in the order of a few volts. The other scenarios monitor the healthy NGR during 9 system faults that happen in different locations of the generator stator winding with different fault resistances.

The monitoring algorithm successfully detects the ground faults and the NGR status except during high impedance or near the neutral ground faults, i.e., somewhere between scenarios 1 and 2. In this condition, the neutral current is less than the GF trip level, i.e., 20% of CT rating equal to 6 A. Moreover, the voltage is more than clamping level. Therefore, the current signal is used for monitoring the status of the NGR. The relay reports a failed NGR because the neutral current is less than 1.8 A. As a conclusion, it should be mentioned that the medium level voltages across neutral during any of the following conditions will lead to an undetected NGR failure.

- A very close to neutral single-line-to-ground fault
- A high impedance fault
- A very distant fault

Case 2 — Monitoring Various NGR Degradations In a Healthy System:

The second case happens when the power network is healthy, and the NGR fails. This situation has been investigated for different kinds of NGR failures. The voltage of the neutral is 12 V peak of fundamental frequency induced due to inherent asymmetry of the power network. The simulation outcomes have been analyzed, and the results of the monitoring are represented in Table 3.2.

As expected, the ground protection elements remain disabled. As shown, the algorithm securely detects all degradations, and does not trip on ground faults since the neutral voltage and current are very low. The only reason behind this performance is nothing but the properly measured voltage of the neutral. In other words, the neutral voltage is less than the 100 V, and well-measured. Therefore, the measured resistance is

Table 3.2: Case 2 –Monitoring various NGR degradations in a healthy system.

Scenario No.	GF Type	V_0/V_{LG}	NGR (p.u.)	NGR Status	GF Trip
11	—	0.0008	0.1	F	0
12	—	0.0008	0.2	F	0
13	—	0.0008	0.4	F	0
14	—	0.0008	0.8	F	0
15	—	0.0008	1.2	F	0
16	—	0.0008	2.0	F	0
17	—	0.0008	5.0	F	0
18	—	0.0008	10.0	F	0
19	—	0.0008	20.0	F	0
20	—	0.0008	30.0	F	0

valid. Since the measured resistance takes place out of the calibration margins, the failed NGR is reported. The only challenge facing this case is the minimum current that the used sensitive CT can measure. In fact, the used CT cannot accurately measure the very low currents recorded in scenarios 19 and 20 which are less than 2 mA. In these cases, the monitoring algorithm should report an open circuit or disconnected NGR because of absence of neutral current. Fortunately, since the calibration margins for NGR resistance are used, absence of neutral current and very low currents are treated the same, considered as open NGR. This scheme has been used in [16] as well.

Case 3 — Monitoring Various NGR Degradations During Line-to-Ground Faulted Condition: In this case study, the NGR fails during a bolted LG ground fault at terminal of the generator, as represented in Table 3.3. These scenarios demonstrate the double faults. Different NGR failures are modeled by different NGR resistance values. During the fault, the neutral node experiences 1 pu or 7200 V of the fundamental power frequency modulated by 15% of each of 2^{nd} , 3^{rd} , 5^{th} , and 7^{th} harmonics resulting 30% THD. A double fault is expected to be detected by the monitoring algorithm. The first detection is the ground fault, and the second one is the NGR failure. It should be mentioned that the NGR is healthy, 288Ω , at the beginning of all scenarios. When the fault happens, the NGR degradation starts after three power cycles with the variation rate considered as 10% in 100 ms. Its resistance changes toward the final value shown in the table.

As shown in Table 3.3, the ground fault is detected successfully for all conditions. As shown in the algorithm of the relay, the ground fault is detected using both overvoltage and overcurrent functions. In scenarios 21 to 25, the sensed current is more than 100% of the CT rating meaning that the NGR resistance has been lower than the rated value. It should be noted that this detection is performed without calculating the resistance of the NGR since the neutral voltage is more than the clamping level of the TVS diode of the sensing resistor. In scenarios 26-28, the sensed current is higher than GF trip level and less than 100% of the neutral let through current. The NGR is reported healthy while its resistance is higher than the normally expected value. In fact, the failed-open NGR conducts a current that forces the neutral current supervision element to report it healthy. However, the failed-open NGR is detected in scenarios 29 and 30 since the sensed current is lower than 5% of the CT rating. Although the ground fault has been detected in all of the scenarios, but the overcurrent element does not operate in scenarios 28-30 because the measured current is less than the GF trip level. However, the overvoltage protection function is activated because the voltage across the neutral is more than 20%. Additionally, the overvoltage ground protection function does not operate in scenarios 21-23 where the overcurrent ground protection function detects the ground fault. Thereby, it should be noted that the ground faults in an impedance grounded system will not be detected always if only one of the aforementioned ground protection functions are used.

Table 3.3: Case 3 –Monitoring various NGR degradations during a solid LG fault.

Scenario No.	GF Type	V_0 / V_{LG}	NGR (p.u.)	NGR Status	GF Trip
21	AG	1.0	0.1	F	1
22	AG	1.0	0.2	F	1
23	AG	1.0	0.4	F	1
24	AG	1.0	0.8	F	1
25	AG	1.0	1.2	F	1
26	AG	1.0	2.0	NF	1
27	AG	1.0	5.0	NF	1
28	AG	1.0	10.0	NF	1
29	AG	1.0	20.0	F	1
30	AG	1.0	30.0	F	1

Case 4 – Monitoring a Failed-Short NGR During Various System Faults:

The previous study is carried out for a failed-short NGR, i.e., 100% to 20% in two consequents steps over 1 s, during different system faults. The outcomes of the monitoring algorithm during different system faults are listed in Table 3.4.

Table 3.4: Case 4 –Monitoring a failed-short NGR during various system faults.

Scenario No.	GF Type	V_N / V_{LG}	NGR (p.u.)	NGR Status	GF Trip
31	—	0.0008	0.2	F	0
32	AG	0.2	0.2	NF	1
33	AG	0.4	0.2	F	1
34	AG	0.6	0.2	F	1
35	AG	0.8	0.2	F	1
36	AG	1.0	0.2	F	1
37	BC	0.0008	0.2	F	0
38	BCG	1.0	0.2	F	1
39	ABC	0.0005	0.2	F	0
40	ABCG	0.0003	0.2	F	0

The NGR status is monitored securely except when the voltage across the neutral system is less than 20% of the phase-to-ground voltage, somewhere between scenarios 31 and 32 including scenario 32 itself. This situation is considered as a shortcoming of this method. In fact, the neutral voltage is more than clamping level. Therefore, the resistance calculation element remains unused while the neutral current supervision functions detecting the failed-short NGR in all scenarios 33 to 40.

Case 5 – Monitoring a Failed-Open NGR During Various System Faults:

In the last case, the same studies as the previous case are repeated for a failed-open NGR, i.e., 1 pu to 20 pu over 1 s. The monitoring and protection outcomes are listed in Table 3.5. The monitoring algorithm relies on the neutral current supervision element since the neutral voltage is not available during these scenarios. Although all the scenarios are well-detected, however, the monitoring algorithm fails to operate properly when the NGR resistance increases to 2-5 pu. In fact, the neutral current is in the safe region, 5-120%, for such resistances at neutral. The very same behavior happened in scenarios 26-28 that were demonstrated in case 3. As such, the imperfection of the neutral current supervision element of the monitoring algorithm is highlighted once more. The other shortcoming

faced this technique is its non-functionality in de-energized operation condition which is inherent to passive methods. However, this method is highly of interest since it operates reliably in unfaulted condition.

Table 3.5: Case 5 –Monitoring a failed-open NGR during various system faults.

Scenario No.	GF Type	V_N / V_{LG}	NGR (p.u.)	NGR Status	GF Trip
41	—	0.0008	20	F	0
42	AG	0.2	20	F	1
43	AG	0.4	20	F	1
44	AG	0.6	20	F	1
45	AG	0.8	20	F	1
46	AG	1.0	20	F	1
47	BC	0.0007	20	F	0
48	BCG	1.0	20	F	1
49	ABC	0.0007	20	F	0
50	ABCG	0.0007	20	F	0

Following, the failed conditions are analyzed using the dead zones characteristic of the monitoring algorithm. In fact, it will be demonstrated that how this algorithm fails to function correctly using the V_N versus R_{NGR} trajectory movement. The trajectories are calculated using sequential networks analysis too. The sequential network of the configuration for a LG fault at 12.47kV bus is used as shown in Figure 3.4, and the voltage across the NGR is derived as a function of NGR and fault resistances, as follows.

$$I_N = I_a + I_b + I_c \quad (3.1)$$

$$\text{hence, } I_N = 3 I_0 \quad (3.2)$$

$$\text{As a result, } V_N = NGR \times I_N = 3 NGR \times I_0 \quad (3.3)$$

Accordingly, the voltage of the generator neutral can be obtained based on resistive potential division law as follows.

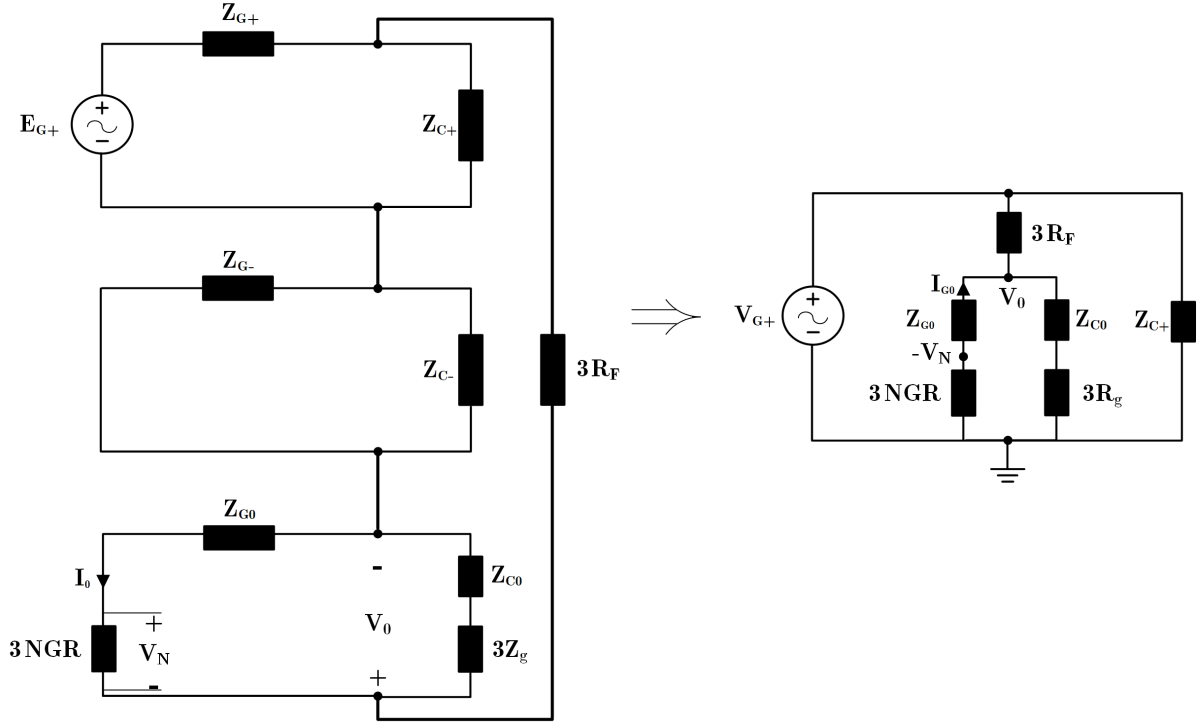


Figure 3.4: Sequential network of the configuration 1 for LG fault at 12.47 kV bus.

$$V_N = -\frac{3 NGR}{3 NGR + Z_{G0}} V_0 \quad (3.4)$$

$$\text{where } V_0 = \frac{(Z_{C0} + 3 Z_g) \parallel (Z_{G0} + 3 NGR)}{(Z_{C0} + 3 Z_g) \parallel (Z_{G0} + 3 NGR) + 3 R_F} V_{G+} \quad (3.5)$$

where Z_C , Z_g , Z_G represent the impedance of the system per phase charging capacitor, earth impedance, and generator stator impedance respectively. This relation is simplified considering that the Z_C is so high that can be neglected.

$$V_N = -\frac{3 NGR}{Z_{G0} + 3 NGR + 3 R_F} \quad (3.6)$$

The dead zones characteristic and the trajectory movement for scenarios 2, 26-30, and 32 are demonstrated in Figure 3.5. In addition, the calculated V_N versus R_{NGR} trajectories, based on Equation (3.6), are also depicted for these cases. It should be noted that the R_F is 600Ω for scenarios 2 and 32 while it is just 0.1Ω for scenarios 26-30.

As shown, the trajectories highly match the obtained curves using Equation (3.6). The description of the characteristics is the same as Figure 3.5. Therefore, the reader

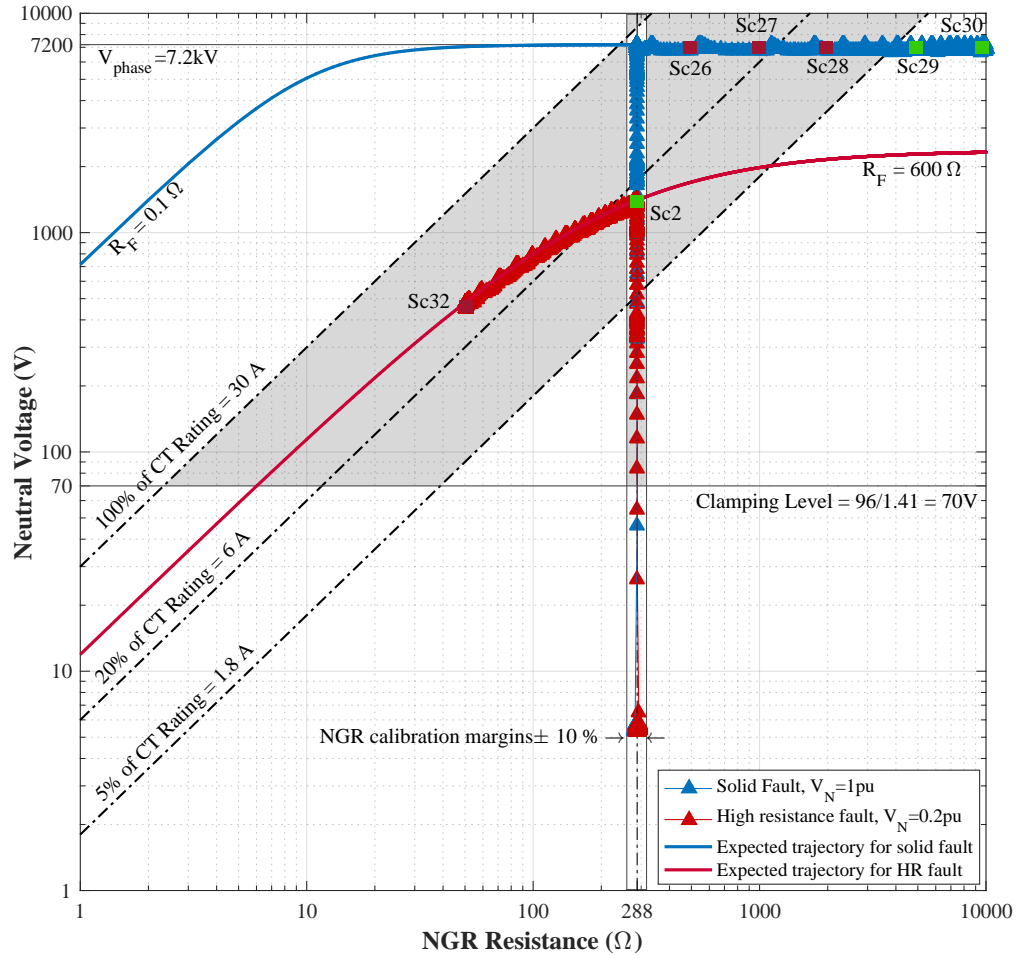


Figure 3.5: Behavior analysis using the dead zones of the algorithm.

is recommended to first understand the according sections. As observed, the trajectory that contains scenario 32 passes through the dead zones and remains inside this region. The main reason is the fault resistance. This parameter affects the voltage across NGR based on 3.6. In fact, NGR is shorted. The neutral current is mainly dependent to fault resistance. This means that even though the NGR resistance decreases but the neutral current remains unchanged. As a result, the trajectory moves along a constant current characteristic. The trajectory remains totally inside the dead zones even if the NGR resistance decreases down to 5Ω .

On the other hand, the failed-open NGR condition, studied in scenarios 26-28, are shown as well. In these scenarios, the fault resistance is very low and the neutral current is completely dependent to NGR resistance. Additionally, the phase-to-ground voltage

appears across the NGR. In other words, the fault resistance does not experience any voltage. As a result, the voltage across NGR remains constant equal to phase-to-ground voltage and the trajectory moves inside the dead zones, as shown in Equation (3.5) by Sc26, Sc27, and Sc28, and the NGR is detected healthy while it is failed-open.

Configuration 2 - High Resistance Grounded DYg Distribution Transformer

In the second configuration, a high resistance grounded utility supplier is studied in the same way as the previous configuration. There is a minor but very important difference, and that is the larger system charging capacitance of the distribution network compared to generation system. Typically, the system charging capacitance of a generator is very low and less than $5\mu\text{F}$, while the system charging capacitance of a distribution system is very high with the maximum of $500\mu\text{F}$. Moreover, the distribution networks are more unbalanced in contrast to generators due to distributed loads across the wide area of the distribution system. As known, higher imbalance of the system will cause more voltage across the NGR specially if the system charging capacitance is high as seen in distribution

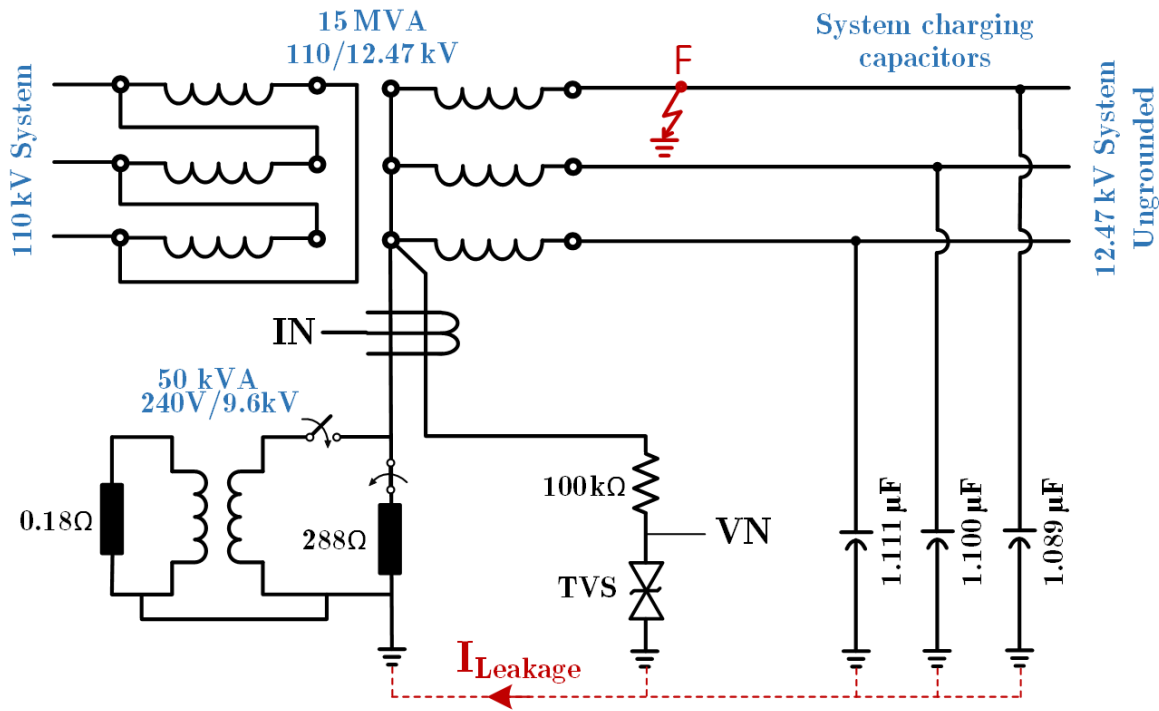


Figure 3.6: High resistance grounded DYg distribution transformer.

networks. As such, higher voltage and current is expected in the new configuration which is referred to as Configuration 2, as demonstrated in Figure 3.6. The NGR can be inserted either directly between the neutral and earthing points, or at the secondary of the NGT. The NGR and NGT are designed based on a step by step methodology provided in [3].

As shown, the voltage level and measurement instruments are identical to the previous configuration to only focus on the performance of the monitoring method.

The same analysis as the previous configuration was carried out for this configuration. With the system charging capacitance of only three times the previous configuration, higher voltage was observed at neutral. As may be realized, higher voltage at neutral during the unfaulted operation condition might disable the impedance supervision logic since the clamping level of the TVS diode is only 100 V peak. However, this clamping level is well-designed since the neutral of most of distribution systems will not experience such a voltage level in the absence of ground faults. As such, the performance of the monitoring method P6 is the same for this configuration. Therefore, it is suggested to read the analysis of the previous configuration, included in Tables 3.1-3.5, to figure out the behavior of this monitoring technique for the new configuration.

Configuration 3 - High Resistance Grounded YD Distribution Transformer

In this section, the operation of method P6 is studied for monitoring the status of a high resistance NGR installed at the neutral of a zig-zag grounding transformer, which grounds the terminals of the secondary of a wye-delta utility supplier that feeds an ungrounded distribution network. The connection diagram of the complete system is depicted in Figure 3.7.

The distributed charging capacitances of the distribution system, considering the transformer phase-to-ground windings, grounding transformer, unbalanced loads, 12.470 kV bus, surge arresters, and circuit breakers, are lumped into one three-phase unbalanced capacitor equal to $1.100\mu\text{F}$ that is connected to 12.47 kV bus. In this configuration, $\pm 0.1\%$ drift in capacitance of the system charging capacitors causes around 10 V and 30 mA in neutral system.

The specifications of the zig-zag transformer have been chosen based on [36, 37, 38].

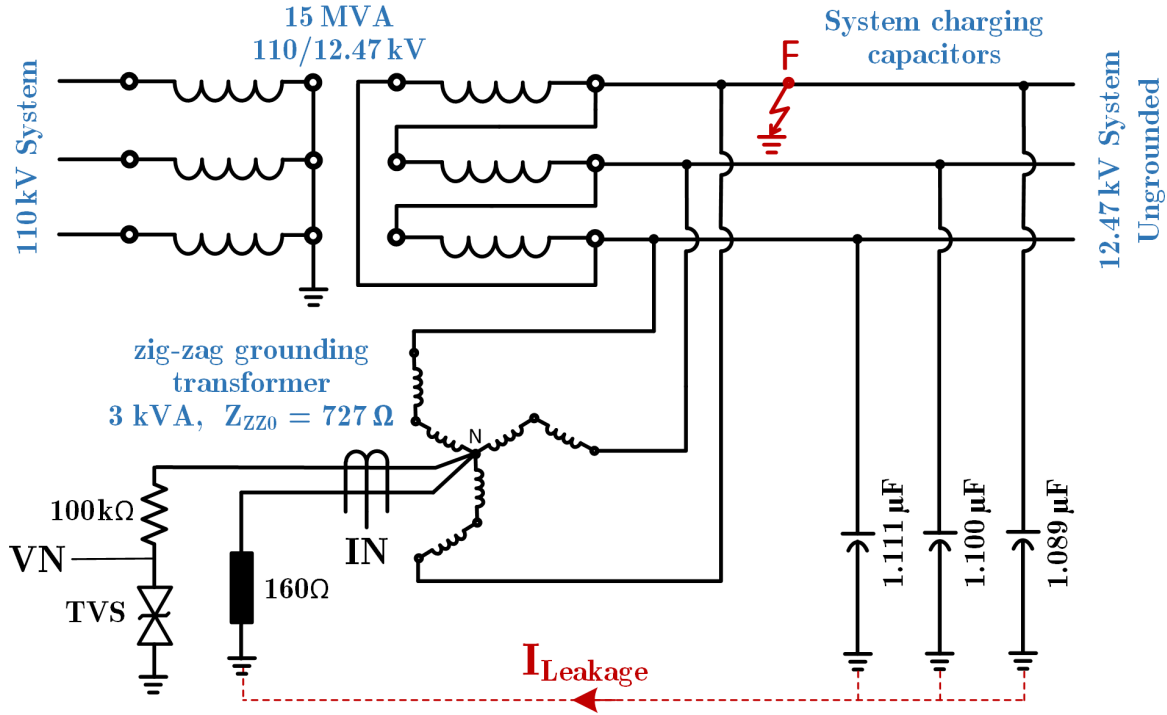


Figure 3.7: High resistance grounded wye-delta distribution transformer.

This connection is obtained by three single-phase transformers. The voltage rating of each phase transformer is less than the phase-to-ground voltage by a factor of $\sqrt{3}$, i.e., $V_{LG}/\sqrt{3}$ or 4.157 kV. Furthermore, the turn ratio of all phase transformers is unit meaning that the voltage rating of the primary and secondary sides are the same. However, the maximum voltage across the neutral system is still equal to V_{LG} , i.e., 7.2 kV. Reminding that the NGR is designed to limit the ground current to 25 A, the capacity of the one-phase transformers is calculated as follows.

$$I_{PH} = \frac{I_{let}}{3} = \frac{25 \text{ A}}{3} = 8.333 \text{ A} \quad (3.7)$$

$$S_{PH} = \frac{V_{LG}}{\sqrt{3}} I_{PH} = S_{PH} = \frac{12.47 \text{ kV}/\sqrt{3}}{\sqrt{3}} 8.333 \text{ A} = 34.64 \text{ kVA} \quad (3.8)$$

where the S_{PH} is the capacity of each of the one-phase transformers, and I_{PH} is the maximum current that each transformer experiences. This current is very weak during the loading condition since the positive sequence impedance of the zig-zag transformer is very high. But, when the line-to-ground faults happen, it rises to its maximum level

equal to $I_{PH} = 8.33 \text{ A}$. Since the neutral is high-resistance-grounded, the I_N should be limited to 25 A. Accordingly, the current flowing through each phase transformer is equal to 8.333 A [37]. Then, the rating of the phase transformers is obtained 34.64 kVA. To meet the 10 s duty requirement, just 3% of the continuous rating is required as per the IEEE Standard 32 [36]. Therefore, three one-phase 1.04 kVA transformers, rounded off to 1 kVA, are chosen. Thereby, the capacity of the zig-zag transformer bank should be 3 kVA.

The zig-zag connection has been modeled in PSCAD based on [38]. Three 1 kVA and 4.157 kV single phase transformers are combined as depicted in Figure 3.8. The leakage reactance of the phase transformers are the same and equal to 4.3%, perunitized based on their own parameters.

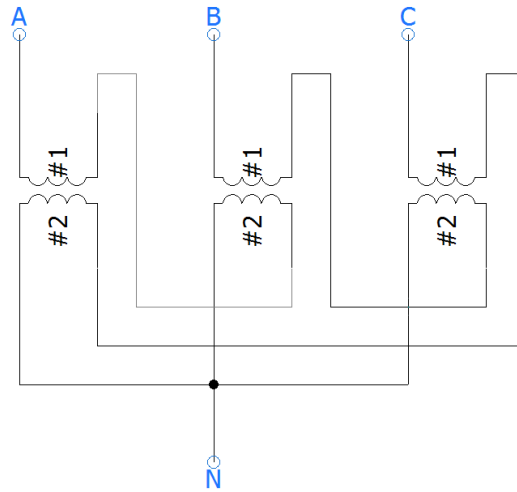


Figure 3.8: The zig-zag connection modeled in PSCAD.

The positive and negative sequence impedances of the connection are very high [38]. But, the zero sequence is so low that it conducts the imbalance current during the unfaulted conditions. The software simulation clearly shows that the positive and negative sequence impedances are indefinite. But, the zero sequence impedance is definite and cannot be simply derived from the simulation. Following, the zero sequence impedance of the zig-zag connection is calculated based on sequence network analysis and a simple test using the software simulation.

In order to calculate the zero sequence impedance of the zigzag connection, assume

that a solid single phase to ground fault, AG, happens at 12.47 kV busbar. The NGR is shorted to avoid its impact on the calculations. The zero sequence impedance of the zig-zag connection is then obtained as follows [39]:

$$Z_{ZZ0} = \frac{V_{LG}}{I_0} = \frac{V_{LL}/\sqrt{3}}{I_N/3} = \frac{\sqrt{3} V_{LL}}{I_N} \quad (3.9)$$

The I_N has been obtained 29.7 A by PSCAD simulation. As such, the Z_{ZZ0} comes equal to 727Ω . Now, the NGR resistance should be calculated. In order to calculate the NGR resistance, the sequential network of the configuration is derived, as depicted in Figure 3.9. The following relationships are then derived based on sequential network analysis.

$$V_0 = \frac{1}{3} (V_a + V_b + V_c) = \frac{1}{3} (3 V_{PH} \angle 180^\circ) = -V_{PH} \quad (3.10)$$

$$\text{also, } V_0 = (Z_{ZZ0} + 3 NGR) I_0 = \left(\frac{Z_{ZZ0}}{3} + NGR \right) I_N \quad (3.11)$$

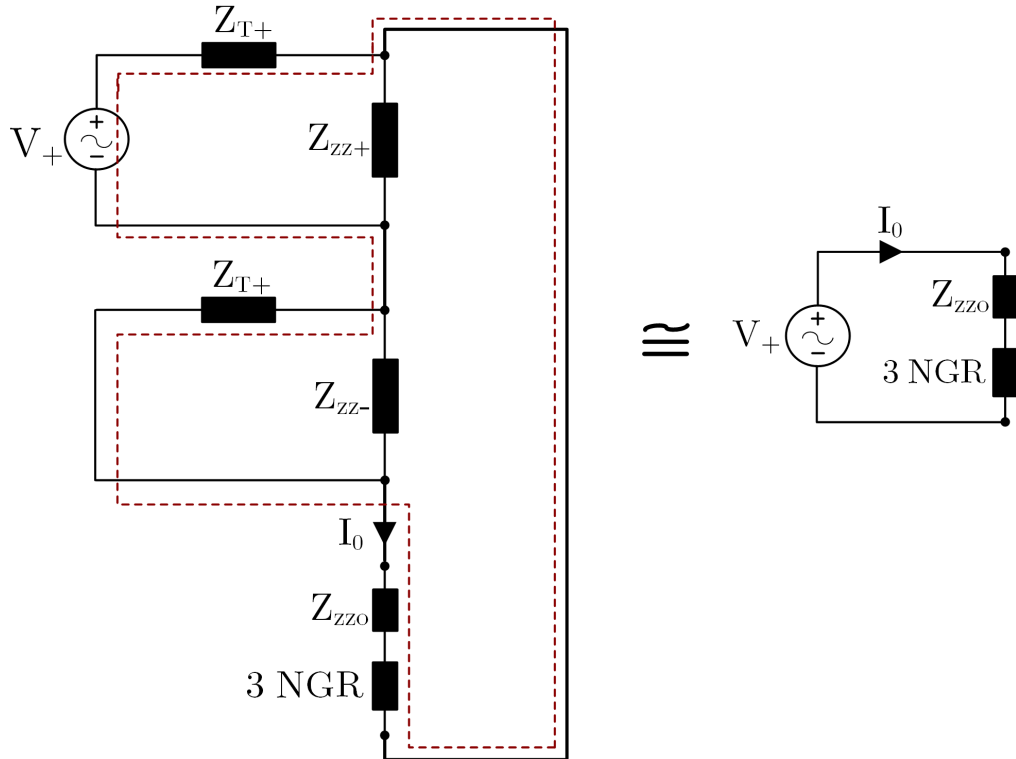


Figure 3.9: Sequential network of configuration 3 for LG fault at 12.47 kV busbar.

$$\text{hence, } \frac{V_0}{I_N} = \frac{-V_{PH}}{I_N} = \frac{Z_{ZZ0}}{3} + NGR \quad (3.12)$$

$$\Rightarrow \frac{-7.2 \text{ kV}}{25 \text{ A}} \angle(\varphi_{V_{PH}} - \varphi_{I_N}) = j242.33 + NGR \quad (3.13)$$

$$(A = B \Rightarrow A \cdot A^* = B \cdot B^*) \Rightarrow NGR = \sqrt{288^2 - 242.33^2} = 155.63 \Omega \quad (3.14)$$

Finally, the NGR is obtained rounded off to 160Ω . As observed, it is less than 288Ω as expected earlier. It should be noted that since the NGR has been changed for this configuration, the VN Trip Level of the overvoltage element of the monitoring algorithm should be updated. This setting is achieved by multiplying the NGR resistance to 20% of the neutral CT rating which comes equal to 13% or 800 V.

The same studies as the previous configurations are carried out for this configuration as well. As expected and as clearly mentioned in [19, 20], the monitoring algorithm operation is satisfactory during the loading condition. However, its performance during the ground faults is not dependable. Following, the results of performance analysis are represented through a few tables that contain 50 scenarios to analyze the operation of the algorithm for the same case studies investigated for the previous configurations.

The status of the NGR is properly monitored when a single fault or failure happens as represented in Tables 3.6 and 3.7. In other words, the algorithm operates reliably when the system is healthy and the NGR fails, or when the NGR is healthy and a fault

Table 3.6: Case 1 – Monitoring a healthy NGR during various system faults.

Scenario No.	GF Type	V_N / V_{LG}	NGR (p.u.)	NGR Status	GF Trip
1	—	0.0005	1.0	NF	0
2	AG	0.2000	1.0	NF	1
3	AG	0.4000	1.0	NF	1
4	AG	0.6000	1.0	---	---
5	AG	0.8000	1.0	---	---
6	AG	1.0000	1.0	---	---
7	BC	0.0004	1.0	NF	0
8	BCG	0.5600	1.0	NF	1
9	ABC	0.0005	1.0	NF	0
10	ABCG	0.0003	1.0	NF	0

happens. In fact, when the neutral voltage is low, and the system is not experiencing any ground faults the monitoring method uses the impedance supervision scheme which functions reliably. In Table 3.6, the dashed cases mean that the scenario is not practical. The main reason is the zero sequence impedance of the zig-zag transformer which limits the voltage across the NGR to 4 kV or 56% of the V_{LG} .

Table 3.7: Case 2 – Monitoring the failed NGR during unfaulted condition.

Scenario No.	GF Type	V_0 / V_{LG}	NGR (p.u.)	NGR Status	GF Trip
11	—	0.0005	0.1	F	0
12	—	0.0005	0.2	F	0
13	—	0.0005	0.4	F	0
14	—	0.0005	0.8	F	0
15	—	0.0005	1.2	F	0
16	—	0.0005	2.0	F	0
17	—	0.0005	5.0	F	0
18	—	0.0005	10.0	F	0
19	—	0.0005	20.0	F	0
20	—	0.0005	30.0	F	0

This monitoring method fails to detect the precise status of the resistor in case the NGR fails during a ground fault which is called double fault condition. In fact, the neutral voltage is not available during this condition. Thereby, the monitoring method relies on neutral current supervision logic which is not dependable. The weakness of this logic is more highlighted while studying this configuration.

When the double faults happen, i.e., system fault followed by an NGR failure, the algorithm mostly fails. The results of monitoring different NGR failures during a LG fault at 12.47 kV busbar are demonstrated in Table 3.8. In these scenarios, the system fault happens first, and then the NGR fails. The voltage across the NGR upon LG fault incidence is 56% of the system phase-to-ground voltage, i.e., 4 kV. The NGR starts failing short or open three power cycles after the ground fault occurrence.

The algorithm fails for all of the scenarios except one case. When NGR resistance falls to very low values, scenarios 21 to 23, the NGR current does not grow noticeably. For the same conditions of the previous configurations, the neutral current increased strikingly. The algorithm reported the NGR failure because the CT sensed a current

more than 100% of its rating. In this configuration, the neutral current is limited by the zero sequence impedance of the zig-zag transformer even though the NGR is failed-short. Hence, the current measured by CT remains less than 100% of the CT rating even when the NGR becomes shorted. The inverse condition happens in scenarios 26-29, but, the neutral current does not decrease enough to set the 5% threshold. Therefore, the failed-open NGR condition remains undetected as well. The scenario 30 is detected correctly because the neutral current is less than 5% of the CT rating.

The scenarios 22 and 29 have been investigated during different system faults as demonstrated in Table 3.9 and Table 3.10. In scenarios 32-36, the algorithm faces the same problem as scenario 22. Since the NGR current is sensed between 5% and 100% of the CT rating, it is reported healthy while it is not. The failed-open NGR is securely

Table 3.8: Case 3 – Monitoring the failed NGR during a LG fault at 12.47 kV busbar.

Scenario No.	GF Type	V_0 / V_{LG}	NGR (p.u.)	NGR Status	GF Trip
21	AG	0.56	0.1	NF	1
22	AG	0.56	0.2	NF	1
23	AG	0.56	0.4	NF	1
24	AG	0.56	0.8	NF	1
25	AG	0.56	1.2	NF	1
26	AG	0.56	2.0	NF	1
27	AG	0.56	5.0	NF	1
28	AG	0.56	10.0	NF	1
29	AG	0.56	20.0	NF	1
30	AG	0.56	30.0	F	1

Table 3.9: Case 4 – Monitoring a failed-short NGR during various system faults.

Scenario No.	GF Type	V_N / V_{LG}	NGR (p.u.)	NGR Status	GF Trip
31	—	0.0005	0.2	F	0
32	AG	0.2000	0.2	NF	1
33	AG	0.4000	0.2	NF	1
34	AG	0.6000	0.2	NF	1
35	AG	0.8000	0.2	NF	1
36	AG	1.0000	0.2	NF	1
37	BC	0.0004	0.2	F	0
38	BCG	0.5600	0.2	NF	1
39	ABC	0.0005	0.2	F	0
40	ABCG	0.0003	0.2	F	0

monitored during different system faults as demonstrated in Table 3.10. The NGR current declines to less than 5% of the CT rating and the NGR failure is detected. However, if the NGR fails partially, e.g., 5 pu, it will be undetected due to higher level of the neutral current which is higher than the 5% threshold. In fact, the partially failed-open NGR remains unidentified for the same reason as the failed-short NGR condition.

Table 3.10: Case 5 –Monitoring a failed-open NGR during various system faults.

Scenario No.	GF Type	V_N / V_{LG}	NGR (p.u.)	NGR Status	GF Trip
41	—	0.0005	20	F	0
42	AG	0.2000	20	F	1
43	AG	0.4000	20	F	1
44	AG	0.6000	20	---	---
45	AG	0.8000	20	---	---
46	AG	1.0000	20	---	---
47	BC	0.0004	20	F	0
48	BCG	0.5600	20	F	1
49	ABC	0.0005	20	F	0
50	ABCG	0.0003	20	F	0

Lastly, it is concluded that the NGR is satisfactorily monitored during the load condition. The algorithm does not function correctly when NGR fails during the faulted condition specially if the grounding is performed using zig-zag grounding transformer. Moreover, this monitoring method cannot function in de-energized operation condition of any of the power systems. However, it is of interest since it guarantees a reliable detection in unfaulted operation condition of the power system.

3.2 Method P5 - NGR Monitoring Using Resistive Potential Divider (RPD) and Neutral CT

In this section, the performance of the fifth passive monitoring method, i.e., method P5, is studied. This method has been implemented, verified and widely employed in distribution systems during recent years [16, 17]. Hence, it will be worthwhile to study and understand its performance. The main concepts and principles of this method have been reviewed in chapter. This section conducts the detailed studies on modeling and

behavior analysis of this method. It employs the Resistive Potential Divider (RPD), and a neutral CT that to measure the neutral voltage and current respectively. As may be realized, the RPD does not exist in most of the applications and is an additionally required apparatus causing more expense compared to the monitoring methods that use the existing measurement instruments.

Following, the detail principles and concepts of the algorithm are covered using an extracted monitoring algorithm. The dead zones of the algorithm are also derived to show the blind regions of its operation. Thereafter, the performance and functionality of the method are investigated for three different power system configurations through 150 scenarios. Finally, learned lessons will be included summarizing the defects, issues, advantages, and disadvantages of this method.

3.2.1 Monitoring Algorithm

Decision-Making Flowchart

In the same way as the previous monitoring method, the main principles of the monitoring algorithm are divided into four major protection/monitoring elements. Two elements provide ground fault protection. The other two elements monitor the status of the NGR. The complete flowchart of the monitoring algorithm is shown in Figure 3.10. It should be noted that the ground fault protection is not a focus of this research work; however, it is believed that the NGR monitoring is very much connected to ground fault protection. As such, the ground fault protection is investigated in parallel with the intended monitoring practice as well.

In order to clearly introduce each part of the scheme, a different color is assigned to each element. For example, the overcurrent ground fault protection element is differentiated by green color and coded as 50G. The other element is the overvoltage ground fault protection, represented in blue and coded as 59G. This element detects the ground faults in case the system becomes ungrounded. The last element, shown in red, is the main focus of the work which is the monitoring scheme. It itself consists of two separate logics, as mentioned on top of the monitoring block. The right side functions during

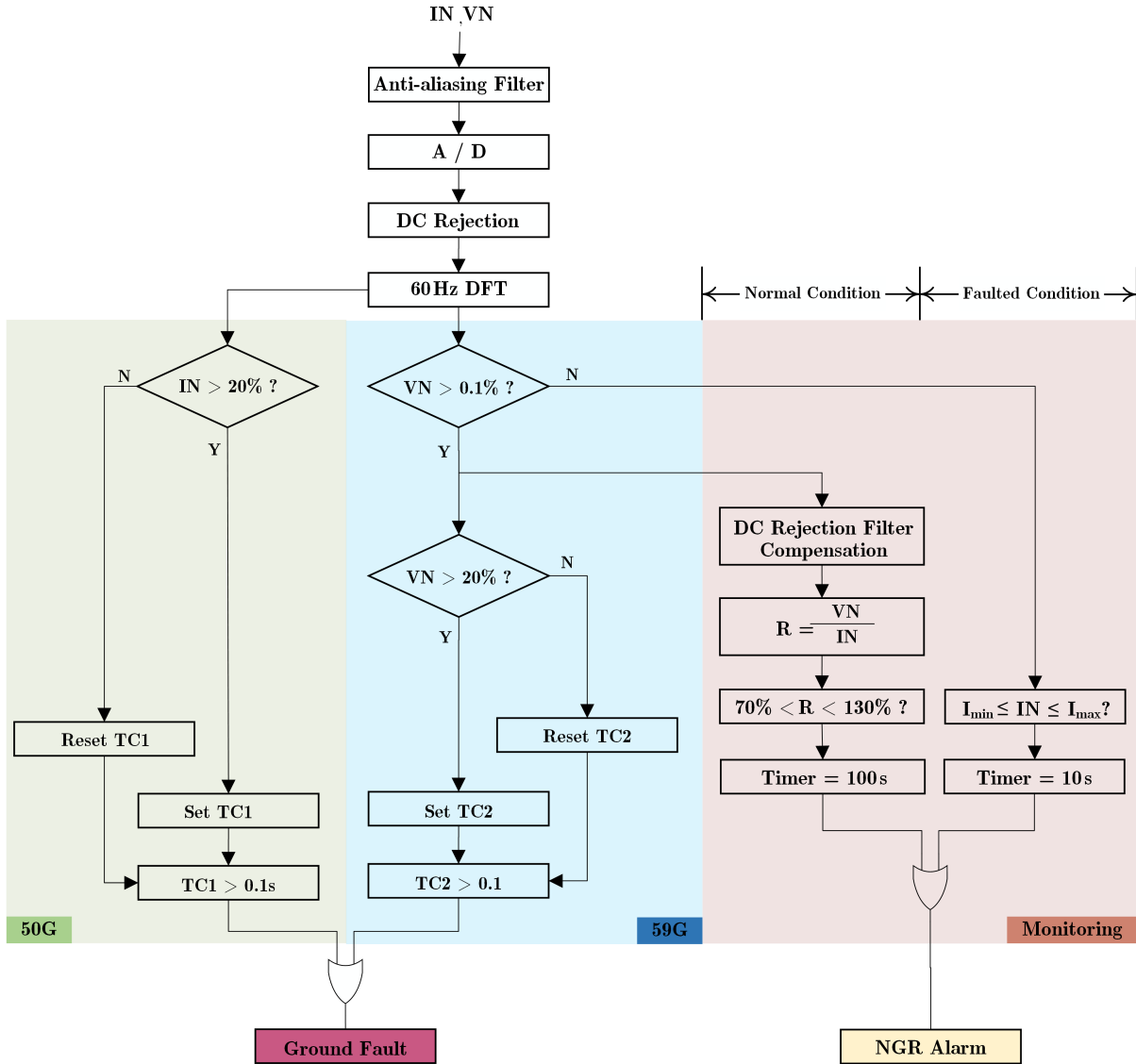


Figure 3.10: Decision making flowchart of the monitoring method P5.

the faulted condition while the left side element operates during the normal operation condition where the voltage across the neutral grounding resistor is very low.

Since the main focus of the work is the monitoring part of the algorithm, the protection elements are not discussed anymore. The main issue facing this method is the minimum accuracy limit of the RPD that measures the neutral voltage. In MV systems, the neutral voltage can be measured with less than 3% error over 0.1-125% using sampling resolution of 4096. This means that the very weak voltage across the neutral system that appears during the normal operation condition can be accurately measured if it is

within this range. If this constraint gets satisfied, both of the voltage and current signals of the NGR become available with an acceptable accuracy. Therefore, the impedance of the NGR can be obtained using Ohm's law. Following, a calibration margin is used to identify the intact NGR considering $\pm 10\%$ measurement inaccuracy and 8% drift due to temperature rise knowing that the temperature coefficient of the well-designed resistors is about 200 PPM/ $^{\circ}\text{C}$.

$$R_{meas1} = \frac{(1 + 10\%)VR/3}{(1 - 10\%)IN} = 1.22R_{NGR} \Rightarrow +22\% \text{ error} \quad (3.15)$$

$$R_{meas2} = \frac{(1 - 10\%)VR/3}{(1 + 10\%)IN} = 0.81R_{NGR} \Rightarrow -19\% \text{ error} \quad (3.16)$$

The maximum error of the obtained resistance of the NGR due 10% measurement inaccuracy is 22%. Adding the 8% drift due to temperature impact, the calibration margin should be set to $\pm 30\%$ drift from the rated value which is 70-100%. If the calculated resistance goes out of this safe zone, the NGR alarm will be initiated considering 10 s time delay.

When the neutral voltage is very weak and not measured accurately, the monitoring algorithm relies on neutral current supervision. It supervises the magnitude of this parameter. If it does not fall within a preset safe region, then the failed NGR is reported considering 100 ms time delay to detect it before circuit breaker disconnects due to ground fault trip. The current supervision logic is defined as follows.

$$I_{min} \leq I_N \leq I_{max} \quad (3.17)$$

$$I_{min} = 0.01\% \quad \text{and} \quad I_{max} = \frac{0.1\% V_{LG_{PT}}}{0.7 \text{ NGR}} \quad (3.18)$$

If the neutral current is less than I_{min} , the failed-open NGR will be reported. In addition, the 0.1% of $V_{LG_{PT}}$ is the minimum accurately measured voltage at neutral. This voltage causes the maximum current to be used by the current supervision element of the algorithm. In other words, if the voltage is less than 0.1%, and the sensed current is more than I_{max} , the failed-short NGR will be indicated.

Dead Zones of The Algorithm

The dead zones of the monitoring algorithm are demonstrated as well. In fact, the conditions that the algorithm fails to function correctly are shown. The complete set of all of the failure conditions make the blind regions or the dead zones of the method. The only way to extract these zones is to examine different conditions and practical levels of the employed parameters. In this case, the voltage and current signals of the neutral system are dominant. Hence, the operation of the algorithm is manually checked for different levels of these parameters. Since the measured current signal is more reliable due to acceptable accuracy of the used CT, the only parameter that remains determinative is the neutral voltage. This means that if any full range voltage measurement mechanism emerges in future, then this algorithm will not have any dead zones at all. Anyways, different levels of the neutral voltage should be investigated for extracting the dead zones of the algorithm.

As mentioned, any voltage greater than 0.1% is accurately measured. Under this condition, the neutral current is also available with acceptable accuracy. Therefore, the resistance of the NGR can be obtained with less than 30% error. Under this situation, there will not be any dead zone for the monitoring algorithm since it functions exactly like an ohmmeter. However, if the voltage level becomes less than 0.1%, the voltage signal cannot be used due to inaccurate metering. But, the current signal is still reliable because the current sensor operates with a very negligible error. In this case, the measured current is supervised. It means that if the current magnitude goes beyond the maximum expected value, a failed-short NGR will be reported. Moreover, a failed-open NGR will be detected if the current declines to less than a minimum predefined value. These values have been addressed as I_{max} and I_{min} in the previous subsection.

The obtained dead-zones characteristic of the algorithm for the chosen high-resistance grounded system is demonstrated in Figure 3.11. In this case, the line-to-ground voltage of the system is 7.2 kV which is the maximum voltage that appears across the neutral-to-ground system. The neutral current is limited to 25 A using a 288 Ω NGR. As known, the calibration margin is 201.6-374.4 Ω , i.e., 70-130% of the NGR resistance. It means

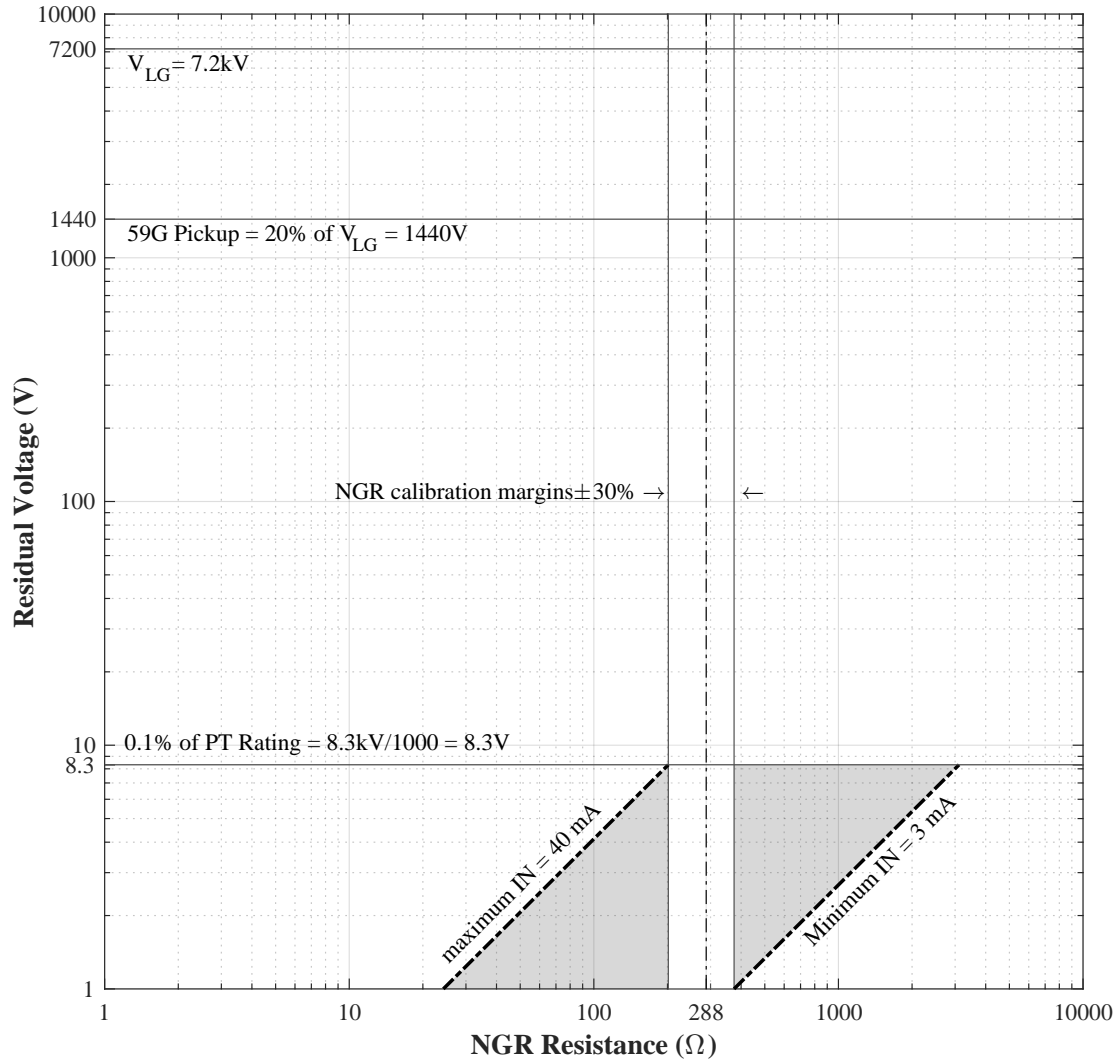


Figure 3.11: The dead zones characteristic of the method P5.

that if the obtained resistance of the NGR falls within this interval, it should be reported healthy. As shown, the dead zones happen only when the NGR voltage is less than 0.1% of the 7200 V. In this case, a failed NGR is reported healthy if its current is within the safe region obtained by 3.17. There are many conditions that although the NGR is not healthy, but, since the measured current is within this region, its status is reported intact or healthy. For example, when the voltage of the NGR is just 2 V, even a highly shorted NGR, $30\ \Omega$, is not detected. The same issue happens when the voltage is a little bit less than 0.1% but the current of the highly open NGR is more than the minimum limit, $V_N=6\ \text{V}$ and $I_N=4\ \text{mA}$.

3.2.2 Performance Analysis

In this section, the performance of the monitoring method P5 is investigated for the same case studies and configurations performed for the previous monitoring method.

Configuration 1 — High Resistance Grounded Generator

The connection diagram of the configuration is shown in Figure 3.12. It is basically the same as the first configuration studied in the analysis of the previous monitoring method. Further details of the system can be found from Section 3.1.2. The only difference is the neutral voltage metering mechanism which is a RPD here. It consists of two series resistors that are inserted between the neutral and earthing points of the generator. The $100\text{ k}\Omega$ resistor provides protection and isolation from the high voltage system. The neutral voltage is obtained by scaling up the sensed voltage by a factor equal to the ratio of the resistors, i.e., 100.

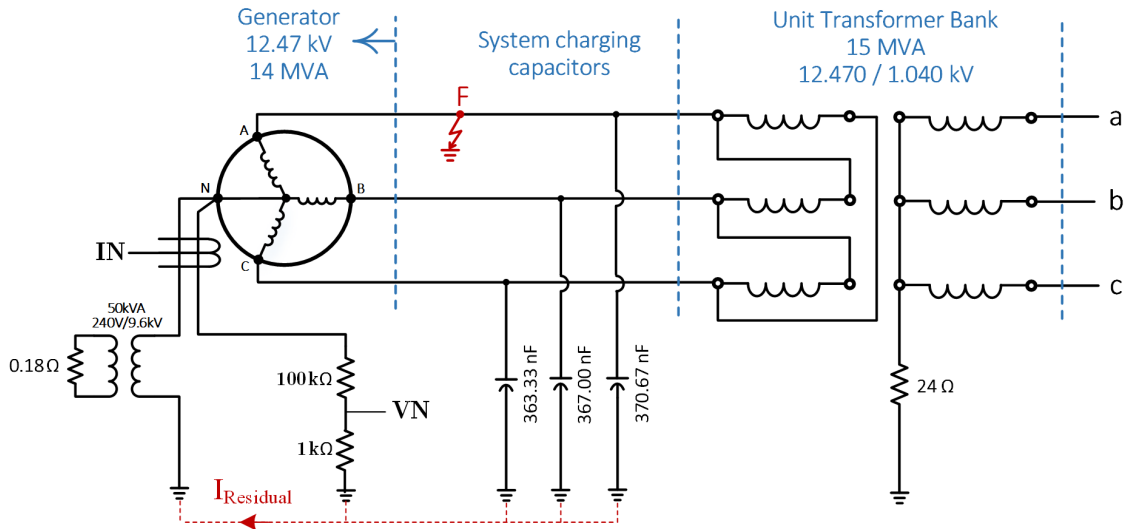


Figure 3.12: High-resistance-grounded unit-connected generator.

Case 1 — Monitoring a Healthy NGR During Various System Faults: The operation of the monitoring method will be investigated for five different cases. The first case is the condition that the NGR is healthy, $288\ \Omega$ with less than 30% degradation, and the neutral voltage can be any value. Different values of neutral voltage occur during

different operation modes of system. For example, the very weak voltages appear during the loading condition while the very high voltages are experienced during the terminal LG fault. The voltage level during the faulted condition is dependent to fault resistance and fault location. Hence, the fault resistance will be the key parameter to induce different voltage levels across neutral system.

In order to monitor a healthy NGR during different operation modes of the system, 10 scenarios are simulated in PSCAD. The captured waveforms of the generator neutral voltage, and neutral current are played back to Matlab-based model of the relay, and its performance is observed as demonstrated in the following table.

Table 3.11: Case 1 - Monitoring a healthy NGR during various system faults.

Scenario No.	GF Type	V_N / V_{LG}	NGR (p.u.)	NGR Status	GF Trip
1	—	0.0008	1.0	NF	0
2	AG	0.2	1.0	NF	1
3	AG	0.4	1.0	NF	1
4	AG	0.6	1.0	NF	1
5	AG	0.8	1.0	NF	1
6	AG	1.0	1.0	NF	1
7	BC	0.0006	1.0	NF	0
8	BCG	1.0	1.0	NF	1
9	ABC	0.0005	1.0	F	0
10	ABCG	0.0004	1.0	F	0

As shown, 10 scenarios have been carried out. The level of the neutral voltage has been shown per-unitized based on the system phase-to-ground voltage, i.e., 7.2 kV. The NGR status is abbreviated by NF or F representing no failure or failure, respectively. Besides, the ground fault protection has been implemented and tested. The ground fault detection outcomes are also represented under GF Trip column. The GF Trip equal 0 means absence of ground faults while GF Trip equal 1 means the ground fault presence. For example, the first scenario shows that the residual voltage magnitude is just 0.0008 pu. This means that the voltage across the NGR is very weak and equal to 5.76 V. This voltage level appears during the load condition and appears due to imbalance of the system three-phase charging capacitors. Since the voltage is very weak, the protection elements should not detect any fault. In addition, the NGR had been healthy, 1 pu or

288 Ω . The monitoring algorithm reports NF meaning that the status of the NGR has been correctly detected healthy. The main reason behind the accurate monitoring is the magnitude of the current which is within the safe region, i.e., within the 3-36 mA interval.

In scenario 2, the voltage level is very high and equal to 0.2 pu. The NGR resistance is 1 pu. The status of the NGR is reported correctly as well as the ground fault. The 0.2 pu voltage appears across neutral system due to LG fault with fault resistance equal to 600 Ω . The main reason behind accurate NGR monitoring is the sufficient voltage and current for accurate measurement. The resistance of the NGR is obtained and compared with the 70% and 130% thresholds. The resistance was measured 288 Ω which falls inside the safe region. The same behavior was observed for other scenarios. The only difference is that the current and voltage levels become high enough to actuate both of the protection elements. As a result, the ground fault is detected as well as the status of the NGR. The level of the voltage and current rise in scenarios 3-6 because the fault resistance is much lower compared to scenario 2.

Furthermore, the other types of faults have been investigated as well. It has been observed that the Line-to-Line (LL) faults do not change the level of the neutral voltage and neutral current. In fact, these kinds of faults do not impact on the zero sequence of the network. In scenario 7, a LL fault was investigated. The fault was not detected because the ground network did not interfere in the event. However, the magnitude of the current behaved the same as scenario 1, and the NGR was reported NF or healthy. If the Double-Line-to-Ground (LLG) fault happens, the ground network is affected and the used parameters rise enough for a reliable protection and monitoring. This condition was investigated in scenario 8. The same behavior as scenarios 2-6 was observed. In addition, the three-phase and three-phase-to-ground faults were studied. In both cases, shown in scenarios 9 and 10, the zero sequence experienced no voltage and no current. Hence, the very weak current caused the monitoring algorithm to assume the NGR is failed-open due to absence of the neutral current. Also, the fault was not detected. In fact, these types of the faults are symmetric. In fact, the solid three-phase fault bypasses the unbalanced capacitors at terminals of the generator. The neutral system does not experience any energy flow resulting a totally wrong detection. These scenarios are the

very prominent shortcomings of this monitoring method. In fact, this case shows that if the neutral system becomes de-energized for any reason then the monitoring system will fail. This issue faces all of the passive methods due to absence of the employed electrical parameters.

Case 2 – Monitoring Various NGR Degradations in Healthy System: In the second case, the performance of the monitoring algorithm is studied when the system is healthy. This study shows how reliable the monitoring algorithm is during the system normal operation condition. As mentioned previously, the neutral voltage is very low in the absence of ground faults, the same as scenario 1 where the neutral voltage was 0.0008 pu or 5.76 V. Such a weak voltage appears due to system inherent imbalance. While the system is healthy, the NGR resistance is changed to various levels, and the performance of the monitoring algorithm is observed. As shown, the entirely failed-short or disconnected NGR conditions are considered in software simulations as well as partial failures. The observations are listed in the following table.

Table 3.12: Case 2 - Monitoring various NGR degradations in a healthy system.

Scenario No.	GF Type	V_N / V_{LG}	NGR (p.u.)	NGR Status	GF Trip
11	—	0.0008	0.1	NF	0
12	—	0.0008	0.2	NF	0
13	—	0.0008	0.4	NF	0
14	—	0.0008	0.8	NF	0
15	—	0.0008	1.2	NF	0
16	—	0.0008	2.0	NF	0
17	—	0.0008	5.0	F	0
18	—	0.0008	10.0	F	0
19	—	0.0008	20.0	F	0
20	—	0.0008	30.0	F	0

As mentioned, the voltage across the NGR is 5.76 V which is less than 0.1% of the PT rating meaning that the neutral voltage cannot be measured accurately. Therefore, the monitoring algorithm relies on only the current supervision element. This issue happens in all of scenarios 11 to 20. As explained in Section 3.2.1, the NGR status will be reported failed if the current declines to less than 3 mA or goes beyond 36 mA

considering a time delay of 10s. For scenarios 11-16, the neutral current magnitude falls inside the safe region, and the NGR is reported healthy. Since the NGR resistance is not 288Ω the algorithm has failed for all of these conditions. In scenarios 14 and 15, the NGR resistance is something different than its rated value, 288Ω , but, the algorithm reports healthy NGR since its resistance is not very much drifted from the rated value. In other words, less than 30% degradation is not assumed as NGR failure. The algorithm operates securely for the other scenarios, 17 to 20. In these scenarios, the resistance of the NGR is so high that the supervised current is less than 3 mA. As a result, the failed NGR is reported meaning that NGR is open. Moreover, the ground fault protection schemes function reliably not reporting any ground fault. The voltage and current of the neutral system are so weak that the protection elements are not even actuated. As such, the GF Trip securely remains off.

As observed, the algorithm mostly fails to detect the shorted NGR during the load condition, highlighted in red. Monitoring the status of the NGR during the load condition is very essential because the failed NGR should be maintained before any ground fault incidence. A failed-short NGR replaces the advantages of a high impedance grounded neutral with disadvantages of a solidly grounded system. As a very early conclusion, it can be claimed that this method is not as secure as initially expected due to imperfection of the neutral current supervision scheme.

Case 3 – Monitoring Various NGR Degradations During an LG Fault: The next case is monitoring the failed NGR during a LG fault. This case is almost the same as case 2. The difference is that the neutral voltage is very high caused by a bolted LG fault at terminals of the generator, instead of the very weak voltage experienced in the previous case. The operation of the monitoring algorithm is investigated through 10 scenarios, 21-30. The algorithm is expected to detect a ground fault and failed NGR for all of the scenarios. As such, the NGR status and the GF Trip signals should be F and 1, respectively.

As shown in Table 3.13, the algorithm functions correctly for all of the scenarios. A ground fault has been detected as well as a failed NGR. The ground fault is detected

because the voltage and current measured in neutral system are high enough to actuate the protection elements. Furthermore, since the measured current is valid, the NGR resistance can be obtained. The calibration margins are used to detect the failed NGR. As a conclusion, the monitoring algorithm functions reliably during the ground faults. The main reason behind this behavior is the sufficient voltage and current for measurement during this condition.

Table 3.13: Case 3 - Monitoring various NGR degradations during a LG fault.

Scenario No.	GF Type	V_N / V_{LG}	NGR (p.u.)	NGR Status	GF Trip
21	AG	1.0	0.1	F	1
22	AG	1.0	0.2	F	1
23	AG	1.0	0.4	F	1
24	AG	1.0	0.8	NF	1
25	AG	1.0	1.2	NF	1
26	AG	1.0	2.0	F	1
27	AG	1.0	5.0	F	1
28	AG	1.0	10.0	F	1
29	AG	1.0	20.0	F	1
30	AG	1.0	30.0	F	1

It should be added that the NGR failure affects the operation of the ground fault protection functions. As observed in this study, the over-voltage ground protection fails in scenarios 21 and 22. In fact, the very low resistance of the NGR implies the solidly grounded neutral situation where the neutral voltage cannot rise very much. In these two scenarios, the residual voltage rises to phase-to-ground voltage of the system, 1 pu. However, it declines to less than 20% once the NGR resistance decreases remarkably as seen in these scenarios. Under this situation, the activated ground overvoltage function is deactivated causing maloperation or disoperation of this protective function. The inverse of this condition happens to overcurrent ground protection, observed in scenarios 28-30, when the NGR resistance increases strikingly. However, the two ground protection functions compliment each other, and the ground fault detection is performed reliably.

Case 4 — Monitoring a Failed-Short NGR During Various System Faults.

In this case, the functionality of the monitoring method P5 is investigated for a shorted

NGR during different system faults. In this case, the profile of the neutral voltage is assumed the same as the first case. The controlled value of the fault resistance causes desired amount of voltage across the neutral system. The specific difference of this case to the other cases is the resistance of the NGR which is assumed very low for all of the considered scenarios, 31-40. The observations are listed in Table 3.14.

Table 3.14: Case 4 - Monitoring a shorted NGR during the ground faults.

Scenario No.	GF Type	V_N / V_{LG}	NGR (p.u.)	NGR Status	GF Trip
31	—	0.0008	0.2	NF	0
32	AG	0.2	0.2	F	1
33	AG	0.4	0.2	F	1
34	AG	0.6	0.2	F	1
35	AG	0.8	0.2	F	1
36	AG	1.0	0.2	F	1
37	BC	0.0008	0.2	NF	0
38	BCG	1.0	0.2	F	1
39	ABC	0.0005	0.2	F	0
40	ABCG	0.0003	0.2	F	0

As shown, the monitoring algorithm functions accurately during the faulted condition even if the residual voltage is very low. The main reason behind this fact is nothing but the sufficient voltage and current causing accurate resistance calculation. The same has happened in scenarios 21-30. The same analysis as Case 3 are applicable to this case. It should be noted that scenario 31 results in a wrong detection because the voltage is very low meaning that there is not any ground fault. The voltage is not sufficient to be safely measured. The current magnitude is identified less than 36 mA and a healthy NGR is reported incorrectly, the same as scenario 11. In scenario 37, the LL fault does not cause very high voltage causing the same situation as scenario 31. In scenarios 39 and 40, the correct detection has happened due to absence of the parameters which applies to failed-open NGR. As mentioned, the NGR is shorted which means that the correct detection in scenarios 39 and 40 is not the result of valid functionality.

Again, the conclusion is the better operation during the ground faults. It securely monitors the shorted NGR and reports F as a failed NGR. However, the NGR failure during LL faults is not guaranteed.

Case 5 – Monitoring a Failed-Open NGR During Various System Faults:

The last case is regarding monitoring a failed-open NGR during various system faults. This study is the same as the previous case except that the NGR is open or disconnected instead of being shorted. The open NGR impedance is assumed 20 pu or 5.760 k Ω . The observed operation of the ground fault protection and the monitoring elements are represented in Table 3.15.

Table 3.15: Case 5 - Monitoring a failed-open NGR during various system faults.

Scenario No.	GF Type	V_N / V_{LG}	NGR (p.u.)	NGR Status	GF Trip
41	—	0.0008	20	F	0
42	AG	0.2	20	F	1
43	AG	0.4	20	F	1
44	AG	0.6	20	F	1
45	AG	0.8	20	F	1
46	AG	1.0	20	F	1
47	BC	0.0007	20	F	0
48	BCG	1.0	20	F	1
49	ABC	0.0007	20	F	0
50	ABCG	0.0007	20	F	0

As shown, the monitoring algorithm securely detects the ground faults and the status of the NGR. A failed NGR has been reported for all of the scenarios as expected. Again, the sufficient voltage and current magnitude support a safe metering providing the possibility of resistance calculation. The calibration margins are then checked, and since the calculated resistance falls outside the safe region, the failed NGR is reported. Furthermore, the Line-to-Line faults in scenarios 47-50 do not cause noticeable rise of neutral parameters, but since the NGR resistance is very high the supervised current is lower than $I_{min} = 3$ mA. Thereby, the monitoring algorithm reports a failed NGR for all of these scenarios which is a correct detection. However, the slightly failed-open NGR condition is not detected as shown in scenario 16.

Following, the most important scenarios are discussed using dead zones characteristic of the algorithm. This analysis shows how and why the algorithm fails under specific conditions while it operates securely for the others. The dead zones characteristic of the algorithm itself has been demonstrated in Figure 3.11. In the following figures, the most

important scenarios are plotted on top of this characteristic.

The shorted NGR conditions investigated in case 2, scenarios 11-14, are demonstrated in Figure 3.13. As shown, the actual and obtained V_N - R_N GR trajectories are not the same. The main reason is unavailability of voltage metering under these conditions. Since the voltage is not available, the resistance of the NGR cannot be monitored. It should be mentioned that the more the trajectories match, the safer and more reliable the algorithm becomes. In fact, when the obtained trajectory does not match the actual one, an estimation of the NGR status is used for monitoring. In this case, the trajectories are completely different, and the operation of the algorithm is expected to be unreliable as it is. The NGR resistance is assumed equal to a predefined value, 288Ω , where the I_N

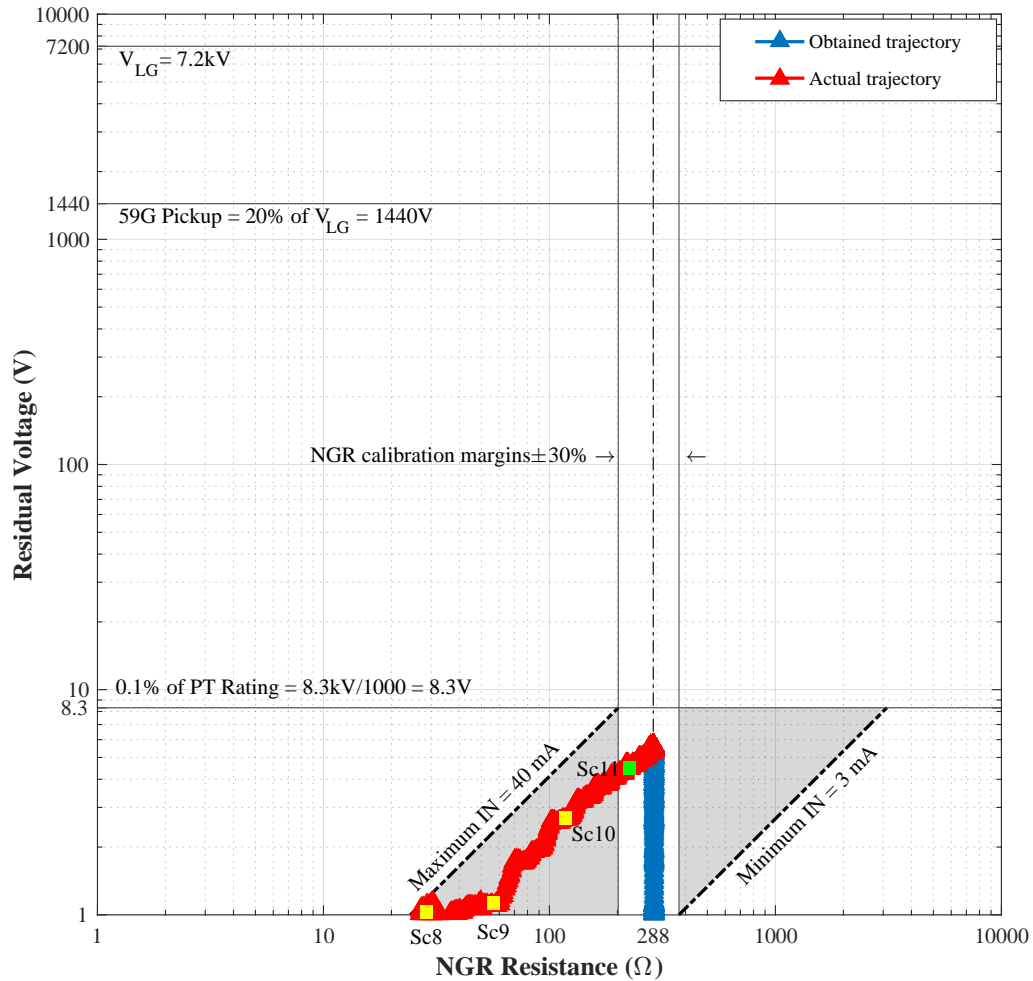


Figure 3.13: Monitoring algorithm operation representation based on dead zones characteristic for scenarios 11-14

is supervised. The obtained trajectory for these conditions, shown in blue, moves inside the NGR calibration margins, and through the safe limits of current. As a result, a healthy NGR is reported for all of scenarios 11 to 14. As represented, scenarios 11 to 13 are marked in yellow to show that the monitoring algorithm functions inaccurately while scenario 14 is marked in green since the NGR is still healthy if its resistance is within the 70-130% zone.

The failed-open NGR conditions investigated in case 2, scenarios 15-20, are demonstrated in Figure 3.14. As shown, both the actual and obtained trajectories are the same. This means that the resistance of the NGR can be obtained if the NGR is becoming open during the loading condition. The only scenario that the algorithm fails to detect the

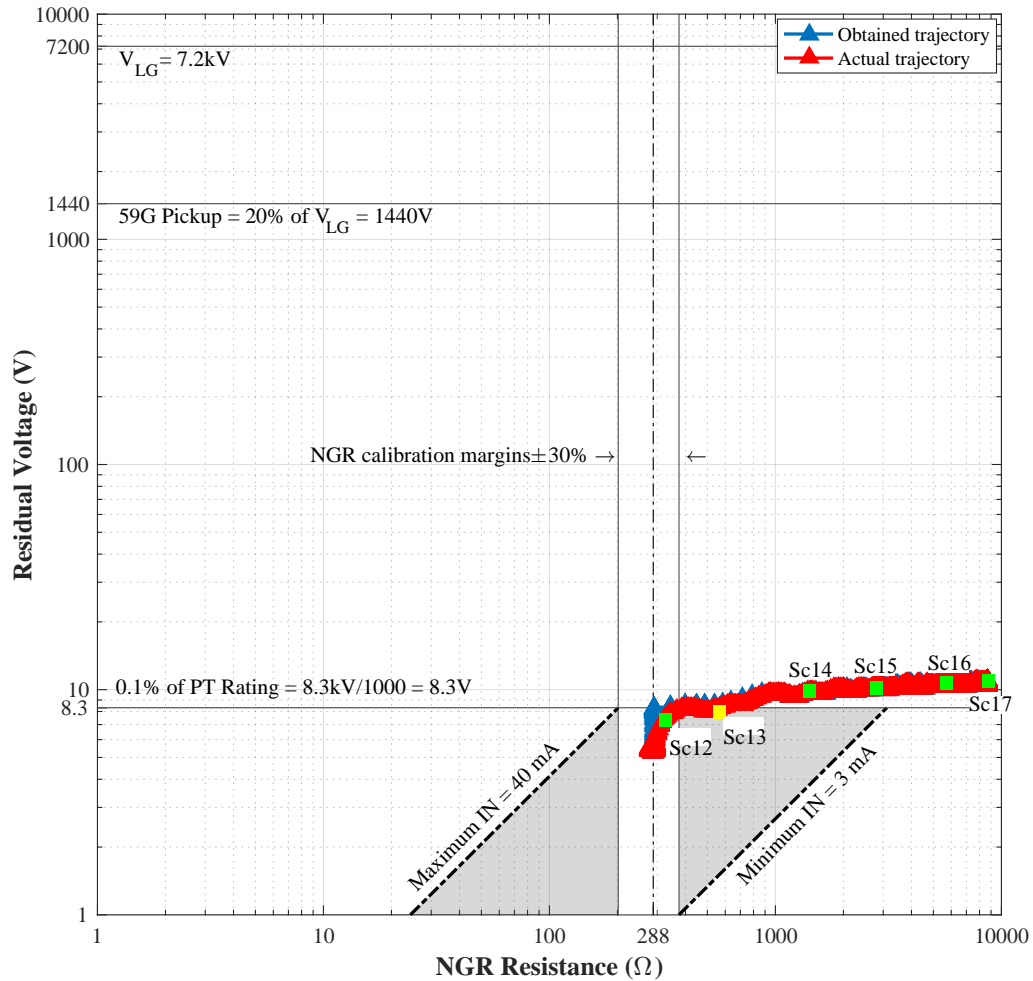


Figure 3.14: Monitoring algorithm operation representation based on dead zones characteristic for scenarios 15-20

failed NGR is scenario 16. The voltage of NGR is less than 0.1% and the current supervision element operates which reports a healthy NGR while its resistance is 2 pu. As shown, the NGR voltage grows as its resistance increases, as experienced in scenarios 17 to 20. Again, the resistance of NGR is calculated, and since it is out of 70-130%, the failed NGR is securely reported for all of the scenarios 17 to 20.

The NGR status during various system faults, scenario 1-5, and 21-24, are shown in Figure 3.15. In these scenarios, NGR becomes shorted during a ground fault at terminals of the generator. As known, the fault resistance is the key parameter to induce the specific levels of voltage across the neutral system. The more the fault resistance grows, the more the neutral voltage becomes. As shown, both the actual and obtained trajectories are exactly the same meaning that precise NGR monitoring is expected as performed in these

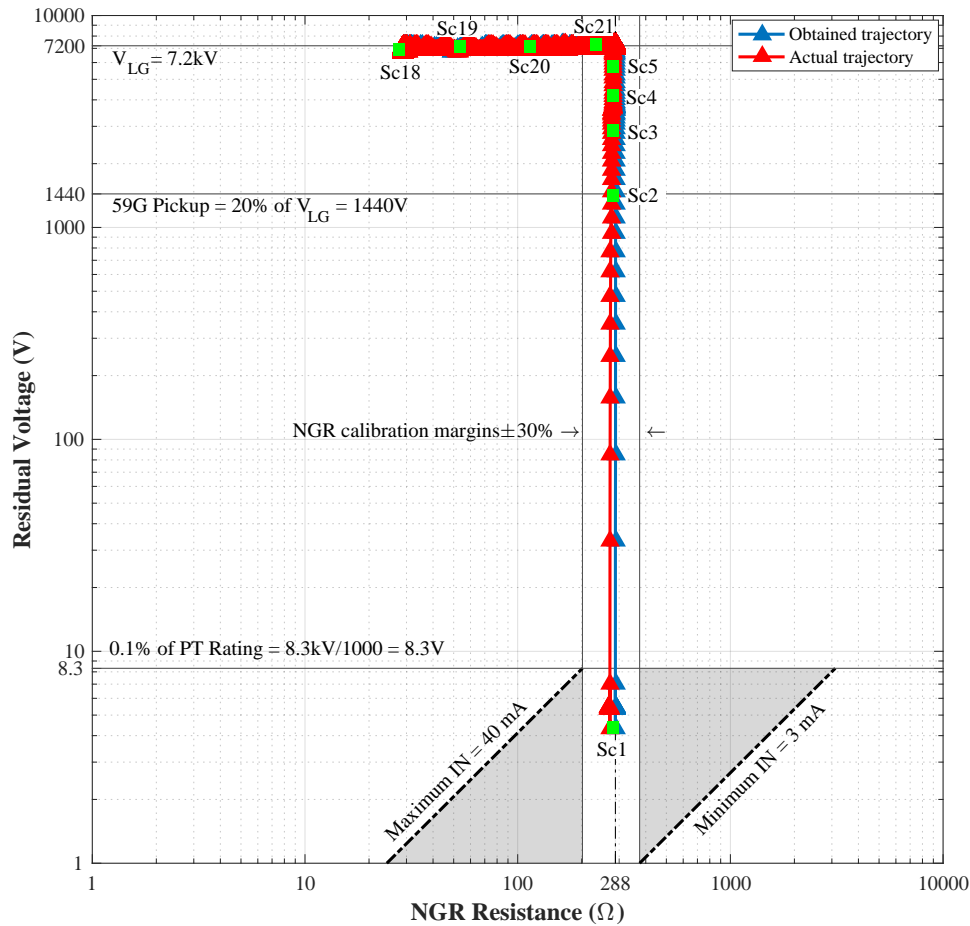


Figure 3.15: Monitoring algorithm operation representation based on dead zones characteristic for scenarios 21-24.

scenarios.

Configuration 2 — High Resistance Grounded DYg Distribution Transformer.

In the second configuration, a high resistance grounded utility supplier is studied in the same way as the previous configuration. There is a minor but very important difference, and that is the higher system charging capacitance in distribution networks compared to generators. Typically, the system charging capacitance of a generator is very low and less than $5\mu\text{F}$, while the system charging capacitance of a distribution system is very high with the maximum of $500\mu\text{F}$. Moreover, the distribution networks are more unbalanced in contrast to generators due to distributed loads across the wide area of the distribution system. As known, higher imbalance of the system will cause more voltage across the NGR specially if the system charging capacitance is high as seen in distribution networks. As such, higher voltage and current is expected in the new configuration demonstrated in Figure 3.16. The NGR can be inserted either directly between the neutral and earthing points, or at the secondary of the NGT. The NGR and NGT are designed based on a step by step procedure provided in [3].

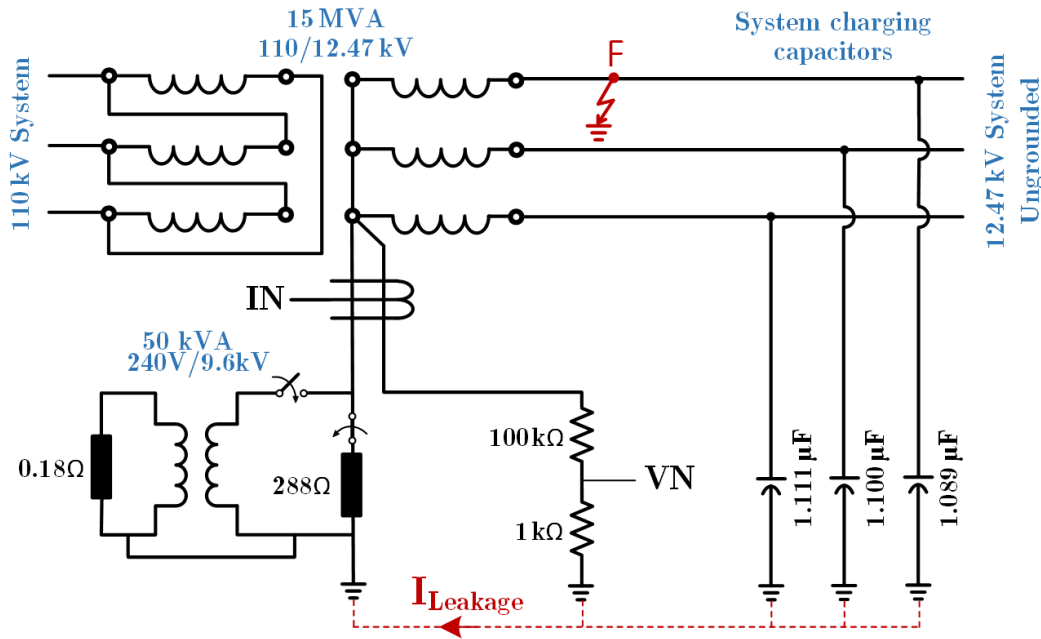


Figure 3.16: High-resistance-grounded DYg distribution transformer.

As shown, the voltage level and measurement instruments are identical to the previous configuration to only focus on the performance of the monitoring method.

The same analysis as the previous configuration was carried out for this configuration. With the system charging capacitance of only three times the previous configuration, higher voltage was observed at neutral. As may be realized, higher voltage at neutral during the unfaulted operation condition is a winning situation for the monitoring method P5 since the higher voltage can be more than the minimum accuracy limit of the RPD. Thereby, the neutral voltage can be measured accurately. Consequently, the NGR at the neutral of a distribution level transformer is monitored better compared to the NGR installed at the neutral of a generator. As a conclusion, this monitoring method is an interesting solution when it comes to monitoring of the NGRs installed at distribution systems.

Configuration 3 — High Resistance Grounded YD Distribution Transformer.

The third studied configuration is the NGR installed at the neutral provided by a zig-zag grounding transformer which grounds the delta side of a wye-delta distribution transformer. The detail explanation and design of this configuration can be found from Section 3.1.2.

In contrast to the previous configuration, the zig-zag connection prevents the appearance of the same voltage at neutral experienced in the previous configuration. In fact, the zero sequence impedance of the zig-zag transformer is in series with the NGR. Therefore, the residual voltage that appears due to system imbalance is divided among the zero sequence impedance of the zig-zag and the NGR with lower contribution of the NGR. However, the system charging capacitance of the distribution system is so high that even 0.1% inherent imbalance of these capacitances causes enough voltage across the NGR. Therefore, the monitoring method mostly relies on NGR impedance supervision which functions reliably. It should be added that if the distribution system is very small, and the system charging capacitances are small, then the probability that the monitoring method relies on neutral current supervision exists. Lastly, the performance of the monitoring method for the delta-delta connected distribution transformer will be the same

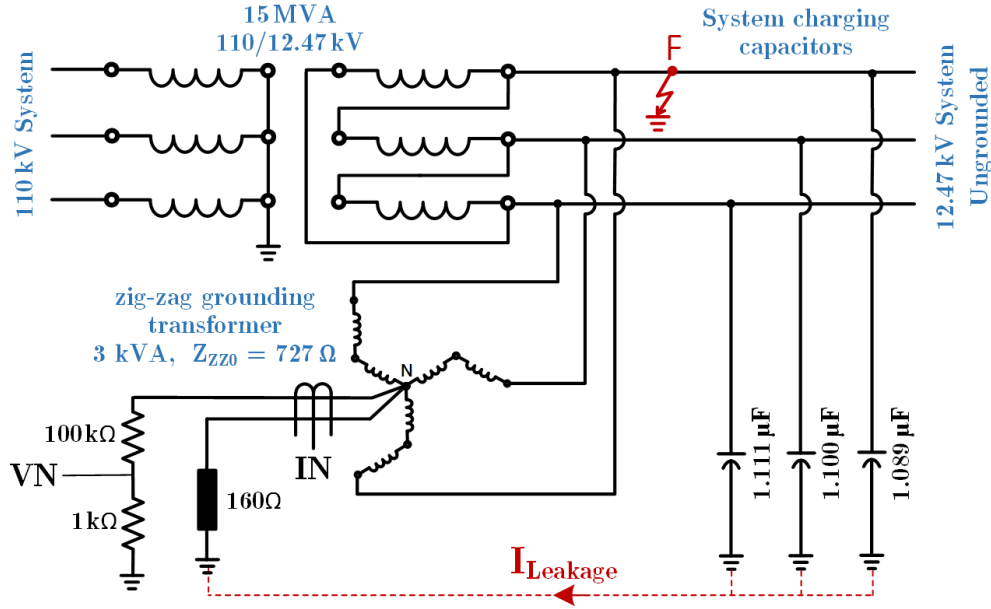


Figure 3.17: High resistance grounded YD distribution transformer.

as presented here.

3.3 Summary

In this chapter, the fundamentals and principles of two existing NGR monitoring methods were used to derive their potential monitoring algorithm. The performance of the methods was investigated under various conditions of the NGR considering three well-known power system configurations that employ the NGRs. The observations were presented through scenario-based tables followed by further analysis using the dead-zones characteristic of the monitoring methods.

The first studied method was the monitoring method P6 which uses a sensing resistor and a sensitive CT. This technique shows reliable performance in loading condition where the neutral voltage is very low. Under this condition, it obtains the NGR resistance and detects any kind of NGR degradation. However, it cannot guarantee a reliable monitoring in the presence of ground fault of any kind. Under this situation, the neutral voltage is not available, and this monitoring method supervises the presence of the neutral current. This kind of monitoring cannot detect the exact status of the NGR and fails in most of

the cases. Moreover, if the NGR is installed at the neutral of the zig-zag connection, the performance of the neutral current supervision monitoring logic is unacceptable. The second analyzed monitoring scheme was the method P5 which uses a resistive potential divider to measure the neutral voltage, and a CT for neutral current measurement. The performance of this monitoring method is the inverse of the monitoring method P6. It cannot function reliably in loading condition except when the neutral voltage is high enough to be measured accurately. However, it guarantees the status of the NGR during the ground faults. As may be realized, the simultaneous use of the monitoring methods P5 and P6 provides a continuous monitor which functions reliably in both unfaulted and faulted operation conditions. That is why these methods were analyzed.

Chapter 4

An Improved NGR and NGL Monitoring Method With Hardware Validation

In this chapter, a new passive and comprehensive monitoring will be proposed. The most prominent advantage of this method is that its functionality is not limited to a specific NGD or power system configuration. The proposed method relies on neutral current measured by a sensitive CT, and neutral voltage measured by a novel wide range voltage measurement instrument. The invented mechanism is actually an enhanced type of the SR which not only clamps and limits the measured voltage to a desired level, but also functions similar to a RPD while clamping the neutral voltage. In other words, it combines the features of the SR and RPD into one instrument that provides accurate measurement of neutral voltage in both normal and faulted conditions of the system.

The monitoring method will be presented in Section 4.1 followed by the fundamentals and concepts of the invented voltage measurement instrument. Thereafter, the performance of the neutral voltage metering instrument will be verified using software studies, and validated using a fabricated prototype. Moreover, the invented voltage measurement mechanism will be employed to monitor the NGDs at neutral of a common configuration of the distribution networks considering various NGDs and different operation modes of the power system. Finally, conclusions will be presented in Section 4.4.

4.1 Proposed Monitoring Method

4.1.1 Monitoring Scheme

A well-designed monitoring technique should continuously check the integrity and intactness of the NGD. As known, the impedance of an element is the most reliable parameter to judge about its integrity and continuity of service. Any change in the physical condition of a component is directly reflected in its impedance. Hence, the more a monitoring technique relies on the impedance of the NGD, the more secure it becomes. However, measuring the impedance of the NGD is not an effortless task. It needs sensitive metering in a high voltage power system which is not supported by conventional measurement instruments.

Using a sensitive CT, full range measurement of neutral current is accomplished. The neutral voltage is measured by a new mechanism which will be explained in next section. Since the current and voltage of the neutral-to-ground circuit are available over their whole possible range, the impedance of the NGD is always obtainable. The normal impedance is the first logic of the monitoring scheme. In fact, if the impedance of the NGD varies significantly, the NGD failure will be reported with a time delay. The NGD failure detection in the presence of ground faults should be as fast as possible which could be achieved using a 100 ms time delay. However, it could be delayed during the normal operation condition, e.g., using a 10 s time delay. On the basis of [19], $\pm 30\%$ change in NGD impedance is sustainable. In fact, the following constraint is the first and the main logic of the monitoring scheme.

$$\text{Logic 1 : } 70\% < |Z_{NGD}| < 130\% \quad (4.1)$$

It should be mentioned that the $\pm 30\%$ margin is obtained considering $\pm 10\%$ inaccuracy of voltage and current measurement, and temperature impact. The second logic is called neutral current supervision. It consists of two sub-logics. The first sub-logic, Logic 2, reports NGD failure in 10s if the neutral current becomes absent, i.e., less than 0.01% of neutral let through current (I_{let}). The other sub-logic, Logic 3, reports NGD failure immediately when the neutral current becomes greater than 120% of I_{let} .

The NGD failure is reported if any of the aforementioned logics is satisfied. In other words, the three logics are ORed, and the outcome identifies NGD Status (NGDS).

4.1.2 Neutral Voltage Measurement

In order to understand how the proposed voltage metering mechanism functions, first two existing voltage metering techniques are explained. The first technique is the Resistive Potential Divider (RPD). It divides the voltage into two portions across two series resistors, as shown in Fig. 4.1(a). The neutral and measured voltages are related as follows:

$$u(t) = \frac{R_1 + R_2}{R_2} v(t) = K v(t) \quad (4.2)$$

where u and v are the neutral and measured voltages, respectively. Obviously, the neutral voltage can be obtained by scaling-up the $v(t)$ by a factor equal to K .

The only issue with this technique is the need for a very high sampling resolution. Indeed, the maximum system voltage cannot be very high if measuring very weak voltage of the neutral is intended.

The second technique, shown in Fig. 4.1(b), is called Sensing Resistor (SR). It benefits from a diode called Transient Voltage Suppressor (TVS). It is actually a bidirectional

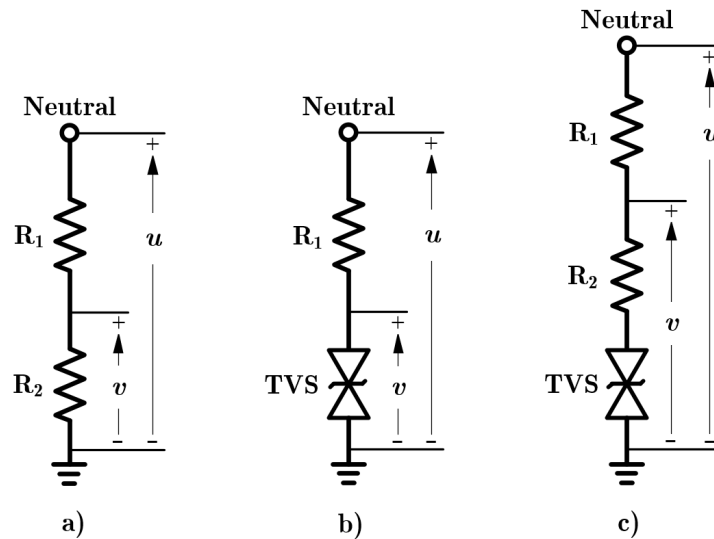


Figure 4.1: Neutral voltage metering techniques. a) Resistive Potential Divider (RPD), b) Sensing Resistor (SR), and c) Advanced Sensing Resistor (ASR).

back-to-back Zener diode. When the u is less than the Breaking Voltage of the diode (V_{BR}), the diode represents a very high impedance so that almost all of the neutral voltage appears across the TVS. This feature provides error-less measurement of the neutral voltage during the load condition where the neutral voltage is less than the V_{BR} . Otherwise, the TVS clamps and limits the v to its clamping level which means falsifying the signal. The altered signal cannot be used under any condition. Hence, the measurement is valid only during the unfaulted condition. The clamping level is considered greater than the maximum voltage that the neutral-to-ground circuit is expected to experience during the unfaulted condition.

Finally, the proposed technique is explained. The main goals behind this technique are: 1) very accurate measurement in unfaulted power system, and 2) acceptable accuracy during the faulted condition. It is, indeed, the combination of the RPD and SR, hereafter referred to as Proposed Method (PM) which is shown in Fig. 4.1(c). It has two modes of operation. The first mode happens when the neutral voltage is weak. The TVS is open, and the neutral voltage is completely delivered to the TVS. The measurement is equal to the neutral voltage with minimum possible error. The second mode of operation occurs when the neutral voltage becomes greater than the breaking voltage of the TVS. Under this condition, the TVS clamps the voltage and represents a constant voltage equal to V_{BR} . The TVS does have an internal resistance, known as dynamic resistance, which is neglected since it is ineffective when being in series with R_2 . Thereby, the following relation is established between the neutral and measured voltage.

$$u(t) = \frac{v(t) - V_{BR}}{R_2} R_1 + v(t) = Kv(t) - (K - 1)V_{BR} \quad (4.3)$$

As may be realized, the original voltage of the neutral is recoverable from the measured voltage. It should be reminded that if the v is less than V_{BR} , the TVS is off, representing infinite impedance which means that the u is equal to v with no modifications. Otherwise, the Equation (4.3) relates the v to u . However, a few practical issues face this technique.

The first issue is the internal resistance of the TVS. As mentioned earlier, the R_2 is designed to be enormously greater than this resistance to eliminate its impact. The

other issue is the nonlinearity of the TVS diode. In fact, the transition from open mode to shorted mode or vice versa of the TVS is not a discrete phenomenon and represents a varying resistance. The very high resistance achieved by R_1 in series to R_2 noticeably attenuates this nonlinearity, as shown in Fig. 4.2.

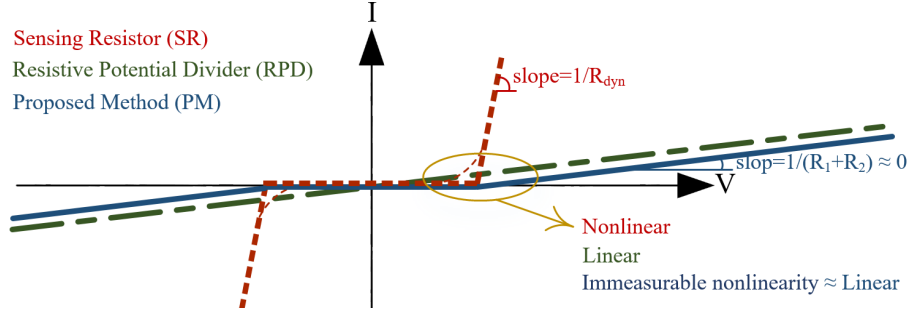


Figure 4.2: I-V characteristics of voltage metering mechanisms.

The last issue is the temperature impact which influences two very critical parameters. The first one is the K . The resistance of resistors R_1 and R_2 changes due to temperature variation. It is believed that choosing the resistors with equal temperature coefficients resolves this issue. Moreover, a common heat sink must be used to keep them operating at equal temperature. Temperature causes the V_{BR} to change too. Digital signal processing is employed for extracting this parameter from the measured signal, $v[t]$, as explained below.

To extract the breaking voltage from the measured voltage, the transition moment between two modes of operation, hereafter called breaking point, is used. As shown in Fig. 4.3, the measured voltage accelerates once the TVS transits from shorted mode to open mode. The detail presented in this figure apply to negative half cycle as well. Using Equation (4.3), it is shown that the v accelerates K -times after the breaking point, i.e., sample $n - 1$.

$$\begin{aligned} \Delta v_{n-1} = v_{n-1} - v_{n-2} &= V_{BR} - \frac{u_{n-2} + (K-1)V_{BR}}{K} = \\ \frac{V_{BR} - u_{n-2}}{K} &= \frac{u_{n-1} - u_{n-2}}{K} = \frac{\Delta u_{n-1}}{K} = \frac{\Delta u_n}{K} = \frac{\Delta v_n}{K} \end{aligned} \quad (4.4)$$

where the parameters used in this calculation can be found in Fig. 4.3. Hence, the sudden acceleration of the waveform is a key parameter that should be used.

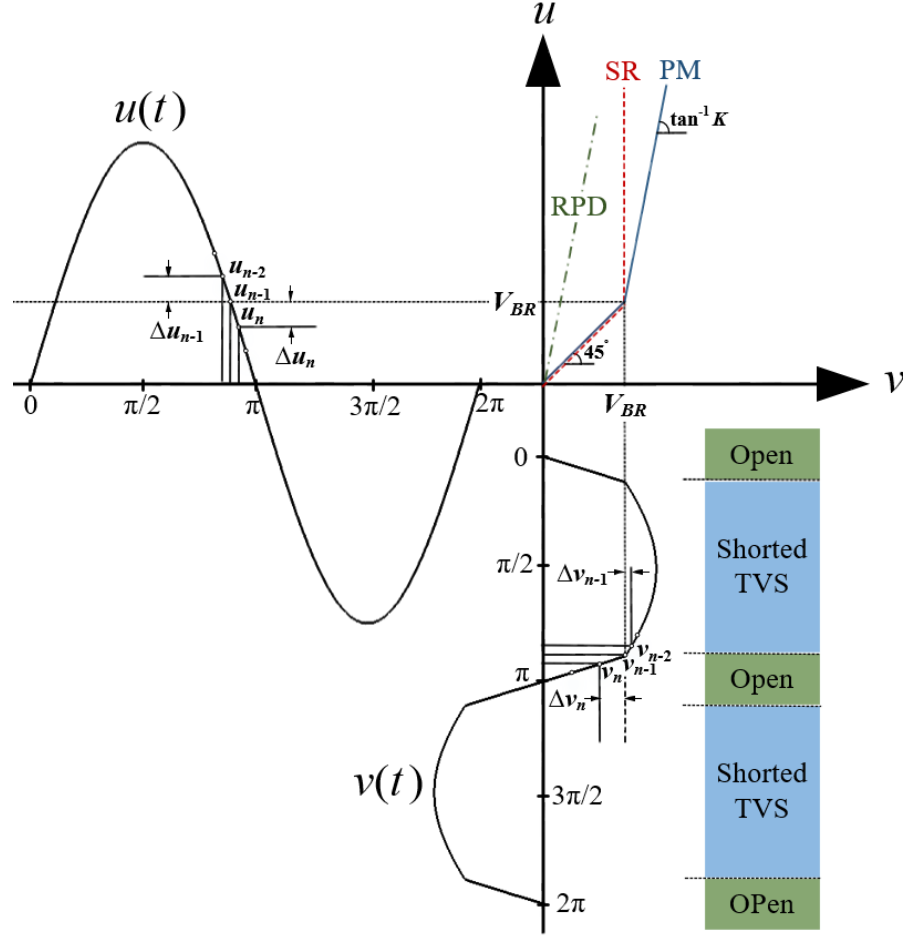


Figure 4.3: Characteristic and operation of the proposed technique.

It is expected that the K -times change in variation rate will not be detected in the positive edge of the sinusoid ($0-\pi/2$ or $\pi-3\pi/2$). The main reason is the anti-aliasing filter effect. It falsifies the breaking point that happens during these intervals. This issue is not expected in negative edges ($\pi/2-\pi$ and $3\pi/2-2\pi$). Therefore, the breaking voltage will be obtained from negative edges as shown in Fig. 4.3. This portion of the sinusoidal waveform is detected by comparing the consequent samples as follows:

$$|v_n| < |v_{n-1}| < |v_{n-2}| \quad (4.5)$$

If this constraint is satisfied and waveform accelerates, the value of sample $n-1$ will be used as the new breaking voltage. A corresponding algorithm is also provided as demonstrated in Fig. 4.4. This flowchart calculates different clamping levels for positive and negative half cycles. It also shows how the neutral voltage is recovered from the

measured signal using the Equation (4.3).

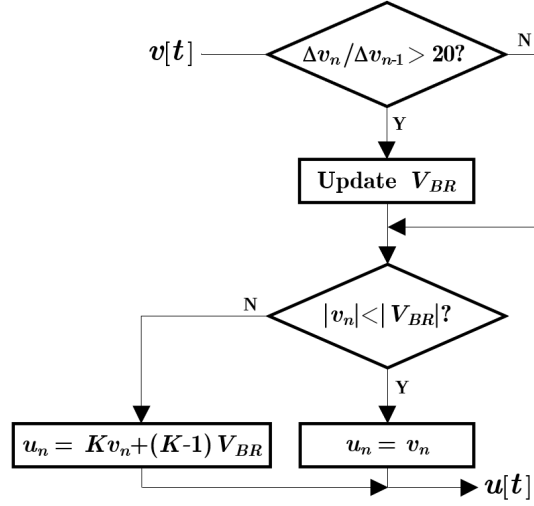


Figure 4.4: Breaking voltage extraction and neutral voltage recovery.

4.2 Modeling and Behavior Analysis of The Proposed Voltage Metering Method

4.2.1 Software Verification

The studies are conducted for NGDs installed at neutral of a 110/12.47kV DYn distribution transformer. The proposed voltage metering mechanism should be designed considering line-to-ground voltage rating of the wye side which is equal to 7.2kV RMS or 10.182kV peak. The breaking voltage of the TVS for such a system is well-designed if set to 100 V. Lastly, the voltage rating of the monitoring equipment is considered 240 V. Using the mentioned specifications and (4.3), the parameter K is obtained as follows:

$$K = \frac{R_1 + R_2}{R_2} = \frac{u_p - V_{BR}}{v_p - V_{BR}} = \frac{10182 - 100}{240\sqrt{2} - 100} = 42.11 \quad (4.6)$$

where u_p and v_p are the peak values of $u(t)$ and $v(t)$, respectively. The R_1 equal to 100 k Ω provides acceptable electrical isolation from neutral node [20]. As a result, the R_2 is obtained equal to 2.375 k Ω . However, the R_2 equal 2 k Ω is chosen since it provides 120% voltage rating for monitoring equipment. Accordingly, the K becomes equal 51.

The PSCAD software was used to perform the software simulations. This software does not provide any model for the TVS diode, and thorough simulations have been performed to obtain an acceptable model of this element. The TVS is nothing but a back-to-back Zener diode. Therefore, first a macro-model of a Zener diode was simulated in this software. It was used for modeling the Thyrector diode based on [33]. Finally, the 100 V TVS diode was obtained by the series combination of 10 Thyrector cells.

The behavior of the simulated voltage metering mechanism was studied for various conditions. A sample case of the thorough performed studies is demonstrated here. The calculated breaking voltage during a sample event is shown in Fig. 4.5. It actually shows the impact of the temperature variation on breaking voltage and its extraction by the algorithm.

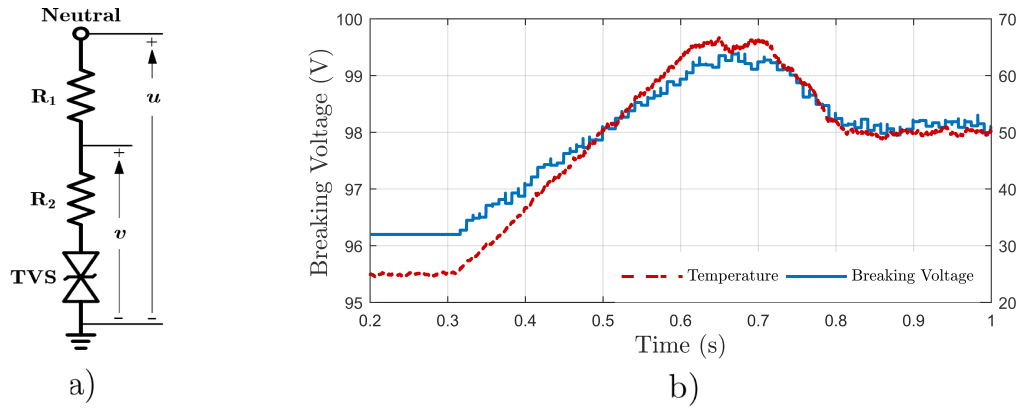


Figure 4.5: Neutral voltage measurement: a) Devise measurement circuit, and b) Temperature impact on breaking voltage and its extraction.

At the beginning of the event, the temperature is 25°C where the breaking voltage is constant and equal to 96.2 V. The TVS is open since the system is operating at its normal condition. Hence, the measured and sensed signals are identical. At $t = 0.3$ s, the system experiences load imbalance causing the neutral voltage to become greater than the clamping level. The TVS starts conducting and heating up. The temperature increases resulting change in breaking voltage. As shown, the proposed algorithm successfully tracks and updates the V_{BR} without using any information of the temperature.

After breaking voltage being updated, the algorithm recovers the neutral voltage. The voltage waveforms of the aforementioned event are shown in Fig. 4.6. The clamped region of the waveform has been magnified to highlight the effect of the R_2 , as well. As

shown, the clamping level is not constant. It carries information about the main signal. The sensed voltage, i.e., $v(t)$, is scaled up resulting the recovered voltage. The recovered voltage is an acceptable approximation of the neutral voltage and the negligible difference is due to sampling resolution which is 12 bits.

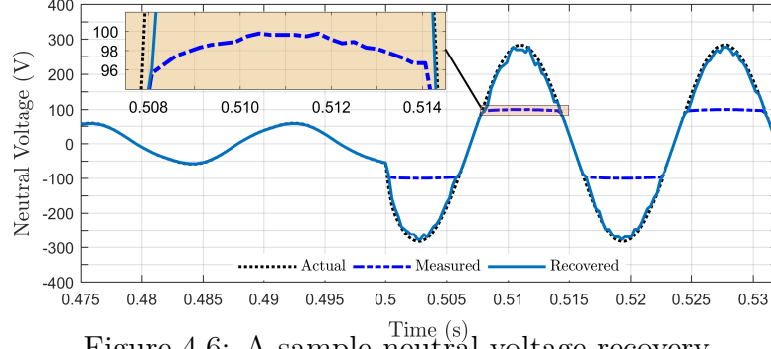


Figure 4.6: A sample neutral voltage recovery.

Lastly, the measurement error of the proposed and existing voltage metering techniques are compared with each other. Fig. 4.7 shows that the measurement error of the proposed voltage metering method is never more than 10% guaranteeing full range 60 Hz measurement. As seen, the RPD operates very accurately when the neutral voltage is more than 1%. However, its error grows exponentially for voltage levels less than 1%. It means that if the neutral voltage is less than 1%, the RPD-based method will not guarantee an accurate voltage and impedance measurement. Performance of SR is exactly inverse of the RPD. Combination of the SR and RPD results in the best performance which is the proposed technique. However, it cannot behave the same as RPD for 1-10%

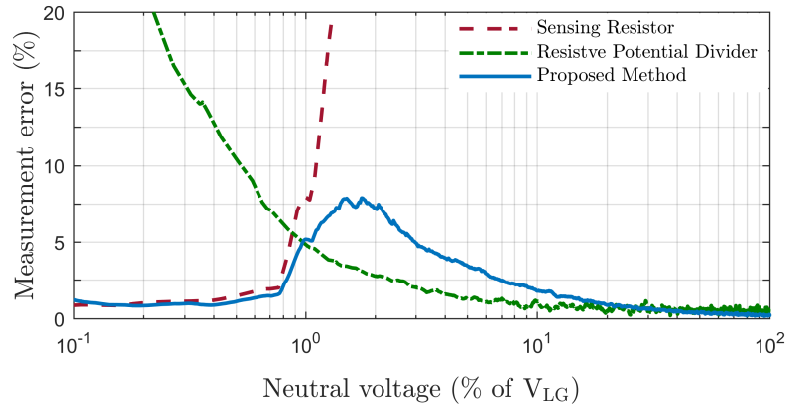


Figure 4.7: Measurement error of the proposed voltage metering technique compared to the other methods, considering 12-bit resolution.

range due to the impact of indefinite sampling resolution and sampling rate that are considered 12 bits and 3840 samples per second, respectively.

4.2.2 Hardware Validation

In this section, the performance of the proposed voltage metering mechanism is validated using a fabricated prototype. The voltage rating of the prototype is 720 V. The electrical isolation at this voltage level was well-achieved by a $10\text{ k}\Omega$ resistance, i.e., R_1 . Considering the transformation factor K equal to 51, the R_2 was chosen $200\ \Omega$. The temperature coefficient of both the resistors are equal. Moreover, a common heat sink was used to equalize their temperature. The breaking voltage of the TVS is 7.5 V. As such, the fabricated device is actually the 10% prototype of the designed voltage metering instrument studied in the previous section. The peak value of the measured voltage is 30 V. Since the voltage rating of used DSP board is $\pm 3\text{ V}$, the measured voltage was scaled-down once more using a conventional RPD. The electrical decoupling was also considered when designing the RPD using operational amplifiers with negligible bias current. The hardware test is shown in Fig. 4.8.

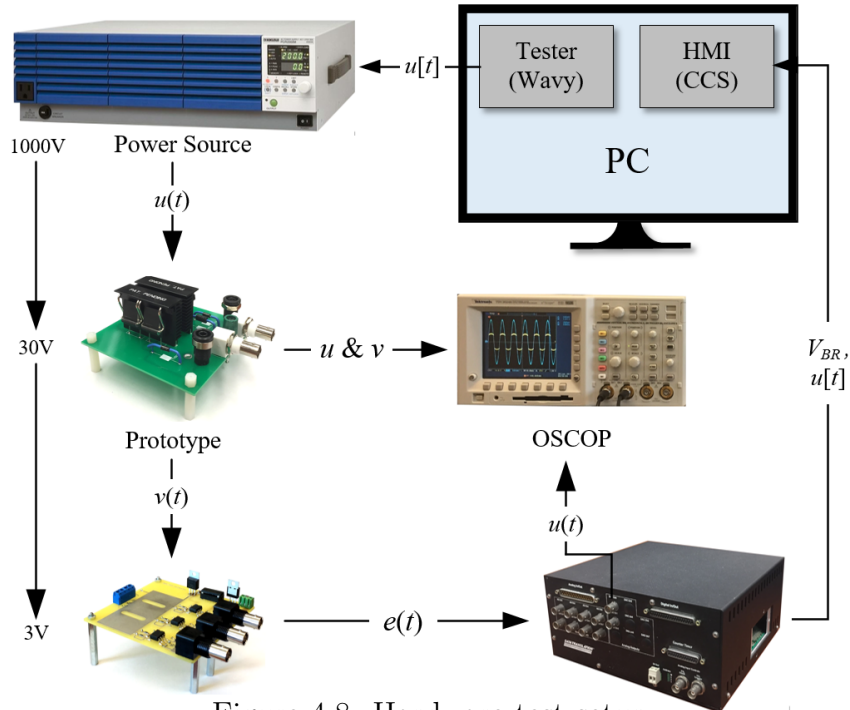


Figure 4.8: Hardware test setup.

The profile of the neutral voltage, $u[t]$, is designed using a software called Wavy. The power source supplies the $u(t)$ to the prototype based on the data received from Wavy. The prototype transforms the $u(t)$ to $v(t)$. The $v(t)$ is scaled-down 10 times by RPD to a new voltage named $e(t)$. The $e(t)$ is sampled by an analog input of the used Digital Signal Processor (DSP) which continuously runs the algorithm presented in Fig. 4.4. The performance of the fabricated prototype and DSP-based algorithm were observed and investigated for various cases. The measurement accuracy obtained from the experimental studies is the same as the characteristic presented in Fig. 4.7 meaning accurate voltage metering. A sample case is shown in Fig.4.9. The obtained breaking voltage is updated at the negative edge of the sinusoidal waveform. Since the TVS diode consists of two back-to-back Zener diodes, the breaking voltage for the positive and negative half-cycles are not equal.

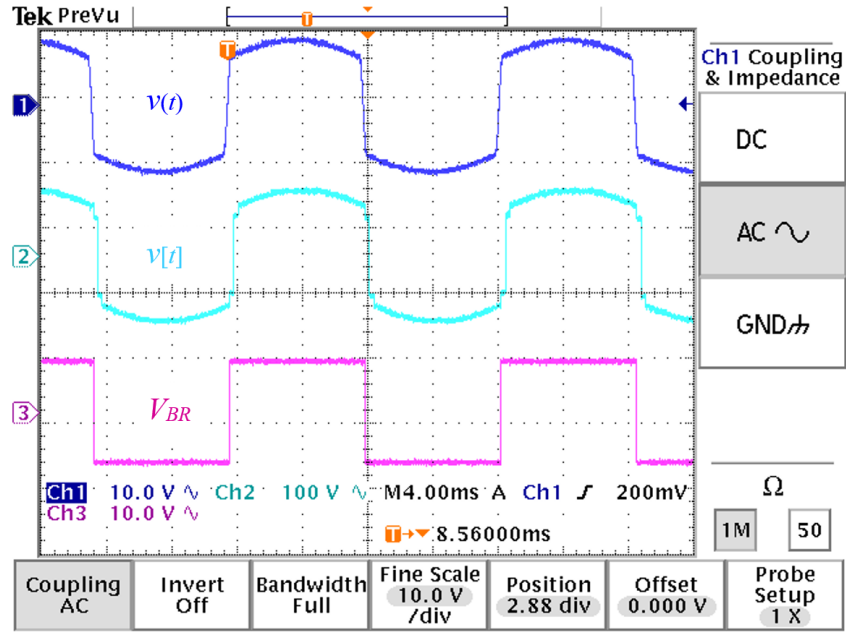


Figure 4.9: Experimental results (150 V across the prototype).

4.3 Performance of The Monitoring Scheme

The proposed monitoring technique is applied to a sample configuration of the distribution system. The DYg distribution transformer is very popular in this field [16, 17]. The

system containing the main details is shown in Fig. 4.10. It supplies an ungrounded 12.47 kV system. As such, the ratings of the neutral voltage measurement instruments are the same as chosen in Section 4.2.1. The only consideration is the second TVS which limits the measured voltage to the rating of the relay which is 240 V RMS or 340 V peak.

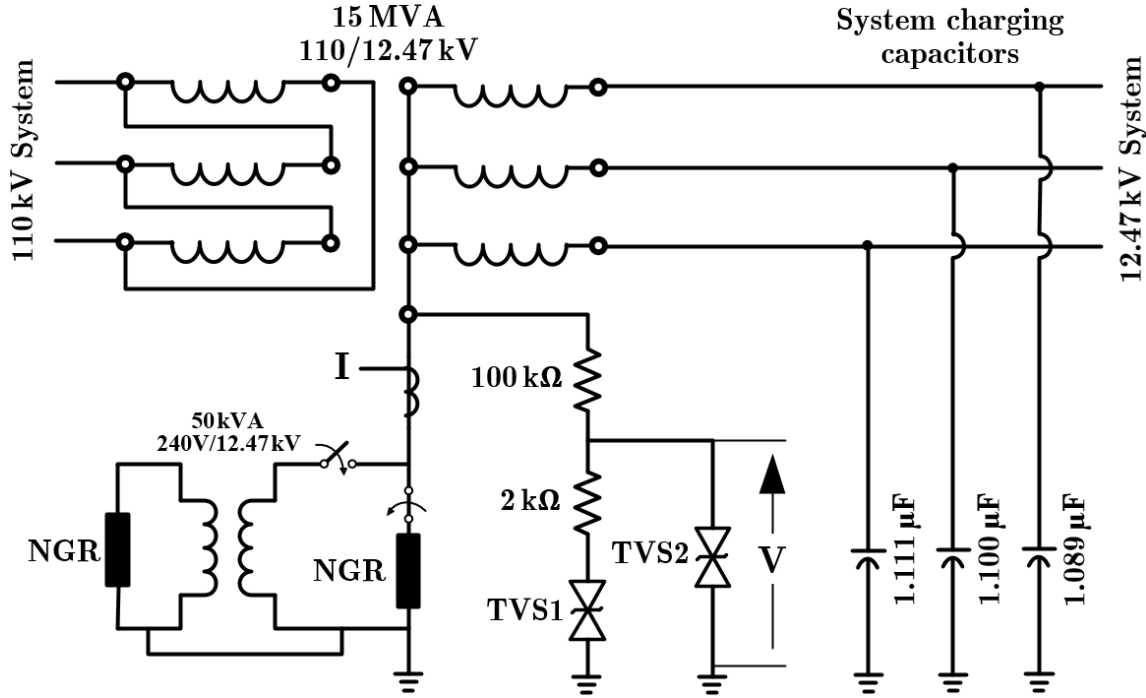


Figure 4.10: Study power system equipped with high or low resistance grounding apparatuses, and the proposed voltage metering mechanism.

The employed grounding methods for this configuration are low-resistance grounding, high-resistance grounding and tuned reactance. The Low resistance Neutral Grounding Resistor (LNGR) and High resistance Neutral Grounding Resistor (HNGR) are so designed that the neutral let through current, I_{let} , is limited to 150 A and 25 A, respectively [3]. In fact, the resistance of the LNGR and HNGR are equal to 50Ω and 288Ω , respectively. The other type of grounding for this configuration is the tuned reactance which is obtained by a High reactance Neutral Grounding Inductor (HNGL). Using the procedure provided by [5], the HNGL is achieved using a small inductor, i.e., 0.72 mH with quality factor equal to 20, at secondary of a 50 kVA, 12.47 kV/240 V Neutral Grounding Transformer (NGT). It should be mentioned that the total capacitive charging current of the 12.47 kV system has been considered 3 A resulting the three phase-to-ground capaci-

tances of $1.1\mu F$. The tuned reactance is supposed to neutralize the parallel equivalent of these phase-to-ground capacitances. To have the minimal current in the neutral during the load condition, some imbalance of these capacitors has been considered, as shown in Fig. 4.10.

Performance of the proposed monitoring technique has been studied during both normal and faulted conditions considering different levels of neutral voltage and NGD degradations. The proposed voltage metering mechanism functions satisfyingly as well. Since the neutral current was also available, the impedance of the NGD helped to identify its status. The failed NGD is reported if its impedance drifts at least $\pm 30\%$. Also, many other events were investigated where the neutral voltage became less than the minimum accuracy limit of the proposed voltage metering mechanism. The minimum voltage that the proposed metering technique can measure, with less than 10% error, is 1.4 V which depends on the selected resolution, here 4096 or 12 bits. Under this condition, the neutral current supervision logic reports the failed-open NGR due to the absence of the neutral current.

To have a better understanding of the performance of the proposed technique, a few most important sample cases of the performed studies are demonstrated and discussed with more details. It should be noted that the measurements might be very low during normal condition, and they shall not be interpreted as secondary level measurements.

Case 1 — The first case is regarding a failed-short LNGR during the load condition, as shown in Fig. 4.11. In this case, a slight imbalance of the system charging capacitances causes the appearance of about 10 V across LNGR and the neutral current less than 1 A. Moreover, the saturation of the DYn transformer generates the third and fifth harmonics that appear in the waveforms. While the voltage is still very low, the LNGR starts failing short. Its resistance decreases to 50%, i.e., 25Ω , over 100 ms. The voltage and current waveforms are filtered and recorded using COMTRADE 91 in PSCAD domain with the sampling rate and resolution of the recorder set to 3840 samples per second and 4096, respectively.

In the next step, the waveforms are applied to monitoring algorithm that is implemented in MATLAB. The resistance of the NGR obtained by all three methods is shown

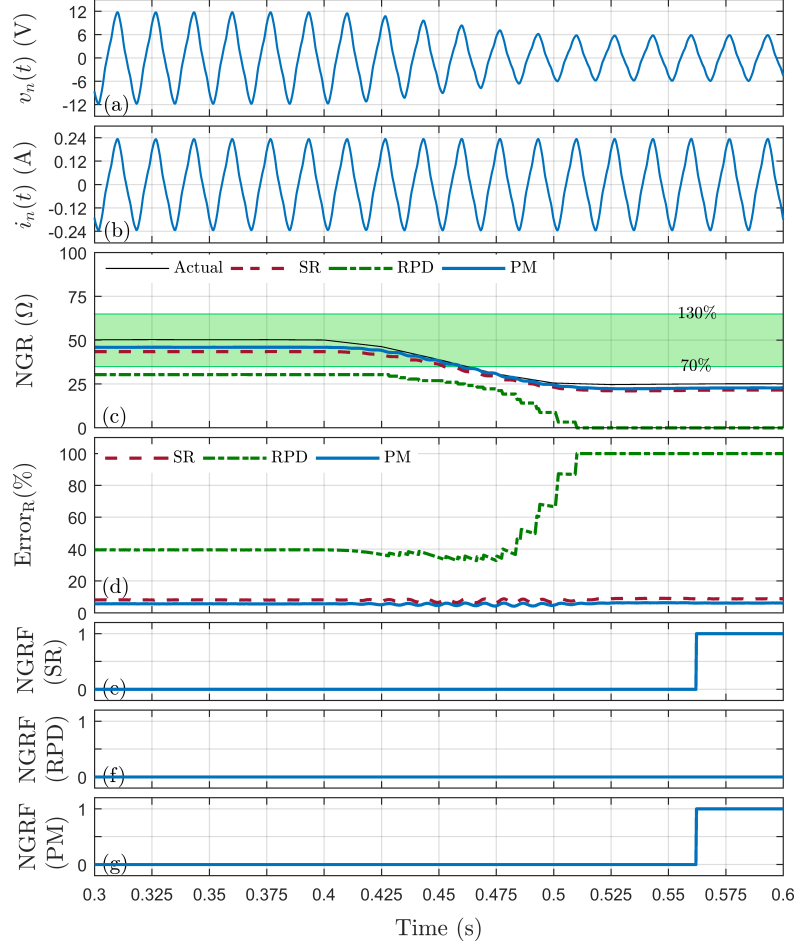


Figure 4.11: Failed-short LNGR during unfaulted condition. a) Neutral voltage, b) Neutral current, c) NGR resistance, d) Measurement error of NGR resistance, e) NGR failure detection by SR-based monitoring method, f) NGR failure detection by RPD-based monitoring method, and g) NGR failure detection by proposed monitoring method.

in Fig. 4.11(c). Since, the neutral voltage is very low, the RPD-based monitoring method experiences a very high error in calculating the NGR resistance, while the other monitoring methods provide an acceptable measurement with less than 10% error. Since the RPD-based method cannot measure the neutral voltage accurately, it relies on neutral current which is present. Thereby, it cannot detect the NGR failure even when the NGR resistance decreases to 50% starting at $t = 0.4$ s. However, the SR-based and proposed monitoring methods calculate the NGR resistance accurately and provide precise status of the NGR during this event. A time delay of 100 ms activated by the 70% threshold safely detects the failed-short NGR. Therefore, the SR-based and proposed method function reliably during the unfaulted condition where the neutral electrical parameters

are very low. However, the RPD-based method cannot function correctly since it cannot measure the very weak voltage of the neutral and relies on the presence of the neutral current. The neutral current supervision logic only detects the entirely failed-open NGR condition.

Case 2 — The failed-open NGR during the unfaulted condition is detected in the same way as demonstrated for this case based on the waveforms shown in Fig. 4.12.

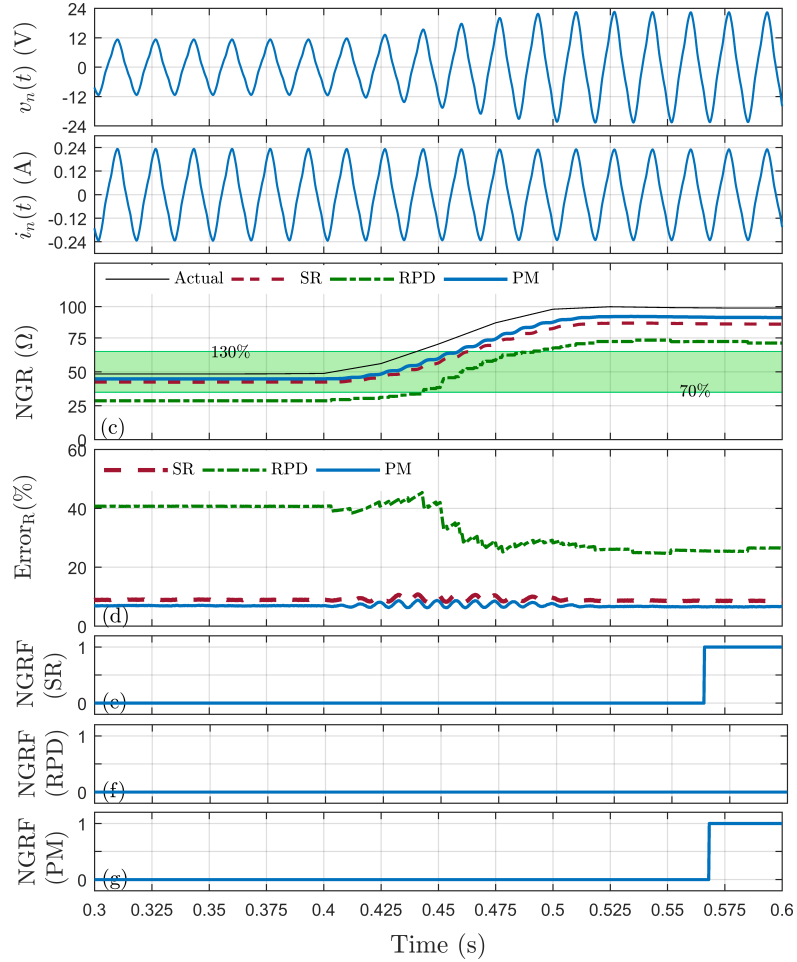


Figure 4.12: Failed-open LNGR during unfaulted condition. a) Neutral voltage, b) Neutral current, c) NGR resistance, d) Measurement error of NGR resistance, e) NGR failure detection by SR-based monitoring method, f) NGR failure detection by RPD-based monitoring method, and g) NGR failure detection by proposed monitoring method.

Case 3 — The third case is regarding a failed-short LNGR during a single-line-to-ground fault, as shown in Fig. 4.13. As a result, the neutral voltage rises to about the line-to-ground voltage of the system, i.e., 7.2 kV. The SR-based monitoring method

cannot measure such a neutral voltage and relies on the presence of the neutral current which is very high but limited to 150 A. Hence, the SR-based monitoring method does not detect the NGR failure since the neutral current is present. However, the RPD-based and proposed monitoring methods provide accurate measurement of the NGR resistance. A time delay of 100 ms activated by the 70% threshold safely detects the failed-short NGR. As such, the RPD-based and proposed monitoring methods monitor reliably during the ground faults while the SR-based monitoring method fails to do so.

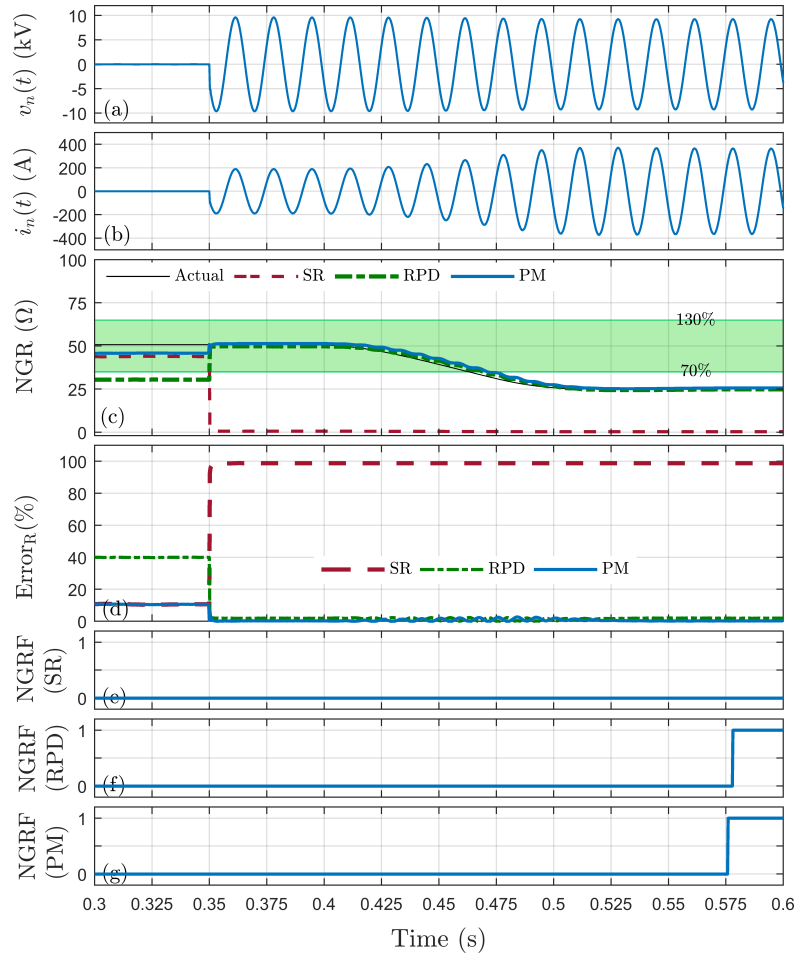


Figure 4.13: Failed-short LNGR during single-line-to-ground fault at terminals of the transformer. a) Neutral voltage, b) Neutral current, c) NGR resistance, d) Measurement error of NGR resistance, e) NGR failure detection by SR-based monitoring method, f) NGR failure detection by RPD-based monitoring method, and g) NGR failure detection by proposed monitoring method.

Case 4 — The failed-open NGR during the faulted condition is detected in the same

way as demonstrated for the previous case, as shown in Fig. 4.14.

As observed, the proposed monitoring method provides accurate monitoring in both normal and faulted conditions while the other methods fail to cover both conditions.

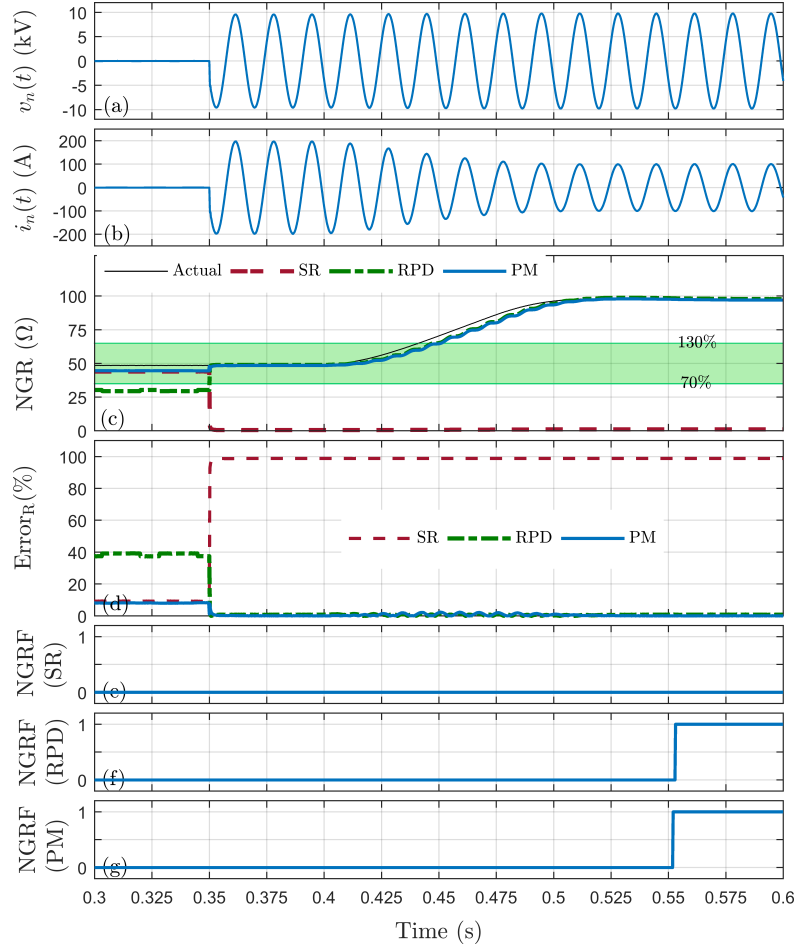


Figure 4.14: Failed-open LNGR during single-line-to-ground fault at terminals of the transformer. a) Neutral voltage, b) Neutral current, c) NGR resistance, d) Measurement error of NGR resistance, e) NGR failure detection by SR-based monitoring method, f) NGR failure detection by RPD-based monitoring method, and g) NGR failure detection by proposed monitoring method.

Case 5 — The fifth case represents a failed-short HNGL during the normal operation condition where the neutral voltage is less than the TVS breaking voltage, as shown in Fig. 4.15. In the same way as shown for the first case, the RPD-based monitoring method relies on neutral current supervision logic since the neutral voltage is very low and cannot be measured by the RPD. The neutral current is present and the NGR

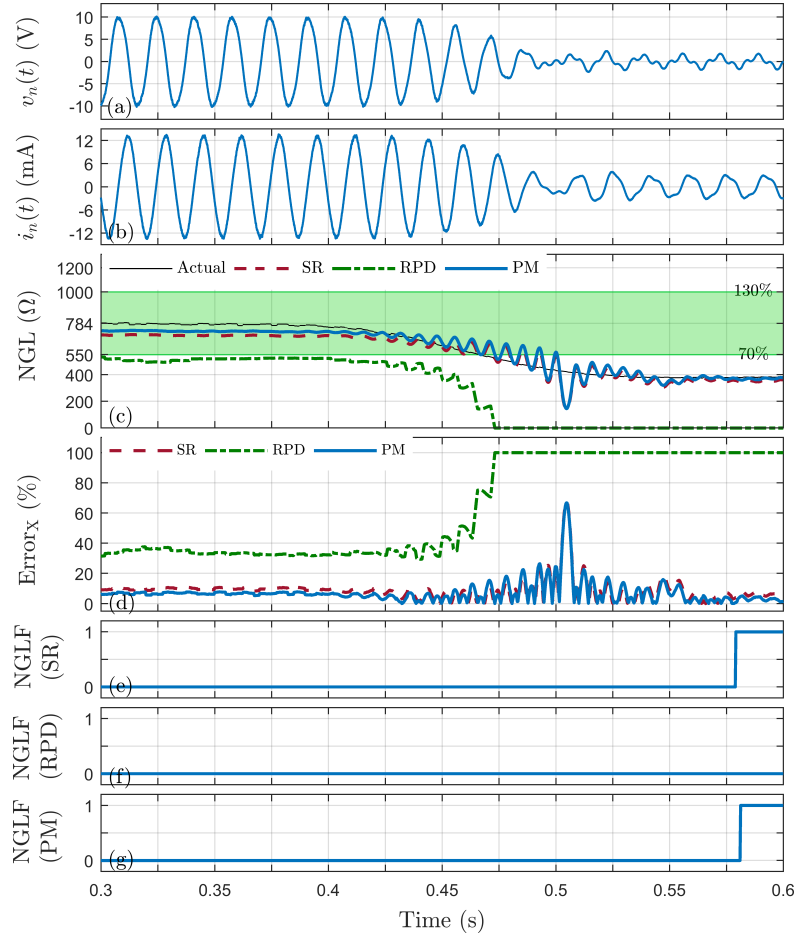


Figure 4.15: Failed-short HNGL during unfaulted condition. a) Neutral voltage, b) Neutral current, c) NGL reactance, d) Measurement error of NGL reactance, e) NGL failure detection by SR-based monitoring method, f) NGL failure detection by RPD-based monitoring method, and g) NGL failure detection by proposed monitoring method.

failure alarm remains off. The RPD-based monitoring method experiences about 35% error in the calculated reactance of the HNGL, as shown in Fig. 4.15(c) and Fig. 4.15(d). However, the SR-based and proposed monitoring methods accurately measure the neutral voltage and current, and calculate the HNGL reactance with less than 10% error. Once the HNGL reactance drifts outside the green region, less than 70% threshold for this case, the NGL failure is detected in 100 ms, as shown in Fig. 4.15. The failed-open HNGL during the unfaulted condition is detected in the same way as demonstrated for this case. As a conclusion, the SR-based and proposed monitoring methods function satisfyingly during the unfaulted condition while the RPD-based monitoring method is not reliable.

It should be added that the very high measurement error of the proposed method, 60% at $t = 0.5$ s in Fig. 4.15(d), is due to DFT filter dynamic which occurs when the neutral voltage and current change due to variation of the HNGL reactance. The resettable time delay resolves the issue of the oscillations seen in the calculated reactance.

Case 6 — The failed-open HNGL during the unfaulted condition is detected in the same way as demonstrated for the previous case, as shown in Fig. 4.16.

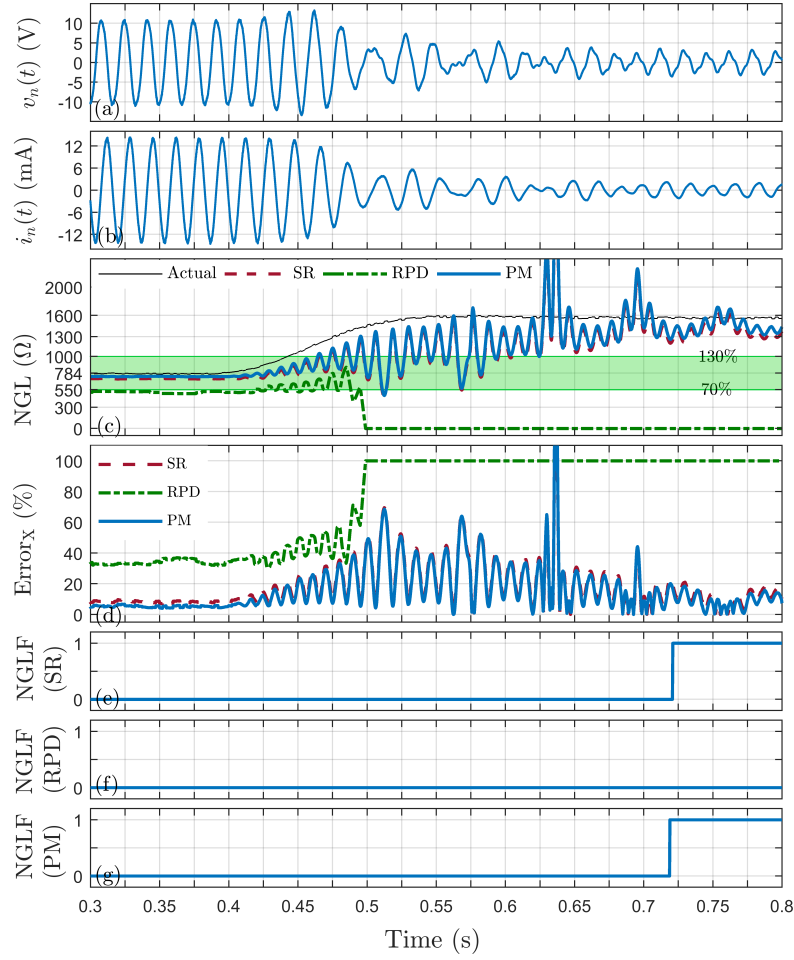


Figure 4.16: Failed-open HNGL during unfaulted condition. a) Neutral voltage, b) Neutral current, c) NGL reactance, d) Measurement error of NGL reactance, e) NGL failure detection by SR-based monitoring method, f) NGL failure detection by RPD-based monitoring method, and g) NGL failure detection by proposed monitoring method.

Case 7 — The seventh case demonstrates a failed-short HNGL during a single-line-to-ground fault, as shown in Fig. 4.17. The neutral voltage grows to about the phase-to-ground voltage level, i.e., 7.2 kV or 100%. In the same way as shown for the

second case, the SR-based monitoring method cannot measure the neutral voltage and relies on the presence of the neutral current which is very high but limited to 5 A. Hence, the SR-based monitoring method does not detect the NGR failure since the neutral current is present. However, the RPD-based and proposed monitoring methods provide accurate measurement of the HNGL reactance. A time delay of 100 ms activated by the 70% threshold safely detects the failed-open NGL. As such, the RPD-based and proposed monitoring methods monitor reliably during the ground faults while the SR-based monitoring method fails to do so. Moreover, the failed-short HNGL during the

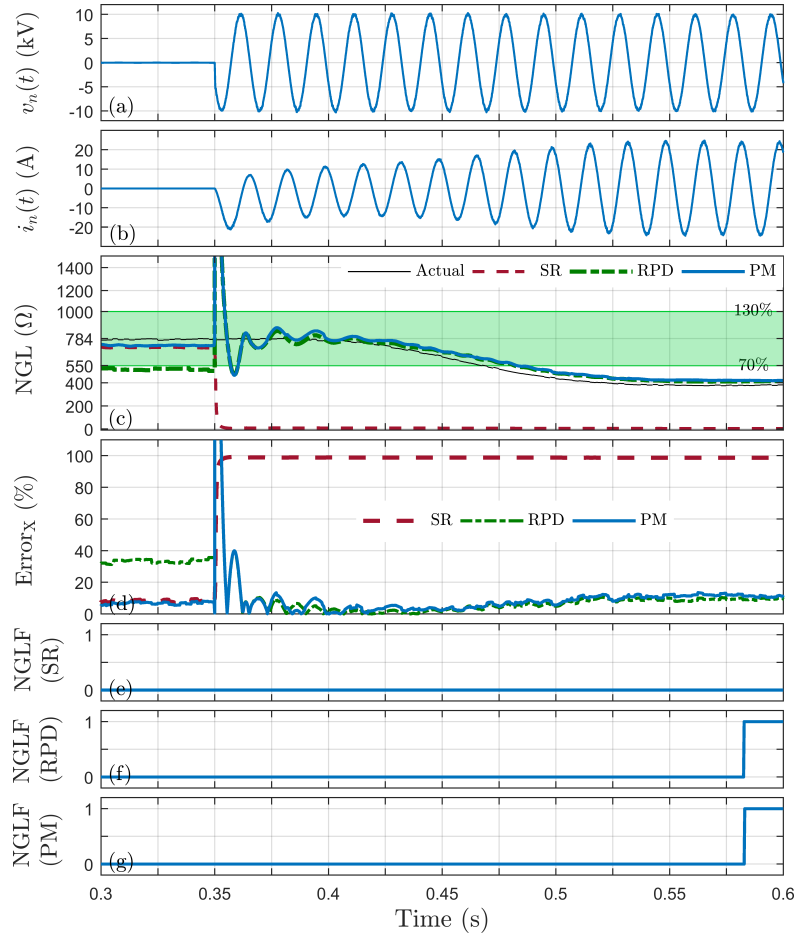


Figure 4.17: Failed-short HNGL during single-line-to-ground fault at terminals of the transformer. a) Neutral voltage, b) Neutral current, c) NGL reactance, d) Measurement error of NGL reactance, e) NGL failure detection by SR-based monitoring method, f) NGL failure detection by RPD-based monitoring method, and g) NGL failure detection by proposed monitoring method.

faulted condition is detected in the same way as demonstrated for this case. Again, the proposed monitoring method provides accurate monitoring in both normal and faulted conditions while the other methods fail to cover both conditions.

Case 8 — The failed-open HNGL during the single-line-to-ground fault at terminals of the transformer is detected in the same way as demonstrated for the previous case, as shown in Fig. 4.18.

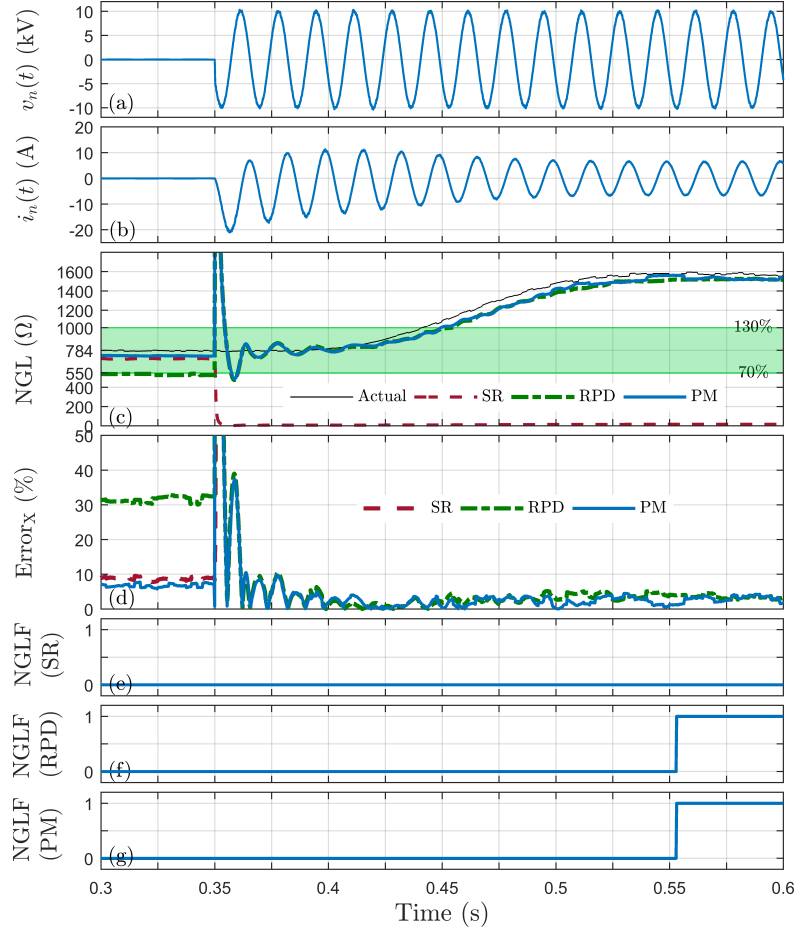


Figure 4.18: Failed-open HNGL during single-line-to-ground fault at terminals of the transformer. a) Neutral voltage, b) Neutral current, c) NGL reactance, d) Measurement error of NGL reactance, e) NGL failure detection by SR-based monitoring method, f) NGL failure detection by RPD-based monitoring method, and g) NGL failure detection by proposed monitoring method.

The demonstrated eight case studies are just a few samples of a comprehensive analysis that has been performed considering different NGDs and system operation modes listed in Table 4.1. This study shows that the functionality of the proposed continuous monitoring

method is not limited to a specific NGD or system operation mode. The monitoring is guaranteed once the neutral node experiences a minimum level of voltage and current. All of these advantages make the proposed monitoring method an advanced passive monitoring method that not only stands with a better performance than the existing passive monitoring method but also proposes monitoring of the other types of the NGDs as well.

Table 4.1: NGD status detection: Normal (NM), Failed-short (SH), or Failed-open (OP)

		No Fault				LG Fault				LLG Fault				LL Fault				
Z(%)	V(%)	0.1	0.5	1.0	2.0	10	20	50	100	10	20	50	100	0.1	0.5	1.0	2.0	
HNCR	50	SH	SH	SH	SH	SH	SH	SH	SH	SH	SH	SH	SH	SH	SH	SH	SH	1
	100	NM	NM	NM	NM	NM	NM	NM	NM	NM	NM	NM	NM	NM	NM	NM	NM	2
	200	OP	OP	OP	OP	OP	OP	OP	OP	OP	OP	OP	OP	OP	OP	OP	OP	3
LNCR	50	SH	SH	SH	SH	SH	SH	SH	SH	SH	SH	SH	SH	SH	SH	SH	SH	4
	100	NM	NM	NM	NM	NM	NM	NM	NM	NM	NM	NM	NM	NM	NM	NM	NM	5
	200	OP	OP	OP	OP	OP	OP	OP	OP	OP	OP	OP	OP	OP	OP	OP	OP	6
HNGL	50	SH	SH	SH	SH	SH	SH	SH	SH	SH	SH	SH	SH	SH	SH	SH	SH	7
	100	NM	NM	NM	NM	NM	NM	NM	NM	NM	NM	NM	NM	NM	NM	NM	NM	8
	200	OP	OP	OP	OP	OP	OP	OP	OP	OP	OP	OP	OP	OP	OP	OP	OP	9
		A	B	C	D	E	F	G	H	I	J	K	L	M	N	O	P	

Furthermore, another type of neutral grounding devices which is applicable to this configuration is the Low reactance Neutral Grounding Reactor (LNGL). Such a reactor was also designed for this configuration which is 0.4 mH without NGT to limit the single-phase-to-ground fault current to less than that of the three-phase-to-ground fault. The voltage that appears across the LNGL is so weak that the selected resolution is not sufficient. The only solution is demanding a better resolution, 20 bits instead of 12 bits.

Lastly, it should be added that for three-phase-to-ground fault, the system charging capacitors are bypassed by the fault impedance. Thereby, the asymmetry of these capacitors which normally causes the minimal current in neutral wire is no longer functional. The three-phase system becomes balanced, and the neutral-to-ground circuit does not experience any energy flow.

Further simulation results can be found in Appendix C.

4.4 Summary

A new and comprehensive method for monitoring neutral grounding devices was proposed which benefits from a novel neutral voltage metering mechanism that guarantees full range voltage and impedance measurement.

The performance of the proposed voltage metering technique was validated using software analysis and a fabricated prototype. It provides full range measurement, 0.01-120%, with the measurement error that is never more than 8%. As a result, the neutral voltage is available during both normal and faulted operation conditions, which cannot happen with existing voltage metering instruments such as neutral PT, line PTs, resistive potential divider and sensing resistor.

Furthermore, the devised voltage metering mechanism was used to monitor the NGDs located at neutral of a distribution transformer. The studies showed that the impedance of the NGDs is available in both normal and faulted conditions regardless of the type of the NGD and the system configuration. Any physical change of the NGD is directly reflected in its impedance which is reliably monitored using its calculated impedance. As such, the proposed monitoring method barely employs the neutral current supervision scheme which is used by existing methods making them imperfect in failure detection. The proposed monitoring method is continuous and comprehensive since it functions in both normal and faulted conditions regardless of the type of the NGD or the system configuration.

Chapter 5

A Passive NGR Monitoring Method for Unit-Connected Generators

In this chapter, a new passive method for monitoring the high-resistance NGR at the neutral of unit-connected generators will be proposed. This configuration is very popular due to third harmonic and zero-sequence isolation. The proposed method relies on the third harmonic (180 Hz) of the neutral and residual voltages that are measured by neutral PT and three-phase terminal PTs, respectively. The residual voltage is obtained by the vector sum of the three-phase voltages measured by terminal PTs that are wye-wye- or wye-broken-delta-connected.

The fundamentals and concepts of the proposed method will be explained in Section 5.1. The monitoring function will be presented in Section 5.2 followed by probable challenges and how the proposed technique is restrained against them. Lastly, the behavior analysis and performance of the monitor method will be shown for different conditions using PSCAD in conjunction with Matlab, and further hardware validations using an available industrial generator protection relay.

5.1 Fundamentals and Concepts

The proposed technique monitors the NGR located at neutral of unit-connected generators as shown in Fig. 5.1. The c_g and c_s are generator and generation-side-system phase-

to-ground capacitances, respectively. The c_{ww} is the inter-winding or primary-secondary capacitance of the step-up transformer.

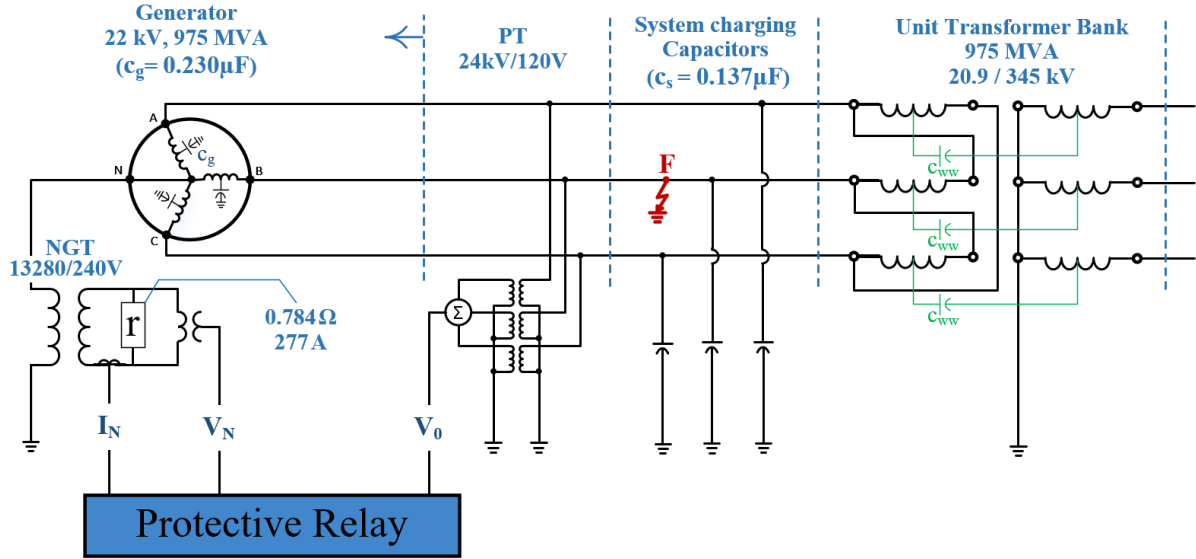


Figure 5.1: High-resistance-grounded unit-connected generator.

As known, generators are often connected to the system through a delta-wye transformer. This configuration, called unit-connection, provides a unique feature which is the third harmonic and zero sequence isolation. It means that the ground faults in transmission system will not have any effect on neutral and residual third harmonic voltages of the generator. Moreover, if the ground fault occurs at generator side, the high voltage system will not feed the third harmonic into the ground fault except through the transformer interwinding capacitance which is very small. Since the proposed technique employs the third harmonic of the neutral and residual voltages, the third harmonic model of the system

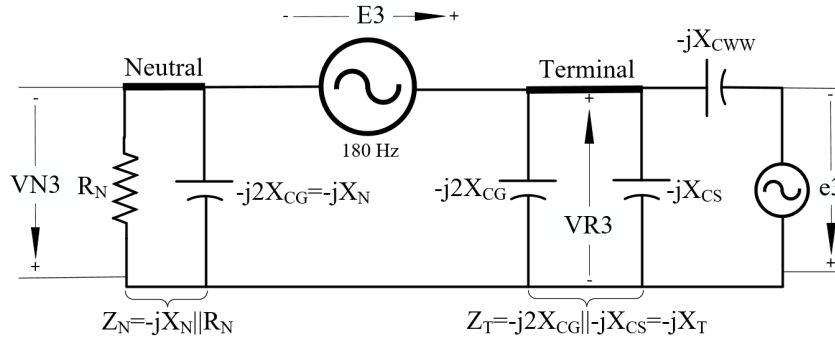


Figure 5.2: Simplified third harmonic model of the system.

system is needed, as depicted in Fig. 5.2.

In this figure, $-jX_{CG}$, $-jX_{CS}$ and $-jX_{CWW}$ are impedances related to c_g , c_s and c_{ww} , respectively. The $-jX_{CG}$ is divided between two ends of the generator stator. Moreover, $E3$ and $e3$ are phasor quantities that refer to third harmonic voltages generated by the generator and step-up transformer, respectively. The $e3$ is generated at star side of the step-up transformer and affects the delta side through $-jX_{CWW}$. Lastly, the R_N is the total grounding resistance seen from the primary of the neutral grounding transformer. Using superposition theorem, the third harmonic of neutral-to-ground voltage phasor, $VN3$, and that of the residual voltage phasor, $VR3$, are derived as below.

$$VN3 = \frac{Z_N}{Z_N + Z_T} E3 + \frac{Z_N \| Z_T}{Z_N \| Z_T - jX_{CWW}} e3 \quad (5.1)$$

$$VR3 = \frac{Z_T}{Z_N + Z_T} E3 - \frac{Z_N \| Z_T}{Z_N \| Z_T - jX_{CWW}} e3 \quad (5.2)$$

These parameters are normalized with respect to $E3$ considering that the magnitude of $-jX_{CWW}$ is remarkably greater than that of the $Z_N \| Z_T$, based on data presented in [40]:

$$\overline{VN3} = \frac{VN3}{E3} = \frac{Z_N}{Z_N + Z_T} - \frac{Z_N \| Z_T}{jX_{CWW}} \frac{e3}{E3} = A - B \quad (5.3)$$

$$\overline{VR3} = \frac{VR3}{E3} = \frac{Z_T}{Z_N + Z_T} + \frac{Z_N \| Z_T}{jX_{CWW}} \frac{e3}{E3} = C + B \quad (5.4)$$

where the bar symbol indicates the normalization in respect to $E3$. In the next section, these parameters are analyzed to derive NGR monitoring function, taking into consideration issues such as load and temperature variation, step-up transformer saturation, and generator stator winding internal and external ground faults.

5.2 Proposed Monitoring Technique and Challenges

5.2.1 NGR Monitoring Logics

The impact of NGR failure on $\overline{VN3}$ and $\overline{VR3}$ is investigated to derive criteria for detecting NGR failure and distinguish it from other phenomena. If $e3$ is ignored, it is clear that

the R_N variation causes an opposite change in the normalized voltages, increasing one while decreasing the other. However, $e3$ is not neglected. To show the opposite behavior of the parameters in case of NGR defect, Equation (5.3) is rewritten as follows:

$$\overline{VN3} = \underbrace{\frac{Z_N}{Z_N + Z_T}}_{\text{term I}} \left(1 - \underbrace{\frac{Z_T}{jX_{CWW}} \frac{e3}{E3}}_{\text{term II}} \right) \quad (5.5)$$

Term II is independent of NGR resistance, while term I is directly proportional to it. Thus, if the NGR resistance increases, the magnitude of $\overline{VN3}$ will also grow and vice versa. On the other hand, the following relations are derived by vector sum of Equation (5.3) and Equation (5.4), and the cosine rule.

$$\overline{VN3} + \overline{VR3} = 1 \quad |\overline{VN3}|^2 + |\overline{VR3}|^2 + 2|\overline{VN3}||\overline{VR3}|\cos\varphi = 1 \quad (5.6)$$

where φ is the angle between the $\overline{VN3}$ and $\overline{VR3}$ phasors. When NGR is healthy and system does not experience any ground faults, these two phasor quantities are approximately in phase [41]. Hence, the φ is always less than 90° meaning that $\cos\varphi$ is positive. Since all terms of (7) are positive, and the right side of (7) is constant, the $|\overline{VR3}|$ must decrease when the $|\overline{VN3}|$ grows due to increase in NGR resistance. In other words, the $|\overline{VR3}|$ is inversely proportionate to NGR resistance. As a result, when the parameters change in opposite directions it suggests NGR failure. A failed-open NGR is expected when $|\overline{VN3}|$ increases and $|\overline{VR3}|$ decreases, and vice versa for a failed-short NGR. This logic is only one criterion for NGR failure detection. However, more specific criteria are needed for reliable detection. Here, the variation rate of the magnitude of the normalized parameters is employed. For intact NGR condition, the following relation is achieved through mathematical work.

The sensitivity of $|\overline{VR3}|$ to NGR resistance variation is proven to be greater than that of the $|\overline{VN3}|$ for intact NGR condition neglecting the $e3$, as proved below.

$$\left| \frac{\dot{\overline{VR3}}}{\overline{VR3}} \right| = \frac{\partial |\overline{VR3}|}{\partial R_N} \frac{\partial R_N}{\partial t} \bigg|_{E3, e3} = \left(\frac{R_N / \sqrt{R_N^2 + X_N^2}}{\sqrt{(1+K)^2 R_N^2 + X_N^2}} - \frac{R_N (1+K)^2 \sqrt{R_N^2 + X_N^2}}{(\sqrt{(1+K)^2 R_N^2 + X_N^2})^3} \right) \frac{\partial R_N}{\partial t} \quad (5.7)$$

$$|\dot{\overline{VN3}}| = \frac{\partial |\overline{VN3}|}{\partial R_N} \frac{\partial R_N}{\partial t} \bigg|_{E3, e3} = \left(\frac{K}{\sqrt{(1+K)^2 R_N^2 + X_N^2}} - \frac{K(1+K)^2 R_N^2}{(\sqrt{(1+K)^2 R_N^2 + X_N^2})^3} \right) \frac{\partial R_N}{\partial t} \quad (5.8)$$

where X_N and X_T are the total neutral-to-ground and terminal-to-ground capacitive reactances, respectively. Moreover, $|\dot{\overline{V}}|$ is the rate of change of the magnitude of the normalized voltage phasor due to change in NGR resistance while $e3$ and $E3$ remain unchanged. Also, K is defined as follows:

$$K = \frac{X_N}{X_T} = \frac{(2\pi f c_g / 2)^{(-1)}}{(2\pi f (c_s + c_g / 2))^{(-1)}} = \frac{c_s + c_g / 2}{c_g / 2} \quad (5.9)$$

The ratio of the $|\dot{\overline{VR3}}|$ to $|\dot{\overline{VN3}}|$ is achieved through basic mathematical work, as below:

$$Ratio = |\dot{\overline{VR3}}| / |\dot{\overline{VN3}}| = \frac{-R_N (K + 2)}{\sqrt{R_N^2 + X_N^2}} \quad (5.10)$$

On the other hand, the high resistance NGR for unit-connected generators is chosen equal to total system phase-to-ground capacitive reactance [5].

$$R_N = |X_N ||X_T| = \frac{X_N X_T}{X_N + X_T} = \frac{X_N}{\frac{X_N}{X_T} + 1} = \frac{X_N}{K + 1} \quad (5.11)$$

Substituting the Equation (5.11) in Equation (5.10) results:

$$Ratio = \frac{-\frac{X_N}{K+1} (K + 2)}{\sqrt{(\frac{X_N}{K+1})^2 + X_N^2}} = \frac{-(K + 2)}{\sqrt{1 + (K + 1)^2}} \quad (5.12)$$

$$\left(\frac{|\dot{\overline{VR3}}|}{|\dot{\overline{VN3}}|} \right)^2 = 1 + \frac{2(1 + K)}{1 + (1 + K)^2} \quad (5.13)$$

The K is always positive and greater than 1. Thus, the right side of Equation (5.13) is greater than one. As such, the absolute value of $|\dot{\overline{VR3}}|$ is always greater than that of $|\dot{\overline{VN3}}|$ in case of NGR defect. Therefore, the criteria for NGR failure detection is enhanced to an opposite change of the $|\overline{VR3}|$ and $|\overline{VN3}|$ while the $|\dot{\overline{VR3}}|$ is greater than $|\dot{\overline{VN3}}|$ by a factor greater than 1, e.g., 1.5. These criteria are combined into one logic referred to as LOGIC12 in the final algorithm.

As further clarifications, if the total charging capacitances at neutral and terminal were equal, and NGR resistance was infinite, the $|\overline{VR3}|$ and $|\overline{VN3}|$ should be equal in magnitude forming a balanced system with equal contribution in $E3$. Under this condition, any change in the NGR would cause an equal change or variation in both parameters. But, the capacitances are not equal in real life practice. In fact, the terminal side capacitance is higher than that of neutral side [41]. Moreover, the NGR resistance is indefinite. Thereby, the impedance of the terminal side is smaller than the neutral impedance at 180Hz specially when the normal resistance of the NGR is considered. As a result, the $|\overline{VR3}|$ becomes smaller than $|\overline{VN3}|$ holding a lower contribution in the mentioned balance. Conceptually, the less-contributing vector shall change or vary more compared to the higher contributing vector upon NGR failure which changes the balance between the parameters. In this case, the $|\overline{VR3}|$ is subjected to higher variation due to its lower contribution in $E3$.

5.2.2 Monitoring Challenges

Load Variation

The generated third harmonic voltage $E3$ depends on the loading condition ($P + jQ$) [40]. Thus, its effect on NGR failure detection logics should be investigated. As understood from [42], terms A , B , and C of Equation (5.3) and Equation (5.4) are almost in the same direction. Thereby, their vector and scalar summations are assumed equal. Terms A and C do not depend on $E3$. Hence, the rate of change of the normalized third harmonic voltages depend on the term B . The magnitude of this term is easily obtained. The sensitivity of the parameters to $E3$ is obtained as follows:

$$\begin{aligned} \left. \frac{\partial |\overline{VN3}|}{\partial |E3|} \right|_{R_N, E3} &= \frac{\partial (|A - B|)}{\partial |E3|} = \frac{\partial (|A| - |B|)}{\partial |E3|} = \frac{\partial |A|}{\partial |E3|} - \frac{\partial |B|}{\partial |E3|} = \\ &= 0 - \frac{\partial |B|}{\partial |E3|} = \left| \frac{Z_N |Z_T|}{jX_{CWW}} \right| \frac{|e3|}{|E3|^2} \frac{\partial |E3|}{\partial t} \end{aligned} \quad (5.14)$$

$$\begin{aligned}
\left. \frac{\partial |\overline{VR3}|}{\partial |E3|} \right|_{R_N, e3} &= \frac{\partial (|C + B|)}{\partial |E3|} = \frac{\partial (|C| + |B|)}{\partial |E3|} = \frac{\partial |C|}{\partial |E3|} + \frac{\partial |B|}{\partial |E3|} = \\
&0 + \frac{\partial |B|}{\partial |E3|} = - \left| \frac{Z_N || Z_T}{jX_{CWW}} \right| \frac{|e3|}{|E3|^2} \frac{\partial |E3|}{\partial t}
\end{aligned} \tag{5.15}$$

The variation rates are equal in magnitude but opposite in sign. As such, the previously established criteria prevents reporting NGR failure in case of $E3$ variation because the variation rates are equal in magnitude. A predefined threshold for variation rates will be considered that provides further security.

It should be mentioned that the assumptions made in this section will not be considered in software analysis. The assumptions and simplifications do not impact the opposite sign of the variation rates. However, it is expected that the magnitude of the variation rates will not be precisely equal. There will be some difference in these values that are supposed to be avoided by the second logic.

Step-up Transformer Bank Saturation

The third harmonic voltage $e3$ affects the parameters as shown in Equation (5.3) and Equation (5.4). This impact is formulated below:

$$\begin{aligned}
\left. \frac{\partial |\overline{VN3}|}{\partial |e3|} \right|_{R_N, E3} &= \frac{\partial (|A - B|)}{\partial |e3|} = \frac{\partial (|A| - |B|)}{\partial |e3|} = \frac{\partial |A|}{\partial |e3|} - \frac{\partial |B|}{\partial |e3|} = \\
&0 - \frac{\partial |B|}{\partial |e3|} = - \left| \frac{Z_N || Z_T}{jX_{CWW}} \right| \frac{1}{|E3|} \frac{\partial |e3|}{\partial t}
\end{aligned} \tag{5.16}$$

$$\begin{aligned}
\left. \frac{\partial |\overline{VR3}|}{\partial |e3|} \right|_{R_N, E3} &= \frac{\partial (|C + B|)}{\partial |e3|} = \frac{\partial (|C| + |B|)}{\partial |e3|} = \frac{\partial |C|}{\partial |e3|} + \frac{\partial |B|}{\partial |e3|} = \\
&0 + \frac{\partial |B|}{\partial |e3|} = \left| \frac{Z_N || Z_T}{jX_{CWW}} \right| \frac{1}{|E3|} \frac{\partial |e3|}{\partial t}
\end{aligned} \tag{5.17}$$

The variation rates are equal in magnitude, but opposite in sign, and thus cannot cause NGR failure detection for the same reasons provided for the load variation.

Ground Faults

A failed-short NGR behaves like a generator stator ground fault near the neutral and causes maloperation of the generator stator ground protection functions such as the third harmonic voltage comparator (59D) [3, 41]. The only difference between a ground fault right at neutral and an entirely failed-short NGR is the initiation speed of the two phenomena; ground faults are catastrophic while resistor failure is a mechanical or thermal incident that takes time [10]. Hence, the only criterion for discriminating ground faults from NGR failure is the rate of change of the employed parameters. The blinders concept, which is well-known in power swing detection field, is employed to capture the initiation speed of the phenomena. When a ground fault occurs, the parameters move through the blinders quickly, while they are expected to pass slowly in the case of NGR failure. Once the first group of blinders are set, a timer starts counting. The timer is held once the second group of blinders, which are the threshold of the 59D, are set. The ground fault is detected if the elapsed time is very low, e.g., less than 5 ms. Otherwise, NGR failure is reported. According to [41], $|\overline{VR3}|$ and $|\overline{VN3}|$ are ideally equal to 0.5 pu but practically vary from 0.2-0.8 pu. Therefore, the first group of blinders are set to 30% deviation from the ideal condition which means 0.2 pu and 0.8 pu. In other words, if $|\overline{VR3}|$ goes beyond 0.8 pu and $|\overline{VN3}|$ declines to less than 0.2 pu, the first blinders are set. The second group of blinders are chosen equal to pickup setting of the generator stator ground protection, i.e., 35% deviation [3]. In other words, the second group of blinders are set when $|\overline{VR3}|$ grows beyond 0.85 pu while $|\overline{VN3}|$ becomes less than 0.15 pu. Since the failed-short NGR can cause ground fault trip, the result of this discrimination is interlocked with the stator ground protection function outcome to prevent its maloperation in case of NGR failure. The blinders build the third logic that is referred to as LOGIC3 in the final monitoring algorithm.

5.2.3 Monitoring Algorithm

Based on the derived monitoring logics and further considerations, a complete monitoring algorithm has been established as shown in Fig. 5.3. It benefits from three elements and

results in two outcomes. NGRS stands for NGR State which identifies whether the NGR is failing short or open. The other outcome is NGR Failure (NGRF).

The first element employs impedance measurement logic which functions only during ground faults where the magnitude of fundamental harmonic of neutral current and voltage, i.e., $IN1$ and $VN1$, are greater than 5% of neutral PT and CT ratings. In fact, neutral CT cannot provide accurate measurement of 60 Hz neutral current in unfaulted condition. This element reports NGR failure if the obtained resistance changes by at least $\pm 30\%$. This function is indicated by LOGIC4 in the comprehensive monitoring

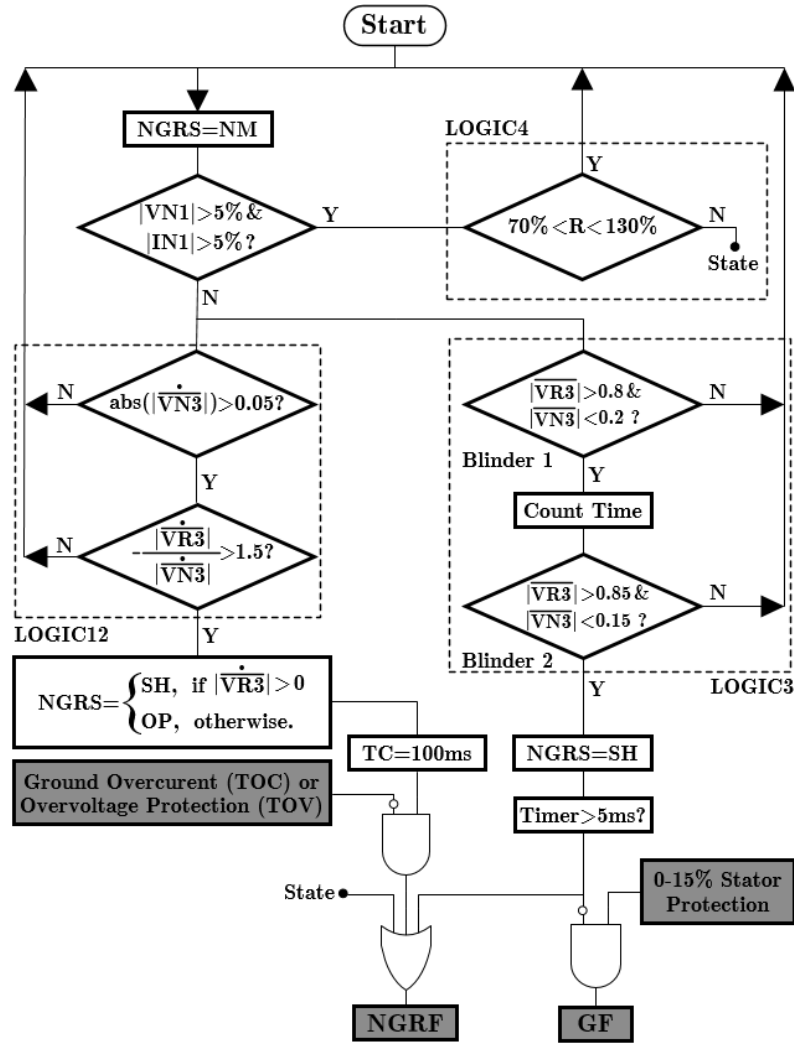


Figure 5.3: Comprehensive algorithm for monitoring the NGR at neutral of the unit-connected generator restrained against ground faults, load and temperature variation, and step-up transformer saturation.

algorithm that is shown in Fig. 5.3. If neutral parameters become less than 5%, the other monitoring elements function.

The second element is the combination of the logics mentioned in Section 5.2.1 and is indicated by LOGIC12. It is activated only if the rate of change of $|\overline{VR3}|$ and $|\overline{VN3}|$ are noticeable, i.e., more than 0.05. This threshold avoids the impact of temperature drifts and signal pollution. If the threshold is activated, LOGIC12 is satisfied only if the parameters change oppositely, and the rate of change of $|\overline{VR3}|$ is at least 1.5 times greater than that of $|\overline{VN3}|$. If LOGIC12 is both activated and satisfied, a digital timer, TC, is set. Once the timer reaches 100 ms, the NGRS and NGRF signals are updated. NGRS is equal to NM by default representing normal or intact NGR condition. It is set to SH if the rate of change of $|\overline{VR3}|$ is positive indicating the failed-short NGR, and is changed to OP otherwise. NGRF is equal to 0 by default and becomes 1 if the overcurrent and overvoltage ground protection elements of the generator remain off or 0.

Finally, the last element, demonstrated as LOGIC3, employs two groups of blinders as described in the previous section. Group 1 is set if $|\overline{VR3}|$ is more than 0.8 pu and $|\overline{VN3}|$ is less than 0.2 pu. If group 1 is set, the time is counted by the Timer. Thereafter, the second group is checked. There is always a time gap between the two groups of blinders which means first the group 1 becomes set and then after a time interval, the group 2. When group 2 of blinders is picked up, the Timer stops counting and the elapsed time is compared to a predefined setting that is 5 ms. This setting has been obtained based on comprehensive software and hardware analysis presented in the next section. If the counted time is less than 5 ms the algorithm does not update NGRS which means the NGR is still intact. Otherwise, NGRS is updated to SH since this logic only detects the failed-short NGR. Additionally, the NGRF signal is triggered to 1 which blocks the 0-15% generator stator ground protection.

It should be added that the designed 5 ms time threshold should be studied to detect the arcing and intermittent ground faults as well. These ground faults show slower evolution than the bolted ground faults. Therefore, a higher threshold should be considered when detecting these kinds of faults is performed using the mentioned 0-15% generator stator ground protection function.

5.3 Validation

In this section, the studied system is introduced. Thereafter, the performance of the proposed algorithm is investigated for various kinds of NGR degradation, considering different conditions of generator loading and step-up transformer saturation. In addition, LOGIC3 is added to an industrial generator protection relay, and its performance is observed.

5.3.1 Study System Specifications and Modeling

The studied configuration, represented in Fig. 5.1, has been simulated in PSCAD. The most important ratings and specifications of the generator and transformer are presented in Table 5.1.

Table 5.1: Power system specifications.

Generator		Transformer	
Capacity	975 MVA	Capacity	975 MVA
Voltage	22 kV	Voltage	20.9/345 kV
c_g	0.230 μ F	c_s	0.137 μ F
NGR	0.784 Ω	c_{ww}	0.012 μ F
NGT	13280/240 V	Knee point	1.17 p.u.

The employed grounding configuration limits the neutral current to 5 A since the achieved resistance at the primary side of the Neutral Grounding Transformer (NGT) is 2.4 k Ω . The distributed model of the generator stator winding has been accomplished using the model presented in [40]. The relation of $E3$ to generator loading has been modeled based on practical data presented in [40]. The parameter K is around 2 for this system. The absolute value of the rate of change of the normalized voltages with respect to the NGR resistance is demonstrated in Fig. 5.4. As shown, the $|\dot{\overline{VR3}}|$ is always securely more than $|\dot{\overline{VN3}}|$ for an intact NGR, as expected and as proven in the previous section. This fact remains valid for a wide range of NGR resistance, i.e., 1.5-5 k Ω . In other words, if the intact NGR fails, the monitoring logic can reliably depend on LOGIC3

of the algorithm shown in Fig. 5.3, where it has been assumed that $|\dot{\overline{VR3}}|$ must be at least 1.5 times the $|\dot{\overline{VN3}}|$.

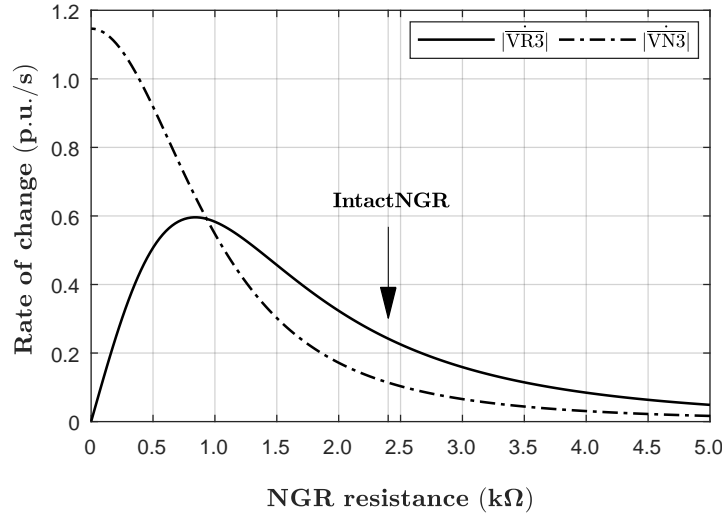


Figure 5.4: Rate of change of magnitude of the third harmonic of neutral and residual normalized voltage phasors in respect to NGR resistance (absolute values).

In the next step, the waveforms are recorded using COMTRADE 91, and the captured data is played back to the monitoring algorithm implemented in MATLAB, and an available industrial generator protection relay.

5.3.2 NGR Failure Detection In Unfaulted Condition

Performance of the algorithm has been investigated for intact, partially failed-short, and partially failed-open NGR conditions considering different loading and saturation conditions as demonstrated in Table 5.2. The proposed algorithm detects the precise status of the NGR for all the cases addressed by SH, NM or OP for failed-short, normal and failed-open NGR, respectively, disregarding the generator loading condition and step-up transformer saturation level. It has also been observed that LOGIC12 detects the slight partial degradation of the NGR, i.e., $\pm 20\%$. In fact, this element of the monitoring algorithm detects all kinds of NGR degradation except when the NGR fails very quickly, completely shorted or disconnected in less than 50 ms, or extremely slowly (which is unlikely). However, the blinder-based monitoring logic detects any slowly failing-short NGR where the resistance of the NGR eventually becomes less than 7%. This study

shows that the proposed technique is well-restrained against the generator loading and saturation of the step-up transformer. These issues will be analyzed independently in following sections.

Table 5.2: NGR failure detection in unfaulted condition. (NGR Status: NM=Normal, SH=Failed-Short, and OP=Failed-Open).

P + jQ (pu)		1.0 + j0.0			0.94 + j0.2			0.85 + j0.4			
e3 (% of 345kV/ $\sqrt{3}$)		0.0	0.5	1.0	0.0	0.5	1.0	0.0	0.5	1.0	
NGR Resistance (Intact NGR = 1 p.u. or 2400 Ω)	0.01 pu	SH	SH	SH	SH	SH	SH	SH	SH	SH	A
	0.05 pu	SH	SH	SH	SH	SH	SH	SH	SH	SH	B
	0.10 pu	SH	SH	SH	SH	SH	SH	SH	SH	SH	C
	0.20 pu	SH	SH	SH	SH	SH	SH	SH	SH	SH	D
	0.50 pu	SH	SH	SH	SH	SH	SH	SH	SH	SH	E
	1.00 pu	NM	NM	NM	NM	NM	NM	NM	NM	NM	F
	2.00 pu	OP	OP	OP	OP	OP	OP	OP	OP	OP	G
	5.00 pu	OP	OP	OP	OP	OP	OP	OP	OP	OP	H
	10.0 pu	OP	OP	OP	OP	OP	OP	OP	OP	OP	I
		1	2	3	4	5	6	7	8	9	

In order to gain a better understanding of behavior of the algorithm, a few case studies are presented in detail. It should be noted that the measurements might be very low during normal condition, and they shall not be interpreted as secondary level measurements.

Case 1 — The scenario B5 of Table 5.2 is represented using recorded waveforms. In this case, the NGR resistance decreases from 100% to 5% in two steps, as shown in Fig. 5.5(e). The loading is $0.94 + j0.2$ pu and the step-up transformer saturation is around 0.5%. The NGR starts failing at $t = 0.1$ s and, the failure takes 700 ms. As shown in Fig. 5.5(c), the $|\overline{VR3}|$ and $|\overline{VN3}|$ are initially equal to 0.51 pu and 0.69 pu, respectively. The saturation of the step-up transformer causes these parameters to not be equal to 0.5 pu. However, they are almost constant with derivatives near zero, as shown in Fig. 5.5(d). Once the NGR starts failing, $|\overline{VR3}|$ grows and $|\overline{VN3}|$ declines. The opposite sign of the derivatives is the first detected sign of failure. As the failure persists, $|\overline{VR3}|$ changes more quickly, confirming that $|\dot{\overline{VR3}}|$ is greater than $|\dot{\overline{VN3}}|$. This behavior persists for more than 100 ms and consequently, NGR failure is reported at $t = 0.235$ s. As shown in Fig. 5.5(c), the blinders of the LOGIC3 are active for this case, as well. The elapsed time

between activation of the two groups of the blinders is 11.8 ms indicating NGR failure. As a result, the ground fault detection, GF, is blocked causing no ground fault detection. Lastly, the status of NGR is updated to SH indicating that the NGR has failed short, as shown in Fig. 5.5(h). This detection is performed based on the direction of change in $|\overline{VR3}|$ and $|\overline{VN3}|$. As demonstrated in Fig. 5.5(c), $|\overline{VR3}|$ increases while $|\overline{VN3}|$ decreases. This behavior occurs only when the NGR resistance declines.

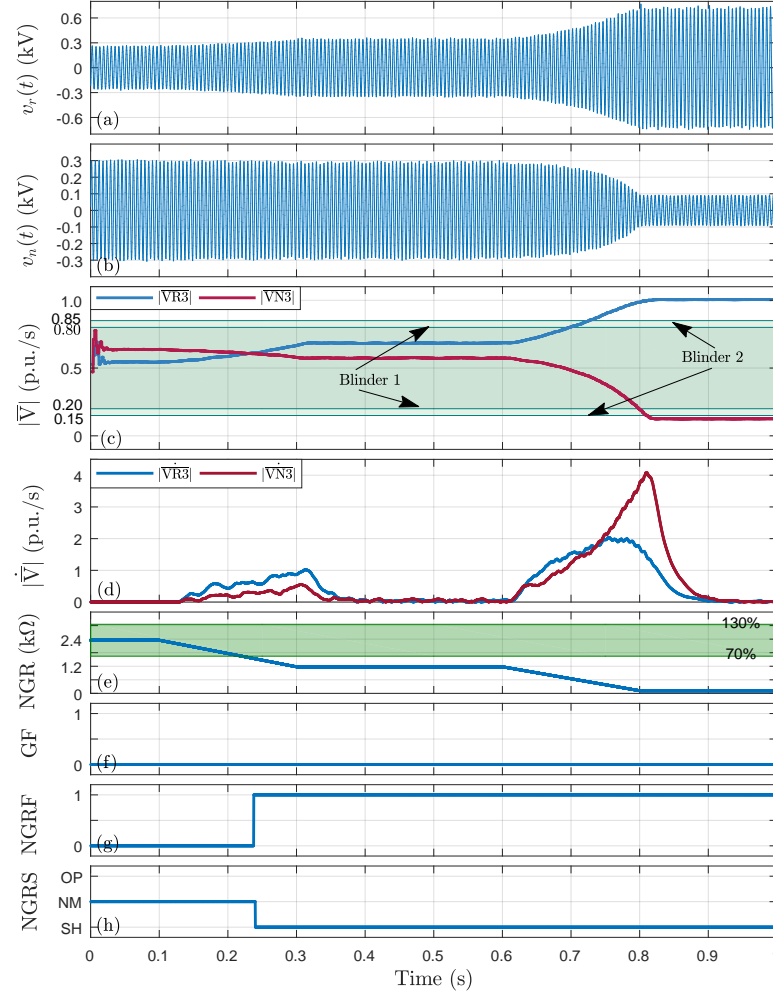


Figure 5.5: Failed-short NGR case (scenario number B5, $r = 1 \rightarrow 0.05$ pu, $Load = 0.94 + j0.2$ pu, and $e3 = 0.5\%$): (a) Residual voltage, (b) Neutral voltage, (c) Normalized neutral and residual third harmonic voltages, (d) Rate of change of the normalized third harmonic voltages, (e) NGR resistance, (f) Ground fault detection, (g) NGR failure detection, and (h) NGRS State.

Case 2 — Another sort of failure similar to previous case is a single step failure where the NGR resistance decreases to a final value in less than a second, e.g., 100% to

60% in 200 ms as shown in Fig. 5.6. In this figure, the $|\overline{VR3}|$ and $|\overline{VN3}|$ vary slightly so that none of the blinders are set. However, the LOGIC12 is activated and satisfied since the $|\overline{VR3}|$ and $|\overline{VN3}|$ change oppositely, while $|\overline{VR3}|$ varies quicker than the $|\overline{VN3}|$ as observed from Fig. 5.6(d). The NGRF signal is enabled by LOGIC12, and NGRS is updated to SH meaning that the NGR is failed-short.

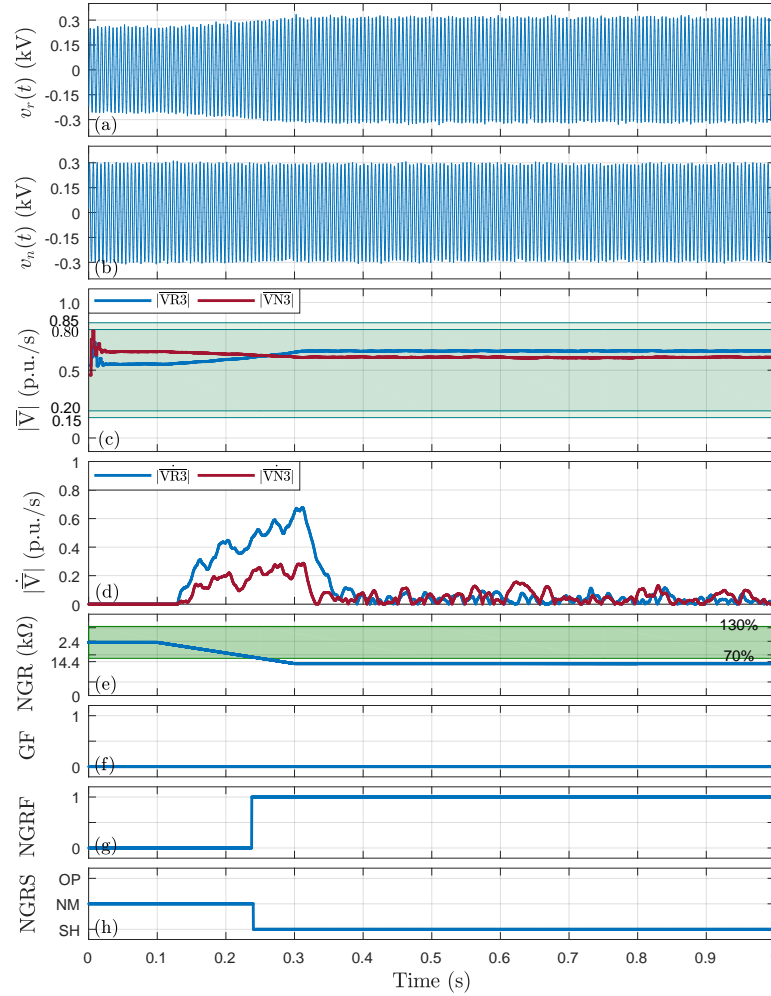


Figure 5.6: Failed-short NGR case ($r = 1 \rightarrow 0.6$ pu, $Load = 0.94 + j0.2$ pu, and $e3 = 0.5\%$): (a) Residual voltage, (b) Neutral voltage, (c) Normalized neutral and residual third harmonic voltages, (d) Rate of change of the normalized third harmonic voltages, (e) NGR resistance, (f) Ground fault detection, (g) NGR failure detection, and (h) NGRS State.

In this scenario, the LOGIC4 does not function since the neutral voltage and current are less than 5% of the system line-to-ground voltage and neutral let through current, respectively.

Case 3 — Scenario number G5 of the Table 5.2 is discussed which is regarding a

failed-open NGR in unfaulted condition where the NGR resistance increases to 200% in 200 ms, as shown in Fig. 5.7. Again, the $|\overline{VR3}|$ and $|\overline{VN3}|$ vary slightly so that none of the blinders are set. In fact, the blinders are not supposed to be activated for failed-open NGR condition. However, the LOGIC12 is activated and satisfied since the $|\overline{VR3}|$ and $|\overline{VN3}|$ change oppositely while $|\overline{VR3}|$ varies quicker than the $|\overline{VN3}|$ as observed from the waveforms. The NGRF signal is enabled by LOGIC12, and NGRS is updated to OP meaning that the NGR is failed-open.

Similar to the previous case, the LOGIC4 does not function since the neutral voltage and current are less than 5% of the system line-to-ground voltage and neutral let through

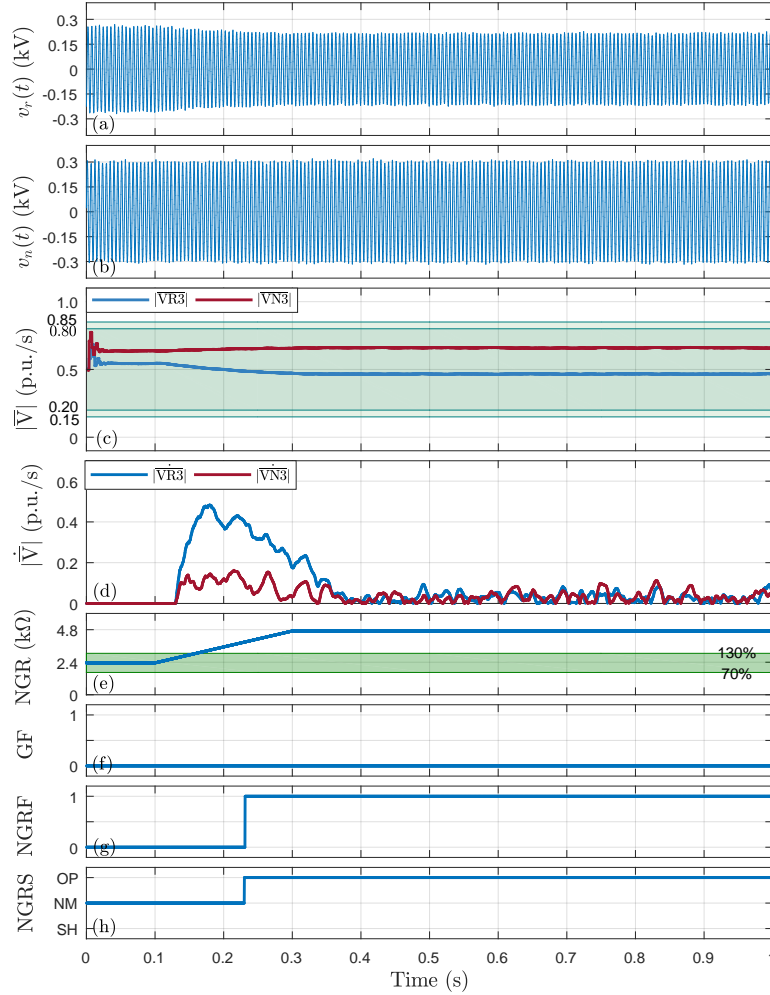


Figure 5.7: Failed-open NGR case (scenario G5, $r = 1 \rightarrow 2$ pu, $Load = 0.94 + j0.2$ pu, and $e3 = 0.5\%$): (a) Residual voltage, (b) Neutral voltage, (c) Normalized neutral and residual third harmonic voltages, (d) Rate of change of the normalized third harmonic voltages, (e) NGR resistance, (f) Ground fault detection, (g) NGR failure detection, and (h) NGRS State.

current, respectively. In this scenario, the LOGIC4 does not function since the the neutral voltage and current are less than 5% of the system line-to-ground voltage and neutral let through current, respectively.

Case 4 — Scenario number H5 of the Table 5.2 is very similar to the previous case, i.e., scenario G5, except a few differences. The NGR fails open in two steps, 100% to 200% and after some time 200% to 500%, as shown in Fig. 5.8(e). The NGR failure is detected in the first step. This study shows that the number of the consequent failures is not important since the proposed technique functions in the first failure.

Similar to the previous case, the LOGIC4 does not function since the the neutral

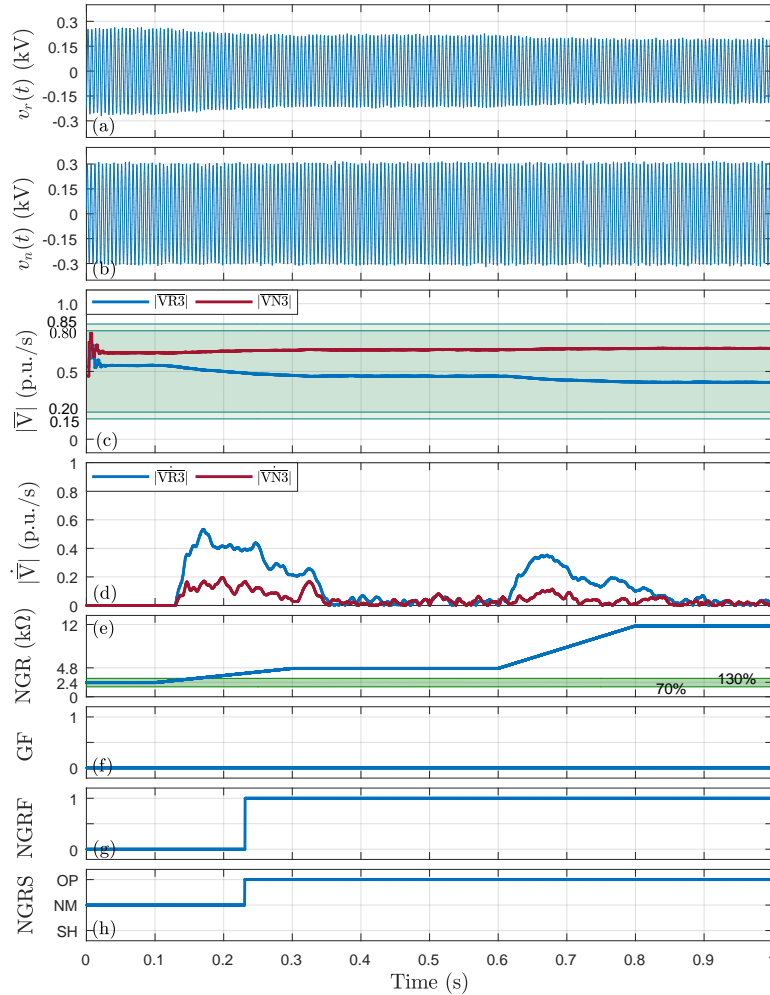


Figure 5.8: Failed-open NGR case (scenario H5, $r = 1 \rightarrow 5$ pu, $Load = 0.94 + j0.2$ pu, and $e3 = 0.5\%$): (a) Residual voltage, (b) Neutral voltage, (c) Normalized neutral and residual third harmonic voltages, (d) Rate of change of the normalized third harmonic voltages, (e) NGR resistance, (f) Ground fault detection, (g) NGR failure detection, and (h) NGRS State.

voltage and current are less than 5% of the system line-to-ground voltage and neutral let through current, respectively.

The effect of the e_3 on LOGIC12 was neglected during the mathematical proof resulting the Equation (5.13). However, it was considered when performing software analysis. As observed, the e_3 is 0.5% of the transmission system line-to-ground voltage, i.e., 0.5% of $345 \text{ kV} / \sqrt{3}$ or 1 kV. However, it does not affect the proven concept. The system faults cause very high saturation levels of the step-up transformer. However, the third harmonic resulted from these phenomena is avoided by 100 ms time delay since the transients last in less than five power cycles.

As mentioned earlier, the shorted NGR behaves similar to ground faults near the neutral of the generator stator. Therefore, the generator stator ground protection might maloperate under this condition. This situation has been observed for the dark gray highlighted cases of Table 5.2. Besides, a hardware test setup was prepared to verify this finding, as shown in Fig. 5.9 and Fig. 5.10. The neutral and three-phase voltage waveforms obtained in PSCAD simulation were recorded using COMTRADE 91. The recorded signals were scaled down to 5V and 1A peak-to-peak using Matlab to comply with digital relay ratings. The captured data was played back to an available industrial generator protection relay utilizing LabVIEW and NI-cDAQ. The adaptive third harmonic level detector protection function provided by the relay trips if the NGR resis-

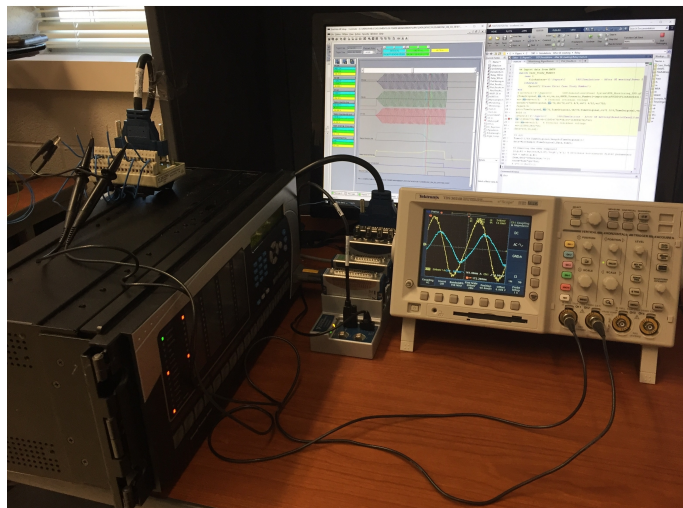


Figure 5.9: Hardware test setup.

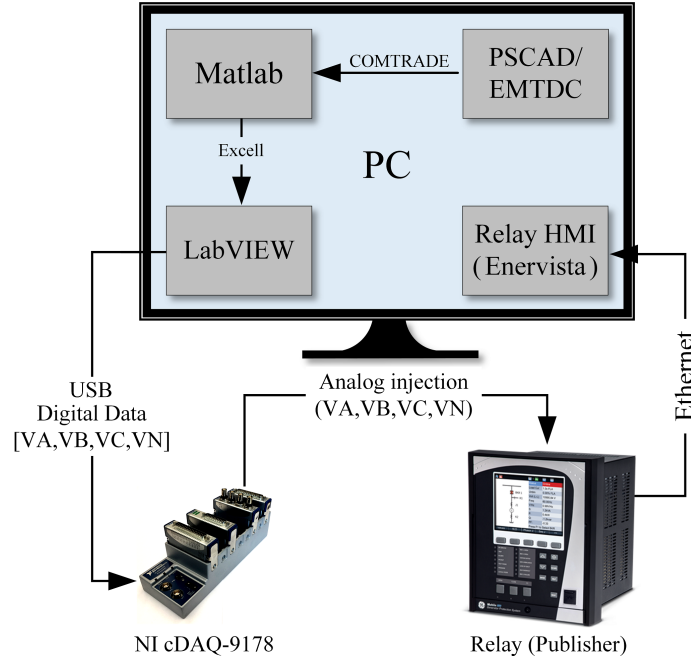


Figure 5.10: Schematics of the hardware test setup.

tance declines to less than 7%.

The blinder-based NGR failure detection logic, LOGIC3, was retrofit to the existing protection relay to detect NGR failure. The enhanced protection function no longer trips in case of NGR failure except when the NGR is shorted very quickly, i.e., completely shorted in less than 50 ms which is unexpected in a real system. The monitored signals by the relay itself and the state of internal variables such as the implemented blinders, enhanced ground fault trip, and NGR failure detection were extracted using the HMI relay software. The performance of the relay for scenario number B5 and another case of a ground fault at 5% of the generator stator winding is demonstrated using the relay measurements and detections.

The first case shows a single-phase-to-ground fault at 5% of the generator stator winding near the neutral. The relay detections are shown in Fig. 5.11. The three-phase voltages at terminals of the generator and neutral voltage are played back to the relay. The magnitude of the total generated third harmonic by the generator, i.e. E_3 , is calculated by vector sum of the three phase-to-ground voltages applied to the relay. As shown, the three phase-to-ground voltages remain unchanged during the single-phase-to-ground fault since the employed high resistance NGR limits the fault current to maximum

of 5 A and suppresses the ground fault.

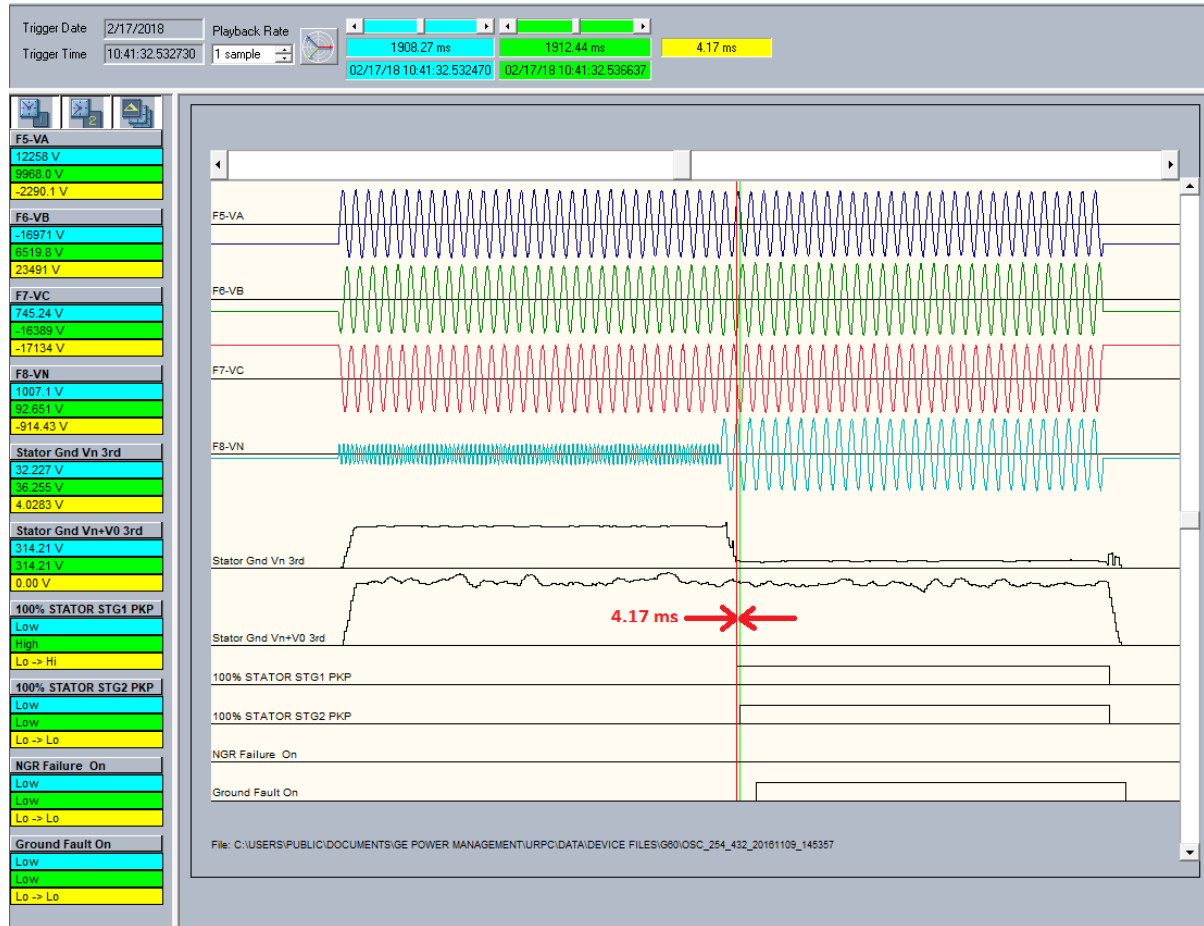


Figure 5.11: Relay detections for LG fault at 5% of the generator stator winding.

On the other hand, the neutral voltage oscillates with 180 Hz frequency before the ground fault incidence where the magnitude of the V_{N3} and total generated third harmonic voltage by the generator, i.e., E_3 , are 208 V and 314 V, respectively. Once the ground fault occurs, the v_n shows oscillations in 60 Hz meaning that its third harmonic has decreased very much, as shown by its magnitude. Since the magnitude of the total generated third harmonic is constant, the $|V_{R3}|$ increases. As a result, the two 100% generator stator ground protection functions are activated. The time duration between activation of the thresholds of the protection functions is very low, i.e., 4.17 ms, as shown in the figure. The red trigger shows the moment that the first 100% stator ground protection function is picked up. There are two other pointers in blue and green. They are mostly used to show the information of specific moments of the waveforms and also the difference

between two moments in volts or time. In this figure, the blue pointer is set on the red trigger which shows the moment that the first blinder, i.e., primary 100% generator stator ground protection, is picked up. It is not visible due to the red trigger. The green pointer is set at the moment that the second blinder, i.e., secondary 100% stator ground protection function, is activated. The time difference between the two pointers, i.e., 4.17 ms, is calculated by the relay and is shown in yellow at the top section of the figure. The relay detects the ground fault, and the NGR failure signal remains off since this time difference is less than the predefined threshold, i.e., 5 ms. This 5 ms setting has been obtained through comprehensive studies of ground faults and NGR failure conditions for the chosen relay.

The second case, shown in Fig. 5.12, is regarding a failed-short NGR in the absence

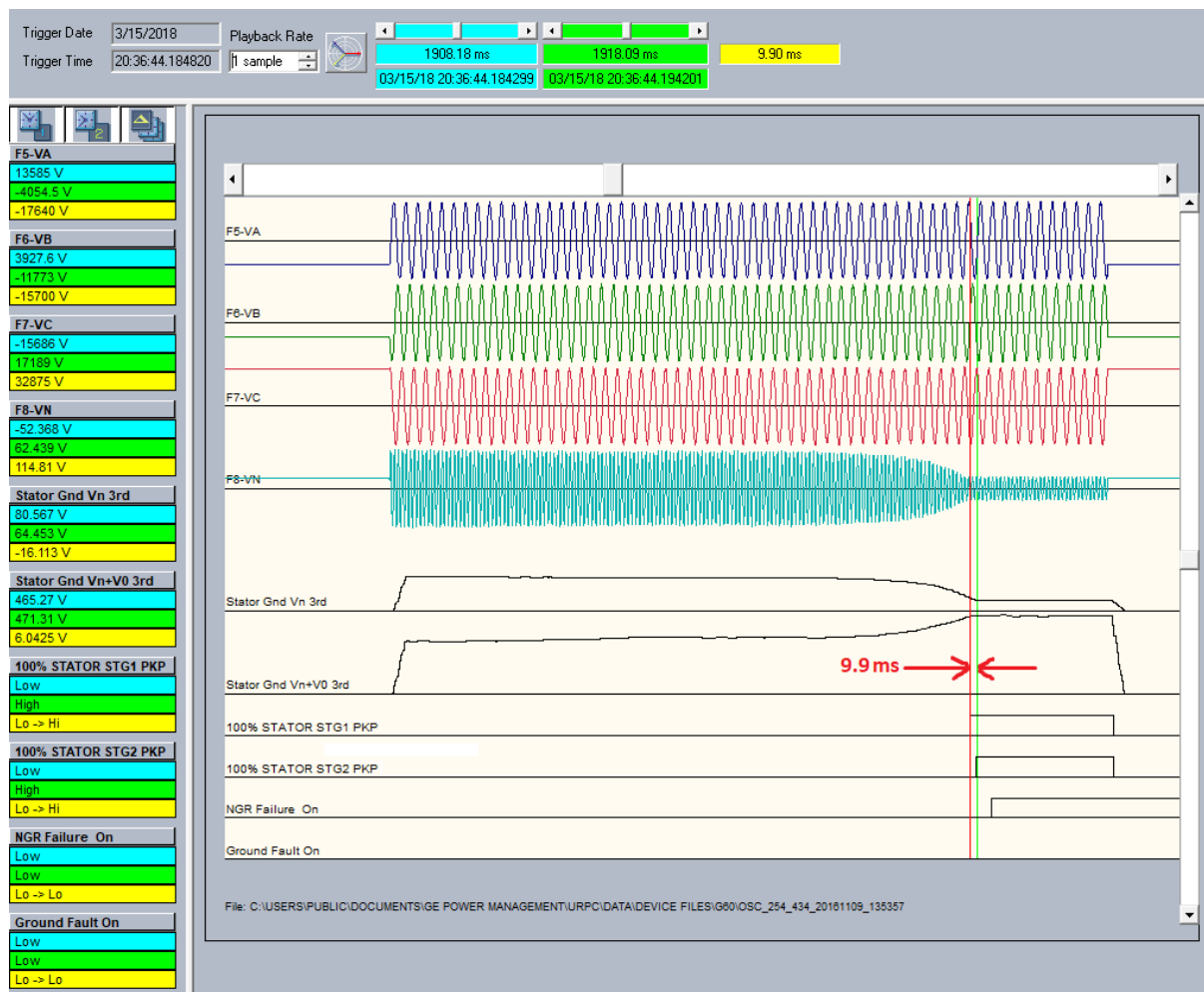


Figure 5.12: Relay detections for failed-short NGR in unfaulted condition.

of the ground faults. In this case, NGR resistance fails short in the same way as shown in Fig. 5.5, i.e., 100-5% in two steps. The neutral voltage remains low during the entire event, and only contains the 180 Hz oscillation. The phase-to-ground voltages behave the same as the previous case even during the NGR failure. Once the NGR starts failing, the neutral voltage starts decreasing. At the same time, the residual voltage starts increasing. As a result, the primary 100% stator ground protection function, with the pickup settings set to 20% and 80%, is activated. After a time delay, the secondary 100% stator ground protection function with the thresholds set to 15% and 85%, is enabled, as well. The time delay between operation of the two protection functions is 9.9 ms. The monitoring scheme reports NGR failure since this time difference is higher than 5 ms. Additionally, the ground fault trip signal remains off.

5.3.3 Distinguishing Ground Faults from NGR Failure

As mentioned, the shorted NGR, and ground faults very close to behave similarly. Therefore, a ground fault in the generator stator could cause undesired NGR failure detection. The performance of the proposed technique for various ground faults has been investigated as well. The proposed algorithm distinguishes the ground faults from NGR failure in two ways. Firstly, ground fault initiation is very faster than NGR failure. In fact, the parameters pass through the blinders in under 5 ms which blocks LOGIC3. Secondly, $|\dot{\overline{VN3}}|$ is greater than $|\dot{\overline{VR3}}|$ which blocks the LOGIC12. A sample case that is regarding a line-to-ground fault at 5% of the generator stator is shown in Fig. 5.13.

Furthermore, NGR can fail during the ground faults as well. Hence, a partially-shortened NGR condition has been considered during the ground fault case represented in Fig. 5.13. The main aim of this case is to show that if the neutral current grows to more than 5% due to ground faults, it is still possible to monitor the NGR status using the impedance measurement, i.e., LOGIC4. Otherwise, the status of the NGR cannot be monitored with the proposed scheme during the ground faults since the ground fault bypasses the NGR. As shown in Fig. 5.13(e), the resistance of the NGR is initially assumed equal to the intact NGR condition and can only be calculated when the fundamental harmonic of the neutral current becomes greater than 5% of the neutral let-through cur-

rent, i.e., 5 A. The resistance decreases to less than 70% at $t = 0.523 \text{ ms}$ and NGR failure is reported 20 ms later.

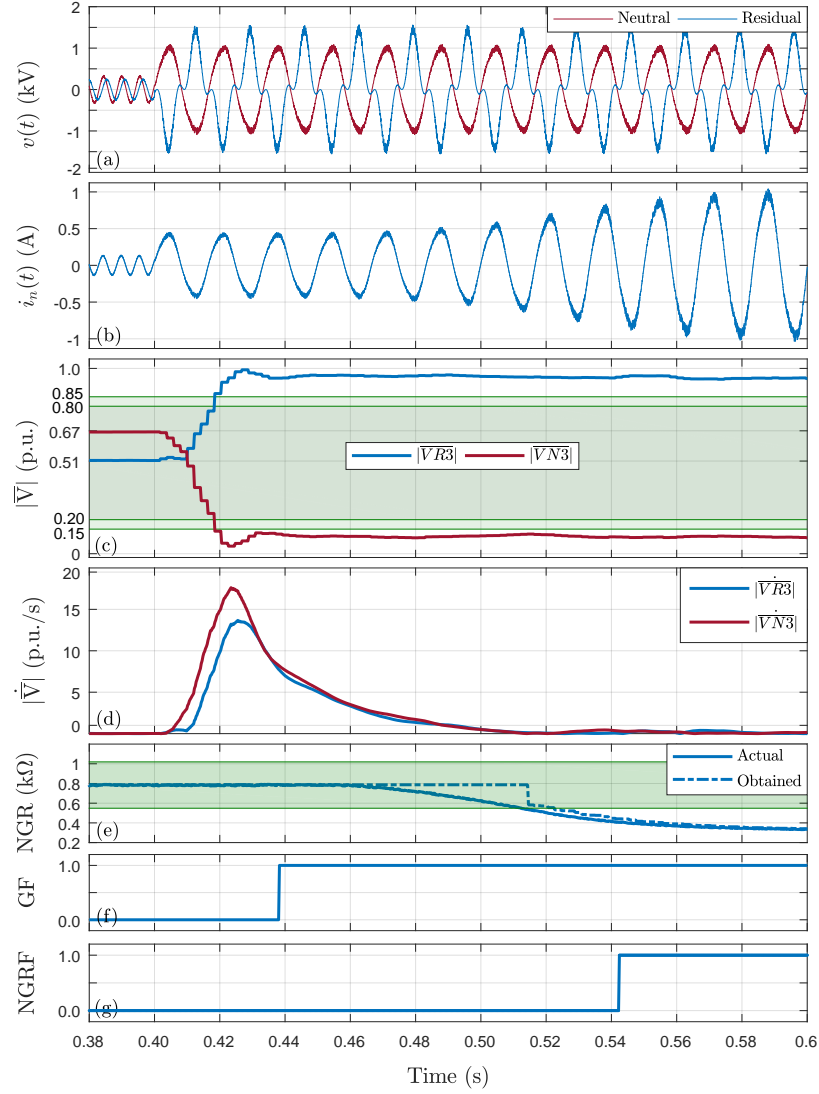


Figure 5.13: Ground fault case followed by NGR failure ($r=1 \rightarrow 0.5 \text{ pu}$, $\text{Load} = 1.0 + j0.0 \text{ pu}$, and $e3 = 0.5\%$): (a) Neutral and residual voltages, (b) Neutral current (c) Normalized neutral and residual third harmonic voltages, (d) Rate of change of the normalized third harmonic voltages, (e) NGR resistance, (f) Ground fault detection, and (g) NGR failure detection.

The external ground faults, outside the generator stator winding, also need to be investigated since they impact on the employed parameters. A study was conducted to investigate the performance of the monitoring algorithm in the presence of ground faults close to the terminal end of the generator stator. The single phase-to-ground and double phase-to-ground faults satisfy LOGIC12. To solve this issue, the ground overcurrent or

overvoltage protection trip is interlocked with the outcome of LOGIC12. Thus, if ground faults in 10-100% of the generator stator occur, LOGIC12 is blocked. This logic has been added to the monitoring algorithm presented in Fig. 5.3. A sample case is represented using the data recorded for an AG fault at terminals of the generator. The results are shown in Fig. 5.14. As shown, LOGIC12 is satisfied, but the ground fault trip has blocked the monitoring algorithm.

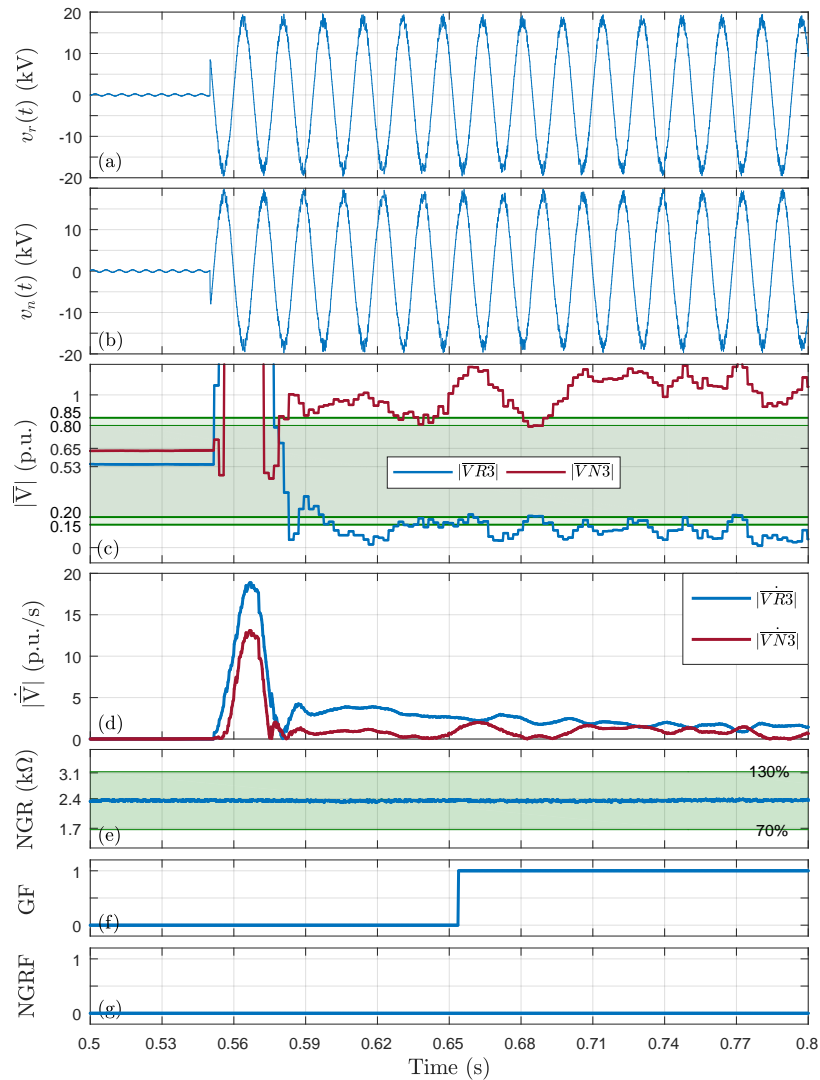


Figure 5.14: Single-phase-to-ground fault at terminal of the generator for intact NGR condition, $E3 = 1\%$, and $e3 = 0.5\%$: (a) Neutral and residual voltages, (b) Neutral current (c) Normalized neutral and residual third harmonic voltages, (d) Rate of change of the normalized third harmonic voltages, (e) NGR resistance, (f) Ground fault detection, and (g) NGR failure detection.

Furthermore, the performance of the proposed method during other kinds of system faults have been studied as well. The system line-to-line and three-phase faults do not change the $|\overline{VR3}|$ and $|\overline{VN3}|$ causing no undesired NGR failure detection. In fact, the third harmonic currents of the three phases are in phase meaning that all system phases are at the same 180 Hz electrical potential. Therefore, the phase-phase faults do not change the third harmonic equivalent network presented in Fig. 5.2 meaning no fault or NGR failure detection. However, the three-phase-to-ground fault changes these parameters. This fault causes the $|\overline{VR3}|$ to decrease noticeably while the $|\overline{VN3}|$ becomes equal to total generated third harmonic. In fact, the ground fault of any type will short the terminal to ground bypassing the Z_T .

5.3.4 Load Variation and Step-up Transformer Saturation

The last case study includes the effect of load variation and step-up transformer saturation on the proposed scheme. On the basis of the analysis presented in Section 5.2.2, the rate of change of the normalized third harmonic voltages is expected to be equal in the case of load variation and step-up transformer saturation. The same has been observed during software analysis. A sample case is shown in Fig. 5.15 which contains 50 ms of load variation starting at $t = 0.54$ s, and 50 ms of step-up transformer saturation starting at $t = 0.66$ s.

As shown, $|\dot{\overline{VN3}}|$ is greater than or equal to $|\dot{\overline{VR3}}|$ for both events, which does not satisfy the LOGIC12. Thus, the algorithm reports neither the ground fault nor the NGR failure. Moreover, the load variation and step-up transformer saturation are very slow phenomena in practice. The 10% change in generator loading takes at least 10 s [41]. Accordingly, the shown variation rates should be scaled-down by a factor of at least 0.1. As such, the threshold block of the monitoring algorithm, i.e., set to 0.05, rejects these phenomena in most of the cases. These variation rates might activate the 0.05 threshold due to sudden disturbances. However, the 100 ms time delay will reject this situation safely. For example, the transformer saturation that happens right after the ground faults lasts in five power cycles. Even though the threshold might be set, but the 100 ms time delay and LOGIC12 will not be satisfied.

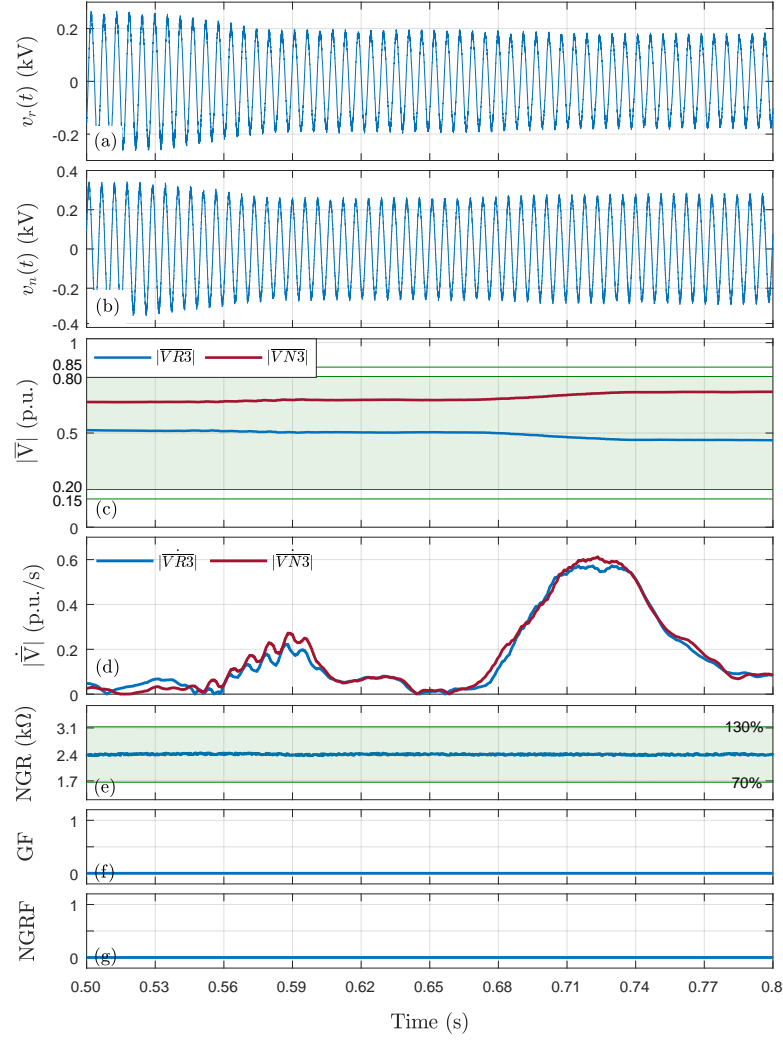


Figure 5.15: Load variation $(1.0 + j0.0) \rightarrow (0.6 + j0.35)$ pu, and step-up transformer saturation ($e3 = 0 \rightarrow 0.5\%$) case for intact NGR: (a) Neutral and residual voltages, (b) Neutral current (c) Normalized neutral and residual third harmonic voltages, (d) Rate of change of the normalized third harmonic voltages, (e) NGR resistance, (f) Ground fault detection, and (g) NGR failure detection.

5.4 Discussion

The following principles should be considered when adapting the proposed method into an actual generator protection system:

- The proposed method can be incorporated into digital protection of generators that are: 1) high-resistance grounded, 2) unit-connected which means that the generator step-up transformer is delta-wye, and 3) equipped with line PTs and neutral PT.

- The blinders employed by LOGIC3 are the simplest possible way to calculate the variation rate. Further, calculation of the rate of change of power system electrical parameters is not a challenge these days, e.g., ROCOF function which calculates the rate of change of frequency. The rest of the proposed technique is just simple and straight forward logics that most logic engine softwares can easily implement.
- The only protection function that is disabled upon NGR failure detection is the 0-15% generator stator ground protection where the NGR is highly shorted. One possible scenario is that the NGR fails completely shorted representing very low resistance. This situation should be behaved as a ground fault at neutral while the proposed method blocks the 0-15% generator stator ground protection function. This situation can be controlled by defining a minimum acceptable level of the third harmonic voltage at neutral, e.g., 1% of E_3 . In fact, the neutral voltage will fade if the NGR becomes entirely shorted.
- Lastly, it should be mentioned that the proposed technique guarantees monitoring only if the employed parameters exist. In fact, this technique only functions in an energized system. The other issue facing this proposed technique is the very severe saturation condition of the step-up transformer. Also, power system parameters do not remain unchanged due to temperature. However, it is expected that the considered threshold and timers will avoid these issues. These limitations need extensive work and are next steps of the studies.

Further simulation results can be found in Appendix D.

5.5 Summary

A new technique was proposed to monitor the high-resistance neutral grounding resistor located at neutral of unit-connected generators. Performance of the technique was studied and discussed for various conditions of the system, resistor, generator loading, step-up transformer saturation, and ground faults. The following conclusions could be derived based on software and hardware observations.

The proposed monitoring logics reliably detect NGR status, including the partially failed-short, partially failed-open and intact conditions, while existing techniques need additional instruments to detect the partial failure of the NGR. In addition, it shows sufficient restraint against load variation and step-up transformer saturation.

Generator stator ground faults were distinguished from the failed-short NGR. Thereby, the conventional generator stator ground protection function was restrained against NGR failure. In addition, an available generator protection relay was enhanced by retrofitting this element. As a result, it no longer maloperates when NGR fails. Since the proposed technique was embedded as part of the generator stator ground protection, it is an economical solution.

As further applications, the proposed method has the potential for use in the delta to high-resistance-grounded-wye distribution transformers that supply the ungrounded or delta-connected loads which are common in industries such as oil and coal. Further analysis and performance evaluation of the proposed technique for this configuration is suggested, with expected results similar to the findings presented in this chapter.

Chapter 6

NGR and NGL Monitoring based on Sub-Harmonic Signal Injection

In this chapter, a new monitoring technique is proposed that benefits from the existing sub-harmonic injection infrastructures that are used to detect the ground faults in 0-15% of the generator stator winding. This technique monitors the generator winding-to-ground impedance and detects the ground faults if the real part of the seen impedance declines to below a very low preset threshold. The available measurements by this technique are the neutral voltage and current. The proposed technique only needs an additional current sensor which can be easily incorporated into digital relays that include the mentioned protection function. Thereby, generators with injection based stator ground protection function can utilize this technique by installing only the additional CT.

The fundamentals and concepts of the sub-harmonic injection based generator stator ground protection will be explained in Section 6.1 followed by the proposed monitoring function. In the next step, the behavior of the proposed monitoring method will be investigated and presented using PSCAD in conjunction with Matlab. The performance of the proposed method will be shown for failed-open and failed-short NGR conditions during both unfaulted and faulted operation modes of the generator. Besides, the performance of the sub-harmonic injection based 0-15% generator stator ground protection will be demonstrated as well. Additionally, the validity of the proposed monitoring method for a resonant grounded unit-connected generator configuration will be studied as well.

6.1 Configuration 1 — High Resistance Grounding

The target configuration is shown in Fig. 6.1 which is actually a high resistance grounded unit-connected generator. The NGR is installed at the secondary of a Neutral Grounding Transformer (NGT) to meet the required current and voltage ratings using a small resistor. The obtained grounding resistor limits the neutral current to 5 A.

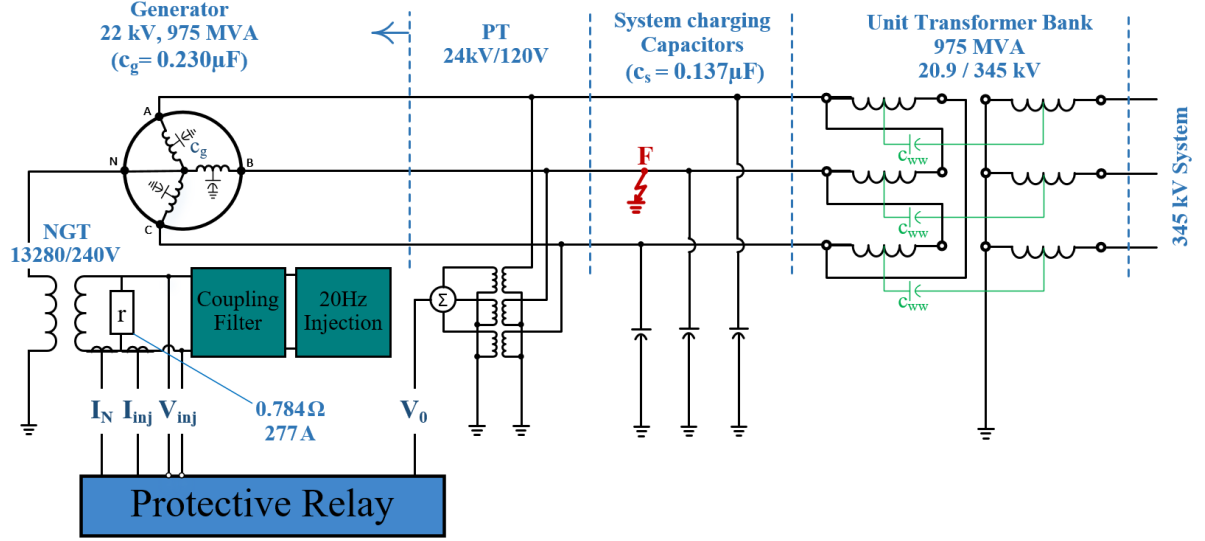


Figure 6.1: Connection diagram of the high resistance grounded unit-connected generator equipped with sub-harmonic signal injection based generator stator ground protection.

Recently, many techniques have emerged towards detecting the internal ground faults of this type of generator. The conventional ground protection functions do not secure the near neutral ground faults and there has been an effort to detect this issue via injecting sub-harmonics or inter-harmonics to neutral and monitoring the stator-to-ground resistance, hereafter referred to as R_{SG} , obtained as follows [34, 35, 31]:

$$R_{SG} = \frac{(N/n)^2}{\text{Real}\left(\frac{I_N}{V_{inj}}\right)} \quad (6.1)$$

where (N/n) is the turn ratio of the NGT which is 13280/240 or 55.33. Also, the V_{inj} is the injection voltage, and the I_n is the neutral current at the secondary of the NGT. The 20 Hz components of the neutral voltage and current are used in this calculation. If the generator stator does not experience any ground faults, then the R_{SG} should be very

high, i.e., in the order of $100\text{ k}\Omega$. Once a ground fault occurs, the R_{SG} is expected to decline to fault resistance. A threshold set to $1\text{ k}\Omega$ detects the ground faults in 0-15% of the generator stator winding near the neutral. Moreover, the overvoltage ground fault protection function detects the ground faults in 5-100% of the generator stator winding if $V_N > 5\%$. The 10% overlap of the two protection functions makes the simultaneous use of them a perfect protective scheme.

6.1.1 Proposed Monitoring Method

In order to be able to monitor the resistance of the NGR, an additional measurement instrument is needed to measure the injected current, shown by I_{inj} in Fig. 6.1. As known, the current through the NGR is equal to vector subtraction of the I_n and I_{inj} . Since the voltage and current of the NGR are available, its resistance is obtained using the following equations:

$$R_{NGR (20\text{ Hz})} = \frac{(N/n)^2}{\text{Real}(Y)} = \frac{(N/n)^2}{\text{Real}\left(\frac{I_{inj}-I_N}{V_{inj}}\right)} \quad (6.2)$$

$$R_{NGR (60\text{ Hz})} = \text{Real}\left(\frac{3V_0}{(n/N)I_N}\right) \quad (6.3)$$

where the I_{inj} is the injected current. The 20 Hz or 60 Hz components of neutral voltage and current can be used depending on the operation mode of the system. During the unfaulted condition, the 20 Hz component is dominant, and it is recommended to employ the 20 Hz admittance. However, when the ground faults occur, the 60 Hz component grows remarkably and filtration of the 20 Hz component becomes challenging. Hence, the 60 Hz impedance is used during the ground faults. Indeed, the sub-harmonic injection based generator stator ground protection alarms and indicates the near-the-neutral ground fault in 100 ms, and just after that the 60 Hz neutral impedance is employed.

The failed NGR is detected if the calculated NGR resistance changes 30% either failed-short or failed-open considering a time delay of 10 s. The complete logic for NGR monitoring is shown in Fig. 6.2. In the shown decision making flowchart, first the total stator-to-ground resistance (R_{SG}) is calculated using Equation (6.1). This resistance is

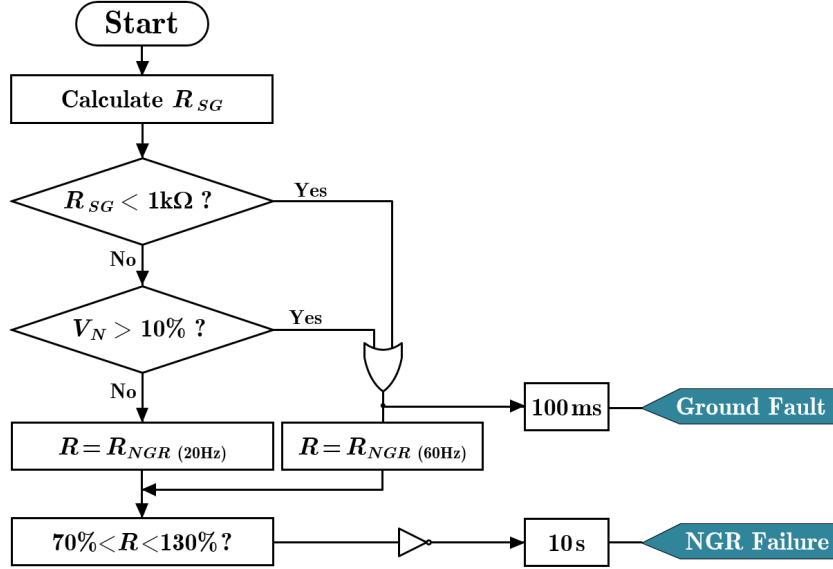


Figure 6.2: NGR monitoring logic and ground fault detection scheme.

used to alarm on ground faults in 0-15% of the generator stator winding. If this resistance is less than $1\text{ k}\Omega$, the Ground Fault (GF) signal will be triggered, and the 60 Hz component of the measurements will be used by the monitoring logic. Otherwise, the ground faults in 5-100% of the generator stator will be investigated using the overvoltage ground fault protection scheme, i.e. $V_N > 10\%$. If any ground fault is detected by this scheme a alarm signal will be initiated in 100 ms, and the 60 Hz component of the measurements will be employed for monitoring. It should be added that the overvoltage ground protection trips immediately and most probably there will not be enough time to monitor the NGR during such ground faults. If no ground fault is detected ($GF=0$), the NGR resistance will be calculated using the 20 Hz component of the measurements, and NGR failure will be detected in case of abnormal resistance, i.e., $\pm 30\%$ from the rated value.

6.1.2 Simulation Verification

In this section, the proposed monitoring technique is studied using PSCAD in conjunction with Matlab. The studies are conducted for an NGR which grounds the neutral of a wye-connected 975 MW, 22 kV generator that is connected to 345 kV transmission system via a 975 MVA, 20.9/345 kV DYg transformer which is chosen from [5], as shown in Fig. 6.1.

The NGR has been designed based on instructions provided in [5]. Its resistance is

0.784Ω which provides high resistance grounding, i.e. 2400Ω at primary, when installed at the secondary of a 50 kVA, 13280/240 V single phase NGT. The generator has been modeled using the 6 segment per phase pi-model presented in [40]. This model provides the opportunity to distribute the generator phase-to-ground capacitances along the winding and also to simulate the internal ground faults.

The proposed monitoring technique successfully detects the NGR resistance variations, reports NGR failure and the type of the defection during both normal and faulted operation conditions. Performance of the monitoring scheme for each condition is presented by a few sample cases, referred to as cases 1 and 2 for normal operation condition and cases 3 and 4 for faulted condition.

During the normal operation condition, the neutral system experiences very weak 60 Hz voltage and current. Hence, the resistance of the NGR is calculated using the injected 20 Hz signals as shown in the proposed monitoring logic. On the basis of the performed software analysis, the proposed technique detects any change of the NGR structure by monitoring its resistance. Few sample cases are presented with more details. It should be noted that the measurements might be very low during normal condition, and they shall not be interpreted as secondary level measurements.

Case 1 — The first case is regarding a failing short NGR, i.e. 50%-shorted over 200 ms, as shown in Fig. 6.3. The neutral voltage and current and also the injected current are shown. The stator-to-ground resistance of the generator winding, R_{SG} , is also represented to demonstrate the protection function. Normally, it is very high in the order of $100\text{ k}\Omega$ which means absence of stator to ground faults. It remains high during the event and no ground fault is detected (GF=0). Hence, the NGR resistance, R_{NGR} , is obtained only using the 20 Hz component of the signals as shown in Fig. 6.3(e). As represented, the NGR resistance starts declining at $t = 1.4\text{ s}$ and decreases to 50% over 200 ms. Once the NGR resistance goes out of the 70-130% region the NGR failure is expected as reported after 200 ms. The failure type is also easily detected since the NGR resistance is in hand. In this case, the NGR state is updated from NM to SH meaning that it was normal and has failed-short. It should be noted that the NGR failure is supposed to be reported after 10 s, but the waveforms are better-represented if a lower time delay,

here 200 ms, is used. Further, the mighty oscillations in the calculated impedance are due to dynamic of the DFT filter used for phasor estimation. This issue is easily solved by using the moving average of the calculated resistance or reactance.

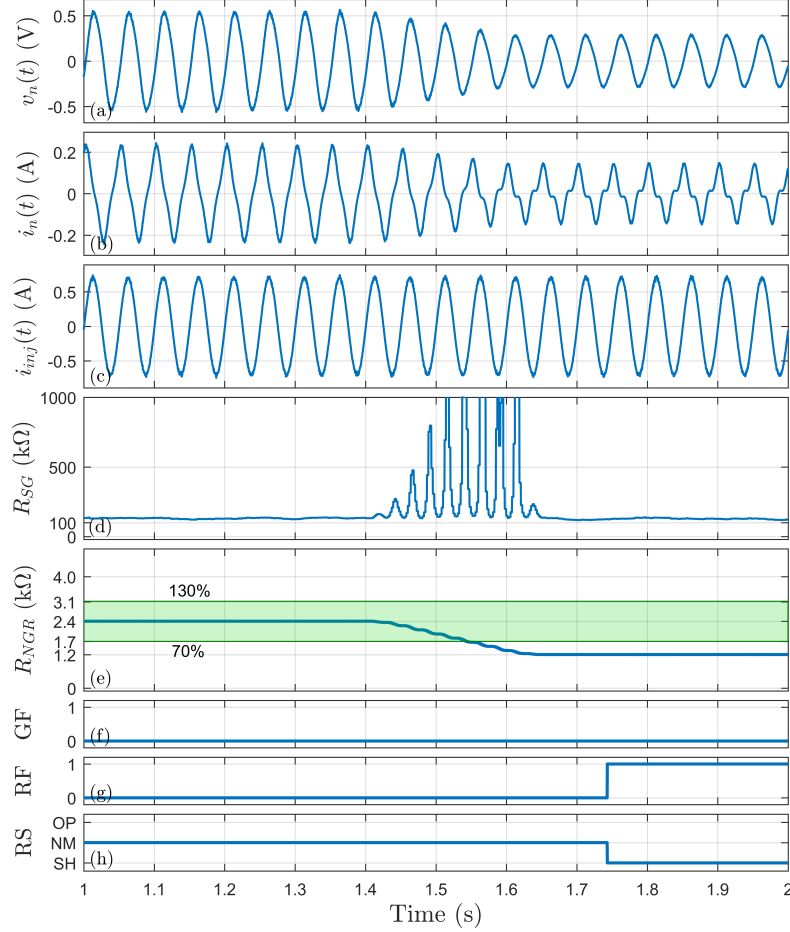


Figure 6.3: Case-1: Failed-short NGR in unfaulted condition: a) Neutral voltage, b) Neutral current, c) Injected 20 Hz current, d) Generator stator winding insulation resistance, e) NGR resistance, f) Ground Fault (GF), g) Resistor Failure (RF), and h) Resistor Status (RS).

Case 2 — The second case, shown in Fig. 6.4, represents the same behavior as the case 1 but for a fail-open NGR. Again, the NGR failure and status are detected correctly using only the 20 Hz component of the measurements. The NGR failure, RF, is reported 200 ms after that the obtained 20 Hz resistance of the NGR rises above the 130% threshold, i.e. 3120Ω . The NGR status is updated from NM to OP meaning that the NGR was normal and is failed-open.

The proposed technique is intended to monitor the NGR even during the ground

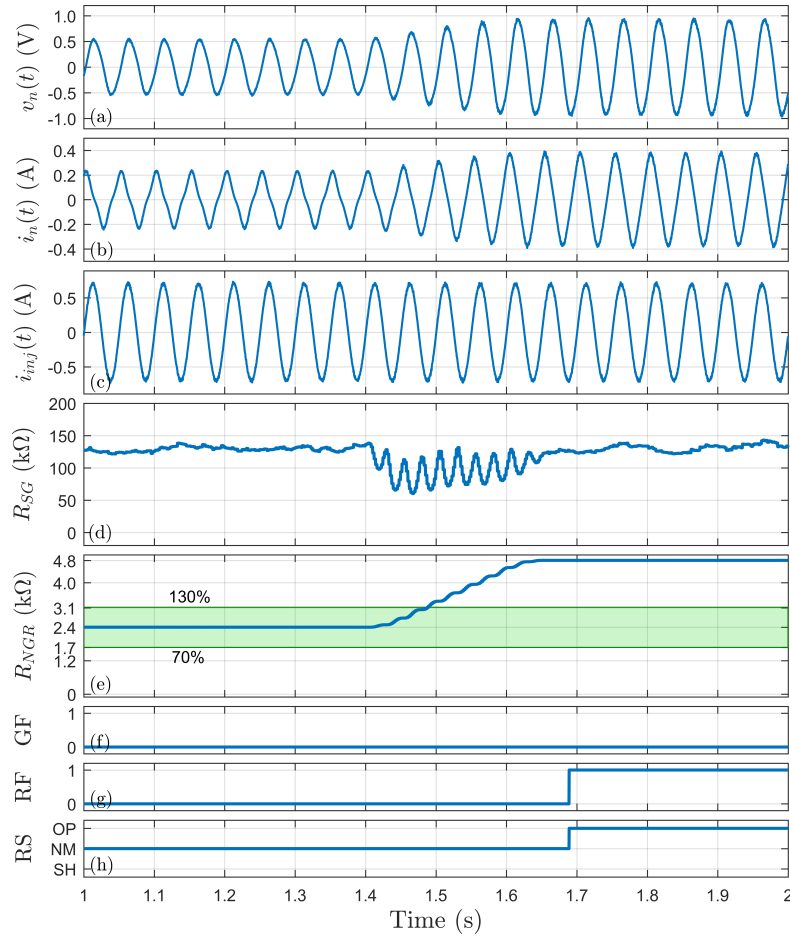


Figure 6.4: Case-2: Failed-open NGR in unfaulted condition: a) Neutral voltage, b) Neutral current, c) Injected 20 Hz current, d) Generator stator winding insulation resistance, e) NGR resistance, f) Ground Fault (GF), g) Resistor Failure (RF), and h) Resistor Status (RS).

faults. The penetration of the 60 Hz fault current into the injection source due to imperfection of the coupling filters is challenging. In fact, the designed filters conduct a very negligible portion of the neutral current during the ground faults near the terminal of the generator stator. Since the 60 Hz component of the neutral voltage and ground current is strikingly greater than the injected 20 Hz signal, the very negligible penetrating 60 Hz current and voltage become comparable to the injected 20 Hz signal. This causes many issues in phasor estimation of the 20 Hz component of the neutral voltage and current yielding completely wrong calculation of the NGR resistance using the 20 Hz component. Hence, the NGR resistance is obtained using the 60 Hz components of the neutral current and voltage during the ground faults. As such, once the ground fault is detected, the

monitoring logic switches to the 60 Hz admittance of the NGR as shown in Fig. 6.2.

Observations show that the performance of the proposed method during ground faults is satisfactory as well. Two sample cases are discussed to illustrate the performance of this technique during the ground faults, shown in Fig. 6.5 and Fig. 6.6, referred to as case 3 and case 4, respectively.

Case 3 — This case shows a failing short NGR during an internal single-line-to-ground fault at 5% of the generator stator winding. The ground fault occurs at $t = 1.2$ s. The calculated resistance of the NGR becomes invalid right after the fault initiation due to adversely affected 20 Hz phasor estimation. Once the ground fault is detected, at $t = 1.34$ s, the monitoring technique switches to 60 Hz phasor estimation and calculates

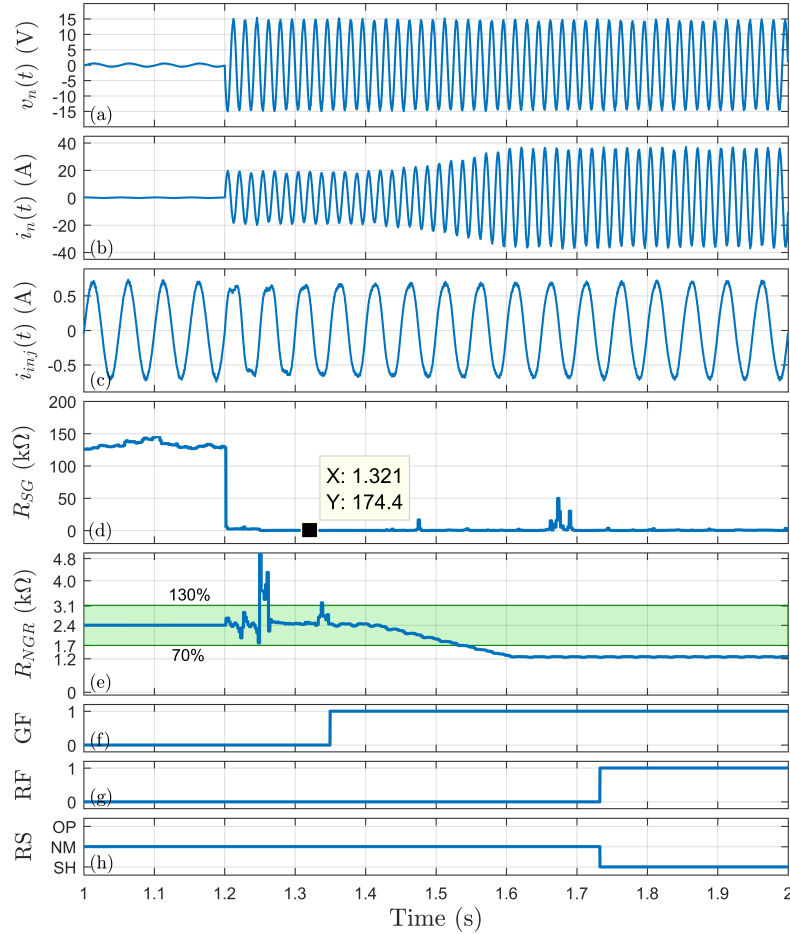


Figure 6.5: Case-3: Failed-short NGR during an internal single-line-to-ground fault: a) Neutral voltage, b) Neutral current, c) Injected 20 Hz current, d) Generator stator winding insulation resistance, e) NGR resistance, f) Ground Fault (GF), g) Resistor Failure (RF), and h) Resistor Status (RS).

the resistance of the NGR using the 60 Hz component of the measurements. As shown in Fig. 6.5(e), the NGR resistance remains in the safe region after the ground fault initiation. Thereafter, the NGR starts failing short at $t = 1.4$ s and the monitoring technique reports the NGR failure in 200 ms after the NGR resistance goes out of the safe region, i.e., less than 70% threshold. Furthermore, the performance of the 20 Hz signal injection based 0-15% generator stator ground protection function is shown as well. The stator-to-ground resistance of the generator is very high before the ground fault incidence and fades to just a few hundred ohms once the ground fault occurs as shown in Fig. 6.5(d).

Case 4 — The fourth case, shown in Fig. 6.6, demonstrates the performance of

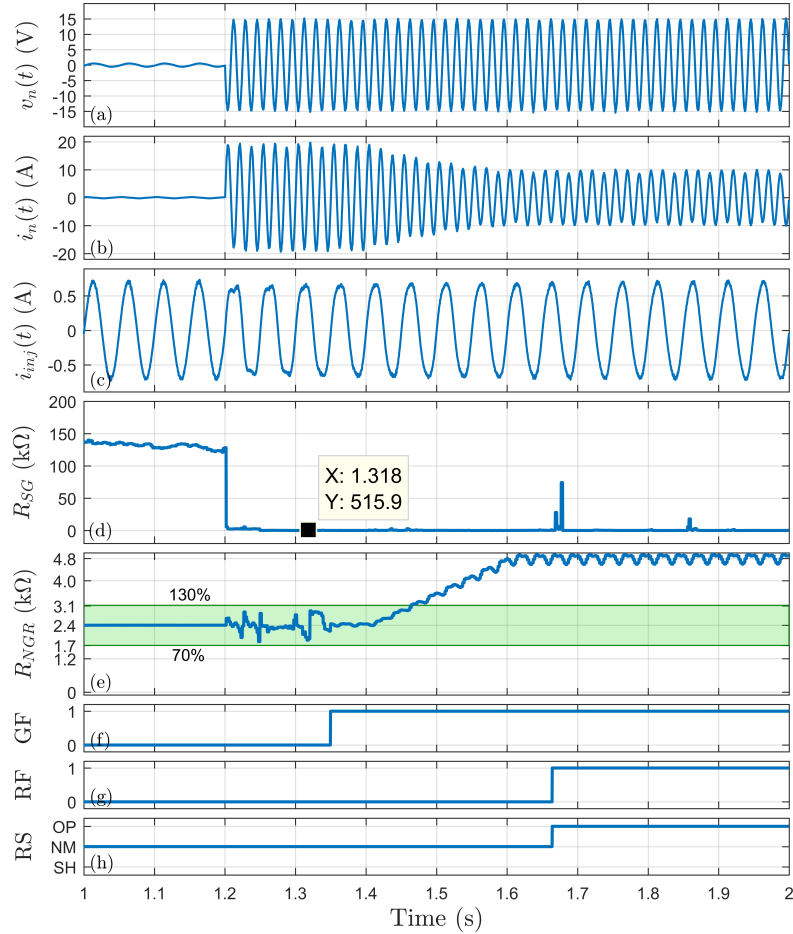


Figure 6.6: Case-4: Failed-open NGR during an internal single-line-to-ground fault: a) Neutral voltage, b) Neutral current, c) Injected 20 Hz current, d) Generator stator winding insulation resistance, e) NGR resistance, f) Ground Fault (GF), g) Resistor Failure (RF), and h) Resistor Status (RS).

the monitoring technique for a failing-open NGR during an internal single-line-to-ground fault at 5% of the generator stator winding. Again, the resistance of the NGR is accurately obtained before ground fault incidence using the 20 Hz component of the measured parameters. However, the 20 Hz impedance of the NGR becomes unreliable once the ground fault occurs. As such, the monitoring logic switches to NGR resistance obtained using the 60 Hz component of measurements detecting intact NGR during fault initiation. However, the NGR fails open and its resistance is detected growing 200 ms after fault incidence resulted in NGR failure detection.

6.2 Configuration 2 — Resonant Grounding

Another type of neutral grounding method applicable to the previously studied configuration is the resonant grounding, as shown in Fig. 6.7. The resonant grounding is achieved using a low inductance reactor at the secondary of a NGT. In fact, this configuration is the same as the configuration 1, but resonantly grounded. The reactor has been designed using the procedure provided by [5], which is 2 mH with the quality factor equal to 20. The leakage impedance of the NGT has been considered when designing the reactor. The combination of the reactor and NGT, hereafter called high reactance Neutral Grounding

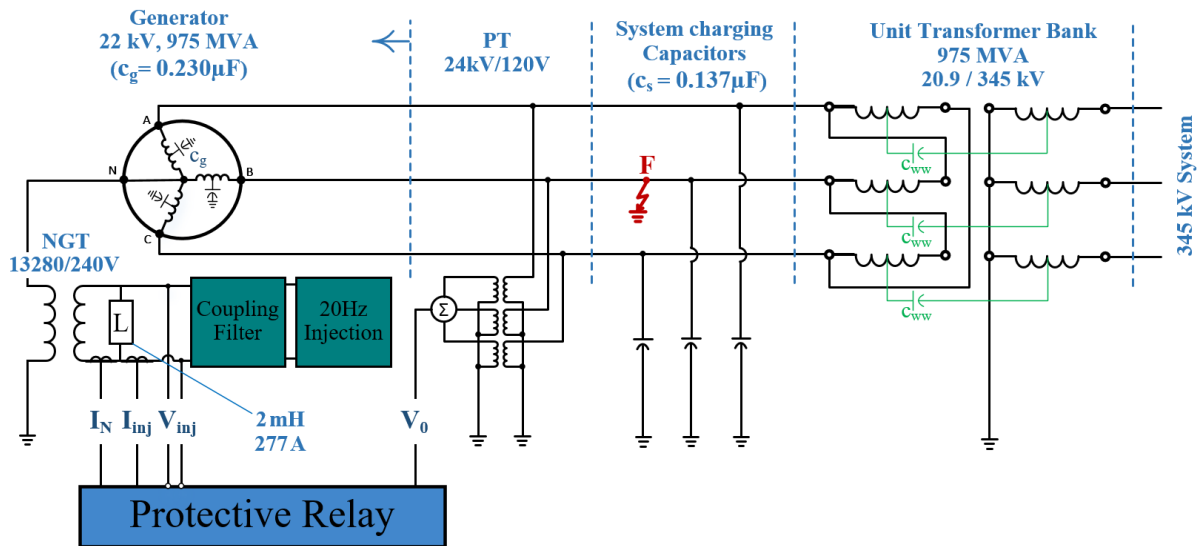


Figure 6.7: Connection diagram of the resonant grounded unit-connected generator equipped with 20 Hz signal injection based generator stator winding ground protection.

Inductor (NGL), limits the neutral current to a very low level, 3.75-5 A since the obtained inductive reactance at the primary of the NGT is equal to and resonates with the capacitive reactance of the total system charging capacitance lumped at neutral point. In the unfaulted condition, a very low voltage and current appears at neutral system which cannot be used for monitoring the NGL. As such, the same sub-harmonic injection based generator stator ground protection infrastructures are used for monitoring in the same way as described for the previous configuration.

6.2.1 Proposed Monitoring Method

The NGL monitoring method employs the same logics and algorithm used for the configuration 1. It only uses the imaginary part of the inverse of the admittance seen from the injection point as formulated below:

$$X_{NGL (20Hz)} = 3 \times \frac{1}{\text{Imag}(Y_{20Hz})} = 3 \times \frac{(N/n)^2}{\text{Imag}\left(\frac{I_{inj}-I_N}{V_{inj}}\right)} \quad (6.4)$$

$$X_{NGL (60Hz)} = \text{Imag}\left(\frac{3V_0}{(n/N)I_N}\right) \quad (6.5)$$

The Monitoring algorithm is updated considering the new equations as shown in the

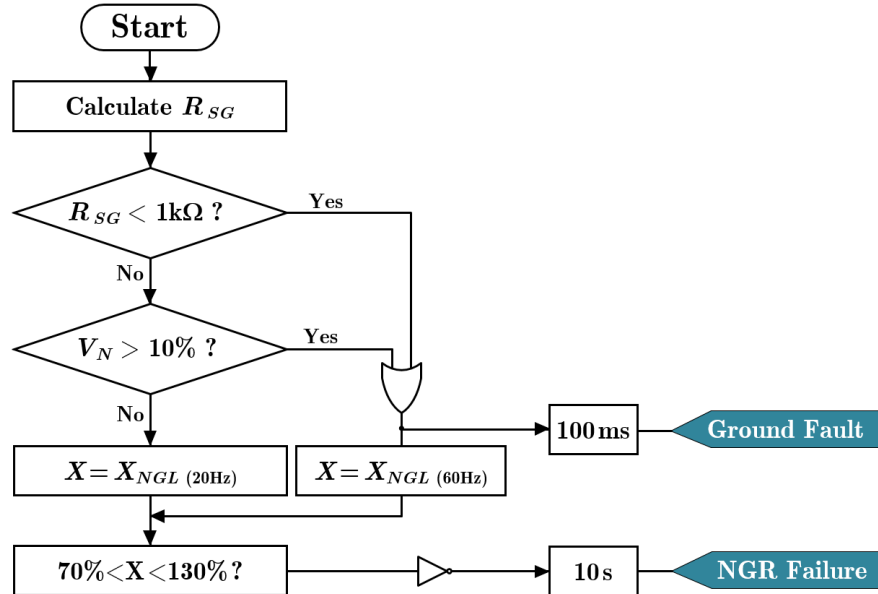


Figure 6.8: NGL monitoring logic and ground fault detection scheme.

following figure.

6.2.2 Simulation Verification

The performance of the proposed monitoring method for configuration 2 is investigated in the same way as the previous configuration. In fact, the failed-short and failed-open NGL conditions during both unfaulted and faulted operation modes of the generator are simulated in PSCAD and the captured data is used to assess the performance of the monitoring algorithm implemented in Matlab. Following, four sample cases are represented using waveforms. It should be noted that the measurements might be very low during normal condition, and they shall not be interpreted as secondary level measurements.

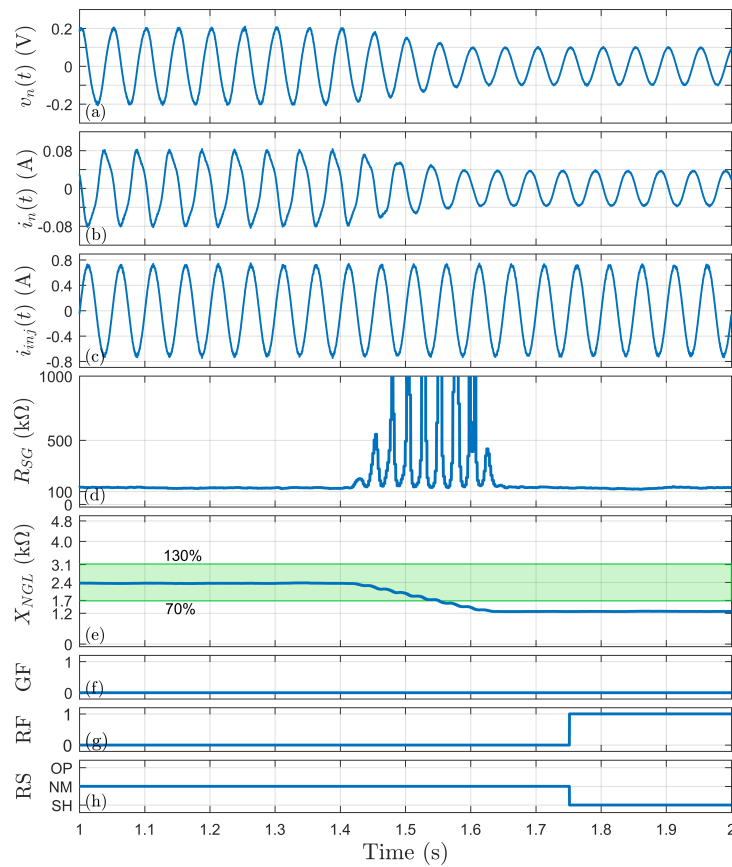


Figure 6.9: Case-5: Failed-short HNGL in unfaulted condition: a) Neutral voltage, b) Neutral current, c) Injected 20 Hz current, d) Generator stator winding insulation resistance, e) HNGL reactance, f) Ground fault, g) Reactor Failure (RF), and h) Reactor Status (RS).

Case 5 — This event is regarding a failed-short NGL, i.e. 50%-shorted over 200 ms, as shown in Fig. 6.9. The neutral voltage and current and also the injected current are shown. The stator-to-ground resistance of the generator winding, R_{SG} , is also represented to demonstrate the protection function. It remains high during this event and no ground fault is detected (GF=0). Hence, the NGL reactance, X_{NGL} , is obtained only using the 20 Hz component of the signals as shown in Fig. 6.9(e). As represented, the NGL reactance starts declining at $t = 1.4$ s and decreases to 50% over 200 ms. Once the NGL reactance declines to less than 70%, the Reactor Failure (RF) is expected as reported after 200 ms. The failure type is also easily detected since the NGL reactance is in hand. In this case, the Reactor Status (RS) is updated from NM to SH meaning that it was normal and has failed short.

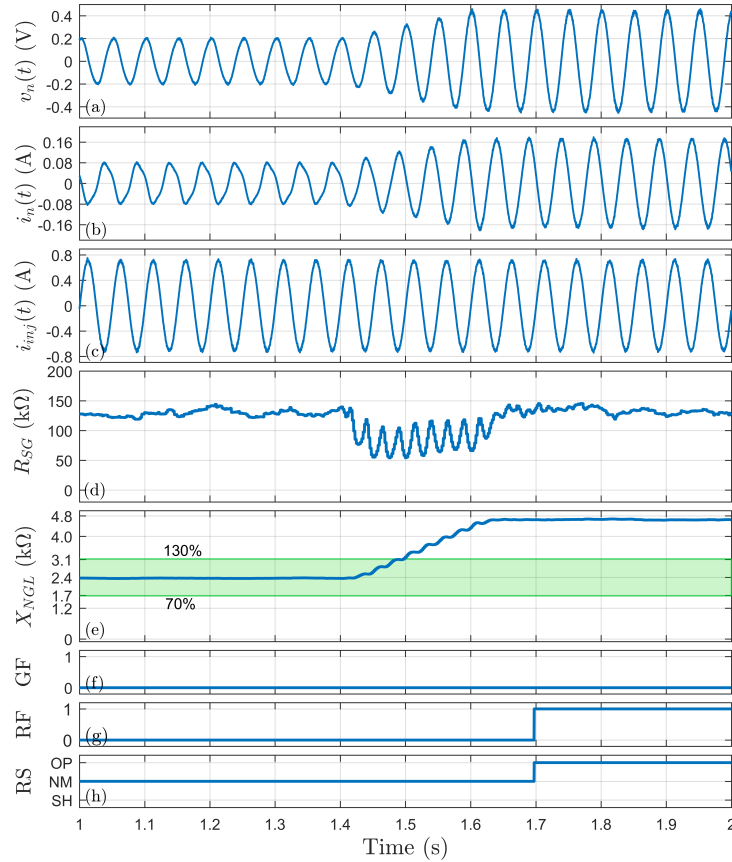


Figure 6.10: Case-6: Failed-open HNGL in unfaulted condition: a) Neutral voltage, b) Neutral current, c) Injected 20 Hz current, d) Generator stator winding insulation resistance, e) HNGL reactance, f) Ground fault, g) Reactor Failure (RF), and h) Reactor Status (RS).

Case 6 — This case, shown in Fig. 6.10, represents the same behavior as the case 5, but for a fail-open NGL. Again, the NGL failure and status are detected correctly using only the 20 Hz component of the measurements. The reactor failure is reported 200 ms after that the obtained reactance of the NGL rises above the 130% threshold, i.e. $3120\ \Omega$. The NGL status is updated from NM to OP meaning that it was normal and has failed open.

Case 7 — This case shows a failing short NGL during an internal single-line-to-ground fault at 5% of the generator stator winding. The ground fault occurs at $t = 1.2\text{ s}$. The calculated reactance of the reactor becomes invalid right after the fault initiation due to adversely affected 20 Hz phasor estimation. Once the ground fault is detected, at

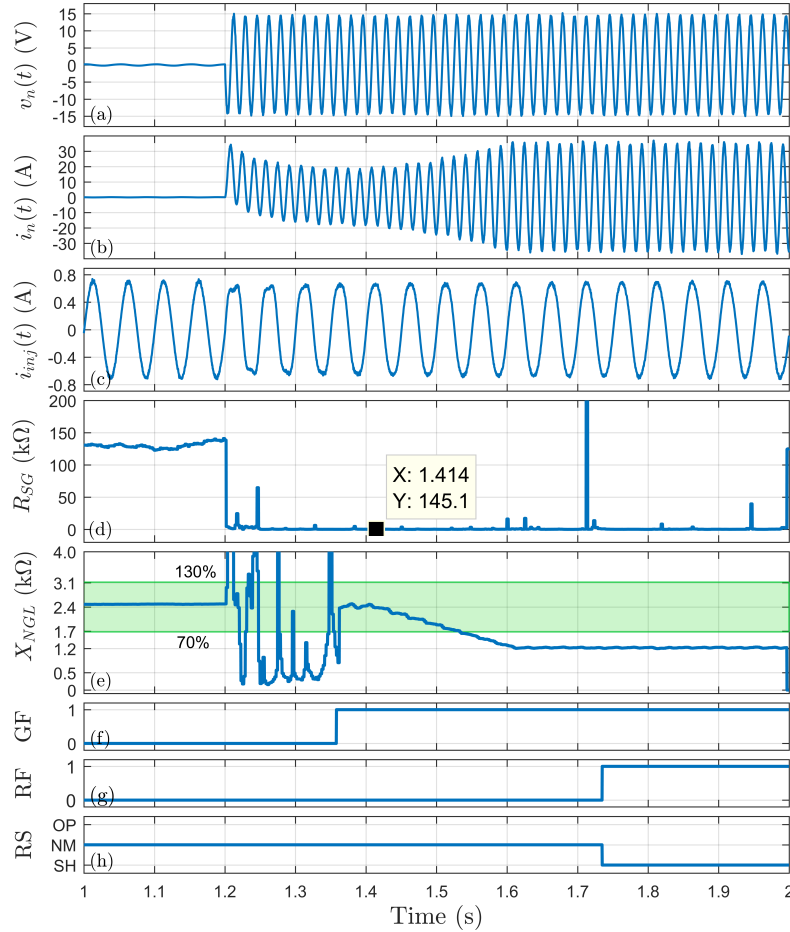


Figure 6.11: Case-7: Failed-short HNGL during an internal single-line-to-ground fault: a) Neutral voltage, b) Neutral current, c) Injected 20 Hz current, d) Generator stator winding insulation resistance, e) HNGL reactance, f) Ground fault, g) Reactor Failure (RF), and h) Reactor Status (RS).

$t = 1.34$ s, the monitoring technique switches to 60 Hz phasor estimation and calculates the reactance of the NGR using the 60 Hz component of the measurements. As shown in Fig. 6.11(e), the reactance remains in the safe region after the ground fault initiation. Thereafter, the NGL starts failing short at $t = 1.4$ s and the monitoring technique reports the NGL failure in 200 ms after its reactance goes out of the safe region, i.e., less than 70% threshold.

Case 8 — The last case shows the performance of the monitoring technique for a failing-open NGL during an internal single-line-to-ground fault at 5% of the generator stator winding, as depicted in Fig. 6.12. Again, the reactance of the NGL is accurately obtained before ground fault incidence using the 20 Hz component of the measured pa-

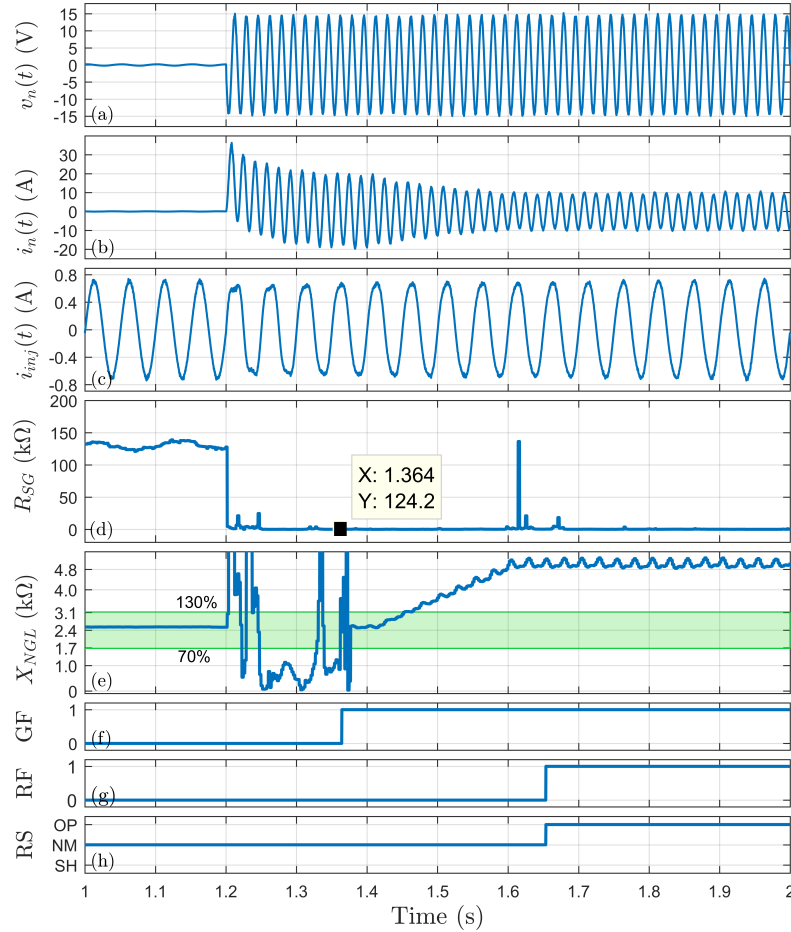


Figure 6.12: Case-8: Failed-open HNGL during an internal single-line-to-ground fault: a) Neutral voltage, b) Neutral current, c) Injected 20 Hz current, d) Generator stator winding insulation resistance, e) HNGL reactance, f) Ground fault, g) Reactor Failure (RF), and h) Reactor Status (RS).

rameters. However, the 20 Hz impedance of the NGL becomes unreliable once the ground fault occurs. As such, the monitoring logic switches to NGL reactance obtained using the 60 Hz component of measurements detecting intact NGL during fault initiation. However, the reactor fails open and its reactance is detected growing 200 ms after fault incidence, as shown in Fig. 6.12(e) resulting reactor failure detection.

Further simulation results can be found in Appendix E.

6.3 Summary

A new NGR monitoring technique was proposed which benefits from the available sub-harmonic injection based generator stator winding ground protection infrastructures. Its performance was further studied for monitoring the status of the neutral grounding reactor used for resonant grounding of the same configuration.

In unfaulted condition, the resistance of the NGR is monitored based the NGR resistance obtained using 20 Hz neutral voltage and current. Any changes in NGR structure are securely detected. However, in case of ground faults, the filtration of the 20 Hz signals is challenging; hence, the 60 Hz component of the neutral voltage and current are employed to monitor the resistance of the NGR. This logic functions satisfyingly, as well. Furthermore, the failed-short NGR is no more counted as a solid ground fault at neutral which prevents ground fault trip. However, an alarm could alert about the issue with the NGR, and switch to a reserved NGR or accelerated ground fault tripping.

Lastly, it should be noted that the proposed monitoring technique is continuous since it monitors in normal, faulted and de-energized operation conditions. Generators with existing injection based stator ground protection function can utilize this technique by installing only an additional CT. The proposed technique does not require any new or additional protection/control infrastructure meaning that it can be incorporated into digital protective relays, which will monitor and alarm in case of the NGR failure.

Chapter 7

Summary, Conclusions, and Future Works

Power system neutral grounding resistors and reactors are used to control transient over-voltages, and limit ground overcurrents to ride through the first ground fault, mitigate the arc-flash hazard, and minimize the ground fault damage to power system equipment. The continuity of service and integrity of the neutral-to-ground circuit, which contains the aforementioned apparatuses, is necessary to ensure the expected advantages of resistance or reactance grounding and avoid false sense of security. That is why the Canadian Electric Code (CEC or CSA C22.1) 2018 mandates the continuous monitoring of the neutral-to-ground path in all applications. Furthermore, the National Electric Code (NEC) mandates neutral-to-ground path monitoring in mining systems.

7.1 Summary

In this research work, first all the existing monitoring methods were reviewed to understand the current recommended practices and avoid intellectual property infringement. These methods were classified into three different categories based on their concepts and principles of operation.

The first category is the passive monitoring methods which rely on existing neutral voltage and current that exist due to inherent asymmetry of the power system compo-

nents. The most prominent advantage of these methods is their cost-efficiency since they mostly employ the available measurement instruments, and control/protection infrastructures for monitoring. However, they cannot function when the neutral voltage and current are very low unless the very sensitive measurement is employed which causes extra cost. Moreover, if these parameters disappear due to any reason such as de-energization or power outage, the passive methods will be disabled.

The second category of existing NGR monitoring methods is active methods which inject a DC/AC signal to neutral. These methods emerged due to aforementioned disadvantages of the passive methods. In fact, the active methods guarantee monitoring in de-energized and unfaulted conditions. However, they fail to monitor in presence of the ground faults. Monitoring the NGRs during the ground faults is only required for high-resistance NGRs that limit the ground fault current to maximum of 10 A to ride through the first ground fault.

The third category, which is called passive-active methods, is actually the combination or simultaneous use of passive and active methods to guarantee a continuous monitor in all de-energized, unfaulted, and faulted conditions of the impedance grounded system. Although these methods cost more than the other two categories, however, they are the emerging generation of the existing methods that offer the best performance.

The performance of the existing methods were compared based on the employed measurement instruments, and the degree of the monitoring that they provide during different system operation modes. The passive methods are of interest due to their lower implementation cost. The active methods provide a well-designed monitor, but expensive. The passive-active methods guarantee 100% and continuous monitoring so that the commissioning cost becomes reasonable. In the next step, the performance of two existing passive methods was investigated through comprehensive analysis since the most advantageous proposal of this research work relies on the principals and concepts of these two methods. The shortcomings and issues facing the methods were identified as well.

On the basis of the understood history and literature of the neutral-to-ground monitoring art, three new or innovative methods were achieved that are mentioned in the

next section.

7.2 Contributions and Conclusions

This research work resulted in three new or enhanced monitoring methods apart from the comprehensively carried-out literature survey.

The first proposed monitoring technique was achieved based on efficient combination of two existing passive monitoring methods. One of the existing methods operates reliably in unfaulted condition, whereas the other one functions satisfactorily in the presence of the ground faults. Therefore, this research work came across the proposal of combining these methods by a minor change of one the techniques, so it can be cost-effective and interesting solution. The proposed method adds a small resistor to the voltage measurement mechanism of an existing passive monitoring method, and performs a reliable monitoring in both unfaulted and faulted operation conditions. Furthermore, it provides continuous monitoring regardless of the type of the neutral grounding device. In other words, it can monitor any kind of neutral grounding apparatuses since it benefits from sensitive, and full-range measurement. However, it still cannot monitor in de-energized condition since it does not utilize the injection technique.

The second and third proposed methods focus on monitoring the high-resistance NGR installed at the neutral of unit-connected generators. The second method is a passive technique which employs the third harmonic of the neutral and residual voltages of the generator. The inverse variation of the mentioned quantities with different rates of change were the main logics of NGR failure detection. The proposed concept was proved mathematically, verified using software analysis, and validated using an available industrial generator protective relay. This method detects any kind of degradation of the NGR using existing measurement instruments and control/protection infrastructures meaning that it is a money-saving alternative. Furthermore, it can be easily incorporated into digital relays using their available logic engine tool and HIM softwares.

The third proposed method, which is a passive-active method, employs the existing sub-harmonic injection based generator stator ground protection infrastructures for

monitoring the same NGR mentioned in the previous paragraph. It guarantees NGR monitoring in all de-energized, unfaulted, and faulted operation conditions meaning that the proposed method offers continuous performance. This method only needs an additional current sensor to equip the signal injection based generator protective relays with a continuous and reliable NGR monitoring scheme. The understood trend of evolution of the monitoring methods implies that the passive-active concept results in the most advantageous solution due to its continuous functionality. Although this concept needs more budget to implement, however, most of the demanding industries perform critical services that deserve such an investment. For examples, the data centers, hospitals, and mines save millions of dollars once they employ high-resistance grounding using NGRs whereas the cost of such a monitoring system is not even higher than \$10,000.00. To such industries, integrity of the NGR ensures operation continuation upon the first ground fault, and mitigating the reconnection cost. All of these benefits show the advantages of the third proposed method. Furthermore, the performance of this method for monitoring the high reactance neutral grounding reactor was studied as well. Observations show that this proposed method can reliably monitor any type of neutral grounding devices.

7.3 Future Works

There exists potential use of the gained knowledge and outcomes of this research work in other fields of power system engineering such as insulation resistance monitoring and equipment internal ground fault detection. Additionally, further improvements of the proposed methods are possible as mentioned below:

- As the next stage of the performed research work, it would be worthwhile to incorporate/retrofit the proposed techniques to available digital protective relays, and study their performance in real life practice, e.g., actual generators or distribution transformers. The results of this study will help to modify or improve the proposed methods. It should be noted that the proposed methods will just alarm on NGR failure and will not trip or disconnect any part of the system meaning that this study is safe and practical.

- Furthermore, the first proposed method, which combines two existing passive methods, provides a reliable monitoring in both unfaulted and faulted operation conditions. The next step of this research work is to make the proposed method continuous through adding the signal injection means in an efficient way. Therefore, the enhanced method will be able to monitor the neutral-to-ground circuit in de-energized condition as well.
- Last but not least, the neutral-to-ground path monitoring art supervises the intactness of an inserted impedance between the neutral and earthing points of the power system. Basically, such an impedance exists between every hot part of the system and the earth potential which is known as insulation resistance. Most of the power system ground faults happen due to defection or degradation of the insulation which isolates the high voltage parts of the system from the earth potential. The insulation is usually modeled by a resistance in parallel with a capacitance. The resistance is normally higher than $1\text{ M}\Omega$ which declines over time due to aging or environmental incidents. A threshold set to $500\text{ k}\Omega$ safely detects the degradation of the insulation before it becomes a ground fault. As a result, the ground faults are detected or predicted ahead of time. The neutral-to-ground path monitoring performs the same but for a lower rated impedance, e.g., NGR. This research work will try to find applications where the proposed methods can be applied for insulation resistance monitoring. It should be added that the third proposed method is basically the enhancement of an existing insulation resistance monitor. However, the first and second methods can be elaborated towards insulation resistance monitoring.

Bibliography

- [1] G. E. Paulson, “Monitoring Neutral-Grounding Resistors,” in *Conference Record of 1999 Annual Pulp and Paper Industry Technical Conference (Cat. No.99CH36338)*, June 1999, pp. 238–241.
- [2] “IEEE Recommended Practice for Grounding of Industrial and Commercial Power Systems (IEEE Green Book),” *ANSI/IEEE Std 142-1982*, pp. 1–135, Sept 1982.
- [3] “IEEE Guide for Generator Ground Protection,” *IEEE Std C37.101-2006 (Revision of IEEE Std C37.101-1993/Incorporates IEEE Std C37.101-2006/Cor1:2007)*, pp. 1–70, Nov 2007.
- [4] “IEEE Draft Guide for the Application of Neutral Grounding in Electrical Utility Systems, Part I - Introduction,” *IEEE P62.92.1/D8, December 2015*, pp. 1–39, Jan 2016.
- [5] “IEEE Guide for the Application of Neutral Grounding in Electrical Utility Systems, Part II - Grounding of Synchronous Generator Systems,” *IEEE Std C62.92.2-1989*, pp. 1–24, Sept 1989.
- [6] “IEEE Guide for the Application of Neutral Grounding in Electrical Utility Systems, Part III - Generator Auxiliary Systems,” *IEEE Std C62.92.3-1993*, pp. 1–30, June 1994.
- [7] “IEEE Guide for the Application of Neutral Grounding in Electrical Utility Systems, Part IV-Distribution,” *IEEE Std C62.92.4-1991*, pp. 1–127, May 1992.

- [8] “IEEE Guide for the Application of Neutral Grounding in Electrical Utility Systems, Part V-Transmission Systems and Subtransmission Systems - Redline,” *IEEE Std C62.92.5-2009 (Revision of IEEE Std C62.92.5-1992) - Redline*, pp. 1–55, June 2009.
- [9] D. Selkirk, M. Savostianik, and K. Crawford, “Why Neutral-Grounding Resistors Need Continuous Monitoring,” in *Petroleum and Chemical Industry Technical Conference, 2008. PCIC 2008. 55th IEEE*, Sept 2008, pp. 1–7.
- [10] M. Al-Hajri, “Neutral Ground Resistor Monitoring Schemes,” in *Electrical Insulation, 2004. Conference Record of the 2004 IEEE International Symposium on*, Sept 2004, pp. 388–393.
- [11] D. Selkirk, M. Savostianik, and K. Crawford, “The Dangers of Grounding Resistor Failure,” *IEEE Industry Applications Magazine*, vol. 16, no. 5, pp. 53–58, Sept 2010.
- [12] W. Labos, A. Mannarino, G. Drobnjak, S. Ihara, and J. Skliutas, “A Possible Mechanism for Neutral Grounding Resistor Failures,” in *Power Engineering Society General Meeting, 2005. IEEE*, June 2005, pp. 1149–1154 Vol. 2.
- [13] *National Electrical Code —Article 250*, ANSI/NFPA, 2005.
- [14] *CSA C22.1 Canadian Electrical Code*, Canadian Standard Association, 2018.
- [15] J. Glenney and D. Selkirk, “The Importance of the Neutral-Grounding Resistor,” in *Conference Record of the 2006 Western Mining Electrical Association Conference*, November 2006.
- [16] Z. Toros, P. Kastelic, T. Kastelic, and S. Maljavac, “Neutral Grounding Resistor Failure Detection,” in *21st International Conference on Electricity Distribution Frankfurt*, June 2011.
- [17] Z. Toros, T. Kastelic, S. Maljavac, and P. Kastelic, “Neutral Grounding Resistor Failure Detection Verification,” in *Electricity Distribution (CIRED 2013), 22nd International Conference and Exhibition on*, June 2013, pp. 1–3.

- [18] J. Campbell and S. Panetta, "Ground Fault Circuit Having Circuit Failure Sensor, and Method," Apr. 22 2003, US Patent 6,552,885. [Online]. Available: <https://www.google.ch/patents/US6552885>
- [19] Littelfuse, *SE-330 Neutral-Grounding-Resistor Monitor*, 5th ed., Startco Engineering Ltd, 406 Jessop Saskatoon, Saskatchewan, Canada, 2011, [Online: <http://www.littelfuse.com>].
- [20] Littelfuse, *SE-325 Neutral-Grounding-Resistor Monitor*, 5th ed., Startco Engineering Ltd, 406 Jessop Saskatoon, Saskatchewan, Canada, 2011, [Online: <http://www.littelfuse.com>].
- [21] Bender, *Ground Fault and Neutral Grounding Resistor Monitor*, RC48N Datasheet, 5810 Ambler Drive Unit 1 Mississauga, ON, Canada L4W 4J5, [Online: <http://www.bender.org/documents/RC48N.pdf>].
- [22] Jan Prins, *A Neutral Grounding Resistor Monitor*, Cypress MicroSystems, Inc., Nov. 2004, [Online: <http://electronix.org.ru>].
- [23] D. Curtis, "Multi-Frequency Ground Monitor Current Sensing," U.S. Patent App. 14/473,568, March, 2, 2015. [Online]. Available: <https://www.google.com/patents/US20150061689>
- [24] S. Meadows, "Ground Wire Monitoring System," U.S. Patent 4,011,483, March, 8, 1977. [Online]. Available: <https://www.google.ch/patents/US4011483>
- [25] JVS, *Neutral Earthing Resistor Monitorng Relay*, 2nd ed., JVS Electronics PVT Ltd, 121 Manchanayakanahalli, Bidadi, Bangalore-Mysore Highway, Ramanagara - 562109, 2013, [Online: <http://www.jvselectronics.in>].
- [26] M. Vangoool and G. Baker, "Neutral Grounding Resistor Monitor," Feb. 19 2015, US Patent App. 14/386,108. [Online]. Available: <https://www.google.ca/patents/US20150048840>

- [27] R. Goldstein, “Apparatus and Method for Continuously Monitoring Grounding Conductor Resistance in Power Distribution Systems,” Jan. 11 1994, US Patent 5,278,512. [Online]. Available: <https://www.google.ca/patents/US5278512>
- [28] i-Gard, *SIGMA Ground Fault Relay - Resistor Monitor*, 1st ed., i-Gard Corporation, 7686 Bath Road, Mississauga, Ontario, Canada,, [Online: <http://www.i-gard.com>].
- [29] i-Gard, *GEMINI High Resistance Grounding Systems - Product Guide*, 1st ed., i-Gard Corporation, 7686 Bath Road, Mississauga, Ontario, Canada,, [Online: <http://www.i-gard.com>].
- [30] Bender, *NGR Monitor*, NGRM700 Datasheet, 5810 Ambler Drive Unit 1 Mississauga, ON, Canada L4W 4J5, [Online: <http://www.bender.org/documents/NGRM700.pdf>].
- [31] T. Bengtsson, Z. Gajic, H. Johansson, J. Menezes, S. Roxenborg, and M. Sehlstedt, “Innovative Injection-based 100% Stator Earth-Fault Protection,” in *Developments in Power Systems Protection, 2012. DPSP 2012. 11th International Conference on*, April 2012, pp. 1–6.
- [32] Post Glover, *Neutral Grounding Resistors*, Post Glover Resistors, 4750 Olympic Blvd., Erlanger, KY 41018 USA, [Online: <https://www.postglover.com>].
- [33] L. Zhou, S. Zhang, W.-Y. Yin, and J.-F. Mao, “Immunity Analysis and Experimental Investigation of a Low-Noise Amplifier Using a Transient Voltage Suppressor Diode Under Direct Current Injection of HPM Pulses,” *Electromagnetic Compatibility, IEEE Transactions on*, vol. 56, no. 6, pp. 1715–1718, Dec 2014.
- [34] M. Kanabar, O. Lapeyra, J. Momic, P. Kreidi, M. Das, and D. Nagalingam, “Experience With Applying Injection based 100% Stator Ground and Rotor Ground Generator Protections,” in *41st Annual Western Protective Relay Conference*, Oct 2014.

- [35] P. Soez, F. Vicentini, V. Skendzic, M. Donolo, S. Patel, Y. Xia, and R. Scharlach, "Injection based Generator Stator Ground Protection Advancements,," in *41st Annual Western Protective Relay Conference*, Oct 2014.
- [36] "IEEE Standard Requirements, Terminology, and Test Procedures for Neutral Grounding Devices," *ANSI/IEEE Std 32-1972*, pp. 1–36, April 1972.
- [37] J. C. Das and E. Perich, "13.8-kV Selective High-Resistance Grounding System for a Geothermal Generating Plant - A Case Study," *IEEE Transactions on Industry Applications*, vol. 49, no. 3, pp. 1234–1243, May 2013.
- [38] M. Shen, L. Ingratta, and G. Roberts, "Grounding transformer application, modeling, and simulation," in *Power and Energy Society General Meeting - Conversion and Delivery of Electrical Energy in the 21st Century, 2008 IEEE*, 2008, pp. 1–8.
- [39] K. R. Hameed, "Zig-zag Grounding Transformer Modeling for Zero-sequence Impedance Calculation Using Finite Element Method, year=2015, volume=8, number=3, pages=63-87, keywords=Finite Element Modeling; Grounding Transformer, doi=10.1109/TIA.2013.2252134, issn=1999-8716, month=September,," *Diyala Journal of Engineering Sciences*.
- [40] R. L. Schlake, G. W. Buckley, and G. McPherson, "Performance of Third Harmonic Ground Fault Protection Schemes for Generator Stator Windings," *IEEE Transactions on Power Apparatus and Systems*, vol. PAS-100, no. 7, pp. 3195–3202, July 1981.
- [41] R. J. Marttila, "Design principles of a new generator stator ground relay for 100% coverage of the stator winding," *IEEE Transactions on Power Delivery*, vol. 1, no. 4, pp. 41–51, Oct 1986.
- [42] J. C. Moreira and T. A. Lipo, "Modeling of Saturated AC Machines Including Air Gap Flux Harmonic Components," *IEEE Transactions on Industry Applications*, vol. 28, no. 2, pp. 343–349, Mar 1992.

- [43] U. Khan, “Modeling and protection of phase shifting transformers,” Ph.D. dissertation, Western University, 2013.
- [44] *PSCAD/EMTDC V. 4.6.2*, Manitoba HVDC Research Center, Winnipeg, MB, Canada., [Online: <http://hvdc.ca>].
- [45] J. Lepkowski, *Zener Macro-Models Provide Accurate SPICE Simulations*, ON Semiconductor, LLC., AND8250/D, January 2006, [Online: <http://www.onsemi.com>].
- [46] J. Lepkowski and W. Lepkowski, “Evaluating TVS protection circuits with SPICE,” *Power Electron. Technol.*, vol. 5, no. 1, pp. 44–49, Jan 2006.
- [47] L. Zhou, S. Zhang, W. Y. Yin, and J. F. Mao, “Immunity analysis and experimental investigation of a low-noise amplifier using a transient voltage suppressor diode under direct current injection of hpm pulses,” *IEEE Transactions on Electromagnetic Compatibility*, vol. 56, no. 6, pp. 1715–1718, Dec 2014.

Appendix A

Simulation Settings

Throughout the entire simulation and modeling carried out with PSCAD, the time step was set to $10\mu\text{s}$. Using the waveform recorder provided by this power system simulation software, i.e., COMTRADE 91, with the recording time step of $50\mu\text{s}$, the required electrical signals were captured and transferred to Matlab [43]. As known, PSCAD uses interpolation to synchronize between the two samples [44]. It should be added that the high frequency rejection was performed using PSCAD Butterworth low pass filter set to 1536 Hz, which is equal to 80% of half of the sampling rate or $0.8 \times 0.5 \times (60 \times 64)$.

The PSCAD recorder samples discretely over every $50\mu\text{s}$, while the Matlab based modeled monitoring relay uses the sampling rate of 3840 samples/sec. As such, a Matlab function should be employed for synchronization between the re-sampled data and the original records from PSCAD. But, the PSCAD simulation time step cannot be adjusted to be an integer multiple of the final $64 \times 60 = 3840$ samples/sec data sampling rate. Therefore, the Matlab interpolation function, called `interp1`, is employed which resolves this issue.

Appendix B

Sensing Resistor Modeling and Verification

The sensing resistor which is a voltage metering instrument consists of a series resistor for overcurrent protection purposes, and a voltage clamper set to 100 V for over-voltage protection at the input gates of the monitoring equipment. This circuit accurately measures the voltage of the neutral point during the normal operation condition. During the faulted condition, the neutral voltage increases to some percents of phase-to-ground voltage. Since the voltage clamper limits the voltage to 100 V, the measured voltage becomes invalid. The resistance of sensing resistor is in the order of kilo-Ohms which limits the measuring circuit current to a few hundred milliamperes, which is a safe current at the input terminals of the monitoring equipment. On the basis of [19], an appropriate sensing resistor for measuring the neutral voltage of a 12.47 kV generator or transformer is ER-15KV with the isolation resistance of 100 k Ω . If a single-line-to-ground (LG) fault happens at terminals of the wye-connected generator or transformer, the phase-to-ground voltage 7.2 kV will appear across the neutral grounding system. This is the maximum electrical potential that appears across the sensing resistor neglecting the transient state. It causes a 72 mA current in the sensing resistor. This is the maximum current that can flow through the voltage sensing circuit which finally could penetrate into the monitoring equipment.

The other element of the neutral voltage measuring system is the voltage clamper that

clamps or limits the voltage to 100 V. This element which is known as Transient Voltage Suppressor (TVS) consists of a few series Thyrector diodes. The Thyrector diode itself is a power electronic device that is nothing but two face-to-face or back-to-back Zener diodes. The power system simulations are carried out in PSCAD; but, this software does not provide any model for Zener diode, which is the main element required for modeling the Thyrector diode and so on for TVS simulation. Hence, the first challenge is to model the Zener diode. The PSCAD is an electrical power systems modeling and analysis software. Whereas the Zener diode is an electronic device that has been implemented in softwares such as Simulink, SPISE, PSPISE, etc. Although the PSCAD does not provide any model for the Zener diode; But, it provides a standard model for other essential electrical elements. Furthermore, its powerful coding library which is based on Fortran programming language makes it possible to simulate any required electrical element like the Zener diode. Hence, there are two alternatives for simulating the Zener diode, and then the TVS.

B.1 Implementation of Zener Diode In PSCAD

The first alternative for modeling the Zener diode in PSCAD is the curve fit model. This way of modeling the Zener diode is also used by SPICE. This method uses the current versus voltage (I-V) characteristic of the Zener diode. The slope of this characteristic is the conductance (B_z) Zener diode. As such, a variable resistance $R_z = 1/B_z$ controlled by a lookup table or a Fortran coded signal can be used to simulate the Zener diode in PSCAD. The disadvantage of this method is that it models the Zener diode mathematical which cannot properly operate with PSCAD electrical elements. However, the second alternative for modeling the Zener diode provides an equivalent electrical circuit for modeling the dynamics of the Zener diode. The I-V characteristic of the Zener diode is simulated by using standard electrical elements which is more of interest [45]. This method is known as macro-model, which is well-addressed in [45] and [46].

The procedure provided in [46] is used for Zener diode simulation and verification. This document is a technical paper which simulates the Zener diode based on macro-model using standard electrical and electronic devices such as resistors, dependent voltage

sources, and diodes, which are available in PSCAD. There are few differences between the way that softwares model the diodes. For example, SPICE uses the mathematic equations of diodes while PSCAD uses the statement-based model (on or off). However, as the operating frequency in power system is very low in contrast to electronic applications, the PSCAD model for standard diode works properly. The operation equations used for simulating the diode by SPICE have been mentioned in [46]. The statement-based model of diode in PSCAD is as depicted in Figure B.1.

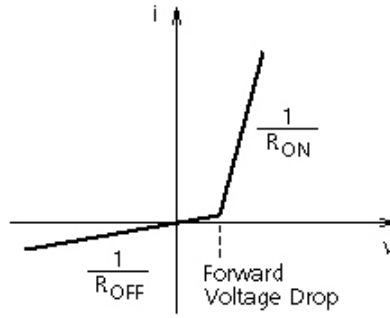


Figure B.1: PSCAD statement-based model of diode.

The macro-model of the Zener diode is shown in Figure B.2. It simulates the I-V characteristic of the Zener diode that is shown in Figure B.3. The definitions of all of the specifications of this circuit are available in [45].

Since the isolation resistor limits the TVS current to a certain limit, simulating the reverse region is not required. Hence, D3, I_{ZG} , and R_{ZG} are not considered in PSCAD

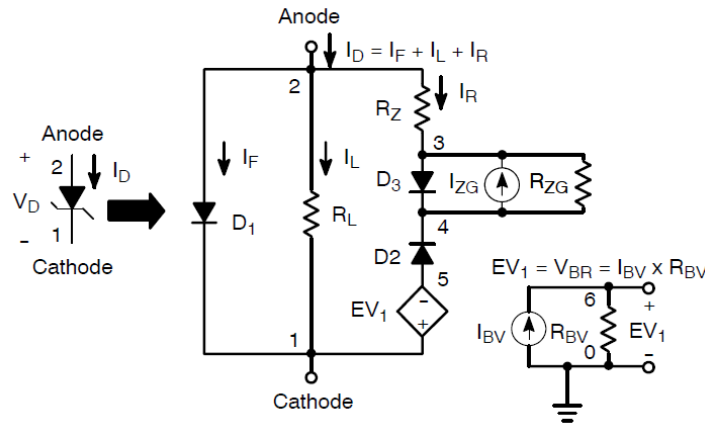


Figure B.2: Zener diode SPICE macro-model[45].

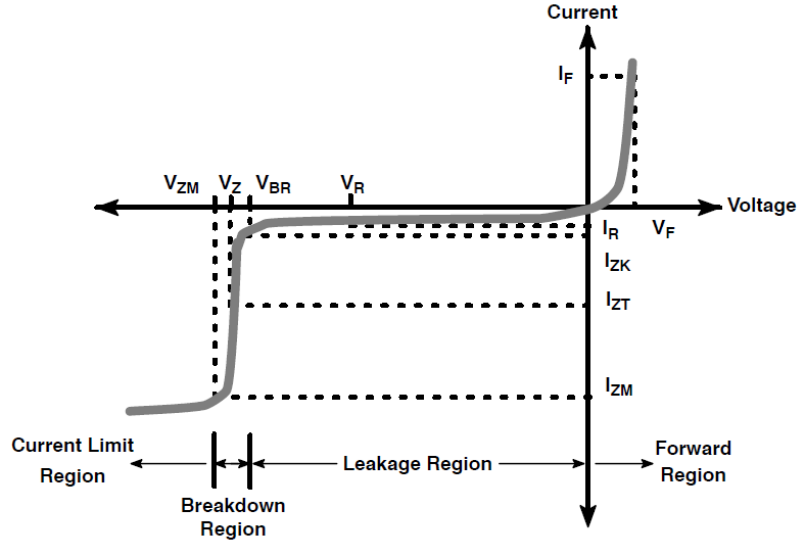


Figure B.3: Zener diode I-V characteristic [45].

model. Therefore, the simplified model is used as represented in Figure B.4.

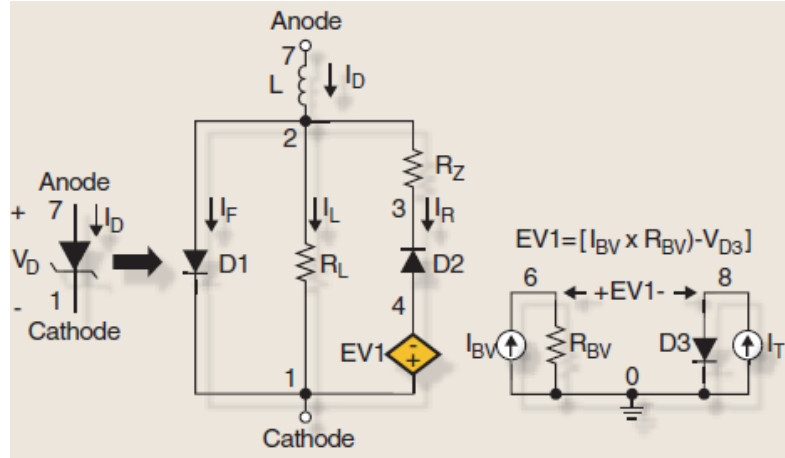


Figure B.4: Zener diode SPICE simplified macro-model[46].

The I-V characteristic achieved by this model is depicted in Figure B.5 which does not model the current limit region. It should be added that when the isolation resistor is added in series with this Zener diode it creates the same characteristic represented in Figure B.3.

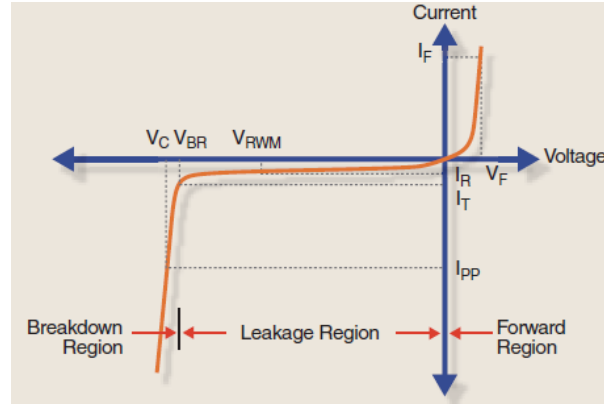


Figure B.5: I-V characteristic of an avalanche Zener diode[46].

The electrical specifications of the utilized elements are listed in Table B.1 and Table B.2, including all the resistive, inductive elements and diodes.

Table B.1: Electrical specifications of the Zener diode [33].

element	symbol	value	unit
Leakage Resistance	R_L	432.244	$M\Omega$
Dynamic Resistance	R_Z	1.28	Ω
Series Inductance	L	1.24	nH
Breakdown Voltage	V_{BR} or $EV1$	26.3571	V

Table B.2: Default specifications of the SPICE diode [46].

Variable	Parameter	SPICE Default Value	Units
IS	Saturation Current	1 E-14	A
RS	Resistance	0	Ω
BV	Reverse Breakdown Voltage	∞	V
IBV	Current at Reverse Breakdown Voltage	1 E-3	A
N	Emission Coefficient (η)	1	-
XT1	Saturation Current Temp. Coefficient	3	-
TT	Transit Time	0	nS
CJO	Zero Bias Junction Capacitance	0	pF
VJ	Junction Potential	1	V
M	Grading Coefficient	0.5	-
EG	Activation Energy	1.11	eV
KF	Flicker Noise Coefficient	0	-
AF	Flicker Noise Exponent	1	-
FC	Depletion Capacitance Forward Bias Coefficient	0.5	-
TNOM	Nominal Temperature	27	$^{\circ}\text{C}$

The simulated macro-model of the Zener diode in PSCAD using the above-mentioned specifications is shown in Figure B.6 accompanied with the current surge testing source.

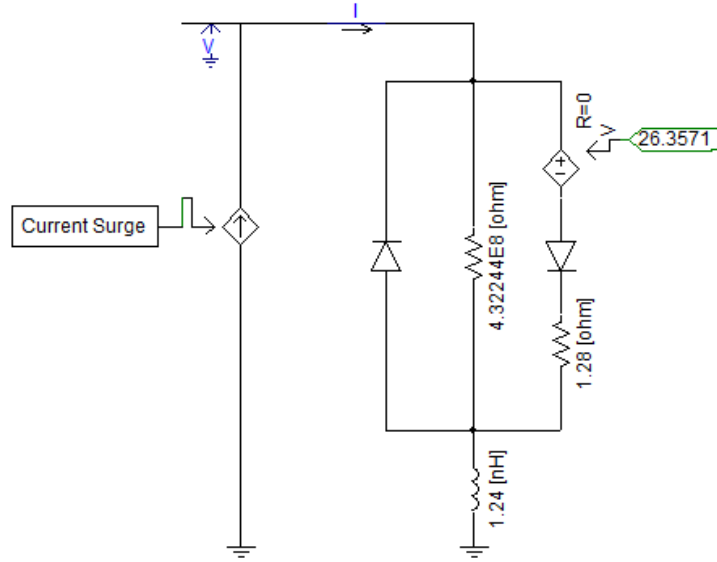


Figure B.6: Macro-model of the Zener diode simulated in PSCAD.

The simulated model is verified with three scenarios based on analysis performed in [46]. The first event is a $8A \times 20\mu s$ current waveform. This signal models the sudden interruption of the current in a load that is connected in parallel with TVS [46]. In this scenario, the current waveform starts at $t=10\mu s$, rises in $6\mu s$, reaches its peak of $8A$ at $t=16\mu s$, damps in $30\mu s$, and finally disappears at $45\mu s$ as represented with blue color in Figure B.7. The resulted voltage across the TVS is depicted in green as well.

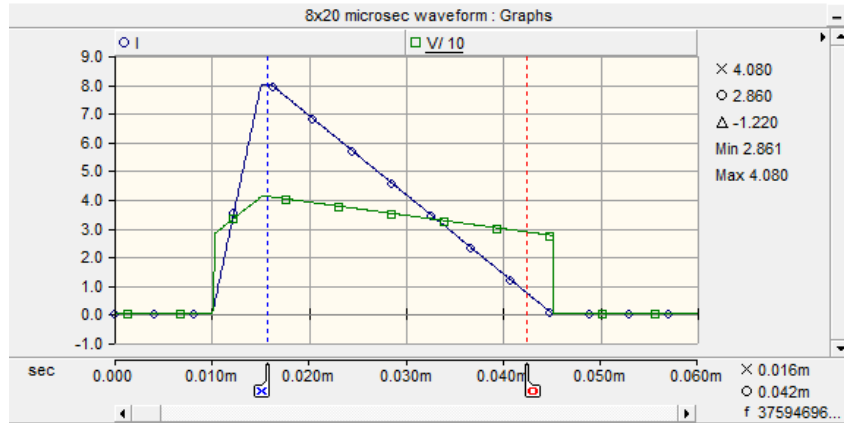


Figure B.7: PSCAD simulation result for $8 \times 20\mu s$ current waveform scenario.

In order to show both the current and voltage in one figure, the voltage is divided by 10. As shown in this figure, the voltage is clamped at 40.8 V. This voltage is highly matching with the result that the authors of the used reference paper have presented, as shown in Figure B.8. The difference is only +0.1 V which is 0.2%.

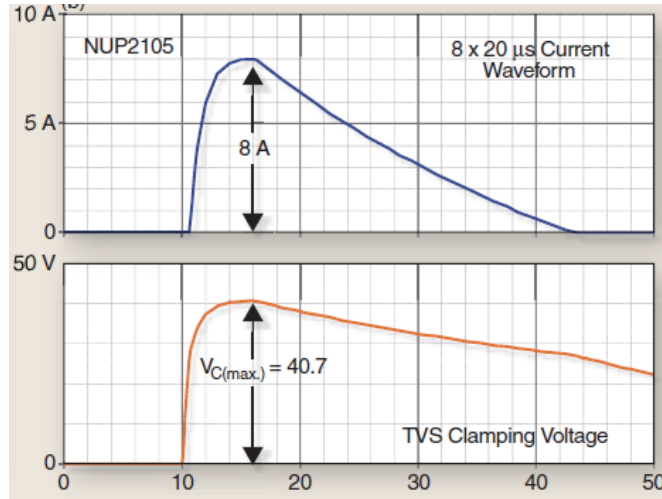


Figure B.8: SPICE simulation result of $8 \times 20 \mu\text{s}$ waveform scenario [46].

The authors also have carried out the bench test measurement for this scenario. The bench test and PSCAD results are represented in Figure B.9 and Figure B.10, respectively.

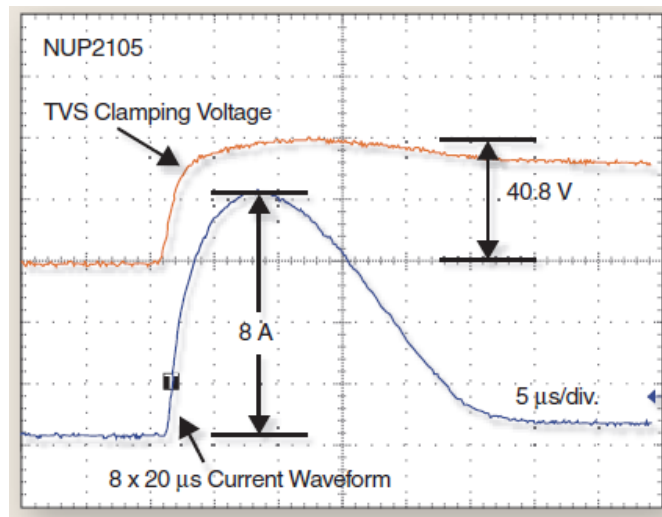
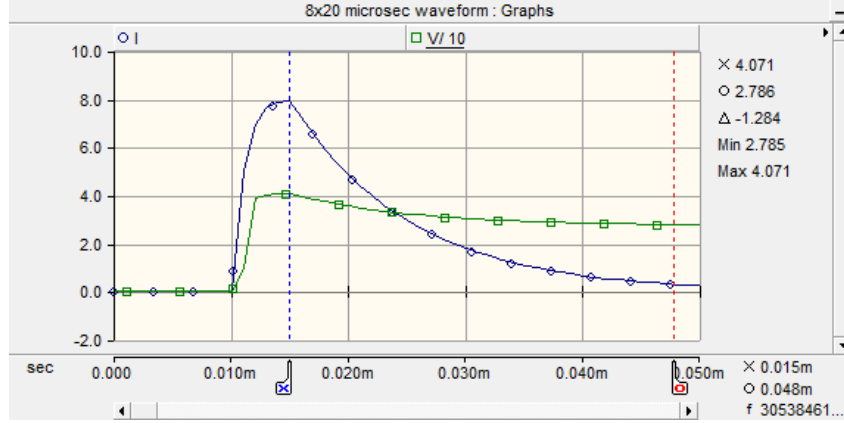
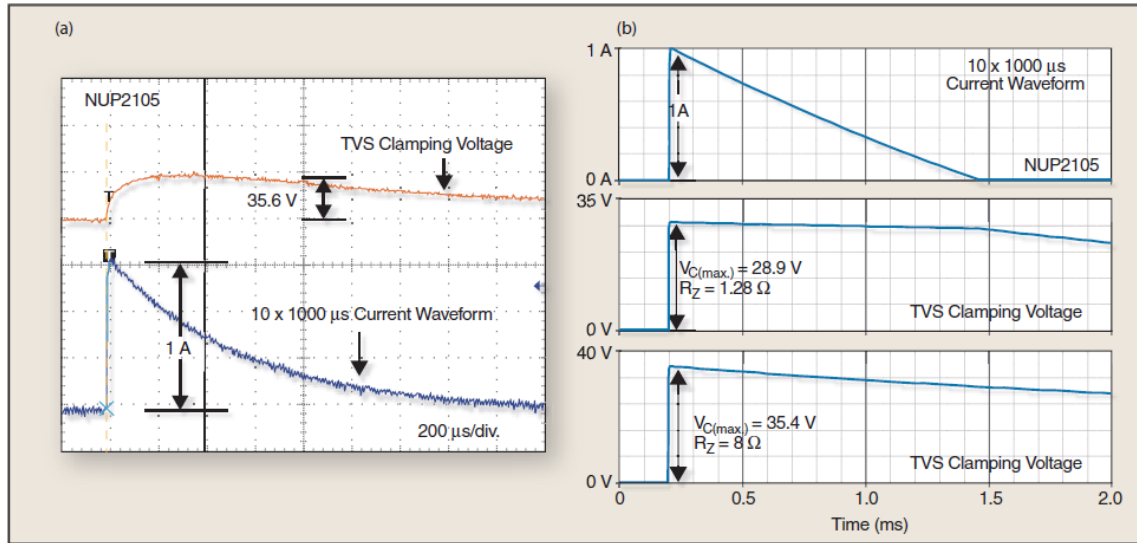


Figure B.9: Bench test measurement result of $8 \text{ A} \times 20 \mu\text{s}$ scenario [46].

Figure B.10: PSCAD simulation result for $8 \times 20 \mu\text{s}$ scenario.

The next scenario is the $1\text{A} \times 1000 \mu\text{s}$ current waveform which occurs when power is removed from an inductive load and the device under test simultaneously. The device remains connected in parallel with the inductance, which produces a negative surge voltage. DC motors, solenoids and relays are common examples of inductive loads that can produce this surge pulse [46]. The results of SPICE simulation, and bench test measurement are presented in Figure B.11.

Figure B.11: $1\text{A} \times 1000 \mu\text{s}$ current waveform scenario a) bench test measurement and b) SPICE [46].

This scenario has been simulated in PSCAD for both SPICE and bench test current waveforms as well as for different dynamic resistances of the Zener diode mentioned in

upper figure. The results are represented in Figure B.12 and Figure B.13. Figure B.12 shows the clamped voltage when the dynamic resistance of the Zener diode is 1.28Ω . In this case, the Zener diode clamps the voltage at 29.04V . The difference with the SPIE simulation result, 28.9V , is only 0.14V or 0.5% .

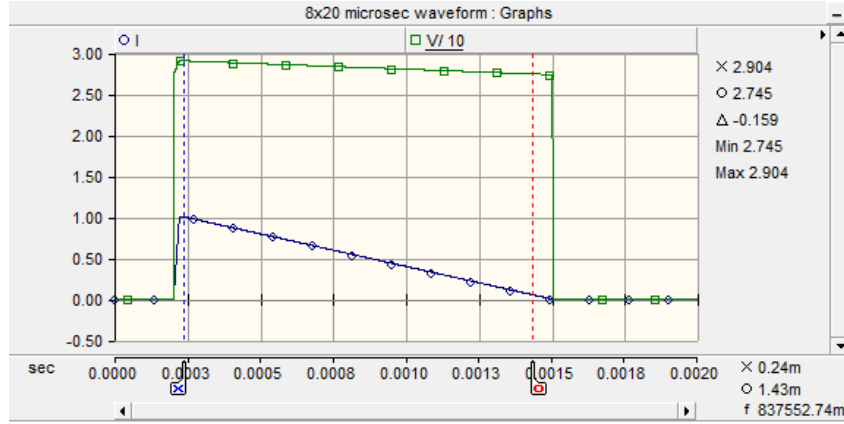


Figure B.12: PSCAD results for $1\text{A} \times 1000\mu\text{s}$ current waveform scenario when $R_z = 1.28\Omega$.

In the next case study, the dynamic resistance of the Zener diode is considered 8Ω . Based on PSCAD simulations, the Zener diode clamps the voltage at 35.76V . Comparing to SPICE simulation, the difference is 0.34V , as represented in Figure B.13. The difference with the SPIE simulation result, 35.4V , is only 0.34V or 1% .

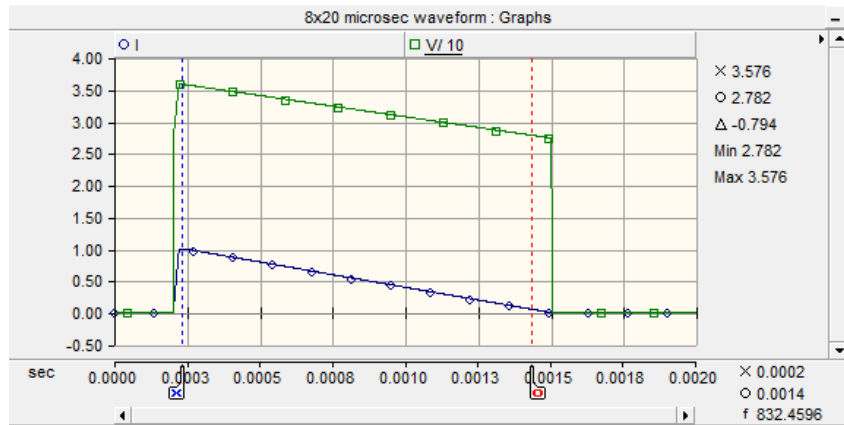


Figure B.13: PSCAD results for $1\text{A} \times 1000\mu\text{s}$ current waveform scenario when $R_z = 8\Omega$.

The last verification using the $1\text{A} \times 1000\mu\text{s}$ waveform is the bench test measurement. This case is also simulated in PASCAD, and the result is shown in Figure B.14. The

voltage is clamped at 35.65V which is 0.05V more than the result that the reference paper presented for this case study. This difference is only 0.1%.

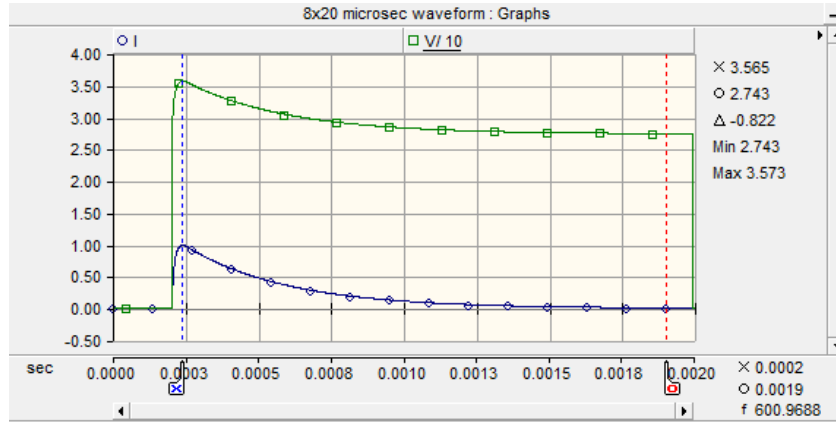


Figure B.14: PSCAD results for $1 \times 1000 \mu\text{s}$ current waveform bench test when $R_z = 8\Omega$.

In addition, the current versus voltage characteristic of the simulated Zener diode in PSCAD is represented in Figure B.15. All of the obtained above-mentioned results can

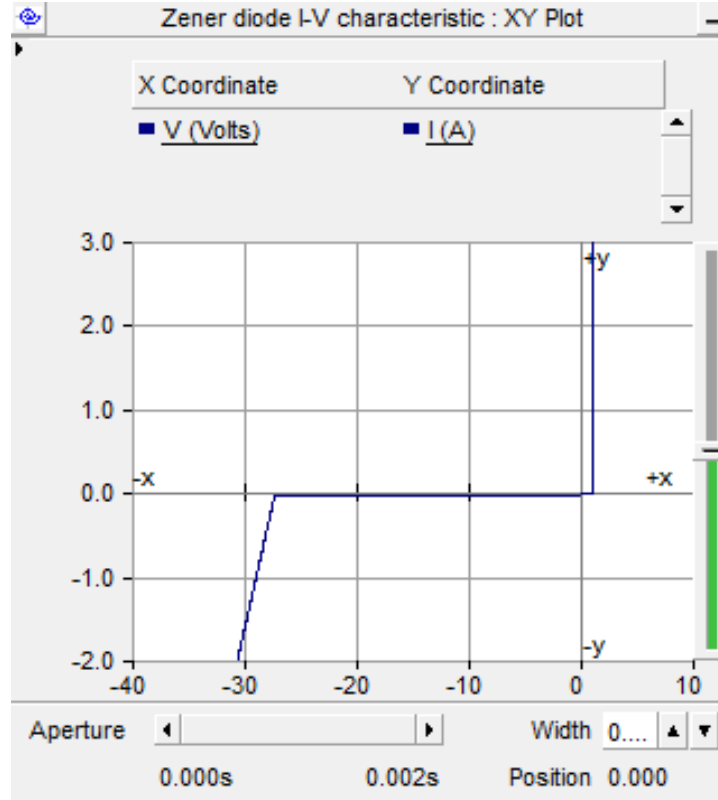


Figure B.15: I-V characteristic of the PSCAD based Zener diode.

be investigated based on this curve as well.

It should be mentioned that the Zener diode is now available in PSCAD. In the next step, the obtained model of the Zener diode is used for developing the Thyrector diode.

B.2 Implementation of A Single Cell TVS DIODE (Thyrector diode)

A Transient Voltage Suppression (TVS) is a diode which is used to protect a circuit against spikes, and transient over-voltages that appear due to switching, lightning strikes, and faults in the circuit. The single cell TVS is called Thyrector diode. The symbolical representation of this element is depicted in Figure B.16.



Figure B.16: Symbolical representation of Thyrector diode.

The I-V characteristic of the Thyrector is similar to the Zener diode. However, the Zener is designed to regulate the voltage while the TVS diode is used to protect against over-voltage by clamping the voltage appeared at the input gates of the DC circuit as shown in Figure B.17 [45].

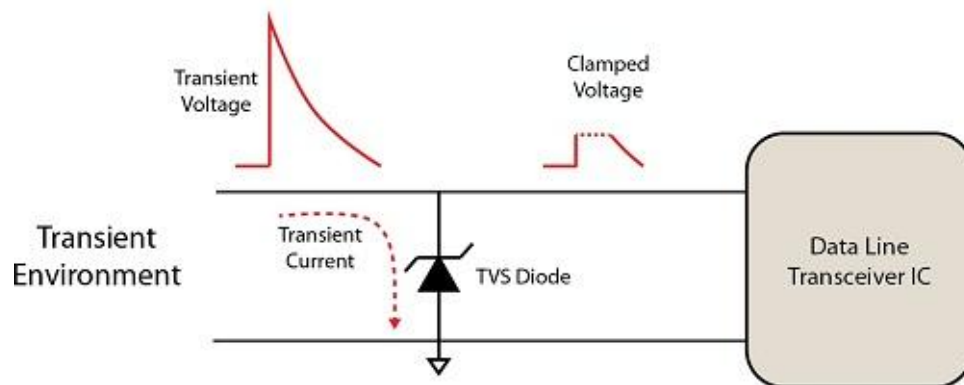


Figure B.17: Voltage clamping by TVS [45].

In [47], first the Thyrector diode model, and then a simple circuit to monitor its

AC performance under DCI High-Power Microwave (HPM) pulses are demonstrated, as depicted in Figures B.18 and B.19, respectively.

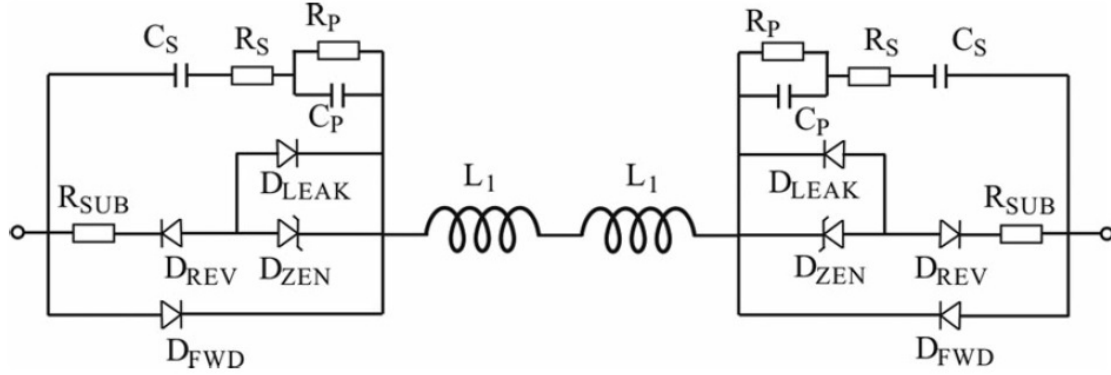


Figure B.18: Thyrector diode macro-model [47].

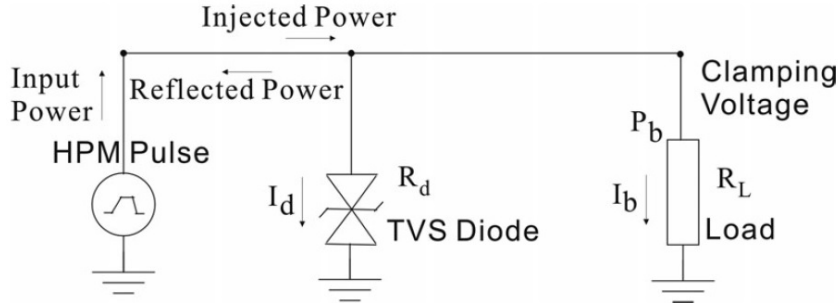


Figure B.19: Test circuit for performance investigation of the Thyrector diode [47].

This Thyrector has been simulated in PSCAD using the specifications provided by [47] supported by following simulation results. First, its dynamic resistance decreases drastically when the power increases to a certain level. In fact, the AC dynamic resistance at high frequency is larger than that at low frequency at a high input power level, as shown in the inset of Figure B.20. This resistance approaches a constant value as the input power continues increasing. For example, the AC dynamic resistance of the TVS diode at 4 GHz is about 9.5Ω , while the DC dynamic resistance is about 2.5Ω at the highest pulse power which is 60dBm.

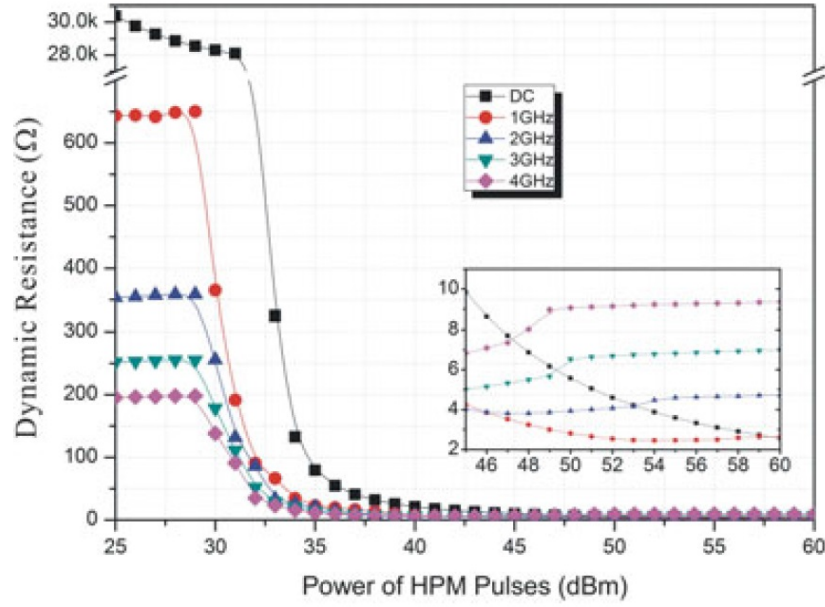


Figure B.20: AC dynamic resistance of the TVS diode versus HPM pulse power at different operating frequencies [47].

Figure B.21 shows the current versus clamping voltage of the TVS diode for different profiles of the HPM pulses. It is seen that the TVS diode exhibits a breakdown characteristic with snap-back effects at higher frequencies. On the other hand, there is no snap-back effect in the DC regime which implies the 60 Hz as well.

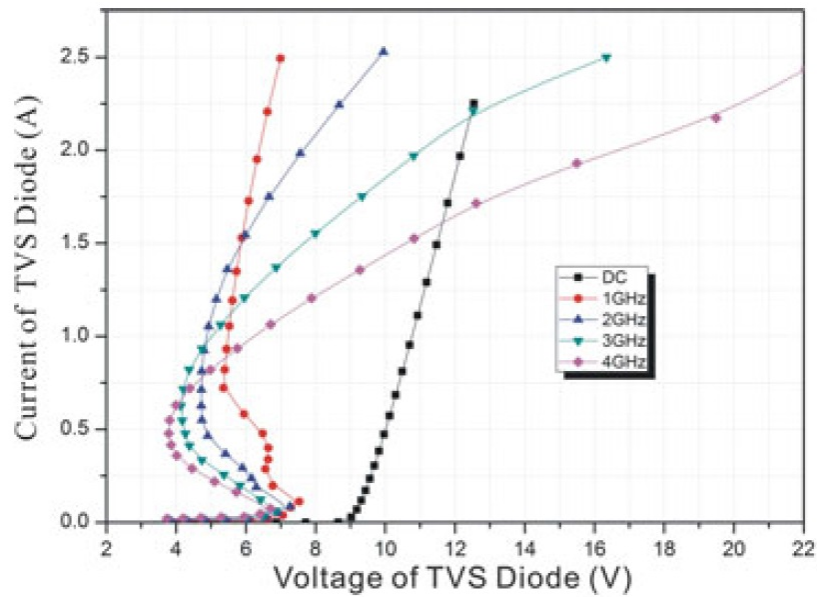


Figure B.21: I-V characteristic of the Thyrector diode at different operating frequencies [47].

Understanding these characteristics, the Thyrector diode has been implemented in PSCAD using the simulated and verified Zener diode model. Its model based on standard electrical elements was shown in Figure B.18. The Thyrector diode mainly consists of two face-to-face Zener diodes. In addition, it includes some other parallel branches modeling the behavior of this element in ultra-frequencies. In the implemented model, the impact of these leakage capacitors on the analysis is negligible because of their significantly high impedance in low frequencies such as the power system frequency, i.e, 60 Hz. The Zener diode is considered to be the same as previously simulated except that the breakdown voltage is considered 7.5 V. Additionally, the forward voltage-drop of the diodes is 0.7 V instead of 1 V. The value of these parameters is chosen based on specifications provided in [47]. Moreover, the dynamic resistance of the Zener diodes has to be investigated. As the R_{SUB} of the Thyrector diode is 0.65Ω , and the slope of the I-V characteristic of the simulated Thyrector diode per [47] is around 1.28Ω , the dynamic resistance of the Zener diode is considered 0.63Ω , as calculated in Equation B.1, as below:

$$Slope_{I-V} - R_{SUB} = R_z = 0.63 \Omega \quad (B.1)$$

The simulated test circuit for the analysis of the Thyrector diode is depicted in Figure B.22. The reference paper [47] investigates both the DC and ultra-frequency AC behavior of the simulated Thyrector diode. But, this research work focuses on monitoring an

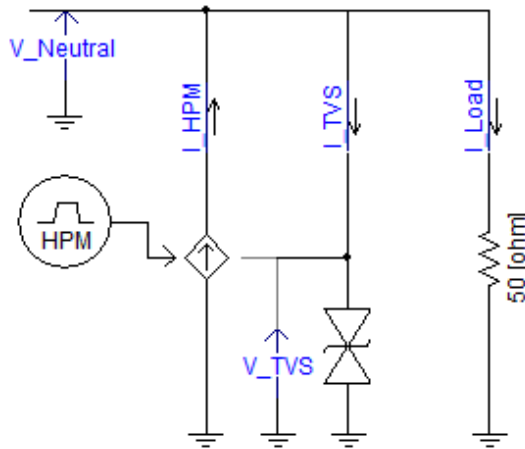


Figure B.22: PSCAD test circuit for analysis of the Thyrector diode.

equipment of the power system that does not experience harmonics oscillating faster than a few kHz. Hence, it is not worthwhile to investigate the simulated model for ultra-frequencies. The DC analysis of this publication is more valid for power systems analysis. On the other hand, the characteristics of all of the electrical elements change dependent to frequency. Even, each resistor has to be modeled as a combination of resistors, capacitors and inductors in ultra-high frequencies. Thus, it is not possible to model the Thyrector in high frequencies using PSCAD standard models.

In Figure B.22, the power profile of the the High Power Microwave source is shown. This signal is a current that the test circuit experiences for 100 ns. As the amplitude of this surge current increases, it is expected that the Thyrector diode clamps the voltage across the $50\ \Omega$ load at approximately 10 V.

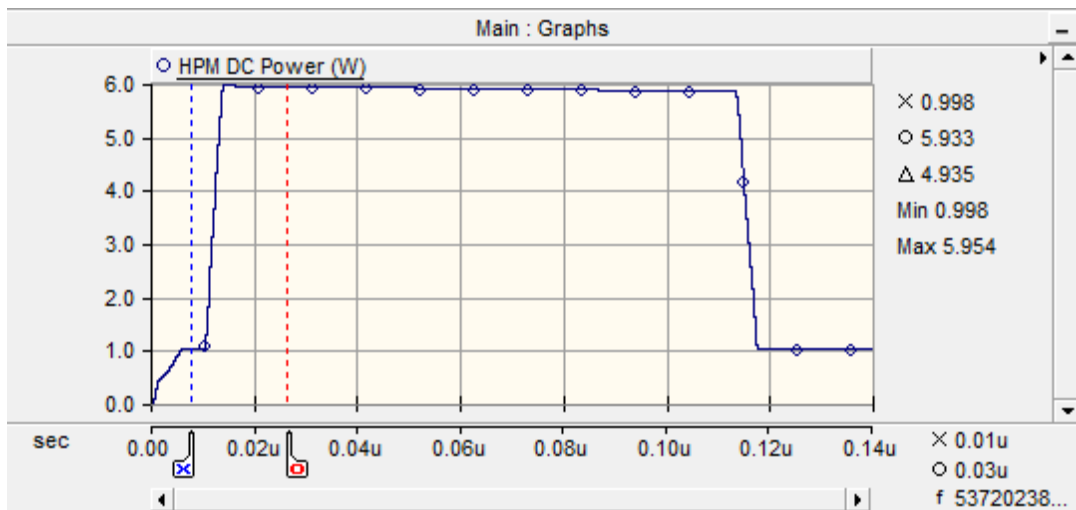


Figure B.23: HPM current profile for DC pulse test.

The macro-model of the PSCAD implementation of the Thyrector is represented in Figure B.23. The capacitive branches have not been considered because they are open at power system frequency. Even if the 10th harmonic of the power system frequency is investigated, the impedance of this branch is so higher than its parallel paths that it could be neglected. Thereby, it will not effect the simulation results.

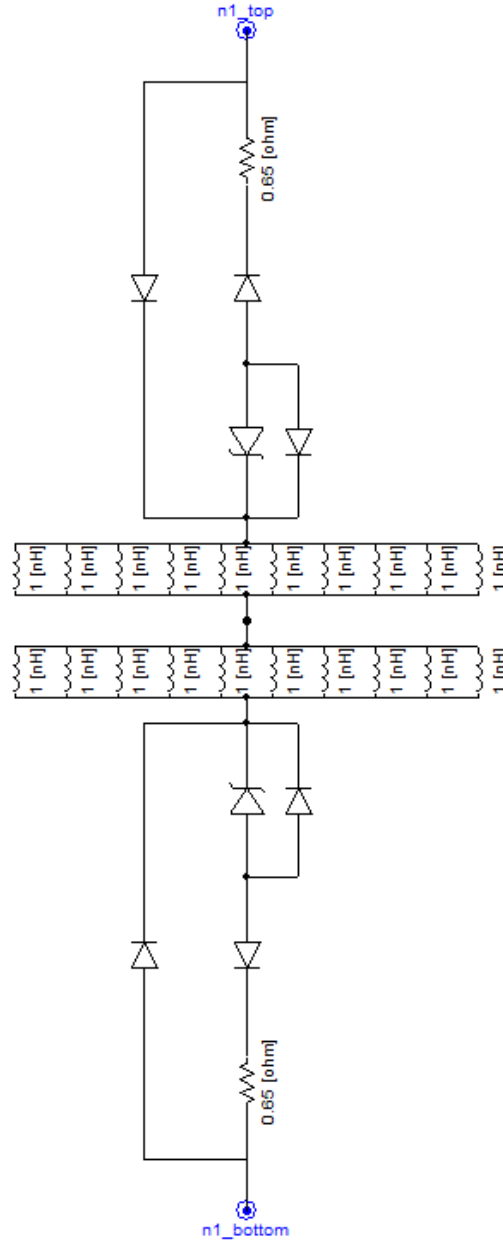


Figure B.24: PSCAD model of the Thyrector diode.

The I-V characteristic of the simulated Thyrector diode is depicted in Figure B.25. In order to obtain this characteristic, the injected power by HPM source has been increased from 25 dBm (316 mW) to 60 dBm (1 kW). The same test has been carried out in [47], and the result has been presented in Figure B.21. As shown, an immeasurable current flows through the Thyrector when the voltage is less than 9.6 V. But, when the voltage becomes greater than 9.6 V, the breakdown region of the reverse Zener diode operates

and creates an I-V characteristic which represents a resistance equal to $1.28\ \Omega$. This resistance is the dynamic resistance of the Thyrector diode.

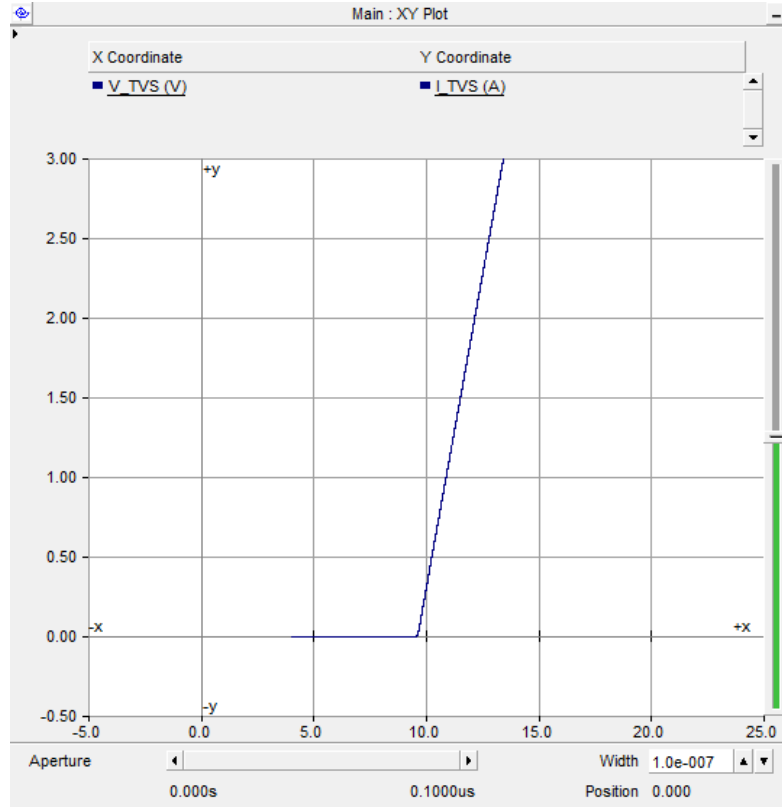


Figure B.25: I-V characteristic of the Thyrector diode in PSCAD.

The other characteristic of the simulated Thyrector diode by [47] is the R_{DYN} versus the power of the HPM pulses. This characteristic has been shown in Figure B.20. It shows that for low power HPMs, the dynamic resistance of the Thyrector diode is very high, i.e., in the order of kilo-Ohms. In fact, the breakdown region of the reverse Zener diode is not activated. However, the forward Zener diode conducts through its forward diode which only needs 0.7 V to conduct the current. This dynamic is valid for voltages less than 9.6 V. This voltage is calculated as follows:

$$V_{BR} = EV1 + 3 \times 0.7\text{ V} + R_{DYN} \times I_{pp} = 7.5\text{ V} + 2.1\text{ V} + 1.28\ \Omega \times 0 = 9.6\text{ V} \quad (\text{B.2})$$

For voltages more than 9.6 V, the breakdown region of the reverse Zener diode of the Thyrector diode operates. In this region, the Thyrector diode is modeled by $R_{DYN}=1.28\ \Omega$

in series with the EV1=7.5 V and $3 \times 0.7 \text{ V} = 2.1 \text{ V}$. The 2.1 V voltage-drop is because in this region of operation, three forward and series diodes also conduct the current. The first one is the forward diode of the forward Zener diode. The second one is the voltage-drop of a diode which models the breakdown region of the reverse Zener diode. Finally, the third one is a diode in series with the reverse Zener diode considered in the model of the Thyrector diode. The R_{DYN} versus the power of the HPM characteristic for DC pulse in PSCAD is represented in Figure B.26.

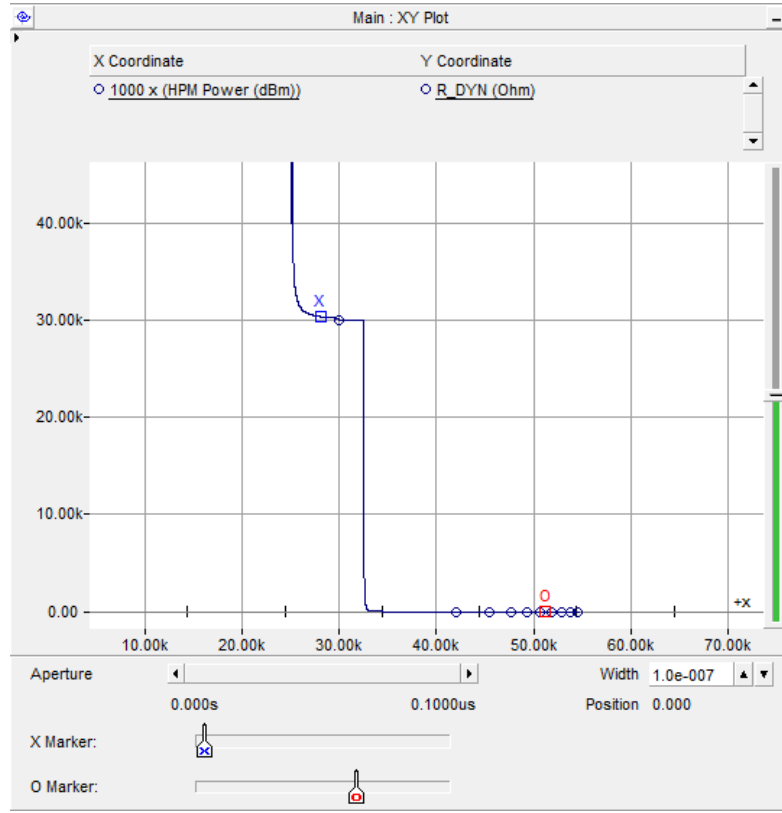


Figure B.26: R_{DYN} versus the power of the HPM DC pulse characteristic of the Thyrector diode in PSCAD.

As shown, when the injected power is low, the resistance of the Thyrector diode is in the order of $\text{k}\Omega$ s. When the injected power rises over approximately 2 W which means that the voltage across the load is 9.6 V, the breakdown region of the reverse Zener diode operates and the resistance of the Thyrector diode decreases suddenly to a few ohms as shown in Figure B.26. The resistance of the Thyrector diode in breakdown region is 1.28Ω as marked with red pointer.

B.3 Implementation of TVS in PSCAD

The next step is adopting the simulated Thyrector diode to the NGR monitoring equipment. This TVS is used for over-voltage protection of the monitoring equipment. It clamps the voltage at 100 V, while the voltages less than the clamping voltage are delivered to input gates of monitoring equipment without any clamping effect. The simulated Thyrector diode clamps the voltage at 9.6 V. In order to provide the clamping at 100 V, 10 Thyrectors are connected in series. The resulted circuit is referred as 100 V TVS. The clamping voltage provided by the simulated TVS, i.e., 96 V, is 10 times greater than that of the Thyrector diode. The simulated test circuit in PSCAD is depicted in Figure B.27.

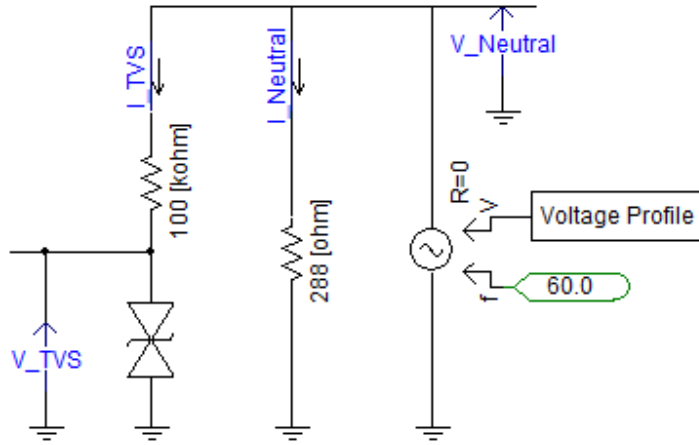


Figure B.27: The TVS simulated test circuit in PSCAD.

The isolation resistor of the sensing resistor, which is 100 k Ω , is selected based on data provided by [19] considering that the system voltage is 12.47 kV. It limits the current through the neutral voltage metering system to 72 mA. This current appears when a LG fault happens at the terminals of the generator, and the TVS is considered short. The neutral grounding resistor is 288 Ω and is chosen so that the neutral current is limited to 25 A. Initially, the neutral voltage is considered to be around 10 V to generate 30 mA current in the neutral wire modeling the normal operation condition. Once the LG fault occurs, the voltage magnitude rises to a significant level. Such a condition is represented in Figure B.28 and Figure B.29 where initially, the neutral point experiences low voltage

and suddenly its voltage jumps to 7.2 kV.

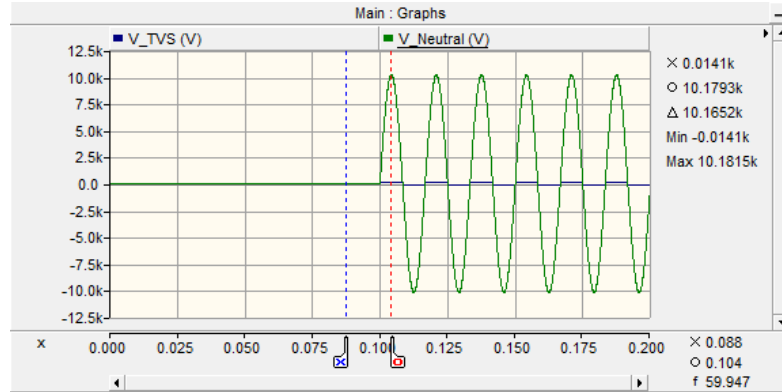


Figure B.28: TVS operation during normal and faulted conditions.

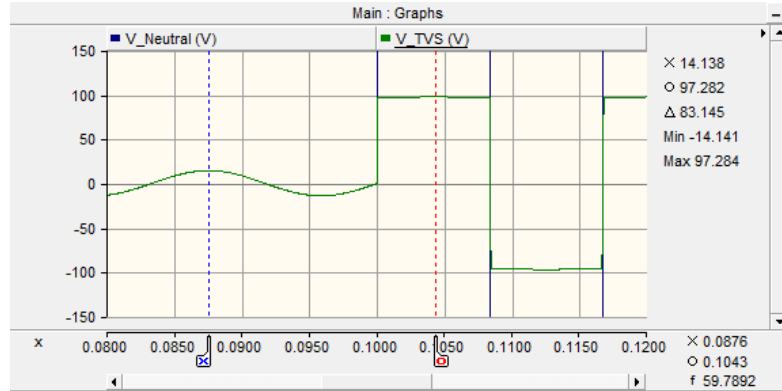


Figure B.29: TVS operation clamping sensed voltage during transition from normal to faulted conditions.

At time equal to 0.1 s, the LG fault happens and the neutral voltage increases suddenly. The TVS clamps the voltage at 97.28 V as soon as the voltage hits the clamping level. The [19] mentions that the clamping voltage is 100 V. The difference between this value and the resulted clamping voltage is because of the difference in the selected Thyrector diode. The resulted clamping voltage can be set to exactly 100 V by modifying the breakdown voltage of the Zener diodes used in the simulation. But, the authors preferred to use the resulted outcome since it is achieved based on the simulation of the previously presented literature of the TVS and technical data of the simulated elements in PSCAD.

Appendix C

Additional Results for Chapter 4

In this chapter, additional simulation results for the first proposed method, presented in Chapter 4, are demonstrated. The performance of the proposed method for monitoring the High resistance Neutral Grounding Resistor (HNRG), designed 288Ω , is investigated. The failed-short and failed-open HNGR during both faulted and unfaulted conditions are just a few represented case studies selected from Table 4.1. Additionally, the performance of the method for disconnected LNGR and HNGL during both unfaulted and faulted conditions are shown as well.

On the basis of the presented results and further performed observations, it is concluded that:

- The neutral-to-ground circuit experiences higher voltage in high resistance grounded systems. In fact, the HNGR has considerable impedance compared to system charging capacitances. But, the LNGR has less impedance than the system charging capacitances causing less voltage across the LNGR. As such, the RPD-based monitoring method performs better when monitoring the HNGR since the neutral voltage is higher. The more the neutral voltage becomes the less its error is due to less impact of the sampling resolution on voltage measurement.
- The proposed method reliably detects the disconnected LNGR, HNGR, and HNGL in both normal and faulted conditions. The other existing methods cannot detect the NGD failure in both mentioned conditions.

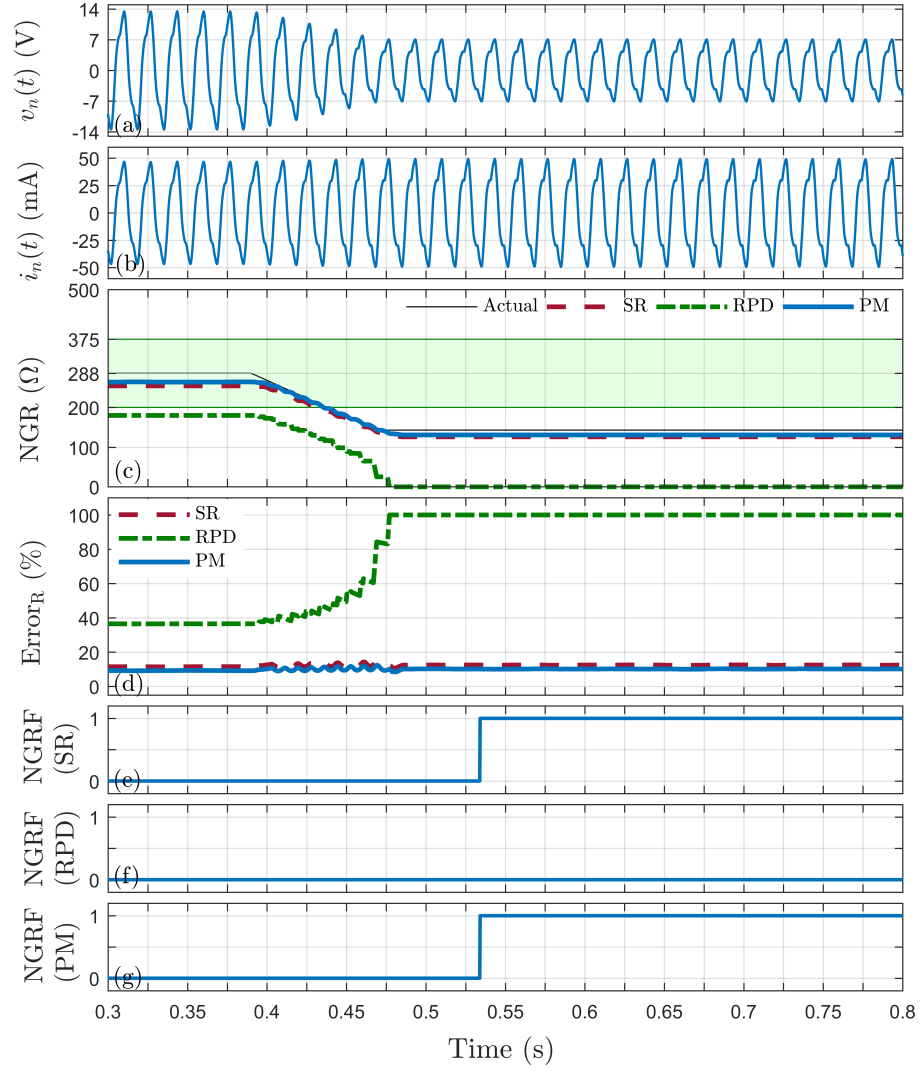


Figure C.1: Failed-short HNGR ($288 \Omega \rightarrow 144 \Omega$) during unfaulted condition. a) Neutral voltage, b) Neutral current, c) NGR resistance, d) Measurement error of NGR resistance, e) NGR failure detection by SR-based monitoring method, f) NGR failure detection by RPD-based monitoring method, and g) NGR failure detection by proposed monitoring method.

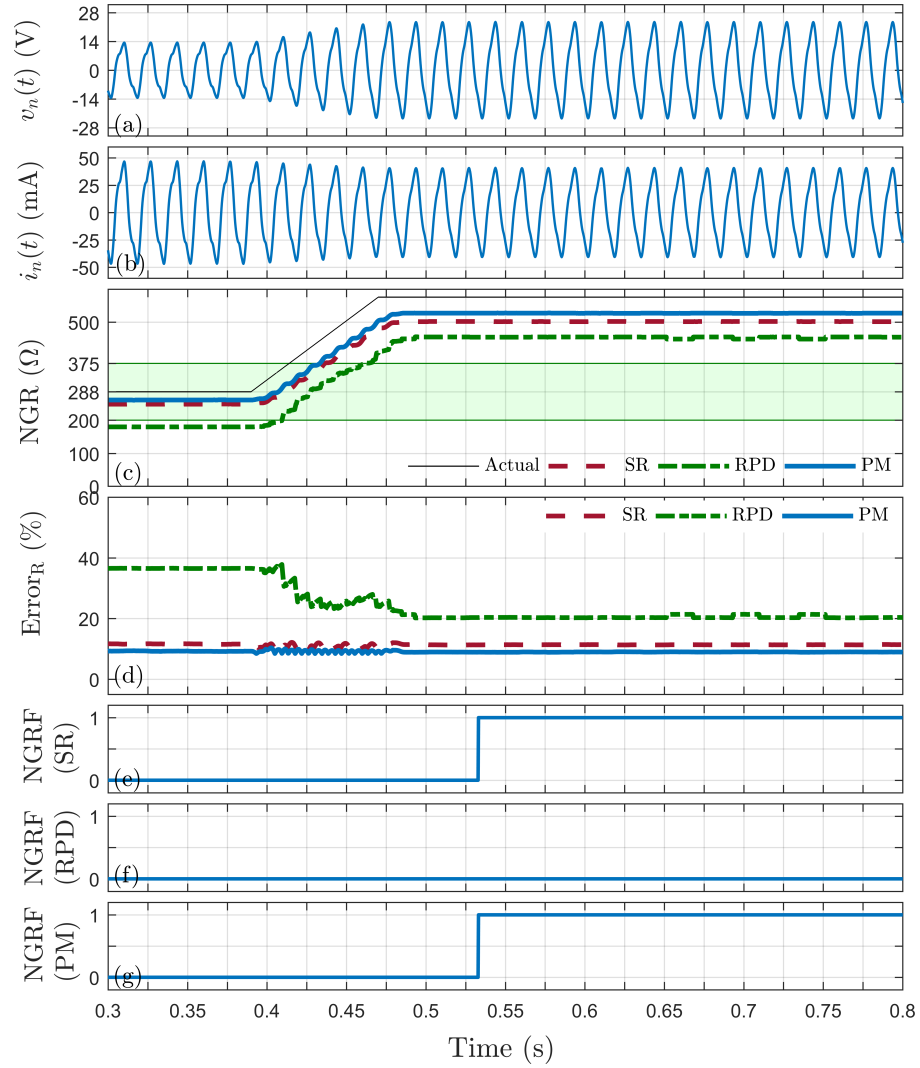


Figure C.2: Failed-open HNGR ($288 \Omega \rightarrow 576 \Omega$) during unfaulted condition. a) Neutral voltage, b) Neutral current, c) NGR resistance, d) Measurement error of NGR resistance, e) NGR failure detection by SR-based monitoring method, f) NGR failure detection by RPD-based monitoring method, and g) NGR failure detection by proposed monitoring method.

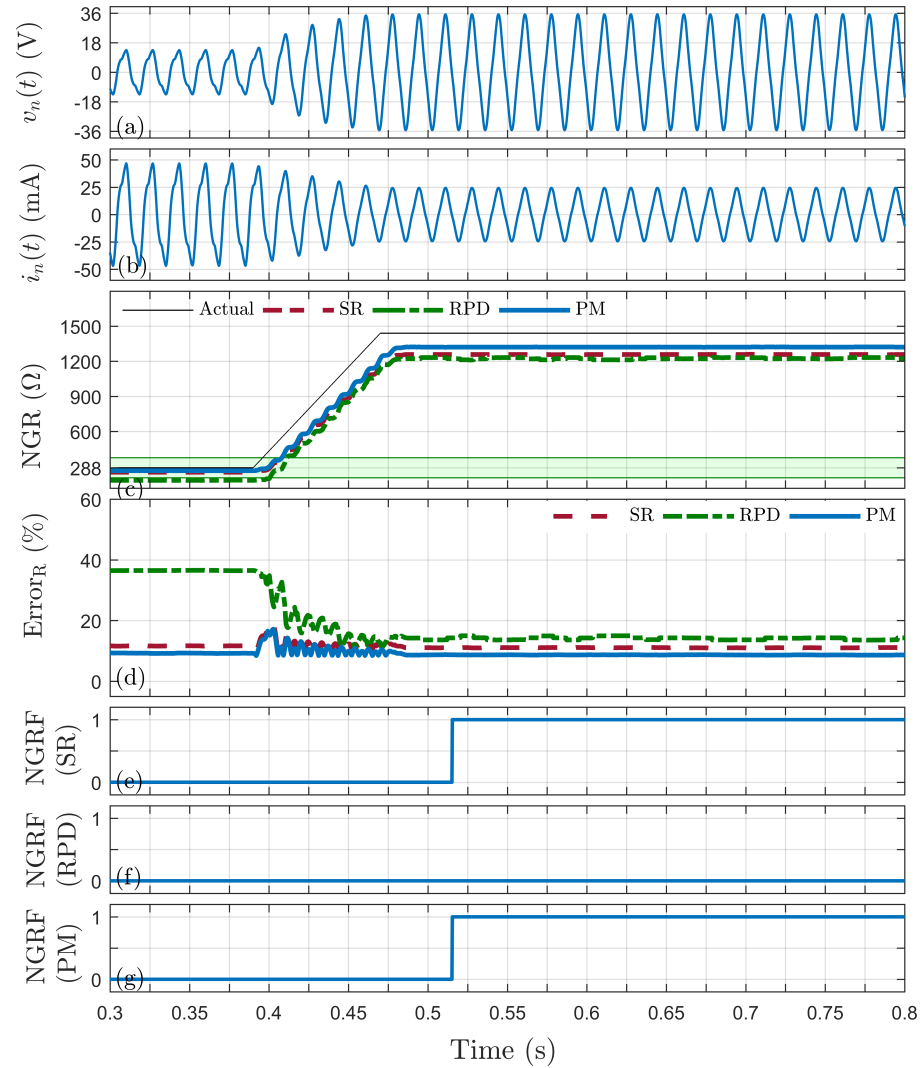


Figure C.3: Failed-open HNGR ($288 \Omega \rightarrow 1440 \Omega$) during unfaulted condition. a) Neutral voltage, b) Neutral current, c) NGR resistance, d) Measurement error of NGR resistance, e) NGR failure detection by SR-based monitoring method, f) NGR failure detection by RPD-based monitoring method, and g) NGR failure detection by proposed monitoring method.

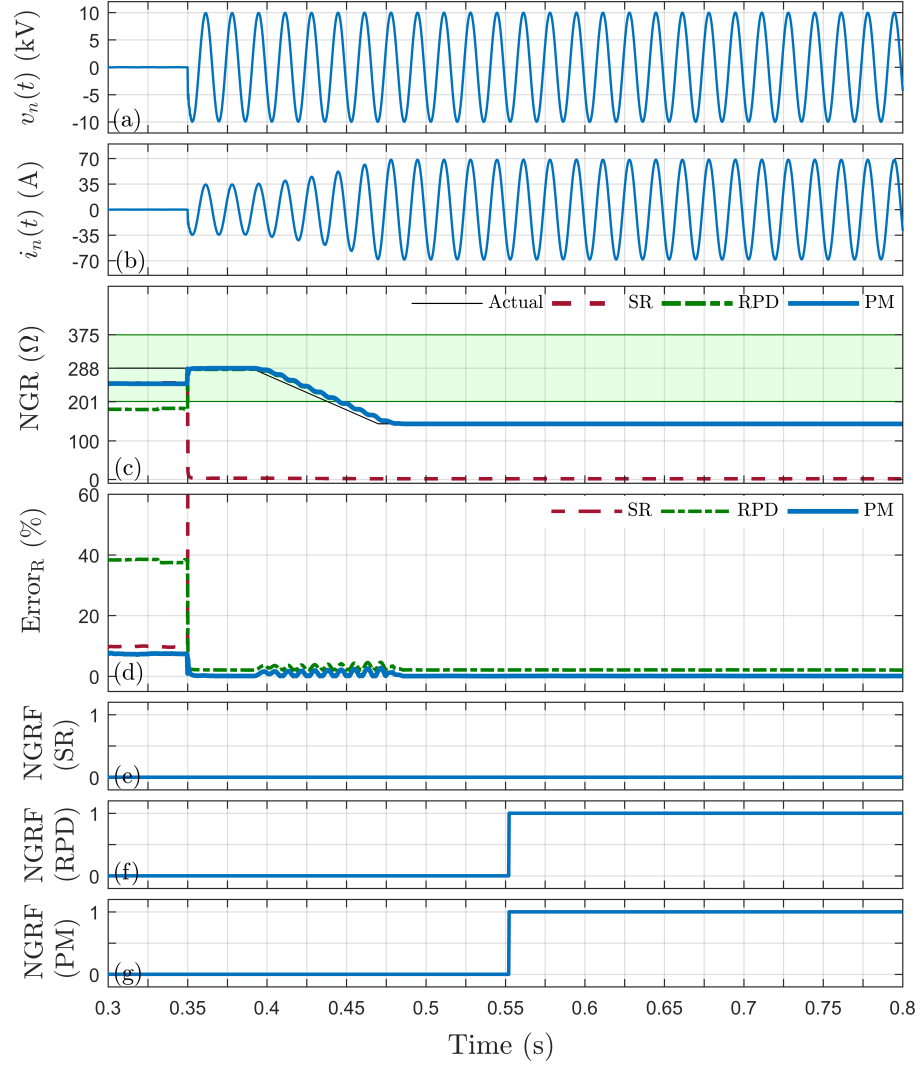


Figure C.4: Failed-short HNGR ($288 \Omega \rightarrow 144 \Omega$) during LG fault. a) Neutral voltage, b) Neutral current, c) NGR resistance, d) Measurement error of NGR resistance, e) NGR failure detection by SR-based monitoring method, f) NGR failure detection by RPD-based monitoring method, and g) NGR failure detection by proposed monitoring method.

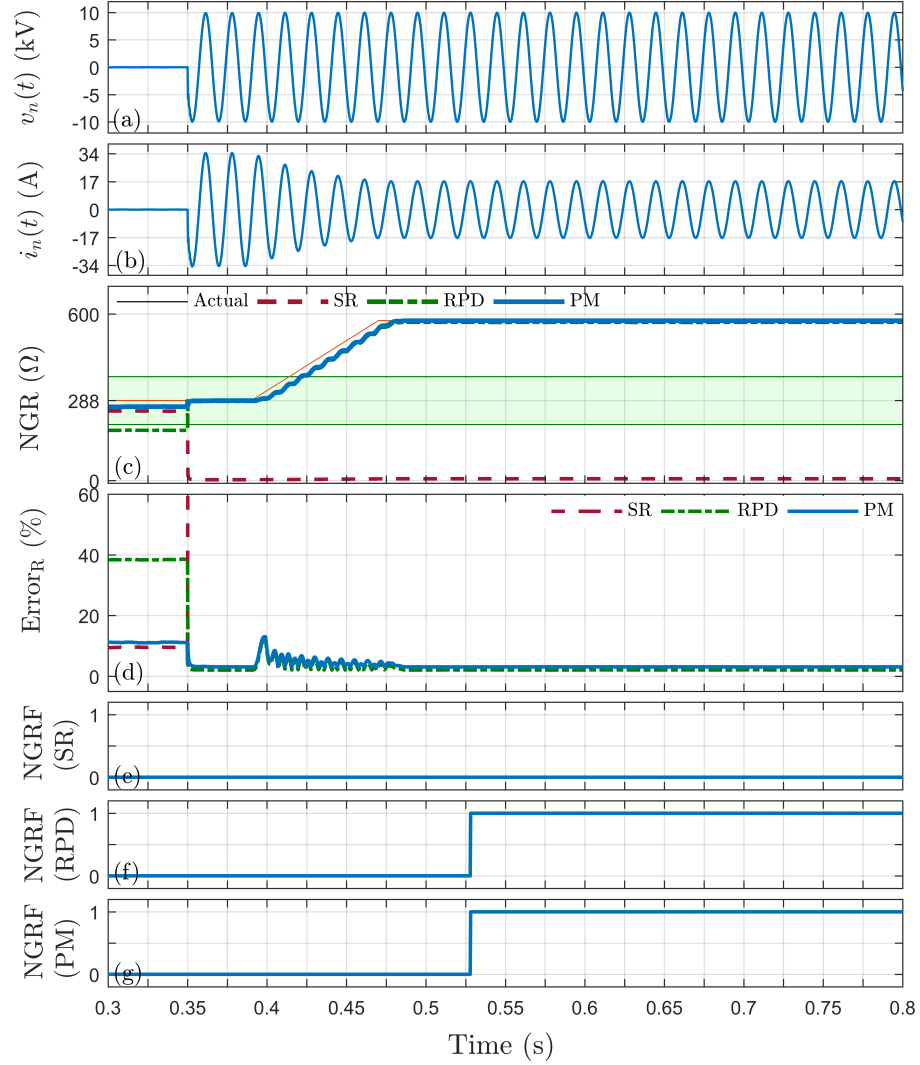


Figure C.5: Failed-open HNGR ($288\ \Omega \rightarrow 576\ \Omega$) during LG fault. a) Neutral voltage, b) Neutral current, c) NGR resistance, d) Measurement error of NGR resistance, e) NGR failure detection by SR-based monitoring method, f) NGR failure detection by RPD-based monitoring method, and g) NGR failure detection by proposed monitoring method.

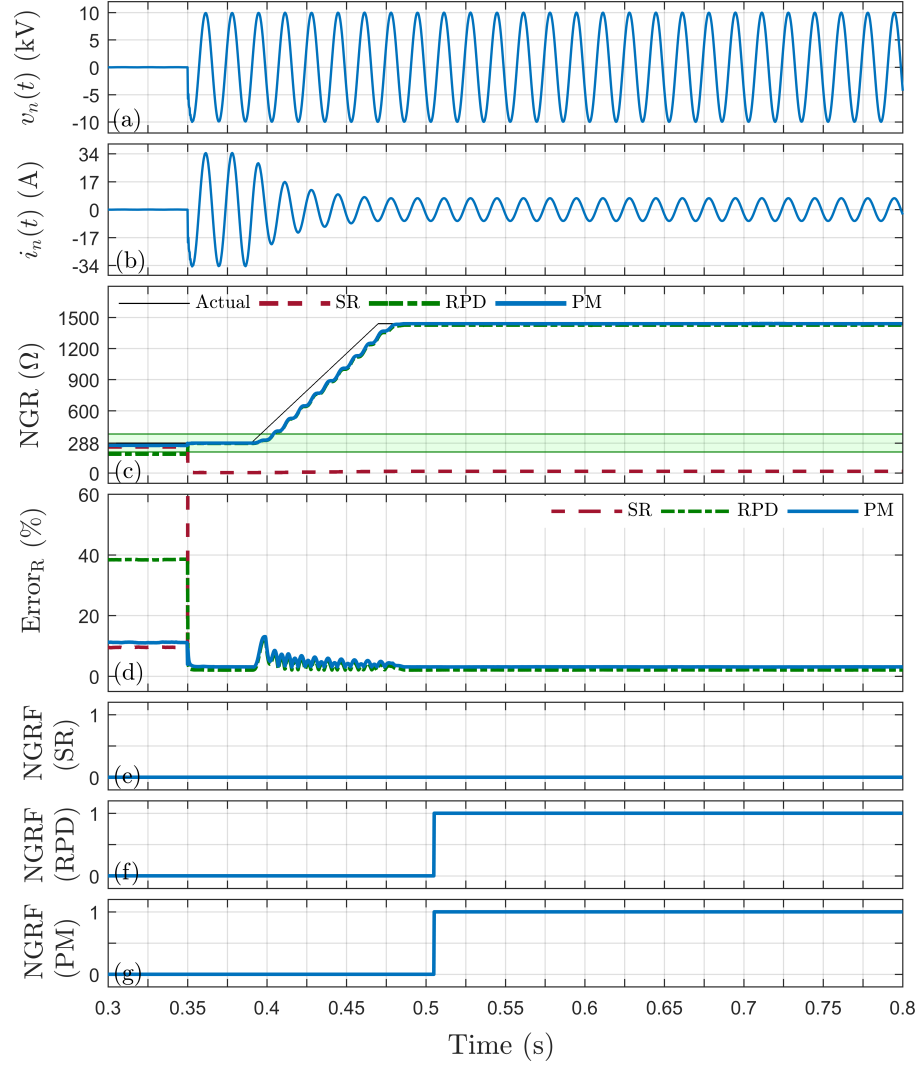


Figure C.6: Failed-open HNGR (288 Ω \rightarrow 1440 Ω) during LG fault. a) Neutral voltage, b) Neutral current, c) NGR resistance, d) Measurement error of NGR resistance, e) NGR failure detection by SR-based monitoring method, f) NGR failure detection by RPD-based monitoring method, and g) NGR failure detection by proposed monitoring method.

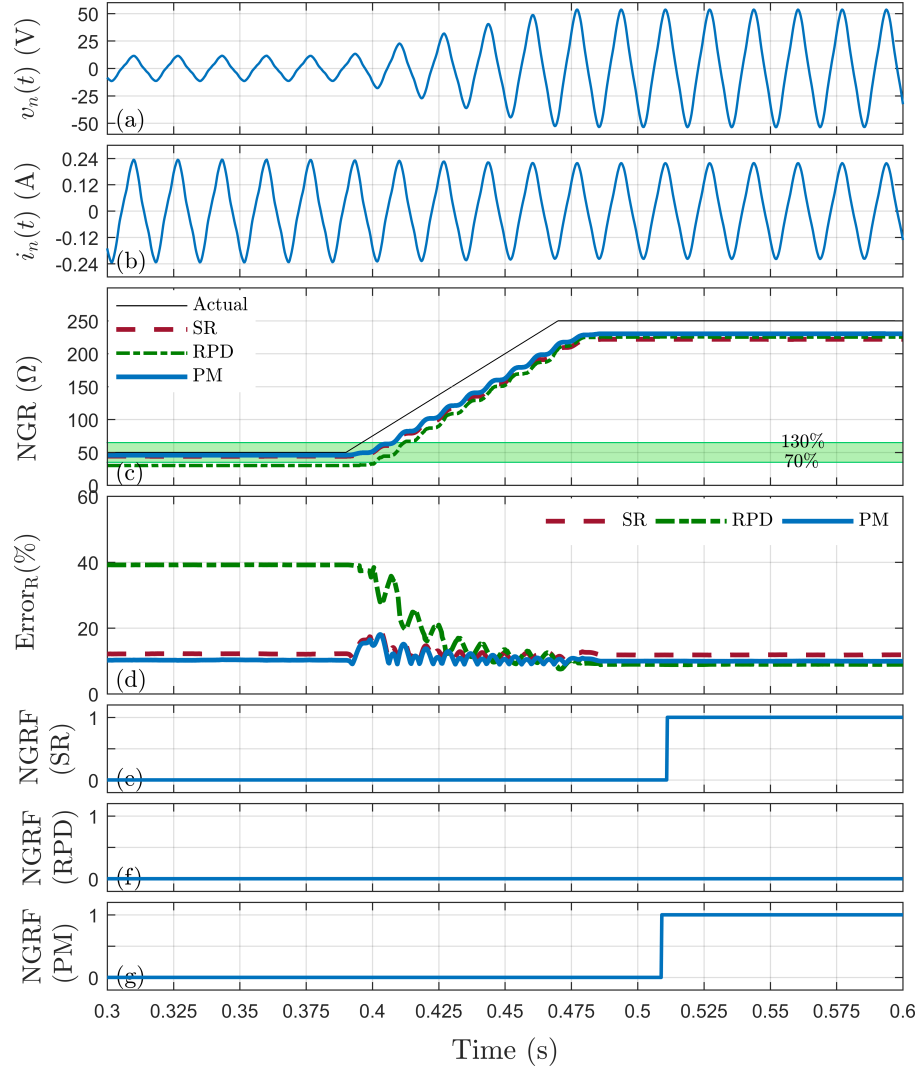


Figure C.7: Failed-open LNGR ($50 \Omega \rightarrow 250 \Omega$) during unfaulted condition. a) Neutral voltage, b) Neutral current, c) NGR resistance, d) Measurement error of NGR resistance, e) NGR failure detection by SR-based monitoring method, f) NGR failure detection by RPD-based monitoring method, and g) NGR failure detection by proposed monitoring method.

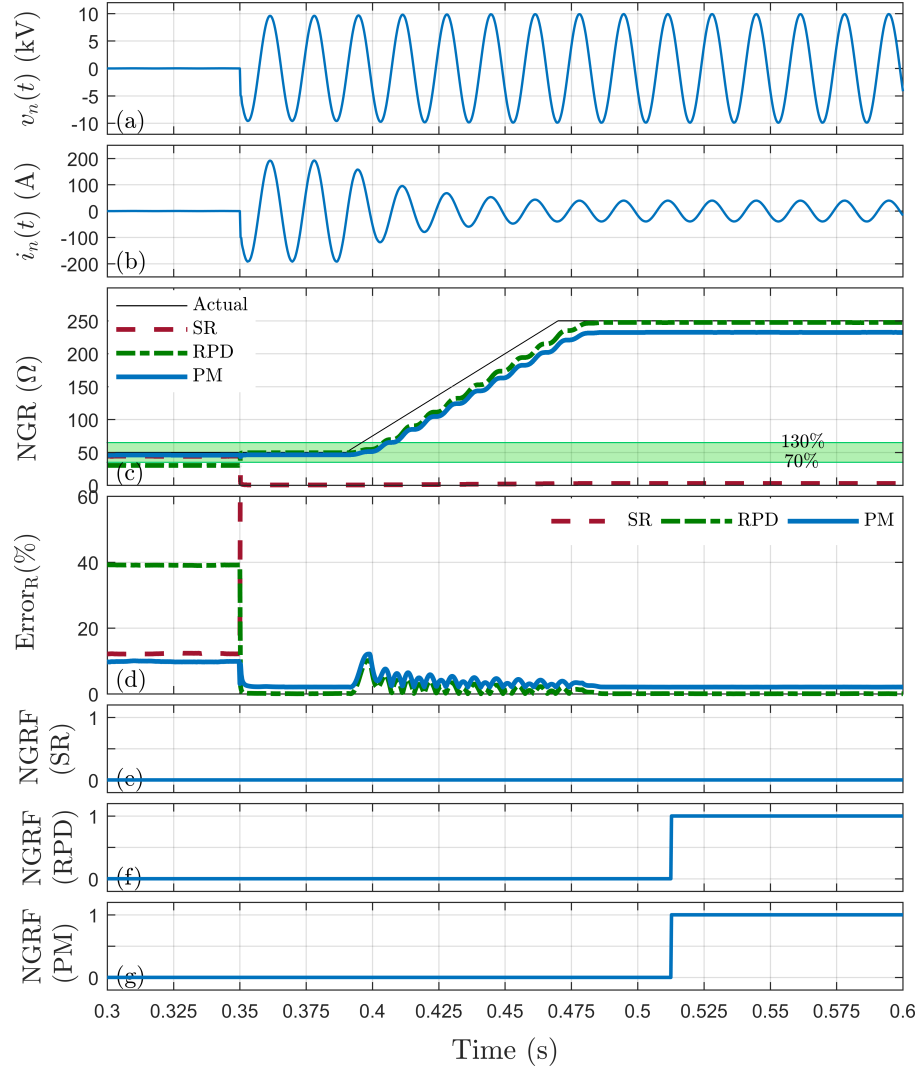


Figure C.8: Failed-open LNGR ($50 \Omega \rightarrow 250 \Omega$) during LG fault condition. a) Neutral voltage, b) Neutral current, c) NGR resistance, d) Measurement error of NGR resistance, e) NGR failure detection by SR-based monitoring method, f) NGR failure detection by RPD-based monitoring method, and g) NGR failure detection by proposed monitoring method.

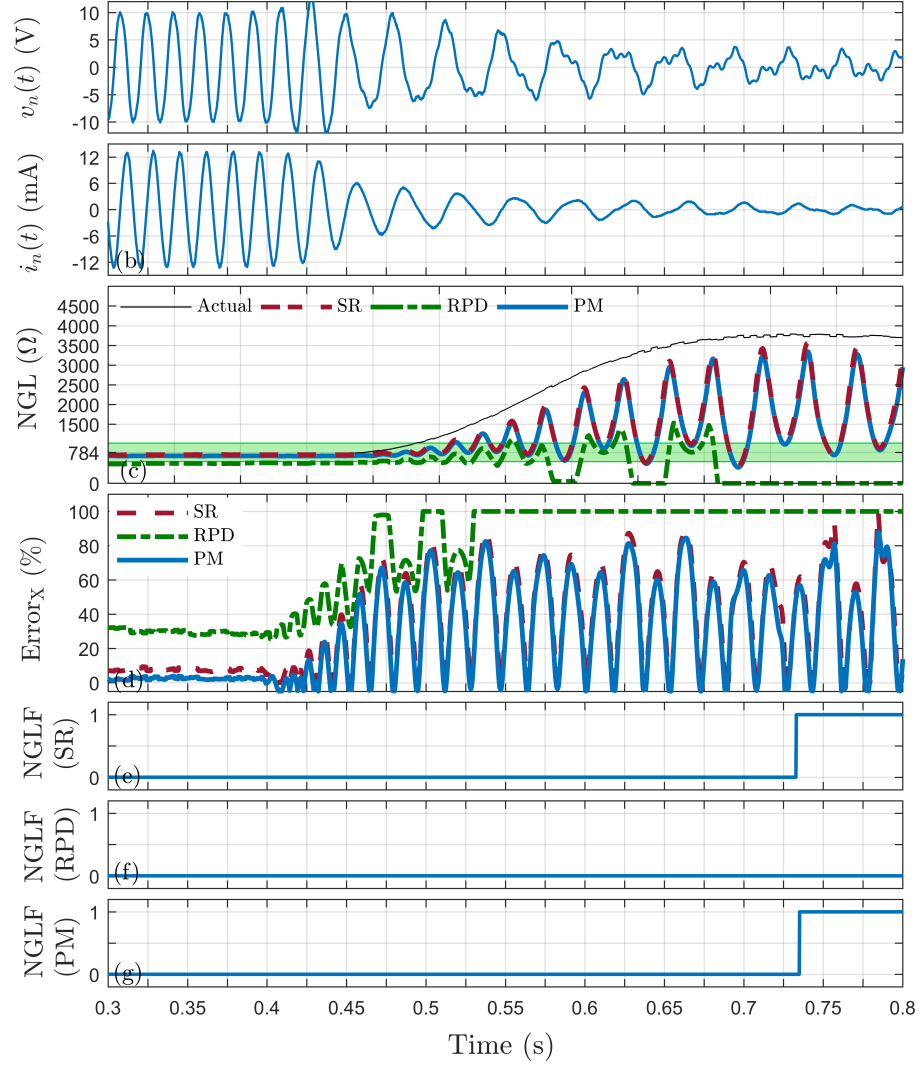


Figure C.9: Failed-open HNGL ($784 \Omega \rightarrow 4 \text{ k}\Omega$) during unfaulted condition. a) Neutral voltage, b) Neutral current, c) NGL resistance, d) Measurement error of NGL reactance, e) NGL failure detection by SR-based monitoring method, f) NGL failure detection by RPD-based monitoring method, and g) NGL failure detection by proposed monitoring method.

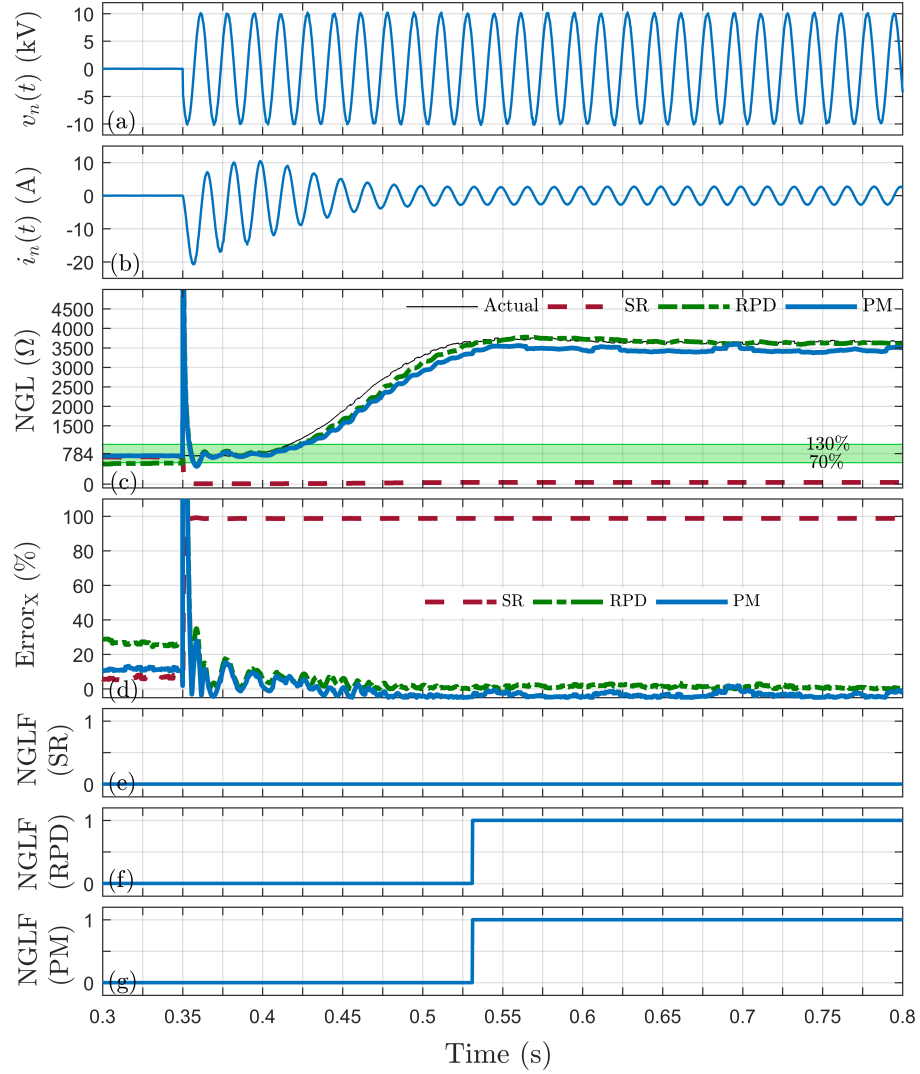


Figure C.10: Failed-open HNGL ($784\Omega \rightarrow 4\text{k}\Omega$) during during LG fault condition. a) Neutral voltage, b) Neutral current, c) NGL resistance, d) Measurement error of NGL reactance, e) NGL failure detection by SR-based monitoring method, f) NGL failure detection by RPD-based monitoring method, and g) NGL failure detection by proposed monitoring method.

Appendix D

Additional Results for Chapter 5

In this chapter, additional simulation results for the second proposed method, presented in Chapter 5, are demonstrated. The impact of step-up transformer saturation, and very high reactive loading on performance of the proposed method are investigated. Furthermore, it will be shown that the catastrophic failure of the NGR elements can be detected as well. In fact, the sudden disconnection of the NGR is possible which can be identified using the proposed method. Lastly, the operation of the proposed method in the presence of different system faults will be examined to show that it distinguishes between system faults and NGR failure. Each of the following figures includes a set of the captured waveforms from PSCAD, and detection made by Matlab-based relay model.

On the basis of the presented results and further performed observations, it is concluded that:

1. Step-up transformer saturation impacts on the neutral and residual 180 Hz voltages. As a result, these two parameters, which should normally be equal to 50% of the total generated third harmonic, deviate from 50% and cause unbalance. However, the NGR failure is detected with the same proposed monitoring algorithm.
2. Loading condition changes the neutral and residual third harmonic voltages, but, it does not affect the proposed method due to normalization.
3. The proposed method is well-restrained against system faults as it distinguishes between system faults and NGR failure.

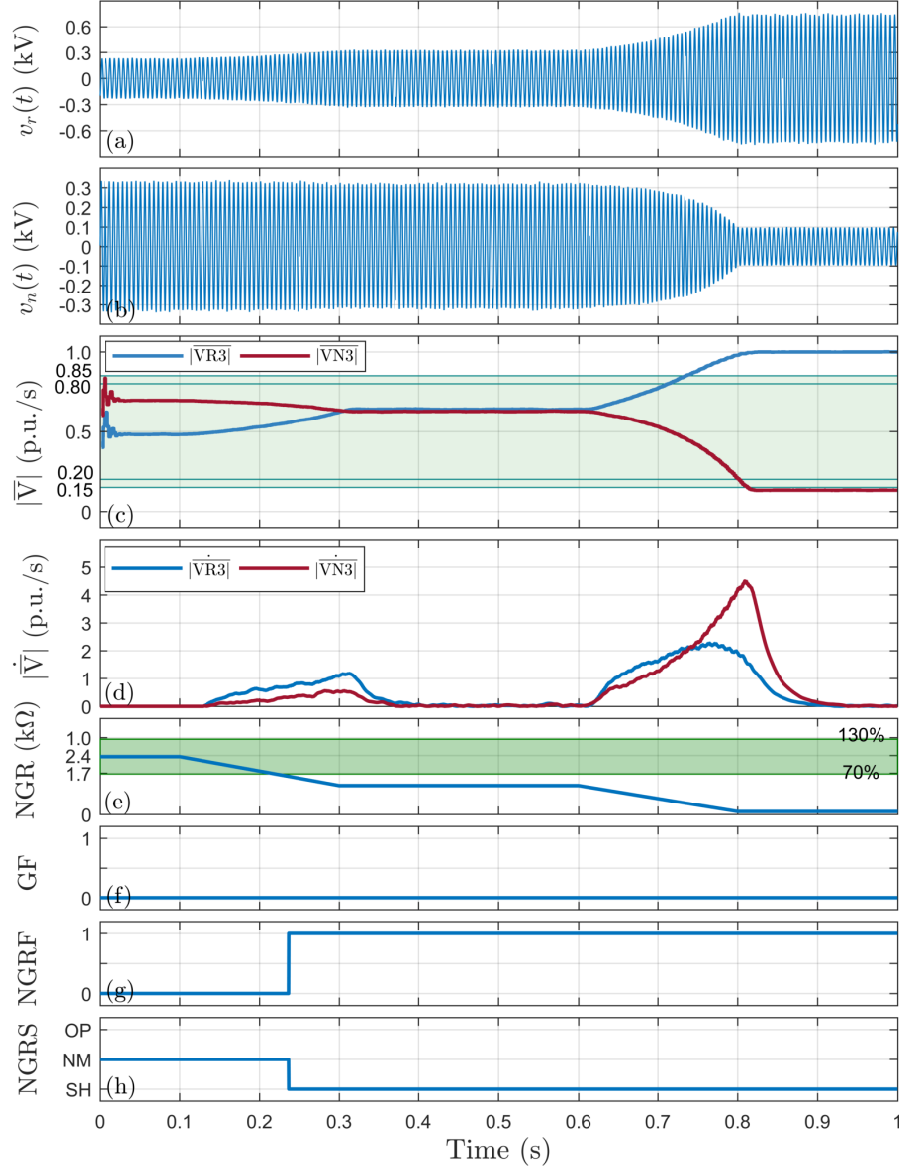


Figure D.1: Failed-short NGR case (scenario number B6, $r = 1 \rightarrow 0.05$ pu, Load= $0.94+j0.2$ pu, and $e3 = 1\%$). (a) Residual voltage, (b) Neutral voltage, (c) Normalized neutral and residual third harmonic voltages, (d) Rate of change of the normalized third harmonic voltages, (e) NGR resistance, (f) Ground fault detection, (g) NGR failure detection, and (h) NGRS State.

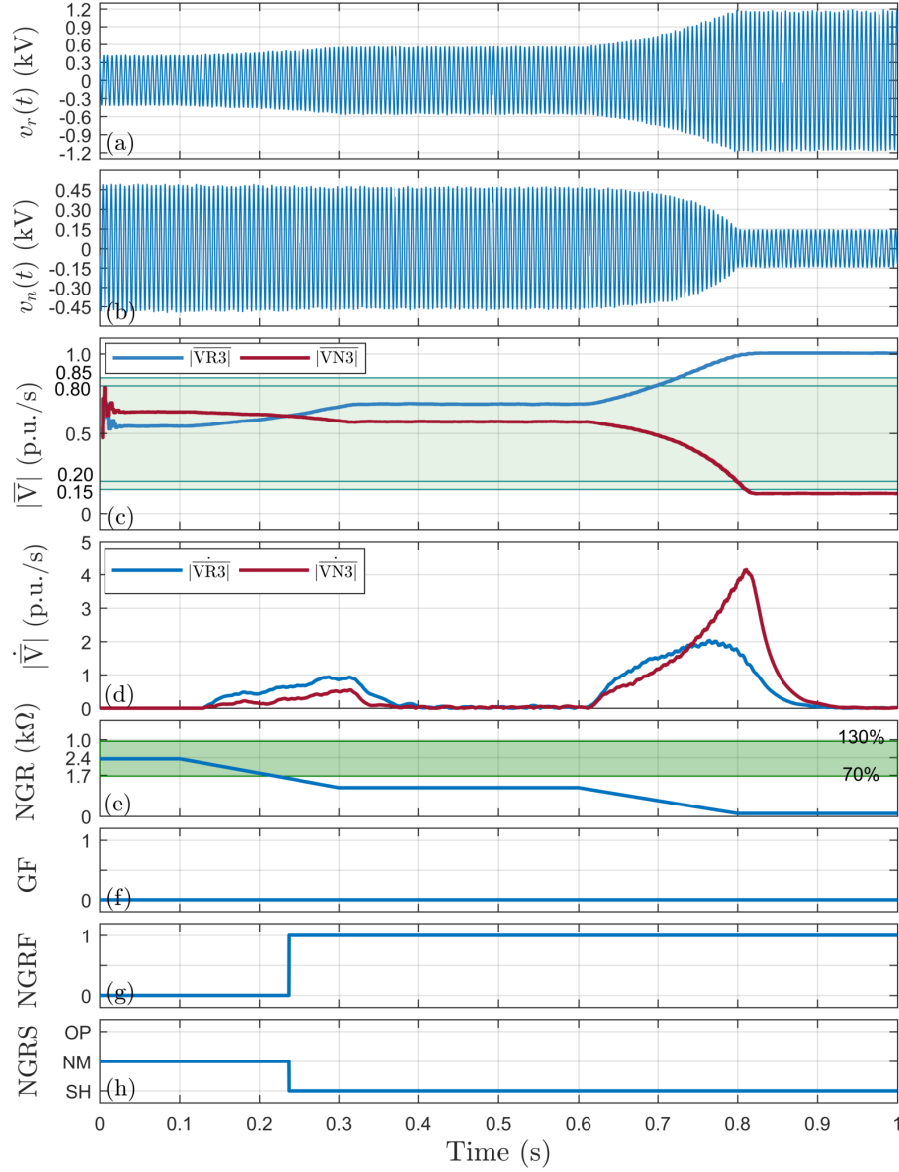


Figure D.2: Failed-short NGR case (scenario number B8, $r = 1 \rightarrow 0.5 \rightarrow 0.05$ pu, Load=0.85+j0.4 pu, and $e3 = 0.5\%$). (a) Residual voltage, (b) Neutral voltage, (c) Normalized neutral and residual third harmonic voltages, (d) Rate of change of the normalized third harmonic voltages, (e) NGR resistance, (f) Ground fault detection, (g) NGR failure detection, and (h) NGRS State.

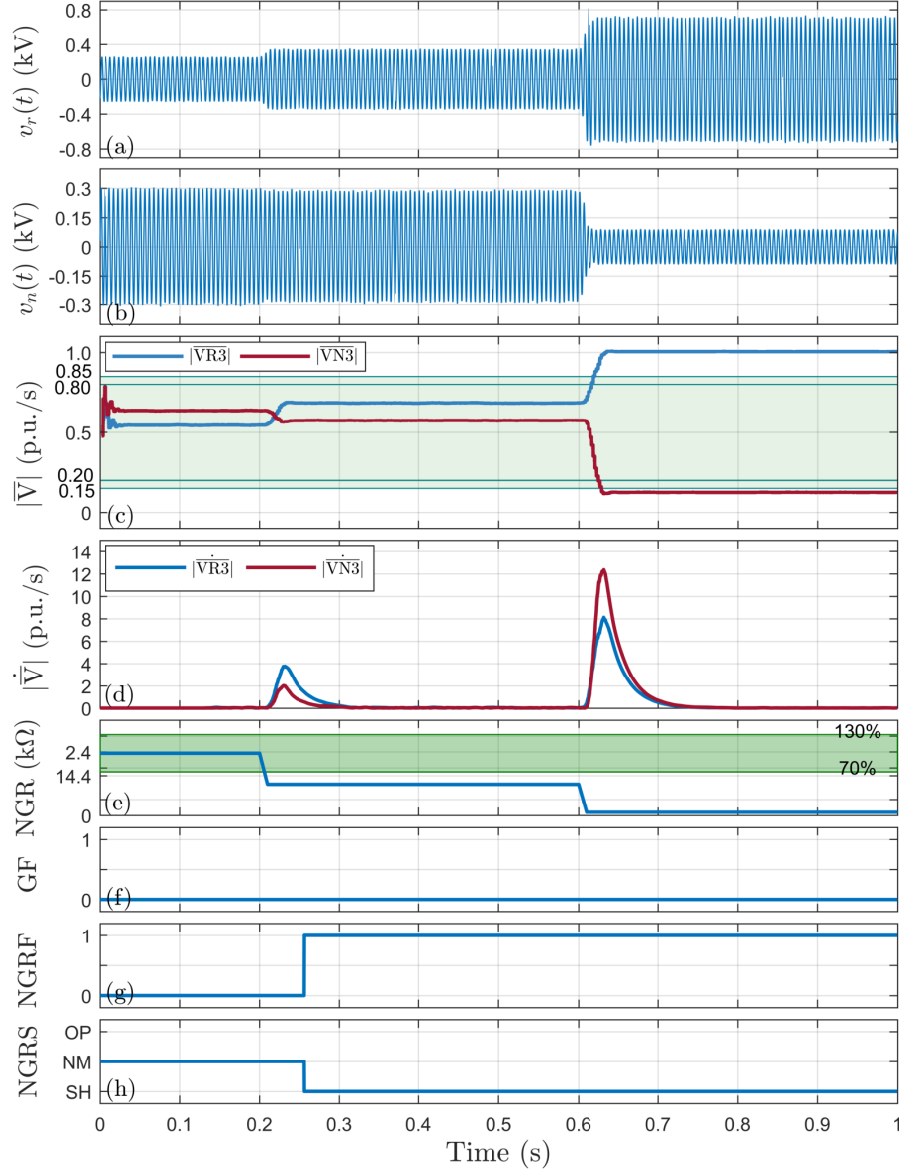


Figure D.3: Failed-short NGR case (scenario number B5 with catastrophic dynamic, $r = 1 \rightarrow 0.5 \rightarrow 0.05$ pu, Load=0.94+j0.2 pu, and $e3 = 0.5\%$). (a) Residual voltage, (b) Neutral voltage, (c) Normalized neutral and residual third harmonic voltages, (d) Rate of change of the normalized third harmonic voltages, (e) NGR resistance, (f) Ground fault detection, (g) NGR failure detection, and (h) NGRS State.

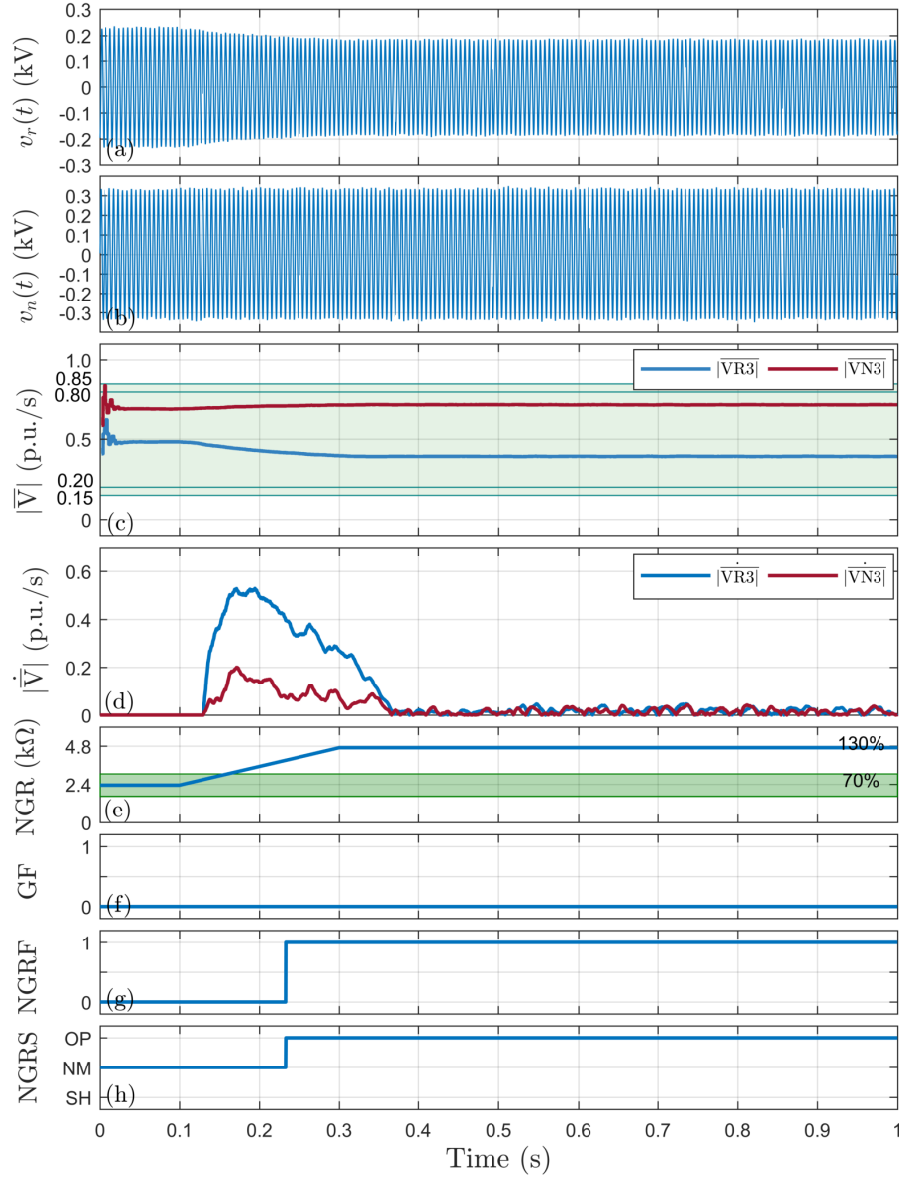


Figure D.4: Failed-open NGR case (scenario number G6, $r = 1 \rightarrow 2$ pu, Load=0.94+j0.2 pu, and $e3 = 1\%$). (a) Residual voltage, (b) Neutral voltage, (c) Normalized neutral and residual third harmonic voltages, (d) Rate of change of the normalized third harmonic voltages, (e) NGR resistance, (f) Ground fault detection, (g) NGR failure detection, and (h) NGRS State.

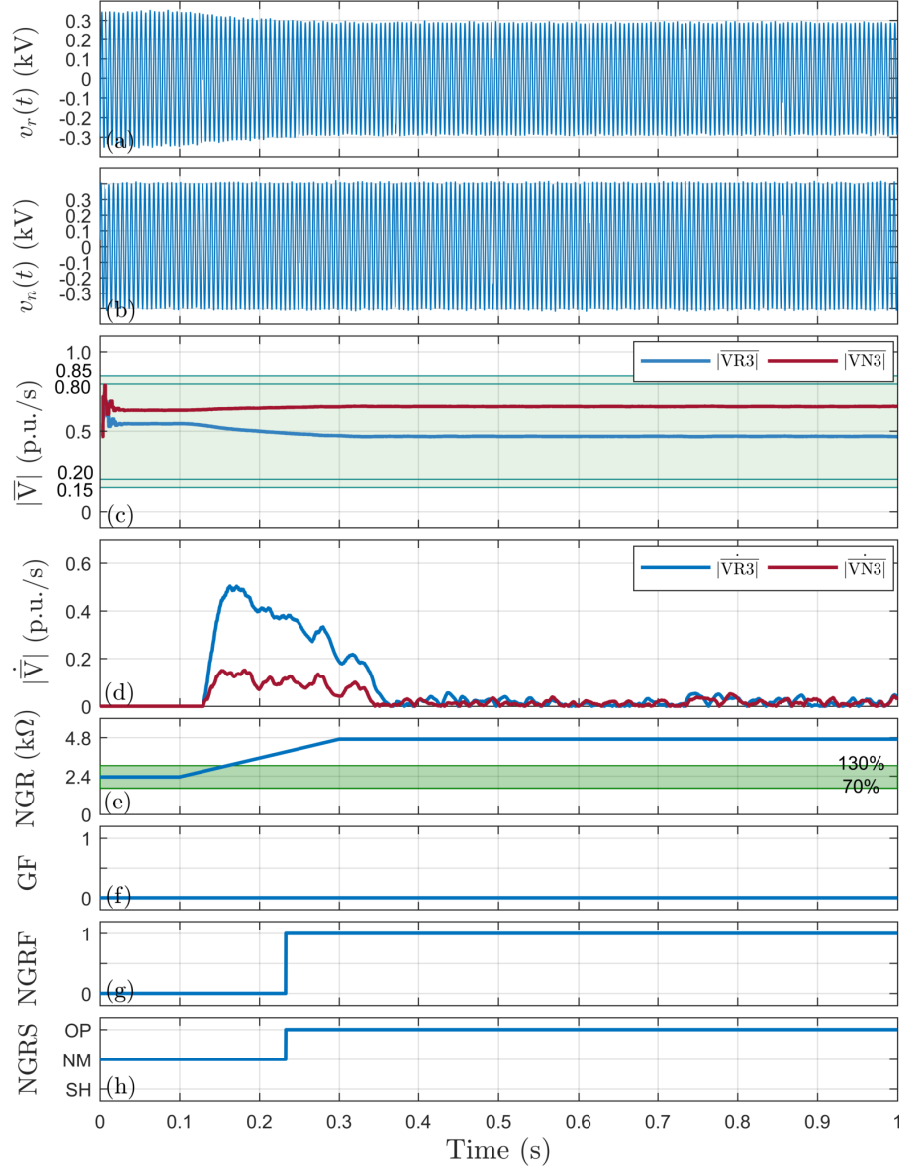


Figure D.5: Failed-open NGR case (scenario number G8, $r = 1 \rightarrow 2$ pu, Load=0.85+j0.4 pu, and $e3 = 0.5\%$). (a) Residual voltage, (b) Neutral voltage, (c) Normalized neutral and residual third harmonic voltages, (d) Rate of change of the normalized third harmonic voltages, (e) NGR resistance, (f) Ground fault detection, (g) NGR failure detection, and (h) NGRS State.

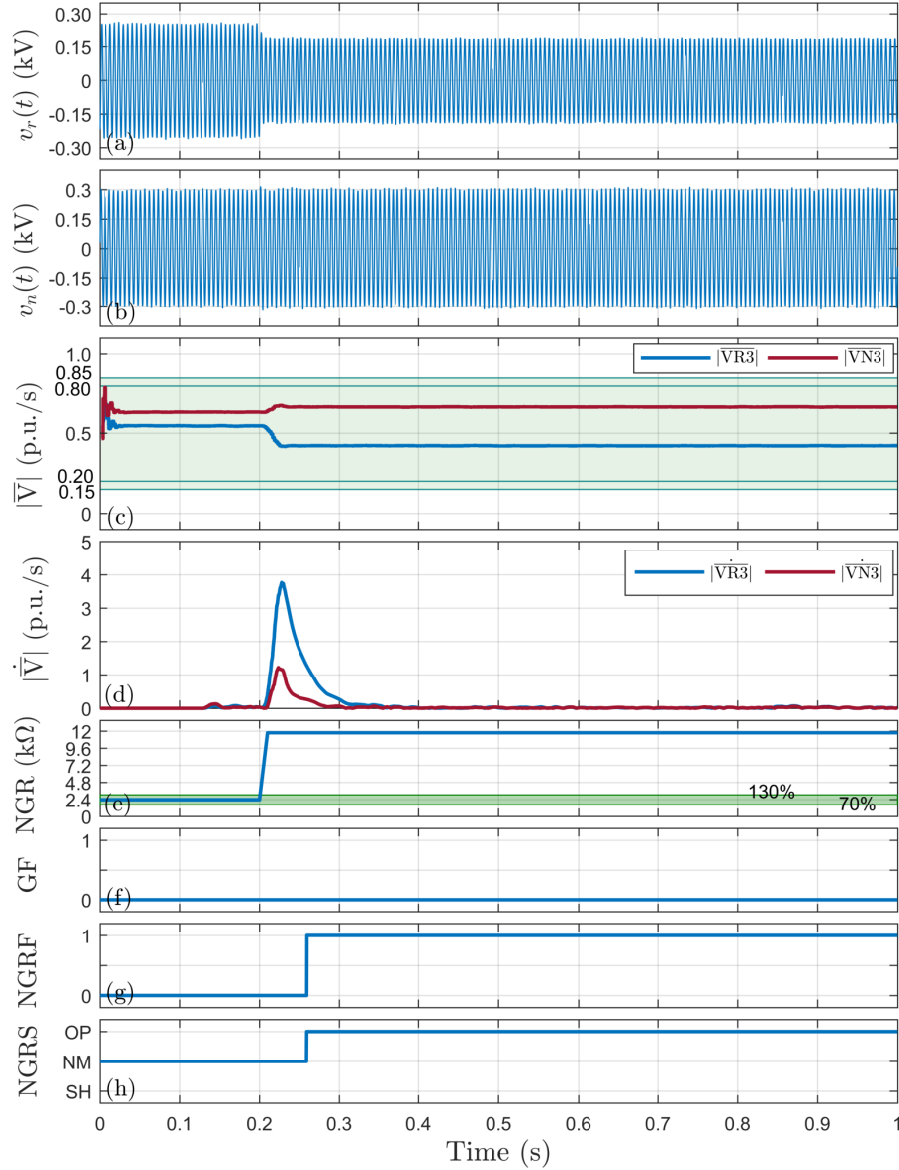


Figure D.6: Failed-open NGR case (scenario number G5 with catastrophic dynamic, $r = 1 \rightarrow 5$ pu, Load=0.94+j0.2 pu, and $e3 = 0.5\%$). (a) Residual voltage, (b) Neutral voltage, (c) Normalized neutral and residual third harmonic voltages, (d) Rate of change of the normalized third harmonic voltages, (e) NGR resistance, (f) Ground fault detection, (g) NGR failure detection, and (h) NGRS State.

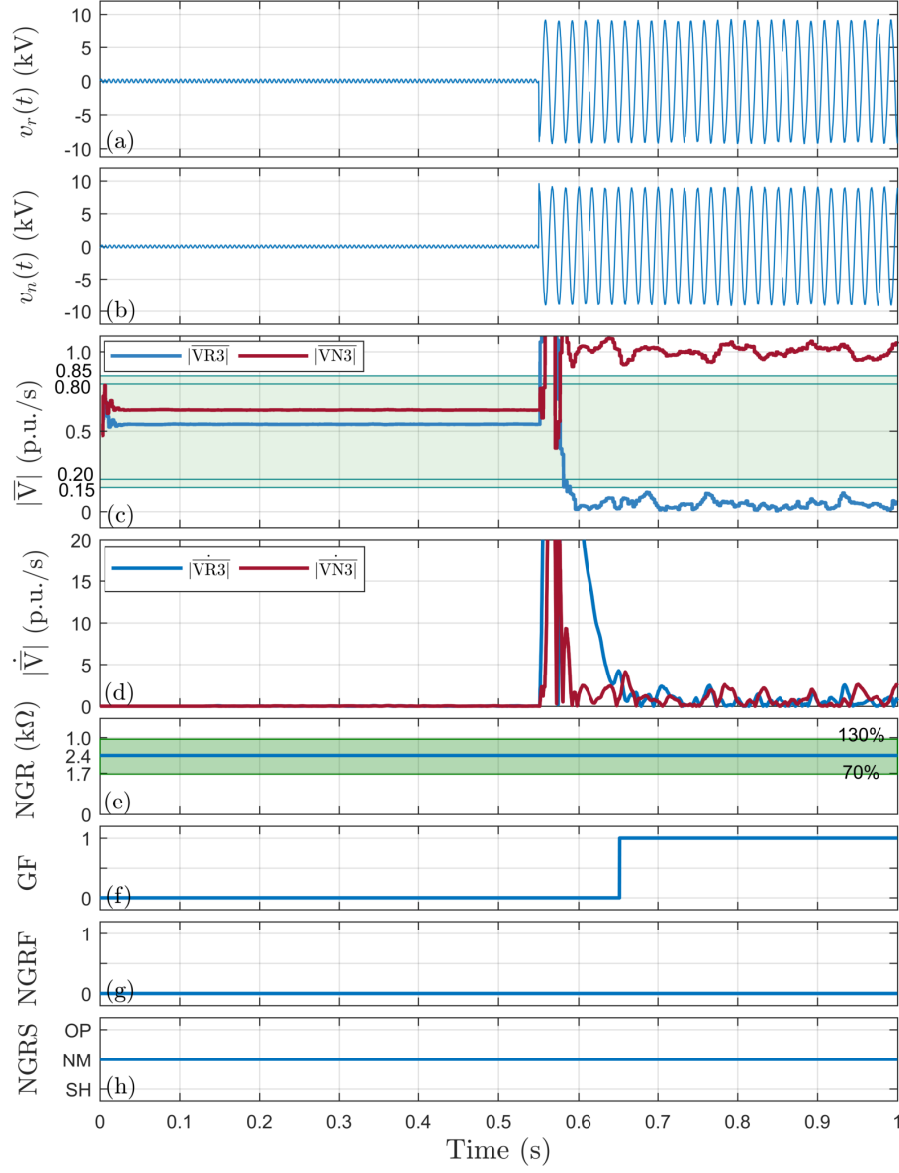


Figure D.7: External double-line-to-ground fault at generator terminals, ($R_{NGR} = 2.4 \text{ k}\Omega$, $R_F = 10 \text{ }\Omega$, Load = $0.94 + j0.2 \text{ pu}$, and $e3 = 0.5\%$). (a) Residual voltage, (b) Neutral voltage, (c) Normalized neutral and residual third harmonic voltages, (d) Rate of change of the normalized third harmonic voltages, (e) NGR resistance, (f) Ground fault detection, (g) NGR failure detection, and (h) NGRS State.

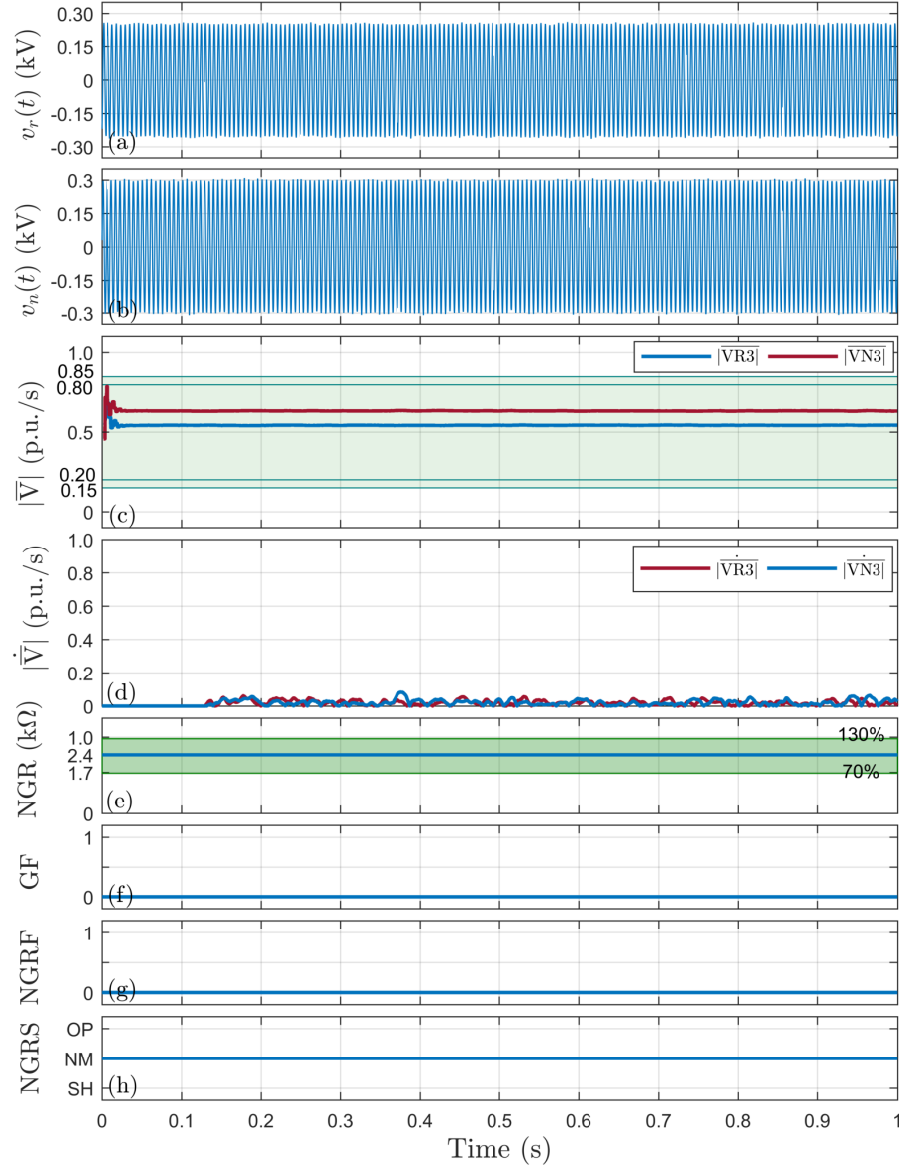


Figure D.8: External line-to-line and three-phase fault in generator terminals, ($R_{NGR} = 2.4 \text{ k}\Omega$, Load = $0.94 + j0.2$ pu, and $e3 = 0.5\%$). (a) Residual voltage, (b) Neutral voltage, (c) Normalized neutral and residual third harmonic voltages, (d) Rate of change of the normalized third harmonic voltages, (e) NGR resistance, (f) Ground fault detection, (g) NGR failure detection, and (h) NGRS State.

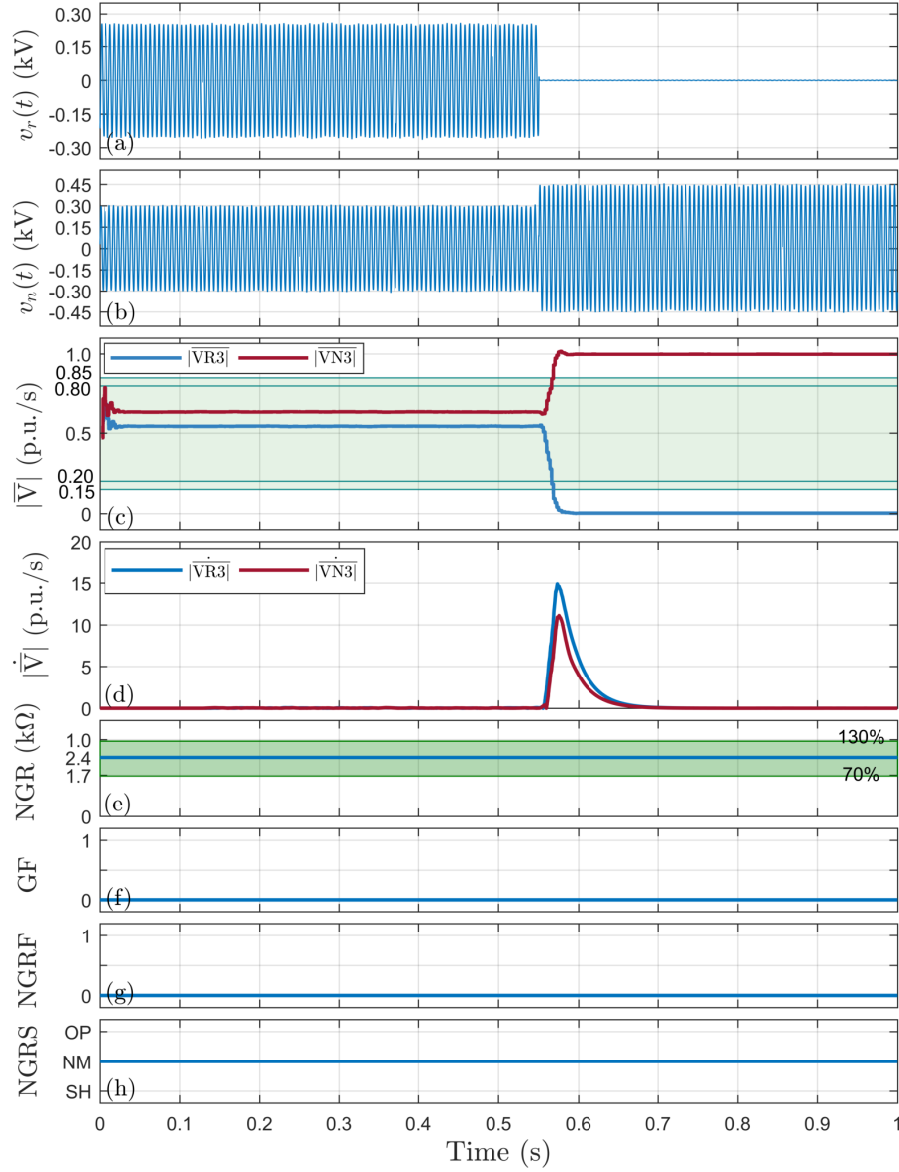


Figure D.9: External three-phase-to-ground fault at generator terminals, ($R_{NGR} = 2.4 \text{ k}\Omega$, $R_F = 10 \text{ }\Omega$, Load = $0.94 + j0.2$ pu, and $e3 = 0.5\%$). (a) Residual voltage, (b) Neutral voltage, (c) Normalized neutral and residual third harmonic voltages, (d) Rate of change of the normalized third harmonic voltages, (e) NGR resistance, (f) Ground fault detection, (g) NGR failure detection, and (h) NGRS State.

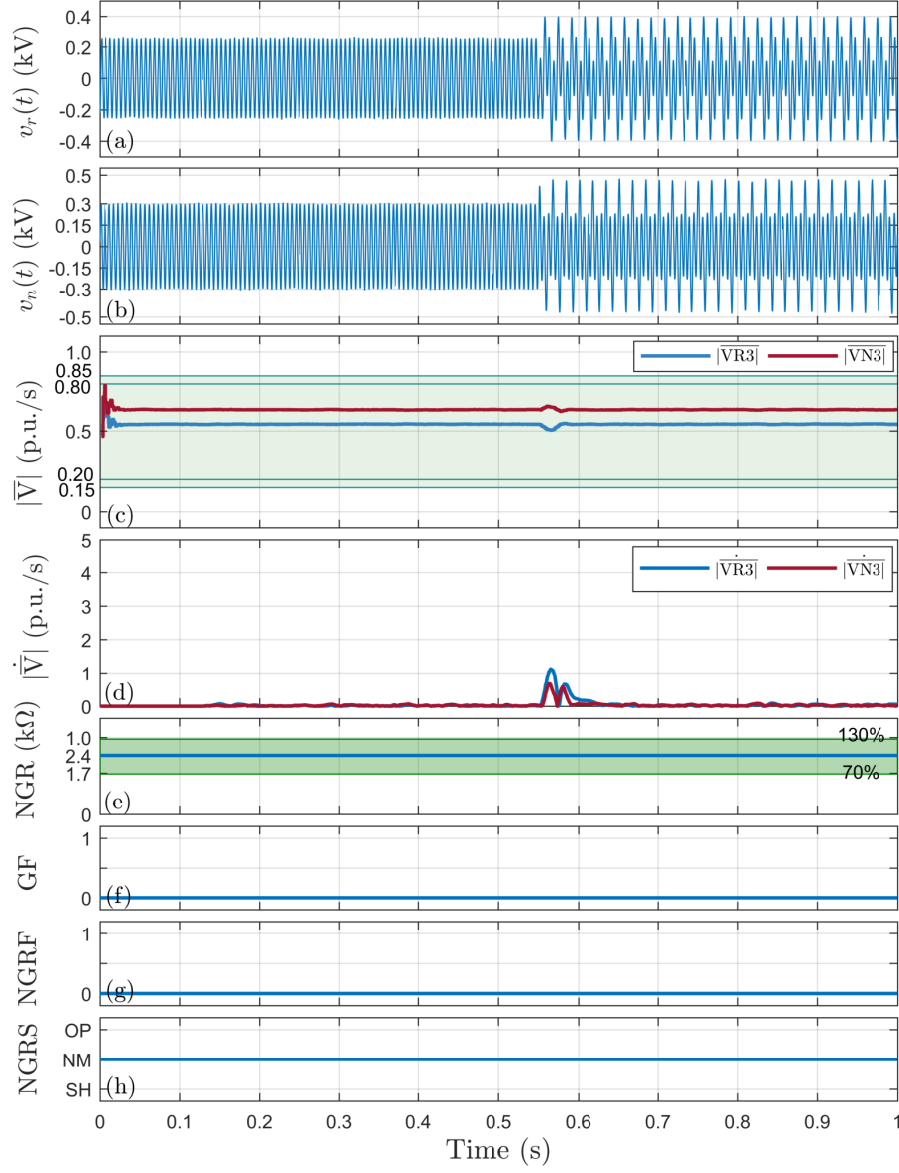


Figure D.10: External line-to-ground fault in 345 kV system, ($R_{NGR} = 2.4 \text{ k}\Omega$, $R_F = 10 \Omega$, Load = $0.94 + j0.2 \text{ pu}$, and $e3 = 0.5\%$). (a) Residual voltage, (b) Neutral voltage, (c) Normalized neutral and residual third harmonic voltages, (d) Rate of change of the normalized third harmonic voltages, (e) NGR resistance, (f) Ground fault detection, (g) NGR failure detection, and (h) NGRS State.

Appendix E

Additional Results For Chapter 6

In this chapter, additional simulation results for the third proposed method, presented in Chapter 6, are demonstrated. The performance of the proposed method in de-energized operation condition is examined. The studied generator operates de-energized before being connected to network meaning that the neutral voltage and current might not be sufficient to perform a reliable monitor. Therefore, the injection system comes to the picture injecting a 20 Hz signal to measure the NGR and generator insulation resistance. It is shown that the proposed method reliably detects the NGR failure and generator insulation fault. Thereafter, it is shown that the proposed method can detect the NGR failure during the ground faults beyond the generator terminals.

On the basis of the presented results and further performed observations, it is concluded that:

1. The performance of the proposed method in de-energized condition is as strong as during the faulted and unfaulted operation conditions. In fact, if the NGR fails during generator star-up or shut-down procedure, it will be detected using the injected voltage and current to the neutral.
2. The NGR failure during the external ground faults, in 22 kV or 345 kV systems, is detected as well. In fact, these ground faults not only do not impact on the proposed method but also provide sufficient neutral voltage and current for NGR monitoring.

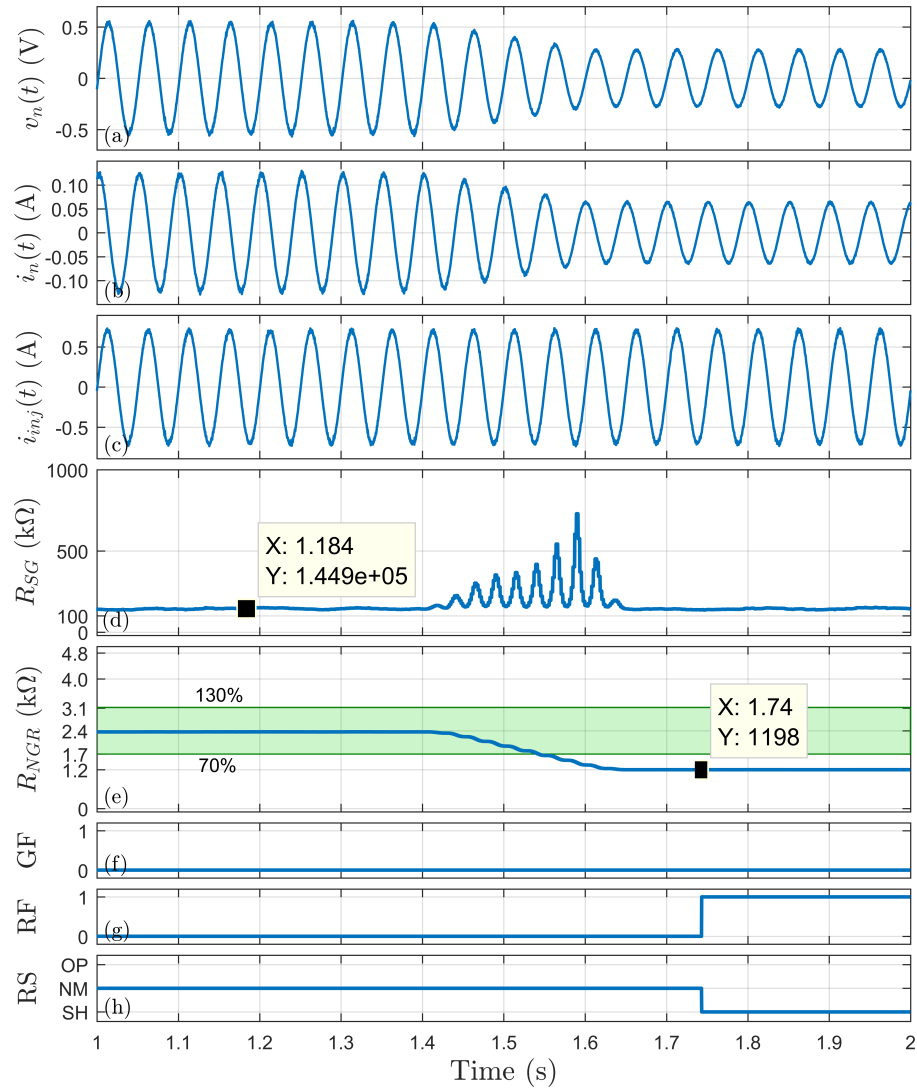


Figure E.1: Failed-short NGR in de-energized condition: a) Neutral voltage, b) Neutral current, c) Injected current, d) Generator stator winding insulation resistance, e) NGR resistance, f) Ground Fault (GF), g) Resistor Failure (RF), and h) Resistor Status (RS).

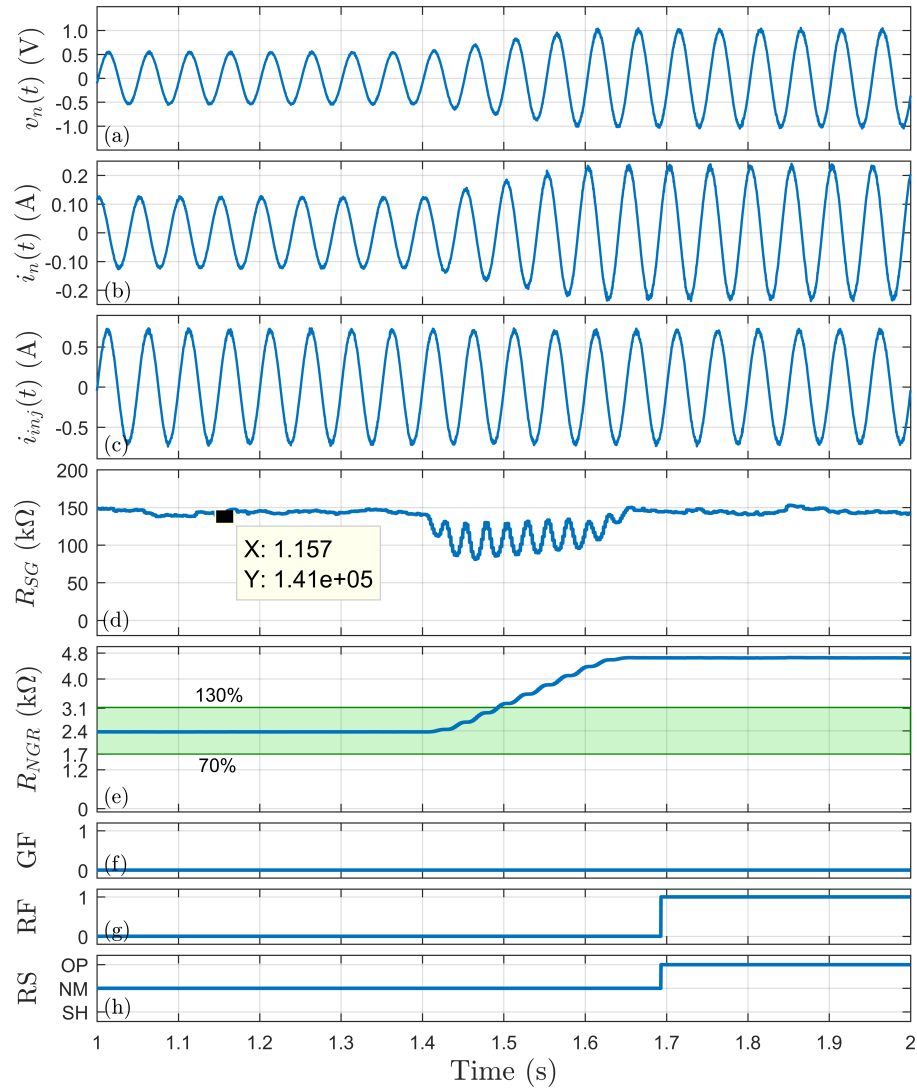


Figure E.2: Failed-open NGR in de-energized condition: a) Neutral voltage, b) Neutral current, c) Injected current, d) Generator stator winding insulation resistance, e) NGR resistance, f) Ground Fault (GF), g) Resistor Failure (RF), and h) Resistor Status (RS).

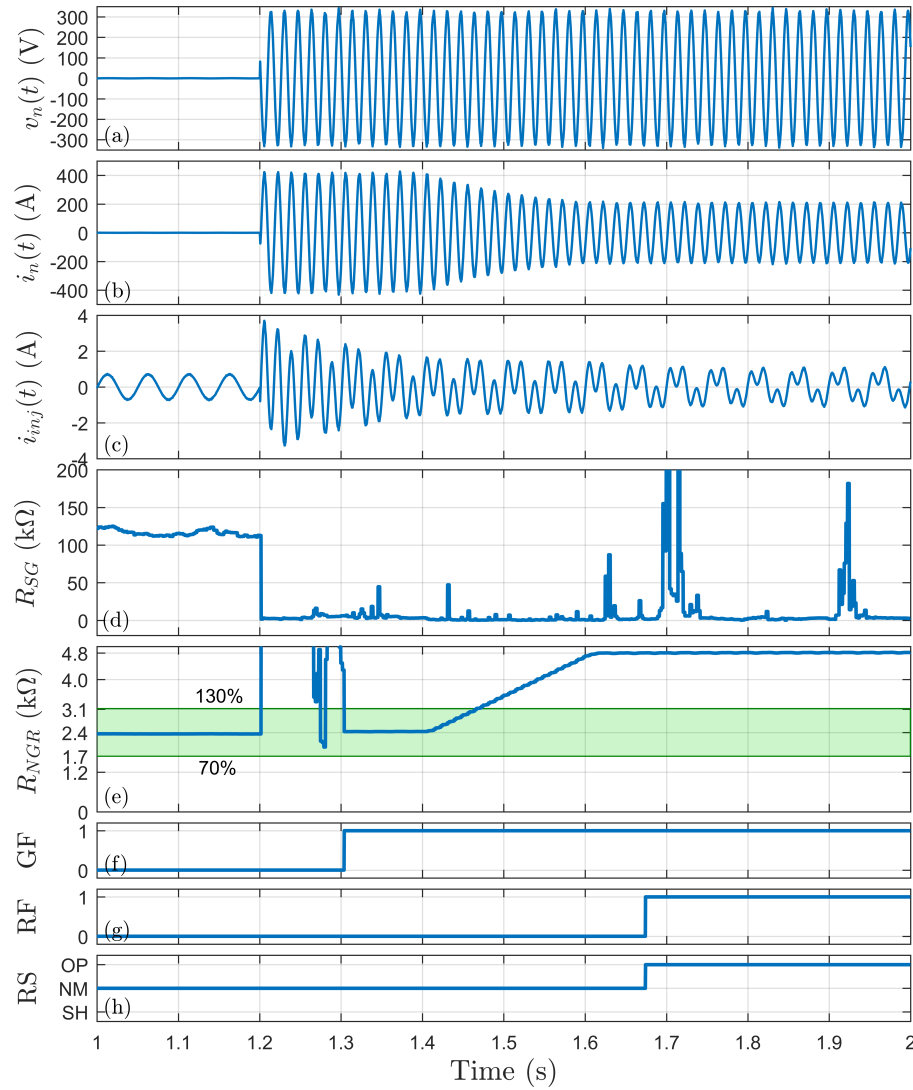


Figure E.3: Failed-open NGR during LG fault at 12.47 kV busbar: a) Neutral voltage, b) Neutral current, c) Injected current, d) Generator stator winding insulation resistance, e) NGR resistance, f) Ground Fault (GF), g) Resistor Failure (RF), and h) Resistor Status (RS).

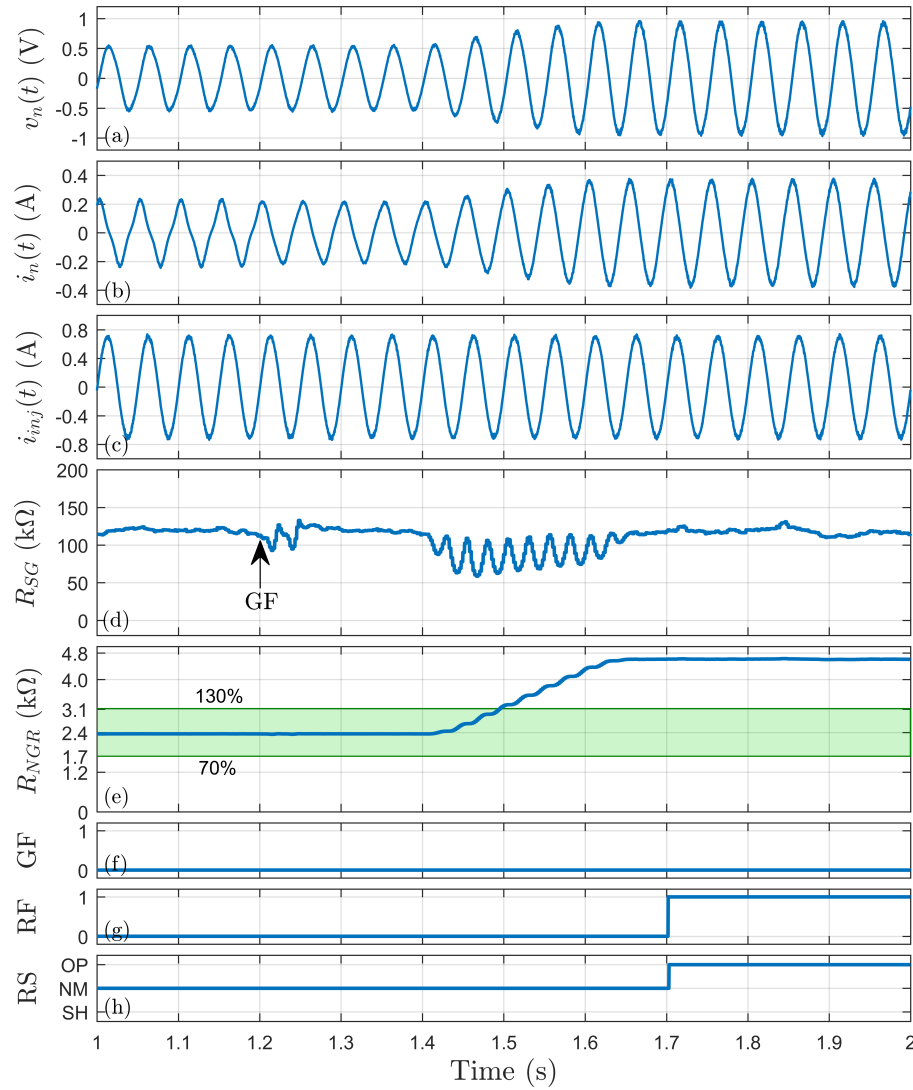


Figure E.4: Failed-open NGR during LG fault in 345kV system: a) Neutral voltage, b) Neutral current, c) Injected current, d) Generator stator winding insulation resistance, e) NGR resistance, f) Ground Fault (GF), g) Resistor Failure (RF), and h) Resistor Status (RS).

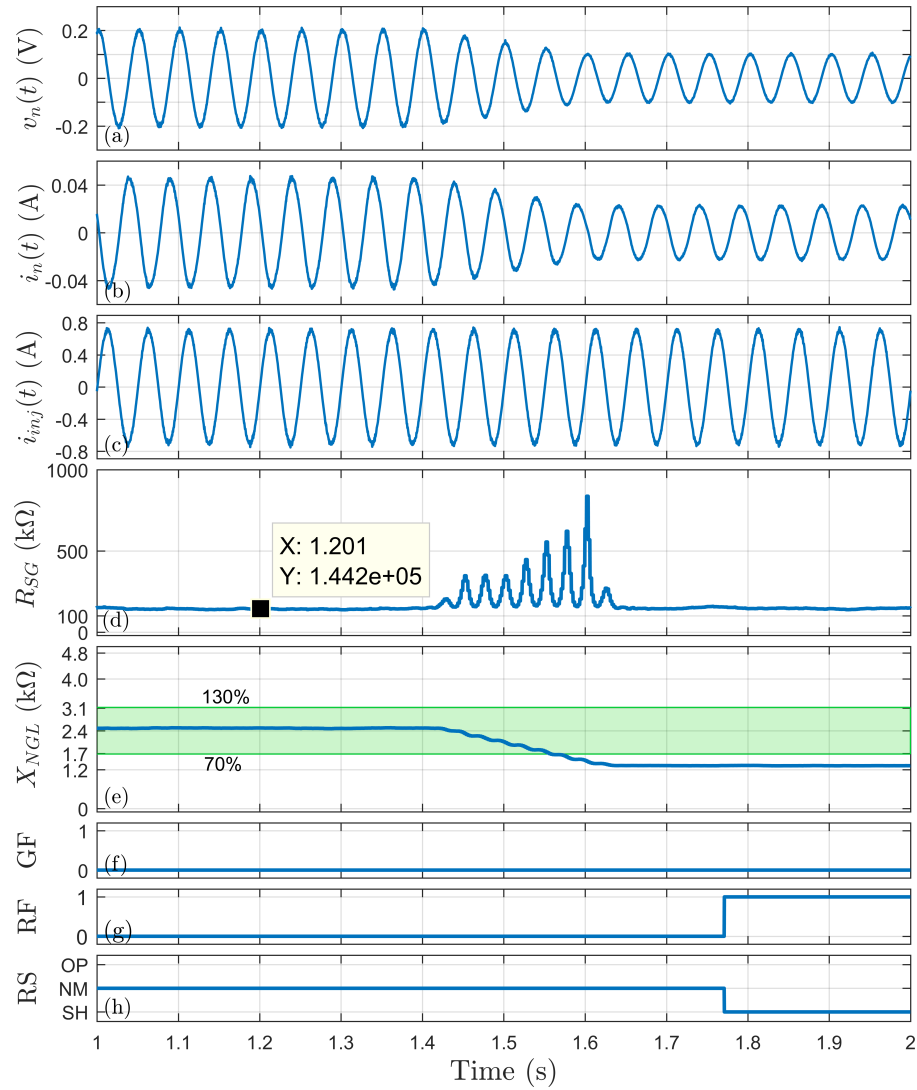


Figure E.5: Failed-short NGL in de-energized condition: a) Neutral voltage, b) Neutral current, c) Injected current, d) Generator stator winding insulation resistance, e) NGL reactance, f) Ground Fault (GF), g) Reactor Failure (RF), and h) Reactor Status (RS).

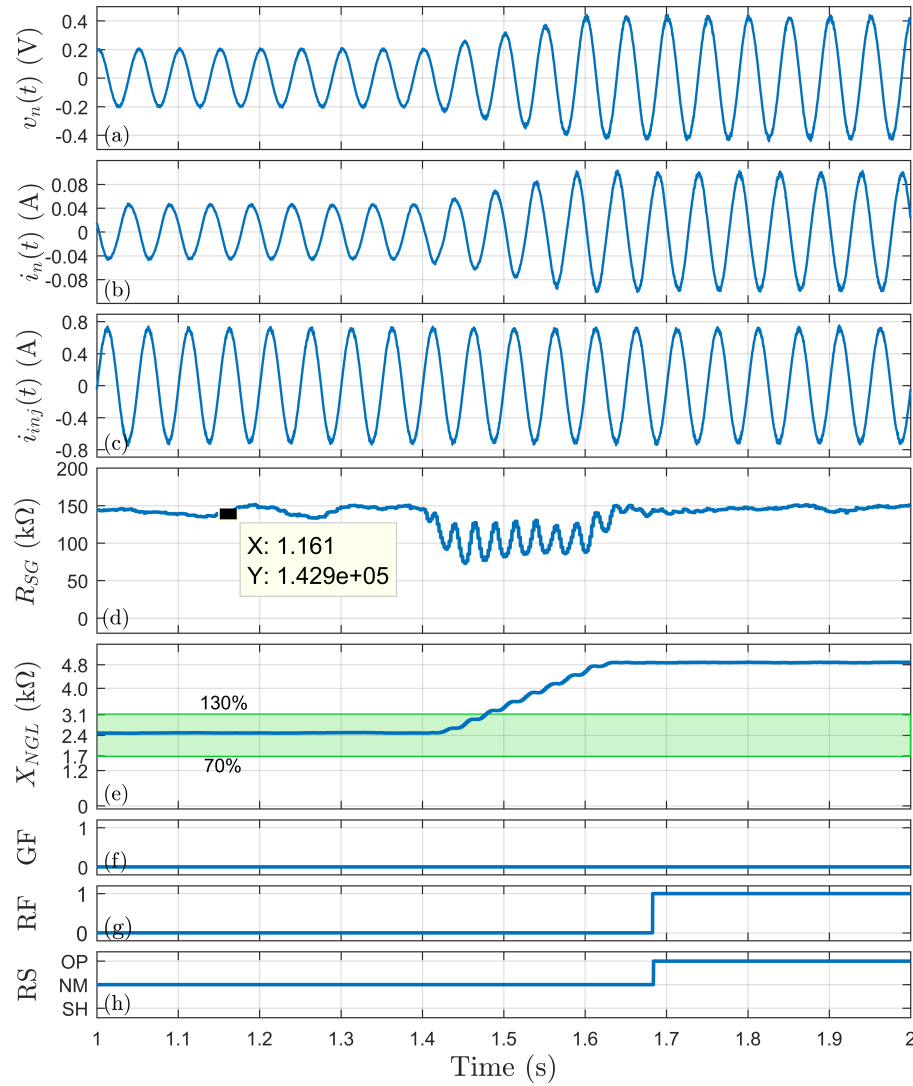


Figure E.6: Failed-open NGL in de-energized condition: a) Neutral voltage, b) Neutral current, c) Injected current, d) Generator stator winding insulation resistance, e) NGL reactance, f) Ground Fault (GF), g) Reactor Failure (RF), and h) Reactor Status (RS).

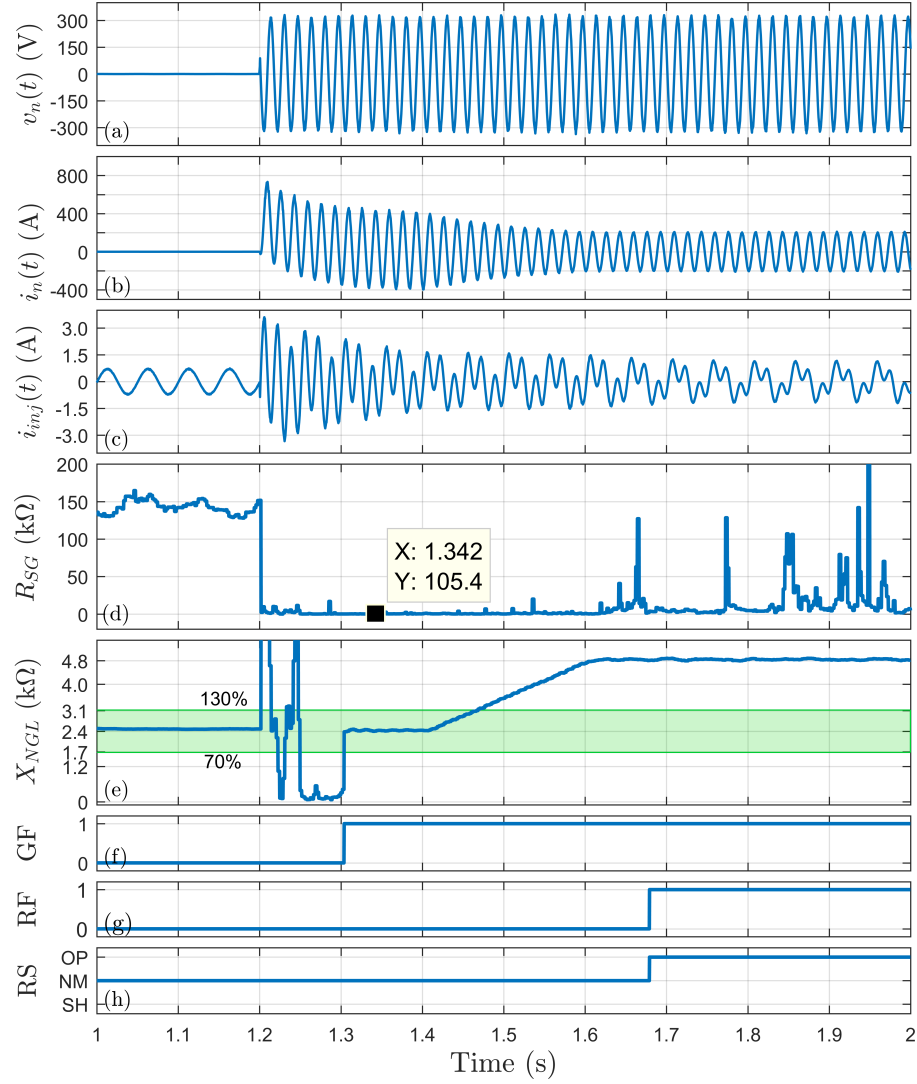


Figure E.7: Failed-open NGL during LG fault at 12.47 kV busbar: a) Neutral voltage, b) Neutral current, c) Injected current, d) Generator stator winding insulation resistance, e) NGL reactance, f) Ground Fault (GF), g) Reactor Failure (RF), and h) Reactor Status (RS).

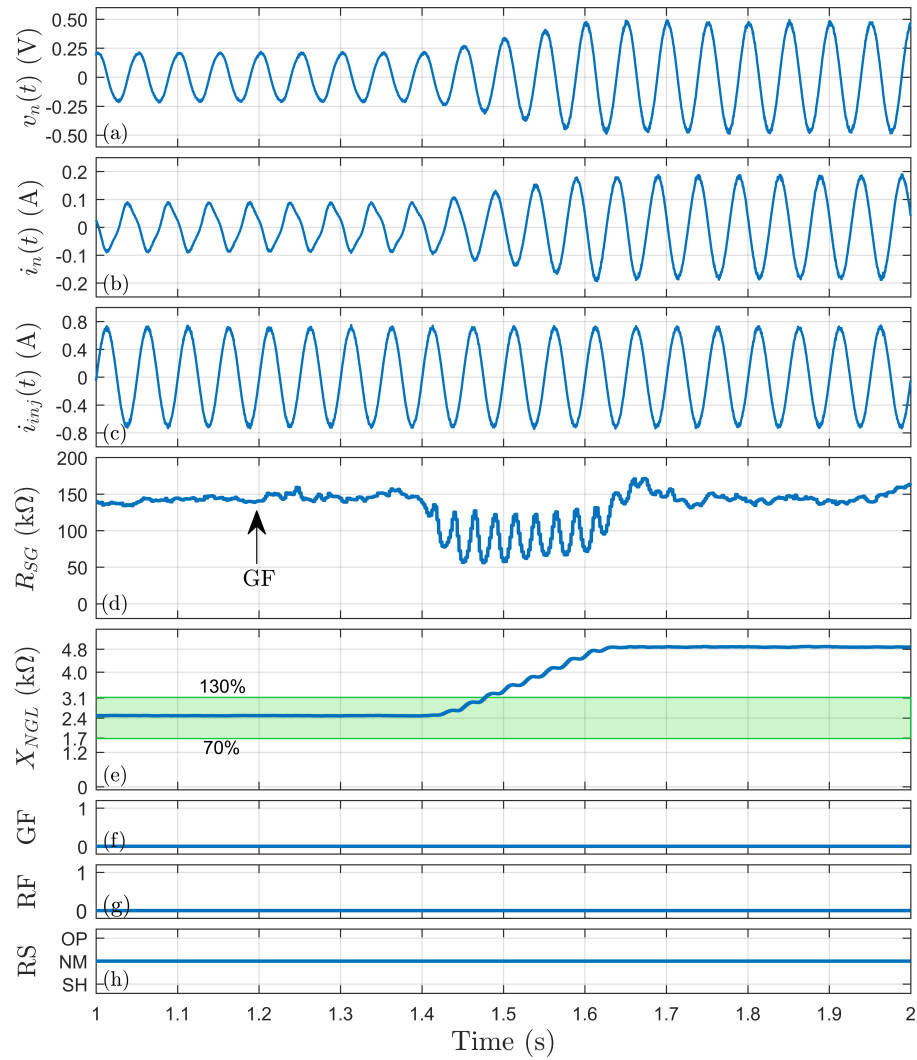


Figure E.8: Failed-open NGL during LG fault in 345 kV system: a) Neutral voltage, b) Neutral current, c) Injected current, d) Generator stator winding insulation resistance, e) NGL reactance, f) Ground Fault (GF), g) Reactor Failure (RF), and h) Reactor Status (RS).

Curriculum Vitae

Name: Rahim Jafari

Education: Ph.D. Electrical Engineering – Power Systems
Western University
London, Ontario, Canada
2014 - 2018

M.Sc. Electrical Engineering – Power System Relaying and Protection
Amirkabir University of Technology (Tehran Polytechnique)
Tehran, Tehran, Iran
2011 - 2013

Bachelor of Electrical Engineering – Power Systems
Tabriz University
Tabriz, East Azarbaijan, Iran
2007 - 2010

Honours and Awards: NSERC CRD Scholarship 2014-2017
Hydro One Award for Excellence in Research 2018

Related Work Experience: Teaching Assistant
The University of Western Ontario
2016 - 2018

Related Publications:

1. R. Jafari, M. Kanabar, T. S. Sidhu and I. Voloh, “Online Neutral Grounding Resistor Monitoring for Unit-Connected Generators with Hardware Validation”, Elsevier International Journal of Electrical Power and Energy Systems, Vol. 105, pp.220-228, February 2019.

2. R. Jafari, M. Kanabar, I. Voloh, and T. S. Sidhu, “New Methods for Monitoring Neutral Grounding Resistors”, IEEE 71st Annual Conference for Protective Relay Engineers (CPRE), College Station, TX, 2018, pp. 1-15.
3. R. Jafari, M. Kanabar, T. S. Sidhu and I. Voloh, “Neutral Grounding Resistor Monitoring based on Sub-Harmonic Signal Injection”, IEEE 31st Canadian Conference on Electrical and Computer Engineering (CCECE2018), Quebec City, QB, May 2018, pp. 1-5.
4. R. Jafari, M. Kanabar, T. S. Sidhu and I. Voloh, “Analysis of A Neutral Grounding Resistor Monitoring Method”, IEEE 31st Canadian Conference on Electrical and Computer Engineering (CCECE2018), Quebec City, QB, May 2018, pp. 1-6.
5. R. Jafari, M. Kanabar, T. S. Sidhu and I. Voloh, “A Comprehensive Neutral Grounding Resistor Monitoring Method with Hardware Validation”, Underreview at IEEE Transactions on Power Delivery.